TENSILE AND SHEAR BEHAVIOR OF ANCHORS IN UNCRACKED

AND CRACKED CONCRETE UNDER STATIC AND

DYNAMIC LOADING

by

Jennifer Marie Hallowell, B.S.

THESIS

Presented to the Faculty of the Graduate School

of The University of Texas at Austin

in Partial Fulfillment

of the Requirements

for the Degree of
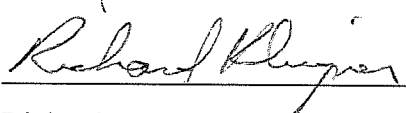
MASTER OF SCIENCE IN ENGINEERING
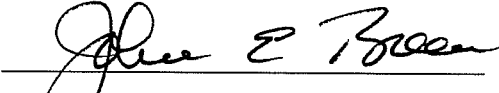
The University of Texas at Austin

December 1996

TENSILE AND SHEAR BEHAVIOR OF ANCHORS IN UNCRACKED

AND CRACKED CONCRETE UNDER STATIC AND

DYNAMIC LOADING

APPROVED BY

SUPERVISING COMMITEE:

Richard E. Klingner

John E. Breen

In loving memory of my father

my hero, my inspiration, my friend

ACKNOWLEDGMENTS

<div align="right">

Jennifer M. Hallowell

June 1996

Austin, TX

</div>

DISCLAIMER

ABSTRACT

TENSILE AND SHEAR BEHAVIOR OF ANCHORS IN UNCRACKED AND CRACKED CONCRETE UNDER STATIC AND DYNAMIC LOADING

by

Jennifer Marie Hallowell, M.S.E.

The University of Texas at Austin, 1996

SUPERVISOR: Richard E. Klingner

This research first examines the behavior of single anchors under static and dynamic tensile loading in uncracked and cracked concrete. Results are analyzed to determine the effect of aggregate hardness on anchor behavior, to compare the behavior of cast-in-place anchors with heavy-duty post-installed anchors, and to evaluate the effect of anchor type on additional crack opening.

The second focus of this thesis is the behavior of single- and double-anchor connections under static and dynamic shear loading in uncracked and cracked concrete. Near-edge single-anchor connections typically fail by concrete cone breakout. The ability of transverse reinforcement to develop the capacity of the anchor beyond concrete cone breakout is evaluated. Double-anchor connections located on a line perpendicular to the free edge are tested and compared with the behavior of single-anchor connections.

TABLE OF CONTENTS

LIST OF TABLES

x

LIST OF FIGURES

xvii

CHAPTER ONE

INTRODUCTION

1.1 INTRODUCTION

In December 1980 the U.S. Nuclear Regulatory Commission (NRC) designated "Seismic Qualification of Equipment in Operating Plants" as an Unresolved Safety Issue (USI). It was determined imperative to develop alternative seismic qualification methods and acceptance criteria that can be used to assess the capability of mechanical and electrical equipment in operating nuclear power plants to perform their intended safety functions. This critical equipment is attached to concrete with anchor bolts; therefore, it is necessary to ensure that the anchors are capable of resisting seismic loads. Although the behavior of anchor bolts under static loading is well understood, the effects of seismic loading and cracked concrete are unclear [Klingner 1991].

1.2 OBJECTIVE AND SCOPE OF RESEARCH PROGRAM

In light of this, the NRC is sponsoring a multi-year testing program at The University of Texas at Austin to evaluate the behavior of anchors located in uncracked and cracked concrete and subjected to static and dynamic loading. The testing program consists of 5 Tasks:

Task 1: Tensile Behavior of Single-Anchor Connections in Uncracked and Cracked Concrete under Static and Dynamic Loading

Task 2: Static and Dynamic Behavior of Multiple-Anchor Connections under Shear and Moment

1

Task 3: Shear Behavior of Single-Anchor and Double-Anchor Connections in Uncracked and Cracked Concrete under Static and Dynamic Loading

Task 4: Dynamic Behavior of Multiple-Anchor Connections

Task 5: Submission of Final Report

1.3 SCOPE OF THESIS

This thesis addresses portions of Task 1 and Task 3. The tensile behavior of anchors in uncracked and cracked concrete under static and dynamic loading is evaluated. In particular, the behavior of cast-in-place anchors, the effect of hard aggregate, and the effect of cracked concrete are evaluated and compared with results presented in [Rodriguez 1995].

The shear behavior of anchors in uncracked and cracked concrete under static and dynamic loading is also evaluated. The ability of transverse reinforcement to increase the capacity and ductility of near-edge anchors is determined. The behavior of double-anchor connections located on a line perpendicular to the free edge is compared to the behavior of single-anchor connections.

1.4 OBJECTIVE OF THESIS

The objective of this thesis is to present and summarize the tensile and shear behavior of anchors in uncracked and cracked concrete under static and dynamic loading. This thesis is intended to add to the understanding of the behavior of anchors in cracked concrete and the behavior of anchors subjected to seismic loading. The results can be combined with those from other Tasks of the research program to develop criteria for evaluating connection capacity under seismic loading.

CHAPTER TWO

BACKGROUND

2.1 INTRODUCTION

Anchors connect structural members and equipment to concrete or masonry. Tensile and shear loads are transferred between the concrete and the attachment through the anchor. This chapter presents background material on the types of anchors and failure modes exhibited in this study. The design methodology is discussed with reference to the ACI Committee 349 design provisions and the Concrete Capacity Design Method. Finally, previous results from this research program are summarized.

2.2 ANCHOR CLASSIFICATION

All anchors can be classified into two main categories: cast-in-place; and post-installed (retrofit). As the name implies, cast-in-place anchors are suspended in the formwork and concrete is cast around the anchor. Headed bolts, headed studs, "J" bolts, "L" bolts, threaded rods, and reinforcing bars are used as cast-in-place anchors. Load is transferred through bearing on the concrete by the head, hook, or deformation [CEB 206 & 207 1991].

Post-installed anchors are placed in hardened concrete. Based on their installation procedures, post-installed anchors are further classified into four groups: self-drilling, bonded, expansion, and undercut. Self-drilling anchors, also known as concrete screw anchors, are inserted into the structural member using a drill. Bonded anchors are inserted into holes larger than the diameter of the bolt and rely on bond between the bolt and an adhesive, and between the adhesive and the concrete, to transfer load. Bonding agents include epoxies, vinylesters, polyesters, and cementitious grout.

3

Expansion anchors are placed in a pre-drilled hole and rely on the expansion of a cone or wedge to transfer force between the anchor and the concrete. Undercut anchors require a bell-shaped cut at the bottom of the pre-drilled hole. The cone of the anchor expands into the bell-shaped hole, and relies on bearing against the concrete to transfer load.

2.3 TYPES OF ANCHORS

This section describes in detail the four anchors used in this study: cast-in-place anchors, wedge-type expansion anchors, sleeve-type expansion anchors and undercut anchors.

2.3.1 Cast-in-Place Anchors

Headed A325 bolts, as shown in Figure 2.1, were used as cast-in-place anchors. Tensile loads are transferred through bearing of the head against the concrete. Shear forces are transferred by bearing of the anchor body against the concrete. Cast-in-place anchors are advantageous for use in heavily reinforced members because there is no concern with drilling into reinforcement. In addition, reinforcement may be configured around the bolt to enhance load transfer.
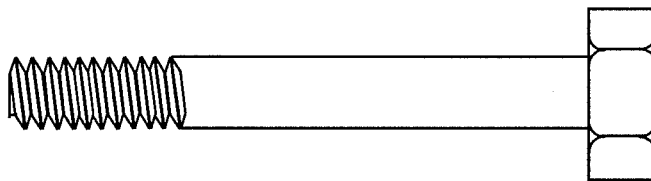
Figure 2.1 Typical Cast-in-Place Anchor (A325 Bolt)

2.3.2 Wedge-Type Expansion Anchors

Figure 2.2 shows the wedge-type expansion anchor used in this study. The anchor is installed in a pre-drilled hole slightly larger than the anchor diameter. The nut is torqued, raising the mandrel and expanding the wedge. Tensile load is transferred through friction between the wedge and the concrete (steel to concrete), and the wedge and the mandrel (steel to steel). Additional load causes the mandrel to continue to rise,

increasing the expansion of the wedge. Shear load is transferred by bearing of the anchor against the concrete.
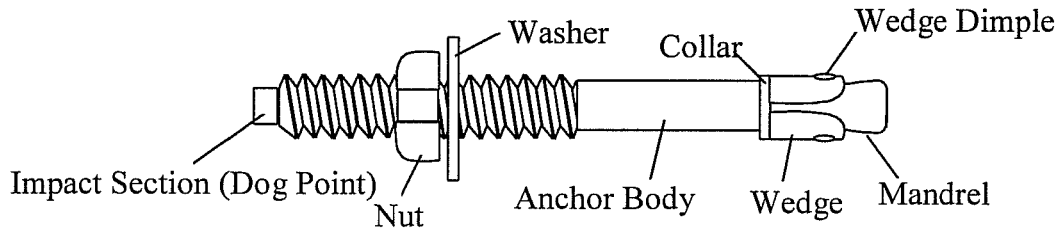
Figure 2.2 Wedge-Type Expansion Anchor [Rodriguez 1995]

2.3.3 Sleeve-Type Expansion Anchor

Figure 2.3 shows the single-cone sleeve-type expansion anchor used in this study. The configuration of this anchor is complex compared to that of the wedge-type expansion anchor. The anchor is set in a pre-drilled hole and torqued to raise the cone and expand the sleeve. Tensile load is transferred through friction between the expansion sleeve and the concrete. Shear load is transferred by bearing of the anchor against the concrete. One unique feature of this sleeve-type expansion anchor is that the expansion sleeve increases in thickness with increasing distance from the cone, as shown in Figure 2.4.
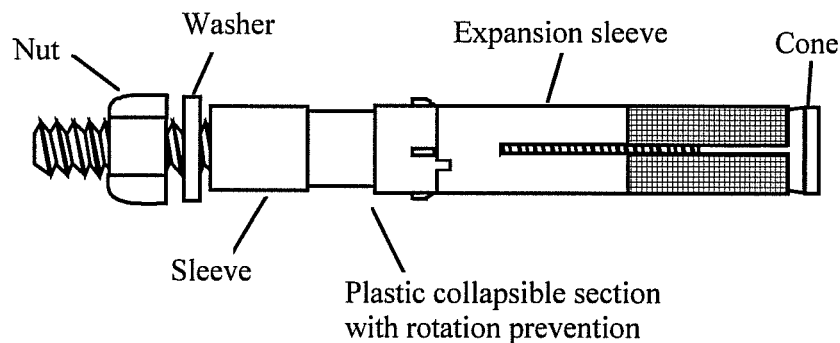
Figure 2.3 Torque-Controlled Sleeve-Type Expansion Anchor [Rodriguez 1995]
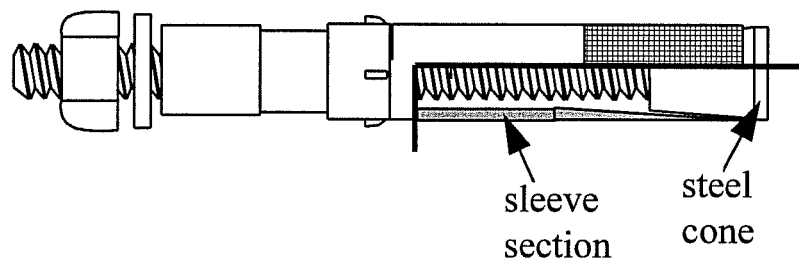
Figure 2.4 Section through Sleeve-Type Expansion Anchor [Rodriguez 1995]

2.3.4 Undercut Anchors

Figure 2.5 shows a typical undercut anchor consisting of a threaded rod with a steel cone at one end and an expansion sleeve. Figure 2.6 illustrates the installation of an undercut anchor. A hole slightly larger than the diameter of the sleeve is drilled in the concrete. A special tool is used to cut a bell-shaped undercut near the bottom of the pre-drilled hole. After the anchor is placed in the hole, the nut is torqued, raising the cone and expanding the sleeve into the bell-shaped undercut. Little or no expansion force is induced into the concrete during the installation procedure [CEB 206 & 207 1991]. Tensile load is transferred by bearing of the sleeve against the concrete. This mechanism is similar to the bearing of the head of a cast-in-place anchor. Shear load is transferred through bearing of the anchor body against the concrete.
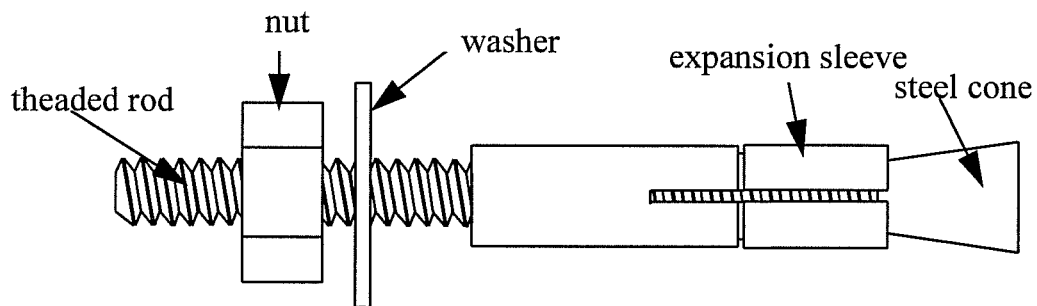
Figure 2.5 Typical Undercut Anchor [Rodriguez 1995]
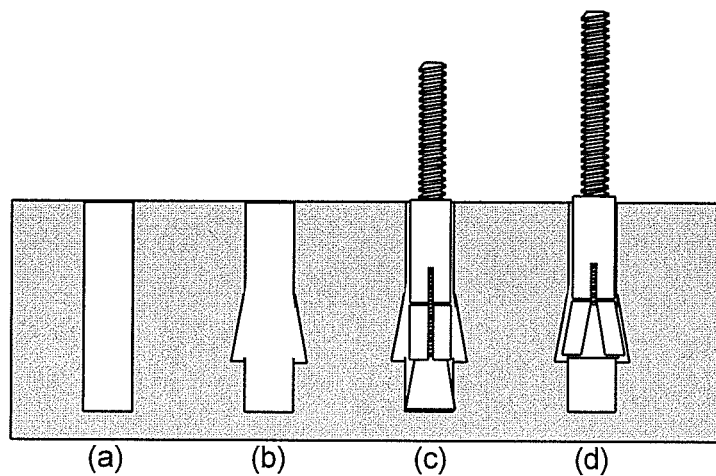
Figure 2.6 Illustration of Installation of One Type of Undercut Anchor: (a) drilled hole; (b) drilled undercut; (c) anchor inserted inside hole; (d) undercut anchor after expansion [Rodriguez 1995]

2.4 FAILURE MODES FOR ANCHORS

Ductile anchor failure is preferable for design against unpredictable loads because it offers large displacement, ample warning before failure, and significant energy absorption. However, brittle failure can sometimes be acceptable, provided that the factor of safety is adequate. In order to ensure proper performance of anchors the failure load must be accurately predicted. Therefore, the failure modes and governing equations must be well understood.

2.4.1 Concrete Cone Breakout Failure

Concrete cone breakout is a brittle failure of the concrete surrounding the anchor. Figure 2.7 shows a concrete cone breakout failure for an anchor under tensile load. Microcracks form in the concrete around the anchor head. These microcracks combine to form larger macrocracks, which propagate to the surface of the concrete. The failure surface is in the shape of a cone with an
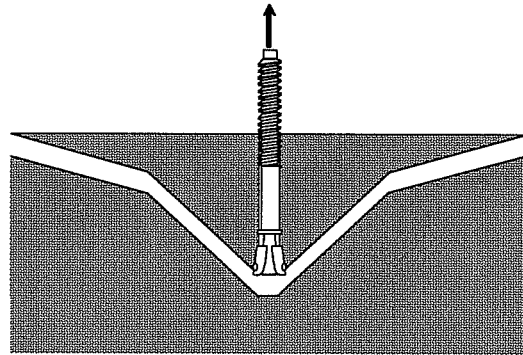
Figure 2.7 Tensile Concrete Cone Breakout Failure [Rodriguez 1995]

inclination of approximately 35-degrees at the base, and flattening out near the free surface. The failure load, predicted by Equation (2-1), is a function of the strength of the concrete and the embedment depth of the anchor [Fuchs, Eligehausen, and Breen 1995].

$$N_{no} = k_{nc} \sqrt{f_c'}\, h_{ef}^{1.5} \qquad \text{(lb)} \qquad \text{(2-1a)}$$

$$N_{no} = k_{nc} \sqrt{f_{cc}'}\, h_{ef}^{1.5} \qquad \text{(N)} \qquad \text{(2-1b)}$$

N_{no} = nominal tensile cone breakout capacity

k_{nc} = multiplicative constant

= 35 for post-installed anchors

= 40 for cast-in-place anchors

f_c' = specified concrete compressive strength, psi

f_c' = specified concrete compressive strength, N/mm^2

h_{ef} = effective embedment
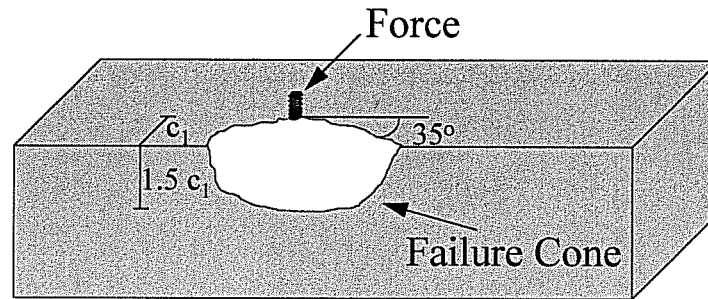
Figure 2.8 Shear Concrete Cone Breakout Failure

When an anchor is loaded in shear, a similar failure occurs as shown in Figure 2.8. Here, the failure surface is a semi-cone. For short, stiff embedments, the failure cone originates near the head of the anchor. For deeper embedments, the failure cone originates near the surface of the concrete [CEB 206 & 207 1991]. The shear breakout cone extends over the top surface of the concrete at an angle of approximately 35-degrees from the anchor. The depth of the failure cone at the side of the member is approximately 1.5 times the edge distance. The load at which the brittle concrete failure occurs is most strongly influenced by the concrete compressive strength and the edge distance in the loading direction. Equation (2-2) predicts the concrete cone failure for shear loading [Fuchs, Eligehausen, and Breen 1995].

$$V_{no} = 13 \, (\ell/d_o)^{0.2} \, \sqrt{d_o} \, \sqrt{f_c'} \, c_1^{1.5} \qquad \text{(lb)} \qquad \text{(2-2a)}$$

$$V_{no} = (\ell/d_o)^{0.2} \, \sqrt{d_o} \, \sqrt{f_{cc}'} \, c_1^{1.5} \qquad \text{(N)} \qquad \text{(2-2b)}$$

V_{no} = nominal shear breakout capacity

ℓ = activated load-bearing length of fastener

d_o = outside diameter of fastener

c_1 = edge distance in loading direction

2.4.2 Concrete Pryout Failure

Anchors located far from an edge and loaded in shear may experience a concrete pryout failure. As shown in Figure 2.9, the concrete in front of the anchor crushes, then as the anchor deforms, the concrete behind the anchor fails due to a "kicking back" of the anchor as it is loaded. Anchors with a small embedment depth-to-diameter ratio and a large tensile capacity are susceptible to this type of failure. Anchor strength, concrete strength, and number and spacing of anchors affect this failure mode.
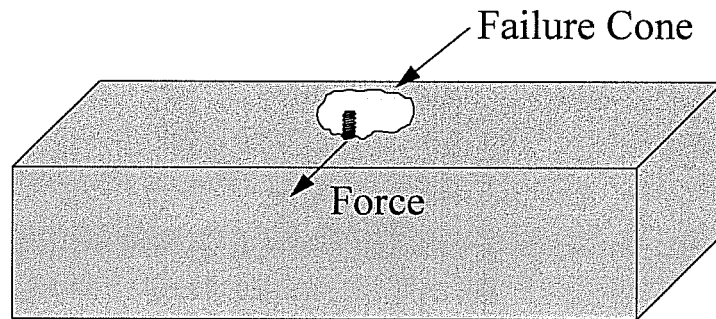
Figure 2.9 Concrete Pryout Failure

2.4.3 Steel Failure

Steel failure is a ductile failure mode characterized by yielding and necking of the steel, followed by fracture. Figures 2.10 and 2.11 show steel failure of an anchor under tension and shear, respectively. Under shear load, the steel failure is preceded by a local concrete spall in front of the anchor. The steel failure load in tension is predicted by Equation (2-3) and the steel failure load under pure shear is predicted from Equation (2-4). The coefficient γ varies depending on whether the failure plane is located through the shank or through the threaded portion of the anchor [Cook 1989].
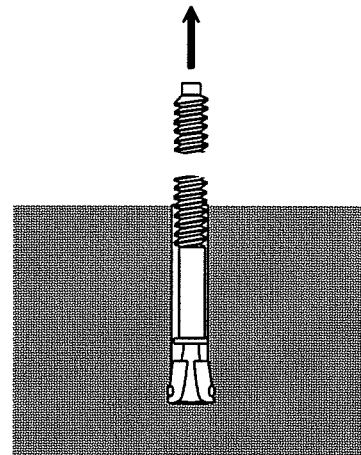
Figure 2.10 Tensile Steel Failure [Rodriguez 1995]

$$N_u = A_s \cdot F_u \qquad (2\text{-}3)$$

$$V_u = \gamma \cdot A_s \cdot F_u \qquad (2\text{-}4)$$

N_u = ultimate tensile capacity

V_u = ultimate shear capacity

$\gamma = 0.75$ for failure through the anchor shank

$\gamma = 0.55 - 0.65$ for failure through the threaded portion
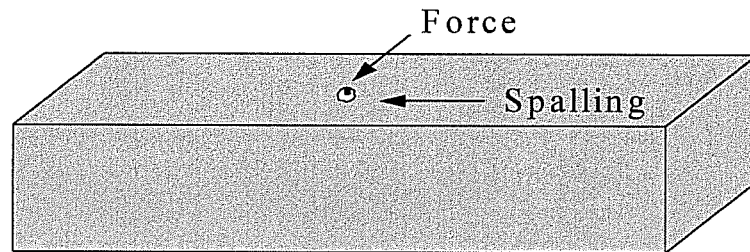
Figure 2.11 Shear Steel Failure

2.4.4 Pull-through Failure
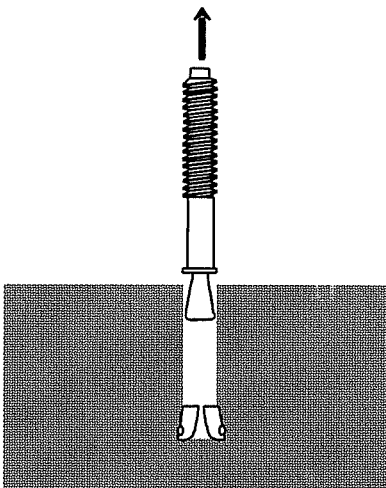
Figure 2.12 Pull-through Failure [Rodriguez 1995]

Pull-through failure, shown in Figure 2.12, occurs with expansion anchors under tensile load when the friction force between the cone and the expansion mechanism is exceeded by the applied force. The cone moves relative to the expansion mechanism, causing the anchor to pull out while the expansion mechanism remains in the concrete. The force necessary to cause pull-through failure is dependent on the inclination of the cone and the surface conditions of the cone and the expansion mechanism. There is no theoretical procedure to predict pull-through failure.

2.4.5 Pull-out Failure

When the friction force between the expansion mechanism and the concrete is exceeded by the applied tensile force, a pull-out failure as shown in Figure 2.13 occurs. The anchor comes out completely from the concrete. The load at which pull-out failure occurs is dependent on the coefficient of friction between the concrete and the expansion mechanism. Currently, there is no theoretical procedure to predict pull-out failure.
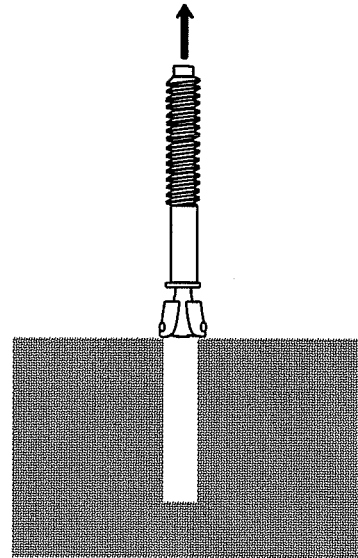
Figure 2.13 Pull-out Failure [Rodriguez 1995]

2.5 DESIGN METHODOLOGY

There are numerous approaches to calculate the concrete capacity of anchorages. Two commonly used design recommendations, the Concrete Capacity Design Method (CC Method) and the ACI 349 design provisions, are summarized below. Information on the approaches not presented here can be found in [Klingner and Mendonca 1982a] and [Klingner and Mendonca 1982b].

2.5.1 ACI 349 Design Provisions for Tensile Loading

The design provisions of [ACI 349 1990] assume a uniform tensile stress of $4 \cdot \sqrt{f_c'}$ over the projected area of the failure cone with a 45-degree inclination. The tensile capacity is predicted by Equation (2-5) which multiplies that tensile stress by the actual projected area of the stress cone. The reduction in capacity due to overlapping cones, edge effects, and member thickness is taken into account by multiplying the ratio of the actual projected area to the projected area of an anchor with no limitations by the

tensile stress, as shown in Equation (2-6). Calculation of the actual projected area when limitations exist is rather complex [Fuchs, Eligehausen, and Breen 1995].

$$N_{no} = 4 \sqrt{f_c'} \, \pi \, h_{ef}^2 \, (1 + \frac{d_u}{h_{ef}}) \qquad \text{(lb)} \qquad \text{(2-5a)}$$

$$N_{no} = 0.96 \sqrt{f_{cc}'} \, h_{ef}^2 \, (1 + \frac{d_u}{h_{ef}}) \qquad \text{(N)} \qquad \text{(2-5b)}$$

$$N_n = \left(\frac{A_N}{A_{No}} \right) N_{no} \qquad \text{(2-6)}$$

N_{no} = nominal tensile breakout capacity

A_N = actual projected area

A_{No} = projected area of a single anchor unlimited by overlapping cones, edge effects, or member thickness

d_u = diameter of anchor head

2.5.2 ACI 349 Design Provisions for Shear Loading

The concrete capacity for anchors loaded in shear is predicted by Equation (2-7) based on a uniform tensile stress acting over the projected area of a semi-cone with a 45-degree angle. When the depth of the member is less than the edge distance, the spacing of two anchors is less than twice the edge distance, or the edge distance perpendicular to the loading direction is less than the edge distance in the loading direction, reductions are taken into account by computing the ratio of the actual projected area to that of an unlimited anchor, as shown in Equation (2-8). Again, the computation of the projected area is quite complex [Fuchs, Eligehausen, and Breen 1995].

$$V_{no} = 4 \sqrt{f_c'} \, \frac{\pi}{2} \, c_1^2 \qquad \text{(lb)} \qquad \text{(2-7a)}$$

$$V_{no} = 0.48 \sqrt{f_{cc}'} \, c_1^2 \qquad \text{(N)} \qquad \text{(2-7b)}$$

$$V_n = \left(\frac{A_V}{A_{Vo}} \right) V_{no} \qquad \text{(2-8)}$$

V_{no} = nominal shear breakout capacity

A_V = actual projected area

A_{Vo} = projected area of a single anchor unlimited by overlapping cones, edge effects, or member thickness

2.5.3 CC Method for Tensile Loading

The CC Method for tensile loading, Equation (2-9), takes into account the concrete tensile stress, the failure area, and the size effect of concrete. This method assumes an inclination of 35-degrees between the failure surface and the concrete surface. Reductions due to overlapping cones, edge effects, and member thickness are based on simple geometric relationships between rectangular prisms [Fuchs, Eligehausen, and Breen 1995].

$$N_{no} = k_{nc} \sqrt{f_c'} \, h_{ef}^{1.5} \qquad \text{(lb)} \qquad \text{(2-9a)}$$

$$N_{no} = k_{nc} \sqrt{f_{cc}'} \, h_{ef}^{1.5} \qquad \text{(N)} \qquad \text{(2-9b)}$$

N_{no} = nominal tensile cone breakout capacity

k_{nc} = multiplicative constant

= 35 for post installed anchors

= 40 for cast-in-place anchors

h_{ef} = effective embedment

2.5.4 CC Method for Shear Loading

The concrete capacity under shear loading is predicted by Equation (2-10). This equation takes into account the concrete tensile stress, the failure area, and the size effect. The angle of inclination between the failure surface and a line through the bolt parallel to the edge is assumed to be 35-degrees. The failure surface is assumed to extend down the side a distance of 1.5 times the edge distance. Reductions for anchor spacing or member thickness are based on simple geometric relationships between rectangular prisms [Fuchs, Eligehausen, and Breen 1995].

$$V_{no} = 13 \, (\ell / d_o)^{0.2} \sqrt{d_o} \sqrt{f_c'} \, c_1^{1.5} \qquad \text{(lb)} \qquad \text{(2-10a)}$$

$$V_{no} = (\ell / d_o)^{0.2} \sqrt{d_o} \sqrt{f_{cc}'} \, c_1^{1.5} \qquad \text{(N)} \qquad \text{(2-10b)}$$

V_{no} = nominal shear breakout capacity

ℓ = activated load-bearing length of fastener

d_o = outside diameter of fastener

c_1 = edge distance in loading direction

2.5.5 Comparison of CC Method and ACI 349

There are three main distinctions between the CC Method and the ACI 349 design provisions. First, the CC Method includes the size effect of concrete. Second, the CC Method assumes the inclination of the failure cone to be 35 degrees, compared to the 45 degrees assumed by ACI 349. Third, the CC Method idealizes the failure surface as a rectangular prism, making capacity reductions easy to compute. ACI 349 uses a conical idealization of the failure surface which is easy to visualize; however, capacity reductions are difficult to compute.

Numerous tests results were compared to the CC Method and ACI 349 by Fuchs, Eligehausen, and Breen. Under tensile loading, the CC Method accurately predicts the failure load in essentially all of the tests, and is conservative for a few tests with deep embedments. ACI 349, however, is conservative for shallow embedments and unconservative for deep embedments. Farrow, Frigui, and Klingner found that for embedments less than 8 inches (200 mm) both methods can be safely used in the design of single tension anchors even though the CC Method fits experimental results more accurately. For embedments larger than 8 inches (200 mm), the CC Method is recommended for design [Farrow, Frigui, and Klingner 1996].

Under shear loading, the CC Method compares well with the test data, while ACI 349 is conservative for small edge distances and unconservative for large edge distances.

The accuracy of the CC Method can be attributed to the fact that the size effect is considered, and that the 35-degree failure cone is closer to measured values [Fuchs, Eligehausen, and Breen 1995].

2.6 SUMMARY OF PREVIOUS RESEARCH

This research reported here is a subset of a five-task research program conducted at The University of Texas at Austin sponsored by the U.S. Nuclear Regulatory Commission (NRC). Task 1 evaluates the response of single anchors under static and dynamic tensile loading. Task 2 examines the behavior of single- and multiple-anchor connections under static and dynamic tension, shear, and oblique loading. Task 3 includes static and dynamic shear tests of single-anchor and multiple-anchor connections in uncracked and cracked concrete. Task 4 investigates full connections subjected to seismic loading. Task 5 is the submission of a final report.

2.6.1 Task 1 Results

The majority of Task 1 testing is reported in [Rodriguez 1995]. The conclusions made by Rodriguez are summarized below. Based on these conclusions, additional tests were conducted and are presented in this thesis.

- Wedge-type expansion anchors have approximately the same capacity under dynamic and static load. This conclusion, however, is deceptive because the reported average is the result of the combination of two distinct failure modes. If failure is by concrete cone breakout, the dynamic capacity exceeds the static capacity. If failure is by pull-through, the dynamic capacity is less than the static capacity. For concrete cone breakout failure, the capacity is evaluated using a multiplicative constant k_{nc} of 35 in the CC Method tensile capacity equation presented in Section 2.4.1.

- Dynamic loading worsens the performance of wedge-type expansion anchors. Under dynamic loading, the coefficient of friction decreases between the cone and the wedge, and between the wedge and the concrete, increasing the tendency for pull-through and pull-out failure.

- At embedments less than that required to produce steel failure, grouted anchors and undercut anchors fail by concrete cone breakout without pull-out. The concrete cone

breakout capacity is evaluated using a multiplicative constant k_{nc} of 40 in the CC Method tensile capacity equation presented in Section 2.4.1.

- Dynamic loading increases the capacity of grouted anchors, undercut anchors, and sleeve anchors. Under dynamic loads, the concrete cone breakout capacity of those anchors is about 30% greater than the capacity under static loads.

- For all anchors tested in Task 1, performance in concrete with limestone aggregate is not much different from performance in concrete with river gravel aggregate. Both aggregates have an identical hardness measured by the LA Abrasion Loss Test, 28%. However, there is reason to believe that aggregate stiffness, not just hardness, may affect the performance of anchors with small bearing areas.

- Heavy reinforcement (#8 bars at 8 inches {200 mm}, 1-1/2 inch {38.1 mm} cover) placed parallel to the surface of the concrete has no appreciable effect on the concrete cone breakout capacity. Had the reinforcement been oriented parallel to the direction of applied load and developed in both the concrete cone and the surrounding concrete, the anchor capacity would probably have increased. In addition, the reinforcement was too shallow compared to the embedment depth. The maximum concrete cone breakout capacity is attained when the crack has propagated toward the surface a distance of approximately 40% of the anchor embedment. Therefore, had the reinforcement been placed with a larger cover, the concrete cone breakout capacity would probably have increased.

2.6.2 Task 2 Results

The following conclusions are the result of static and dynamic eccentric tension tests of double-anchor connections in unreinforced, uncracked concrete, with the anchors spaced at 1.5 and 2.5 times the embedment [Lotze 1996].

- Under dynamic loading, the concrete breakout capacity is approximately 15% to 25% higher than the static capacity. This result agrees well with the results for single-anchor connections.

- The spacing between anchors is based on the size of the failure cone for a single anchor. There is no indication that the spacing should be increased beyond that of two adjacent single cone failures when using multiple-anchor connections.

- There is no indication of an enlarged fracture cone under dynamic loading.

- The load-displacement behavior of connections is independent of loading rate. Larger displacements at failure for dynamic tests are the result of large failure loads and local crushing in the region of the anchor.

The results from the investigation of single anchors under tensile, shear, and oblique loading are summarized below. The embedment depth was adjusted to achieve both concrete and steel failure [Lotze 1996].

- The elliptical interaction equation, $\left(\dfrac{V}{V_u}\right)^\alpha + \left(\dfrac{T}{T_u}\right)^\alpha = 1$ with exponent $\alpha = 1.67$-1.8 for steel failure and $\alpha = 1.6$ for concrete failure, adequately models the results obtained.

- Shear displacement at failure under oblique tension is larger than the shear displacement under direct shear, due to larger spalling in front of the anchor.

- Steel fracture does not necessarily guarantee ductile behavior of the anchorage. Low-strength steel and/or high-strength concrete can result in brittle steel failure. High strength, ductile steel with the sleeve extending through the baseplate, and large edge distances are recommended to ensure ductile failure.

The results from tests conducted on double-anchor connections under shear and bending are summarized below [Lotze 1996].

- There is no redistribution of shear from the tension anchor to the shear anchor in the fracture region.

- Anchors on the compression side take a considerable amount of tension in the failure range. The transferable friction force increases and the shear decreases, leading to a small increase in the failure load. This effect is dependent on the baseplate extension length.

- As the eccentricity of the shear decreases, the ductility of the anchor group decreases. The displacement of the anchor group is controlled by the displacement of the shear anchor.

- Anchor displacement at maximum load is larger in low-strength concrete. Anchor displacement under direct and oblique tension is larger than that under shear.

- When the anchor sleeve is extended through to the top of the baseplate, the maximum load and peak load displacement are increased.

- At average eccentricities of loading, the higher friction coefficient leads to higher failure loads.

CHAPTER THREE

TEST PROGRAM

3.1 INTRODUCTION

This chapter provides information on the tests conducted as part of Task 1 and Task 3 of the U.S. Nuclear Regulatory Commission (NRC)-sponsored research program. This chapter begins with a description of the variables investigated in each Task. The test matrices are discussed, showing the variables investigated in specific series. Design and construction of the specimens are explained. The experimental setup is described and portrayed. Finally, the test procedure is listed.

3.2 SCOPE OF TEST PROGRAM

3.2.1 Scope of Task 1

Based on the results of Task 1 as reported in [Rodriguez 1995], additional testing was conducted to fully understand the behavior of single anchors loaded in tension in cracked and uncracked concrete. In this section, the variables investigated in the extension of Task 1 are discussed.

3.2.1.1 Anchor Type for Task 1

Previous Task 1 testing employed the use of wedge-type expansion anchors (referred to as "Expansion Anchor" and "Expansion Anchor II"), undercut anchors (referred to as "Undercut Anchor 1" and "Undercut Anchor 2"), and heavy-duty sleeve-type single-cone expansion anchors (referred to as "Sleeve Anchor"). The diameters of the anchors tested ranged from 3/8 inch (9.5 mm) to 1 inch (25 mm), with an emphasis on 3/4-inch (19-mm) diameter. Task 1 tests reported in this thesis were conducted with Expansion Anchor II and Undercut Anchor 1, as well as with Cast-in-Place Anchors, all

with 3/4 inch (19 mm) diameters. Figures 2.1 through 2.6 show the details of these anchors. Expansion Anchor II had a 3/4-inch (19-mm) diameter mandrel and shank. Undercut Anchor 1 had a 3/4-inch (19-mm) diameter shank, and a 1.1-inch (28-mm) diameter sleeve and cone. The Cast-in-Place Anchor was a 3/4-inch (19-mm) diameter A325 bolt.

3.2.1.2 Anchor Embedment Depth for Task 1

Ductile failure of anchors under static and dynamic loading is directly related to the behavior of the anchor steel, and is well understood [Rodriguez et al. 1994]. However, the behavior of anchors with shallow embedments under dynamic loading is not well understood. Therefore, as in previous Task 1 tests, the embedment depth was chosen to ensure that failure would be governed by pull-through, pull-out, or concrete cone breakout. To achieve this, anchors were embedded 4 inches (100 mm) into the concrete. Due to the installation technique for Expansion Anchor II, the effective embedment after installation was reduced to 3.44 inches (87.4 mm), for this anchor.

3.2.1.3 Load Type for Task 1

Tests were conducted using two different load types, static and dynamic. In the static case, shown in Figure 3.1, load increases linearly at a rate such that failure occurs within two to four minutes. The dynamic case, shown in Figure 3.2, is a shock load in which the anchor is loaded at a constant rate to failure, with failure occurring between
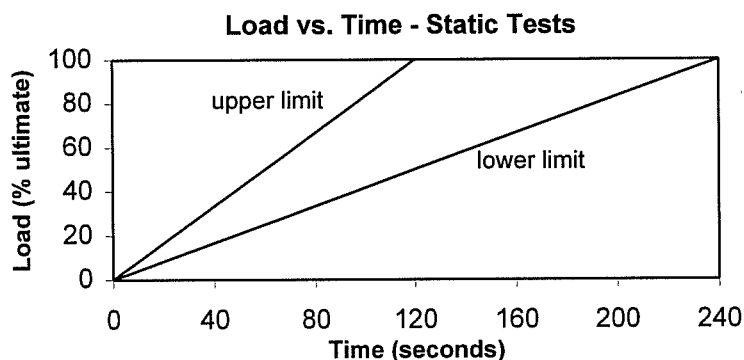
Figure 3.1 Applied Load for Static Tests

0.1 and 0.2 seconds. Dynamic loading represents the time variation of load on an anchor

holding equipment that responds dynamically to a strong earthquake.

Load vs. Time - Dynamic Tests
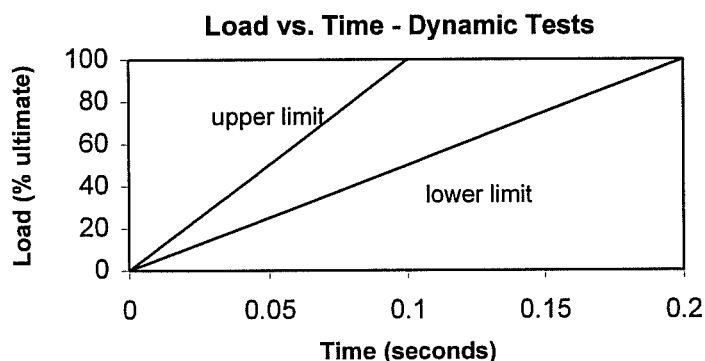
Figure 3.2 Applied Load for Dynamic Tests

3.2.1.4 Concrete Strength for Task 1

All tests were conducted in concrete varying in compressive strength from 4200

psi (29.0 MPa) to 5200 psi (35.9 MPa), which is representative of the concrete strength

in existing nuclear power plants. Tests in lower-strength concrete of 3000 psi (20.7

MPa) are discussed in [Rodriguez 1995].

3.2.1.5 Concrete Aggregate for Task 1

Two types of aggregate, soft limestone and river gravel, were investigated

previously in Task 1. These aggregates have approximately the same hardness (28%) as

measured by the Los Angeles Abrasion Loss Test [ASTM C 1131-81 1987]. No

difference in anchor performance was observed with these two aggregates. In light of

this, tests were conducted in concrete with river gravel aggregate since this aggregate

absorbed less water from the mix design, allowing for better control of the effective

water-cement ratio. To investigate the effect of aggregate hardness on anchor behavior,

some tests were conducted in concrete with granite aggregate, a hard aggregate with a

Los Angeles Abrasion Loss value of 18%.

3.2.1.6 Concrete Condition for Task 1

Since this research is concerned with the seismic behavior of anchors, it was necessary to investigate the change in maximum load-carrying capacity and peak-load displacement of anchors in cracked concrete [Rodriguez et al. 1994]. Previous tests indicate that a reduction in tensile capacity and an increase in peak-load displacement occurs for post-installed anchors located in cracked concrete. However, the anchoring mechanism of cast-in-place anchors is slightly different from that of post-installed anchors. Tests were conducted with cast-in-place anchors to determine if the same reduction in peak load capacity and increase in peak load displacement would occur. Similar tests were conducted by [Eligehausen and Balogh 1995].

3.2.2 Scope of Task 3

The concrete capacity design method (CC Method) describes the behavior of single and multiple shear anchors placed close to a free edge. In Task 3, the shear capacity of near-edge anchors and double-anchor connections is studied and experimental results are compared with those predicted by the CC Method. This section describes the variables investigated in the study.

3.2.2.1 Anchor Type for Task 3

The majority of the tests were conducted using the Cast-in-Place Anchor. A few tests were conducted using Expansion Anchor II and Undercut Anchor 1 in order to determine how anchor type affects behavior. The anchor diameter for all tests was 3/4 inch (19 mm). Figures 2.1, 2.2, and 2,5 show the details of these anchors. Expansion Anchor II had a 3/4-inch (19-mm) diameter mandrel and shank. Undercut Anchor 1 had a 3/4-inch (19-mm) diameter shank, and a 1.1 inch (28-mm) diameter sleeve and cone. The Cast-in-Place Anchor was a 3/4-inch (19-mm) diameter A325 bolt.

3.2.2.2 Anchor Embedment Depth and Edge Distance for Task 3

An embedment depth of 4 inches (100 mm) was selected to ensure brittle concrete cone breakout failure. This is the same embedment depth used for the majority of the Task 1 tests.

Single-anchor connections were tested at an edge distance of 4 inches (100 mm). Double-anchor connections were composed of a front anchor with a 4-inch (100-mm) edge distance, and a back anchor with a 12-inch (300-mm) edge distance. The spacing between the two anchors was 8 inches (200 mm), twice the embedment depth.

3.2.2.3 Number of Anchors for Task 3

Tests were conducted on single anchors to evaluate the accuracy of the CC Method and the effect of transverse reinforcement for anchors located close to a free edge and loaded in shear. In addition, previous Task 2 testing showed the importance of load sharing between the shear-dominated anchor and the tension-dominated anchor of a pair of anchors oriented perpendicular to a free edge and loaded in eccentric shear [Lotze 1996]. In light of this, it was deemed important to investigate the load sharing behavior of a pair of anchors located perpendicular to a free edge and loaded in direct shear.

3.2.2.4 Hairpin Reinforcement for Task 3

It is well understood that anchors located close to a free edge and loaded in direct shear toward that free edge will fail by concrete cone breakout. In some situations placing anchors close to a free edge is unavoidable. Therefore, some tests were conducted with a U-shaped #6 reinforcing bar, referred to as a hairpin, restraining the anchor. The hairpin was placed directly against the anchor in some tests (close hairpin) and at 1-1/4 inches (32 mm) clear from the anchor in other tests (far hairpin). These tests were an effort to extend knowledge about methods for increasing the strength of near-edge shear anchors [Klingner, Mendonca, and Malik 1982].

3.2.2.5 Load Type for Task 3

As in Task 1, tests were conducted under static and dynamic loading. Static loads were applied in a monotonically increasing manner such that failure occurred in two to four minutes, as shown in Figure 3.1. Dynamic loads were also applied in a linearly increasing manner with ultimate failure occurring in 0.1 to 0.2 seconds, as shown in Figure 3.2.

3.2.2.6 Concrete Strength for Task 3

All concrete in Task 3 ranged in compressive strength from 4200 psi (29.0 MPa) to 5200 psi (35.9 MPa). This range was chosen since NRC data indicates that most existing nuclear plants have concrete with compressive strengths of 4000 psi (27.6 MPa) to 5500 psi (37.9 MPa). All concrete was made with river gravel aggregate.

3.2.2.7 Concrete Condition for Task 3

Tests were conducted in uncracked concrete as well as in cracked concrete to examine the effect of a 0.3-mm initial crack width on anchor capacity and peak load displacement. Previous testing indicates that a reduction in tensile capacity and an increase in peak-load displacement occurs for anchors located in cracked concrete.

3.3 TEST MATRIX

3.3.1 Test Matrix for Task 1

The majority of Task 1 testing is reported in [Rodriguez 1995]; however, additional tests were conducted to examine the effect of hard aggregate on anchor behavior, to compare the behavior of cast-in-place anchors to that of post-installed anchors, and to evaluate the effect of anchor type on additional crack opening. This section outlines the test matrix for the additional Task 1 tests.

3.3.1.1 Series 1-9 and 1-10

This series, outlined in Table 3.1, investigated the effect of a hard aggregate on the performance of anchors under tensile loading. Previous tests were conducted with

limestone and river gravel aggregates which both have a Los Angeles Abrasion Loss value of 28%. Granite aggregate has a Los Angeles Abrasion Loss of 18%. For ease in comparison, these tests were conducted using the most common anchor types, anchor diameter, embedment depth, and concrete strength from previous Task 1 tests.

Table 3.1 Test Matrix for Series 1-9 and 1-10

Series Label	Description	Concrete	Anchors Tested (5 Replicates)
1-9	Static tensile test	4700 psi Granite	Expansion Anchor II ¾ in.
	Static tensile test	4700 psi Granite	Undercut Anchor 1 ¾ in.
1-10	Dynamic tensile test	4700 psi Granite	Expansion Anchor II ¾ in.
	Dynamic tensile test	4700 psi Granite	Undercut Anchor 1 ¾ in.

3.3.1.2 Series 1-11 and 1-12

Series 1-11 and 1-12, summarized in Table 3.2, were intended to evaluate the tensile behavior of cast-in-place anchors in uncracked and cracked concrete, and to compare the performance of cast-in-place anchors and post-installed anchors. Tests were conducted using the most common variables: 3/4-inch (19-mm) anchor diameter, 4-inch (100-mm) embedment depth, and 4700-psi (32.4-MPa) concrete.

Table 3.2 Test Matrix for Series 1-11 and 1-12

Series Label	Description	Concrete	Anchors Tested (5 Replicates)
1-11	Static tensile test in uncracked concrete	4700 psi River Gravel	Cast-in-Place Anchor ¾ in.
	Static tensile test in cracked concrete	4700 psi River Gravel	Cast-in-Place Anchor ¾ in.
1-12	Dynamic tensile test in uncracked concrete	4700 psi River Gravel	Cast-in-Place Anchor ¾ in.
	Dynamic tensile test in cracked concrete	4700 psi River Gravel	Cast-in-Place Anchor ¾ in.

3.3.2 Test Matrix for Task 3

Task 3 examined the behavior of single- and double-anchor connections loaded in direct shear under static and dynamic loading in cracked and uncracked concrete. Some tests were conducted with hairpin reinforcement oriented perpendicular to the anchor and located adjacent to or far (1-1/4 inch or 32 mm clear) from the anchor. All tests in this Task were conducted at an embedment depth of 4 inches (100 mm), and an anchor diameter of 3/4 inches (19 mm). Single-anchor tests were conducted at a 4-inch (100-mm) edge distance. Double-anchor tests were composed of a front anchor with a 4-inch (100-mm) edge distance and a back anchor with a 12-inch (300-mm) edge distance. The spacing between the anchors was 8 inches (200 mm), twice the anchor embedment depth.

3.3.2.1 Series 3-1

This series, shown in Table 3.3, investigated the static behavior of single anchors located close to a free edge and loaded in direct shear. All tests in this series were conducted in uncracked concrete. Tests were conducted with a close hairpin, a far hairpin, or no hairpin at all. Cast-in-Place Anchor, Expansion Anchor II, and Undercut Anchor 1 were tested.

Table 3.3 Test Matrix for Series 3-1

Description	Concrete	Anchors Tested (5 Replicates)
Static shear test on single anchors in uncracked concrete without hairpins	4700 psi River Gravel	Cast-in-Place Anchor ¾ in.
Static shear test on single anchors in uncracked concrete with close hairpins	4700 psi River Gravel	Cast-in-Place Anchor ¾ in.
Static shear test on single anchors in uncracked concrete with far hairpins	4700 psi River Gravel	Cast-in-Place Anchor ¾ in.
Static shear test on single anchors in uncracked concrete with far hairpins	4700 psi River Gravel	Expansion Anchor II ¾ in.
Static shear test on single anchors in uncracked concrete with far hairpins	4700 psi River Gravel	Undercut Anchor 1 ¾ in.

3.3.2.2 Series 3-2

This series, summarized in Table 3.4, is similar to Series 3-1 except that all tests were conducted under dynamic loading. This was intended to compare static and dynamic responses.

Table 3.4 Test Matrix for Series 3-2

Description	Concrete	Anchors Tested (5 Replicates)
Dynamic shear test on single anchors in uncracked concrete without hairpins	4700 psi River Gravel	Cast-in-Place Anchor ¾ in.
Dynamic shear test on single anchors in uncracked concrete with close hairpins	4700 psi River Gravel	Cast-in-Place Anchor ¾ in.
Dynamic shear test on single anchors in uncracked concrete with far hairpins	4700 psi River Gravel	Cast-in-Place Anchor ¾ in.
Dynamic shear test on single anchors in uncracked concrete with far hairpins	4700 psi River Gravel	Expansion Anchor II ¾ in.
Dynamic shear test on single anchors in uncracked concrete with far hairpins	4700 psi River Gravel	Undercut Anchor 1 ¾ in.

3.3.2.3 Series 3-3

This series, outlined in Table 3.5, examined the behavior of anchors located close to a free edge and loaded in direct shear under static loading in cracked concrete. Comparison with Series 3-1 will provide an understanding of the effect of cracked concrete on the behavior of shear anchors.

Table 3.5 Test Matrix for Series 3-3

Description	Concrete	Anchors Tested (5 Replicates)
Static shear test on single anchors in cracked concrete without hairpins	4700 psi River Gravel	Cast-in-Place Anchor ¾ in.
Static shear test on single anchors in cracked concrete with close hairpins	4700 psi River Gravel	Cast-in-Place Anchor ¾ in.
Static shear test on single anchors in cracked concrete with far hairpins	4700 psi River Gravel	Cast-in-Place Anchor ¾ in.

3.3.2.4 Series 3-4

The behavior of anchors located in cracked concrete and subjected to dynamic loading is examined in this series, outlined in Table 3.6. Comparison with earlier tests is intended to provide knowledge about the effect of cracked concrete on the behavior of anchors subjected to seismic forces.

Table 3.6 Test Matrix for Series 3-4

Description	Concrete	Anchors Tested (5 Replicates)
Dynamic shear test on single anchors in cracked concrete without hairpins	4700 psi River Gravel	Cast-in-Place Anchor ¾ in.
Dynamic shear test on single anchors in cracked concrete with close hairpins	4700 psi River Gravel	Cast-in-Place Anchor ¾ in.
Dynamic shear test on single anchors in cracked concrete with far hairpins	4700 psi River Gravel	Cast-in-Place Anchor ¾ in.

3.3.2.5 Series 3-5

This series, summarized in Table 3.7, investigated the behavior of pairs of anchors oriented perpendicular to a free edge and loaded in direct shear toward the free edge. Tests were conducted with static loading in uncracked concrete.

Table 3.7 Test Matrix for Series 3-5

Description	Concrete	Anchors Tested (5 Replicates)
Static shear test on two anchors in uncracked concrete without hairpins	4700 psi River Gravel	Cast-in-Place Anchor ¾ in.
Static shear test on two anchors in uncracked concrete with close hairpins	4700 psi River Gravel	Cast-in-Place Anchor ¾ in.

3.3.2.6 Series 3-6

Similar to Series 3-5, pairs of anchors were studied; however, these tests were conducted under dynamic loading, as outlined in Table 3.8.

Table 3.8 Test Matrix for Series 3-6

Description	Concrete	Anchors Tested (5 Replicates)
Dynamic shear test on two anchors in uncracked concrete without hairpins	4700 psi River Gravel	Cast-in-Place Anchor ¾ in.
Dynamic shear test on two anchors in uncracked concrete with close hairpins	4700 psi River Gravel	Cast-in-Place Anchor ¾ in.

3.3.2.7 Series 3-7

This series, shown in Table 3.9, investigated the behavior of pairs of anchors located in cracked concrete subjected to static shear loading.

Table 3.9 Test Matrix for Series 3-7

Description	Concrete	Anchors Tested (5 Replicates)
Static shear test on two anchors in cracked concrete without hairpins	4700 psi River Gravel	Cast-in-Place Anchor ¾ in.
Static shear test on two anchors in cracked concrete with close hairpins	4700 psi River Gravel	Cast-in-Place Anchor ¾ in.

3.3.2.8 Series 3-8

In this series, outlined in Table 3.10, the behavior of pairs of anchors located in cracked concrete and subjected to dynamic loading was studied.

Table 3.10 Test Matrix for Series 3-8

Description	Concrete	Anchors Tested (5 Replicates)
Dynamic shear test on two anchors in cracked concrete without hairpins	4700 psi River Gravel	Cast-in-Place Anchor ¾ in.
Dynamic shear test on two anchors in cracked concrete with close hairpins	4700 psi River Gravel	Cast-in-Place Anchor ¾ in.

3.4 TEST DESIGNATION

Each test received a specific designation. Figure 3.3 explains the meaning behind the test designation 1SCR5701. The first character, 1, represents the series extension (in this case Series 3-1). The second character, S, represents the loading type: S designates static loading, and D designates dynamic loading. The anchor type is indicated by the third character: K represents Expansion Anchor II, M represents Undercut Anchor 1, and C represents Cast-in-Place Anchor. The concrete aggregate is designated by the fourth character: R indicates River Gravel, L indicates Limestone, and G indicates Granite. Concrete strength is indicated by the fifth character: 5 represents 4700-psi concrete. The diameter of the anchor is designated by the next character: 7 represents a 3/4 inch diameter. Finally, the last two characters are an indicator of the test number within the series (in this example, the first test).

SERIES EXTENSION
1 = Series 3-1
2 = Series 3-2
3 = Series 3-3
4 = Series 3-4
5 = Series 3-5
6 = Series 3-6
7 = Series 3-7
8 = Series 3-8

9 = Series 1-9
10 = Series 1-10
11 = Series 1-11
12 = Series 1-12

ANCHOR
C = Cast-in-Place
K = Expansion Anchor II
M = Undercut Anchor 1

CONCRETE STRENGTH
5 = 4700 psi

TEST NUMBER
01 = first test

1SCR5701

LOAD TYPE
S = Static
D = Dynamic

ANCHOR DIAMETER
7= 3/4"

AGGREGATE
R = River Gravel
L = Limestone
G = Granite
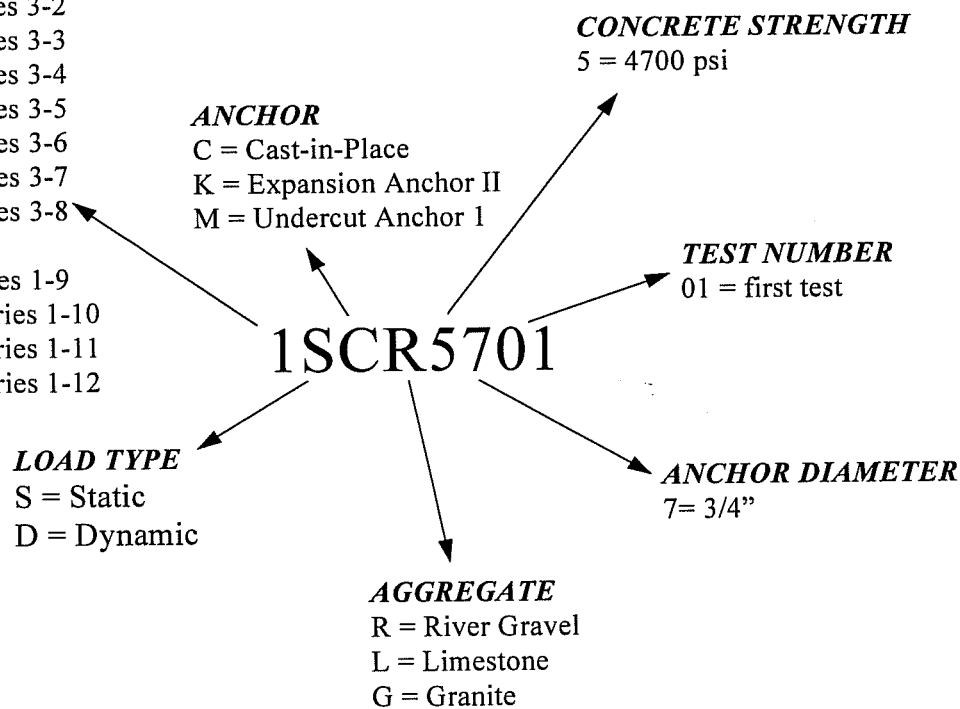
Figure 3.3 Test Designation

3.5 SPECIMEN CONSTRUCTION

3.5.1 Specimen Design

3.5.1.1 Specimen Design for Task 1

Specimens for Task 1 were cast in slabs of dimensions 74 inches x 54 inches x 10 inches (1.88 m x 1.37 m x 2.54 m) reinforced with #4 bars at the top and bottom of the slab with a 1.5 inch (38 mm) cover, as shown in Figure 3.4. The reinforcement was located so as not to interfere with the concrete cone formed at failure. The size of the reinforcement was determined based on the requirement that the steel restrain the splitting forces induced, which can be as large as four times the anchor failure load.
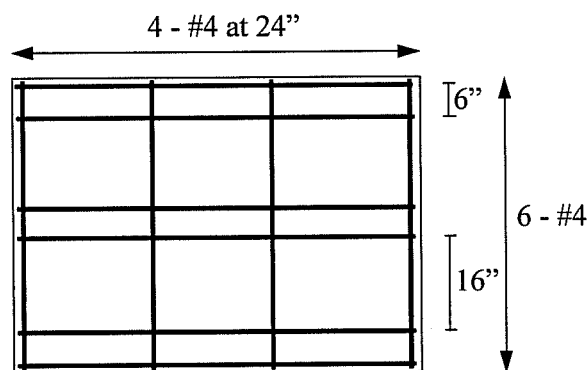
Figure 3.4 Location of Steel Reinforcement for Tension Tests - Plan View

When cast-in-place anchors were used, special wooden frames were constructed to suspend the anchors in the correct position at the correct embedment, as illustrated in Figure 3.5. A bolt was inverted and connected with a nut to the anchor to be cast. The inverted bolt was supported by a 2 x 4 running over the form. The anchor to be cast was painted from 4 inches (100 mm) above the head to the top of the threads, to indicate the portion of the anchor that should extend above the concrete surface. To check that the anchor was located in the proper position, a string was pulled taut across the form.
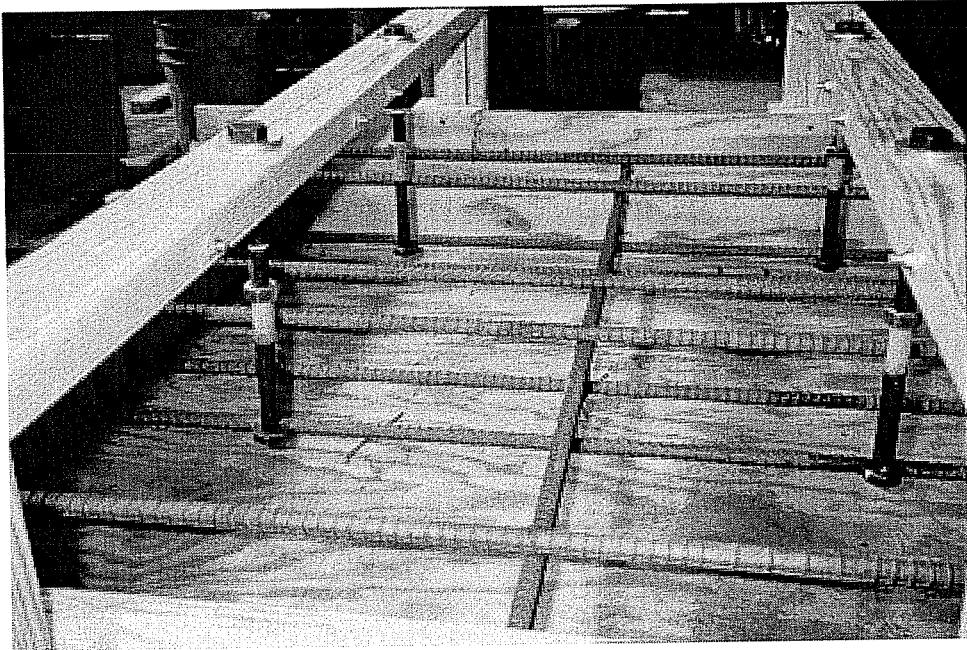
*Figure 3.5 Wooden Frame Work used to Hold Cast-in-Place Anchors
Prior to Casting of Tension Tests*

In previous tests with cracked concrete, a 0.3-mm crack was formed using a split tube and wedge assembly placed in the hardened concrete on both sides of the desired anchor location. The post-installed anchors were then placed in the concrete with the crack running through the middle of the anchor. It is extremely difficult to obtain a perfectly straight crack; for that reason the method needed to be adapted to ensure that the crack would run through the center of cast-in-place anchors. To achieve this, sheet metal was cut as shown in Figure 3.6 and cast in the concrete at specific locations to direct the crack. Care was taken to surround the anchor at least 1 inch (25 mm) in each direction with concrete. Holes were cut in the sheet metal plate to prevent the buildup of uneven pressure from the fluid concrete, which might cause the plate to bulge out of position. The sheet metal was tied to the bar chairs at the bottom of the form and gripped by the 2 x 4 above the form to prevent the plate from displacing during casting. Figure 3.7 shows a form prior to casting tension tests in cracked concrete.
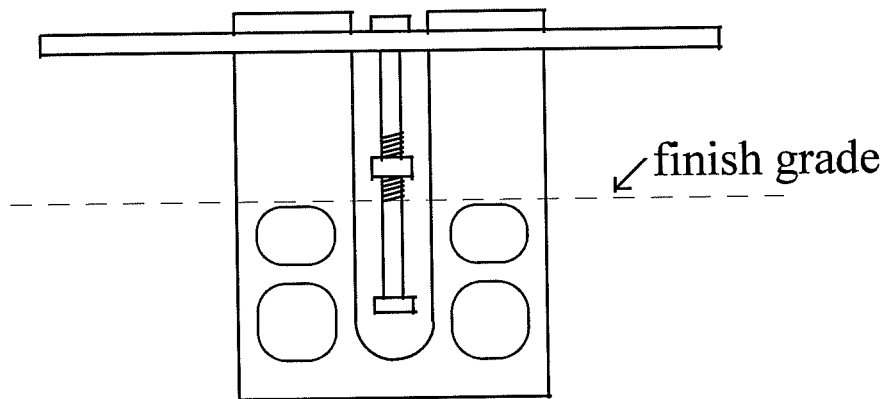
Figure 3.6 Shape of Sheet Metal for Tension Tests
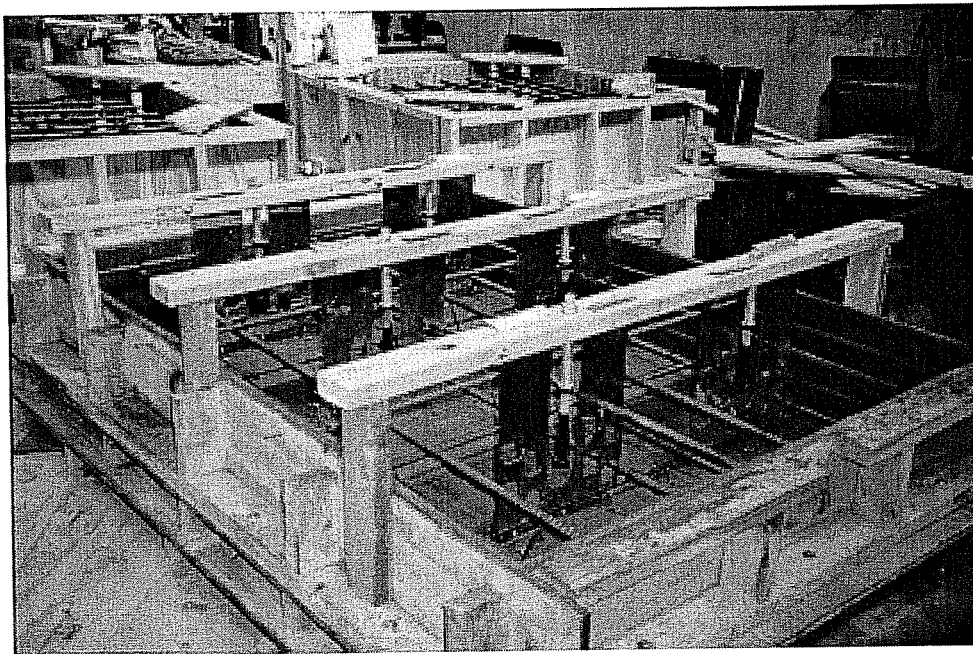
Figure 3.7 Form Prior to Casting Tension Tests of Cast-in-Place Anchors in Cracked Concrete

3.5.1.2 Specimen Design for Task 3

Specimens for Task 3 were cast in blocks of dimensions 87 inches x 30 inches x 14 inches (2.21 m x 0.36 m x 0.76 m) with reinforcement located as shown in Figure 3.8. Number 6 bars were used in the longitudinal direction and number 5 bars were used in the short direction at the top and bottom of the form with a 1-1/2 inch (38 mm) cover. The top reinforcement was located behind the front anchor so that it did not interfere with the concrete breakout cone formed at failure. These specimens are heavily reinforced to resist the splitting forces caused by failure of the anchor, and to resist the forces induced when splitting the concrete for cracked tests.
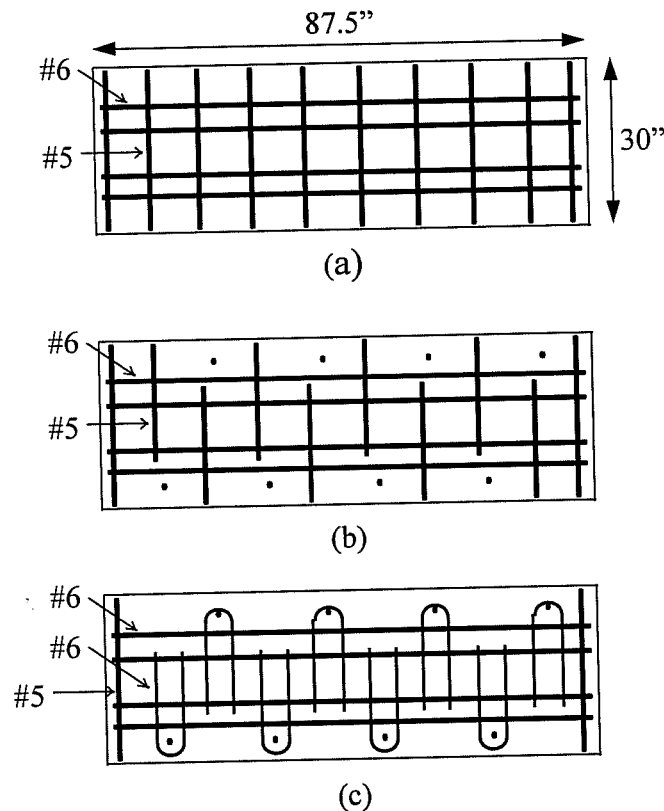
Figure 3.8 Reinforcement for Shear Tests: (a) bottom reinforcement in blocks for shear tests (b) top reinforcement when no hairpins are used (c) top reinforcement when hairpins are used

Cast-in-place anchors were attached to an inverted bolt with a nut, and were suspended from a 2 x 4 running in the short direction over the form. The 2 x 4 was attached to the edge of the form with a threaded rod. The ends of the 2 x 4 were slotted, allowing for adjustment to achieve the proper edge distance. The 4-inch (100 mm) embedment depth was checked as in Task 1, with a string pulled taut across the form. The 2 x 4 was raised and lowered by adjusting nuts on the threaded rods to achieve the proper embedment depth. This setup is shown in Figure 3.9

Since these were near-edge shear tests, no disturbance was allowed between the anchor and the edge of the concrete. This, the splitting tubes for cracked tests could not be located on either side of the anchor. Instead, one splitting tube was placed behind the anchor and one was placed in the side of the form under the anchor to be tested. Since it is difficult to drill a horizontal hole in the side of the specimen, and a vertical hole close to steel reinforcement, PVC pipes were cast in the form to make holes for the splitting tubes. The PVC pipes were split down the middle and held together with rubber bands. The location of the split in the PVC was positioned to match with the split in the tube allowing the PVC to expand with the tube as the wedge is driven into the concrete. Figure 3.10 shows the PVC pipes in the form prior to casting.

The sheet metal plates were redesigned so that they did not extend between the anchor and the edge of the concrete. As in Task 1, holes were cut in the sheet metal to prevent the buildup of uneven pressure and bulging of the sheet metal. The sheet metal was tied taut to nearby reinforcement and chairs, and was gripped at the top by the 2 x 4 and at the bottom by the horizontal PVC pipe to prevent movement during casting. Figures 3.11 and 3.12 show the shape of the sheet metal plates for the single- and double-anchor tests.
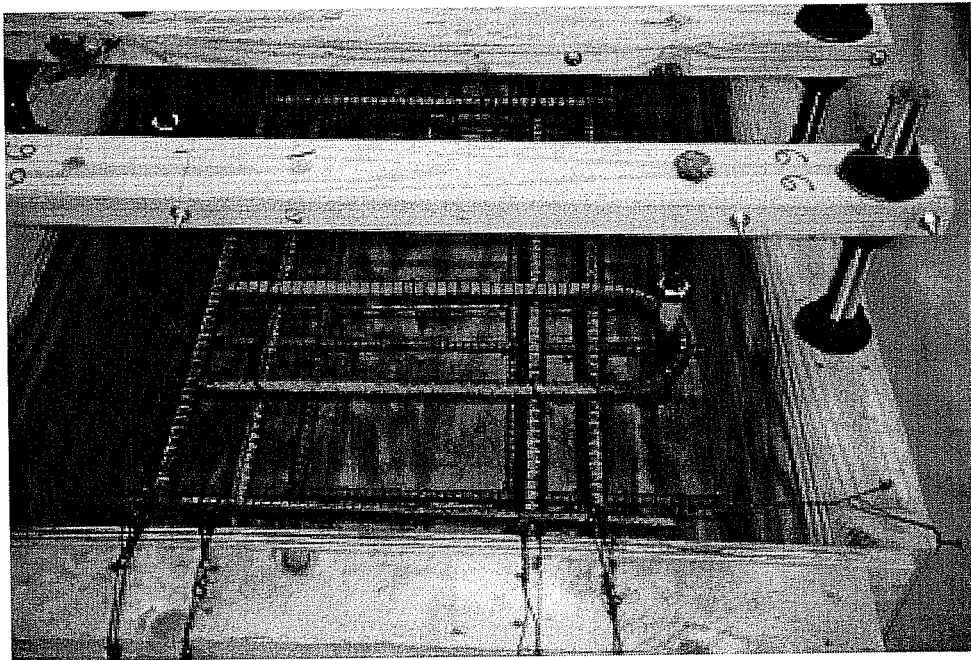
Figure 3.9 Anchors Suspended from 2 x 4 for Shear Tests
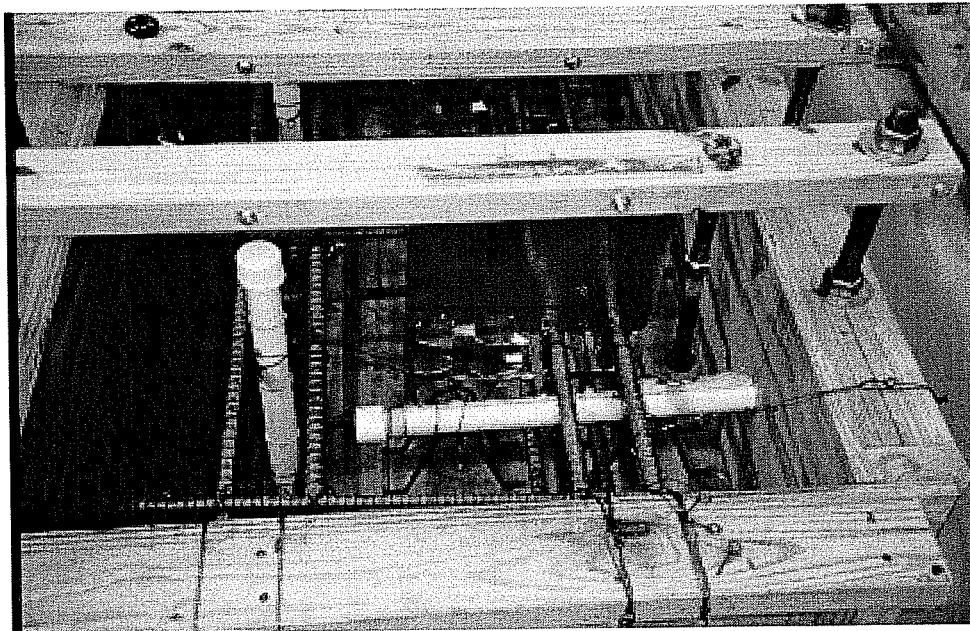
Figure 3.10 Location of PVC Pipes for Shear Tests in Cracked Concrete
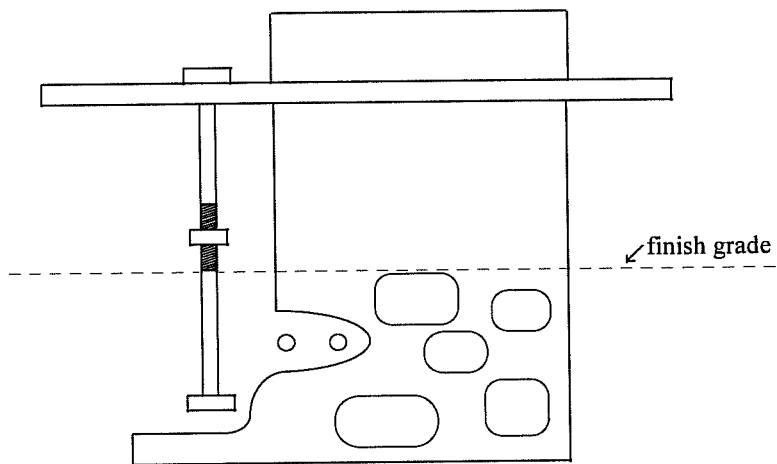
Figure 3.11 Sheet Metal Shape for Single-Anchor Shear Tests
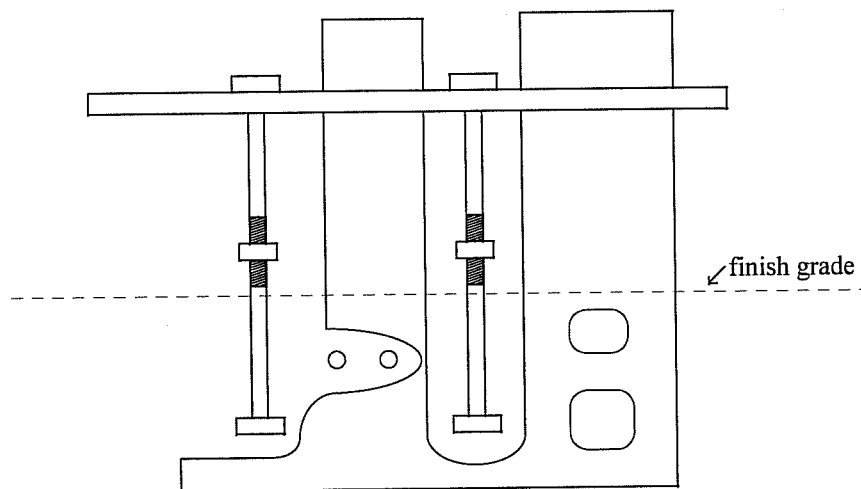
Figure 3.12 Sheet Metal Shape for Double-Anchor Shear Tests

3.5.2 Casting and Curing

Concrete was placed in each form and vibrated using an electric concrete vibrator. Care was taken to place concrete evenly on both sides of the sheet metal plates to prevent bulging. Extra concrete was struck off using a 2 x 4 and the surface was finished.

All specimens and cylinders were covered with heavy-duty plastic and cured in the forms for 7 days, after which the specimens were removed from the wooden forms and kept in the lab until they reached a compressive strength between 4200 psi (29.0 MPa) and 5200 psi (35.9 Mpa). Concrete compressive strengths measured at the time of testing are located in the Appendix.

3.5.3 Concrete Mix Design

The concrete mix was obtained from a single ready-mix plant. The amounts of each component are indicated in the table below. The desired slump was 4 inches (100 mm), although slumps ranging from 3 inches (76 mm) to 5 inches (127 mm) were accepted. Superplasticizer was added to the mix to retard the reaction of the cement keeping the concrete from setting before it was placed in the forms. The coarse aggregate used was river gravel with the exception of the concrete for Series 1-9 and 1-10 in which granite was substituted for river gravel.

Table 3.11 Concrete Mix Design

Cement	Coarse Aggregate	Fine Aggregate	Water	Superplasticizer
(lb/yd^3)	(lb/yd^3)	(lb/yd^3)	(lb/yd^3)	(oz/yd^3)
390	1876	1432	250	48.0

3.6 TEST SETUP

3.6.1 Test Setup for Task 1

3.6.1.1 Crack Initiation for Task 1

For tests conducted in cracked concrete, the first task was to form a 0.3-mm ± 0.02-mm hairline crack in the concrete. Three holes were drilled, one in the center of the slab and one near each of the edges as shown in Figure 3.13. Steel tubes split down the length were placed in the holes with the split placed in the desired location of the crack. Wedges were placed in the split tubes and were hit with a sledge hammer to open the crack the desired amount, as indicated by two DCDT's and two digital displacement gages located on opposite sides of the anchors to be tested. The crack was examined to ensure that it passed through the center of the Cast-in-Place Anchors.

```
   13"        24"          24"        13"

      X           X            X           16"

      ●           ●            ●

      X           X            X           22"

      ●           ●            ●

      X           X            X           16"
```

● = Anchor Location

X = Wedge Location

········ = Crack Location
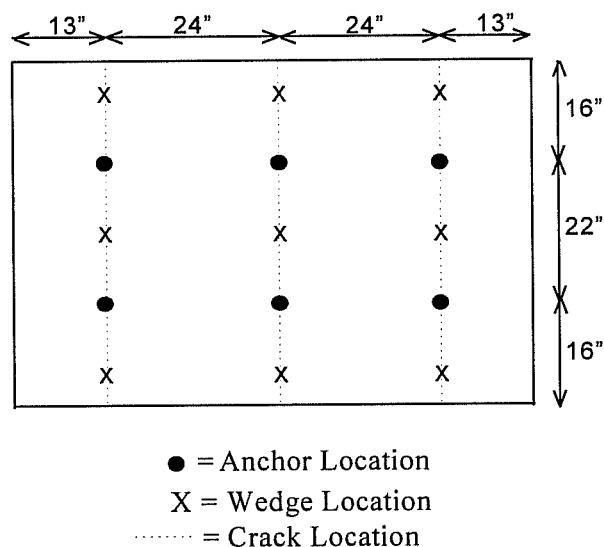
Figure 3.13 Location of Splitting Wedges and Anchors for Tension Tests

3.6.1.2 Anchor Installation for Task 1

For the post-installed anchors, holes were drilled with rotary hammer drill. Expansion Anchor II was lightly tapped with a hammer into the hole to the desired depth, and then torqued to the level specified by the manufacturer. Prior to installation of Undercut Anchor 1, a special tool was attached to the drill to cut the bell-shaped

undercut. The anchor was installed using a special apparatus provided by the manufacturer to expand the anchor into the undercut. This anchor was then torqued as specified by the manufacturer. The Cast-in-Place anchor was installed prior to casting as described in Section 3.5.1.1. Prior to testing the anchor was torqued to a level equal to that of Undercut Anchor 1. After 5 to 10 minutes, the torque of each anchor was released and the anchor was re-torqued to half of the original torque in order to simulate loss of preload due to concrete relaxation over an extended period of time.

3.6.1.3 Loading Equipment for Task 1

A hydraulic ram resting atop a steel reaction ring applied load to the anchor. A 100-kip (450-kN) load cell was placed on top of the ram and was secured in place with a nut to a threaded rod which ran through the load cell, ram, and reaction ring. Connected to the anchor was a threaded baseplate with a thickness equal to the diameter of the anchor. This baseplate was locked in place with a nut and washer, as shown in Figure 3.14. The bottom of the loading shoe was connected to the threaded insert. A 1-1/4 inch (32 mm) threaded rod of high-strength steel ran through the load cell, ram, and reaction ring and connected to the opposite end of the loading shoe, as shown in Figure 3.15. A schematic of the whole test setup is shown in Figure 3.16. As the ram extended, it compressed the load cell between a nut and the ram piston, and the threaded rod moved upward, pulling on the anchor until failure occurred.
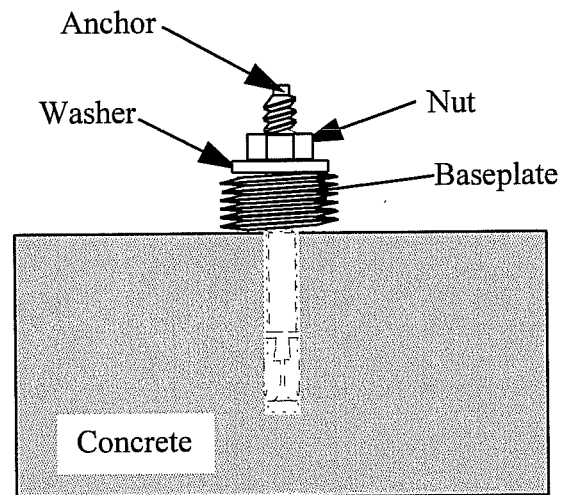
Figure 3.14 Detailed View of Anchor and Baseplate [Rodriguez 1995]
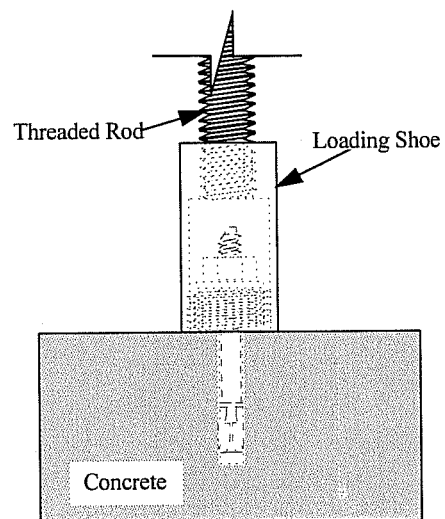
Figure 3.15 Detailed View of Loading Shoe [Rodriguez 1995]
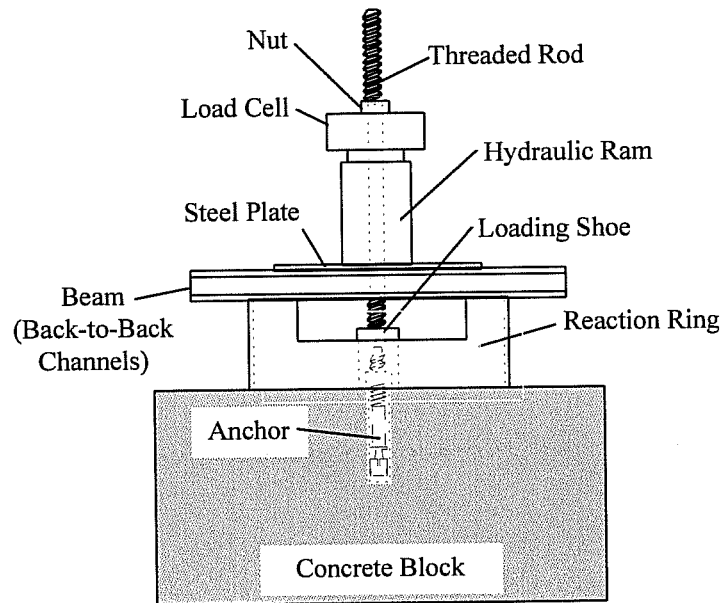
Figure 3.16 Diagram of Test Setup [Rodriguez 1995]

For static tests, a 60-ton (534-kN) centerhole hydraulic ram controlled by an electric pump applied load to the anchor. Dynamic tests were conducted with a 60-ton (534-kN) Enerpac double-action hydraulic centerhole ram. Oil was supplied to the ram through an electric pump, a line tamer, and a servo-valve controlled by an MTS micro-console servo-controller and function generator. Figures 3.17 shows the tensile test setup.
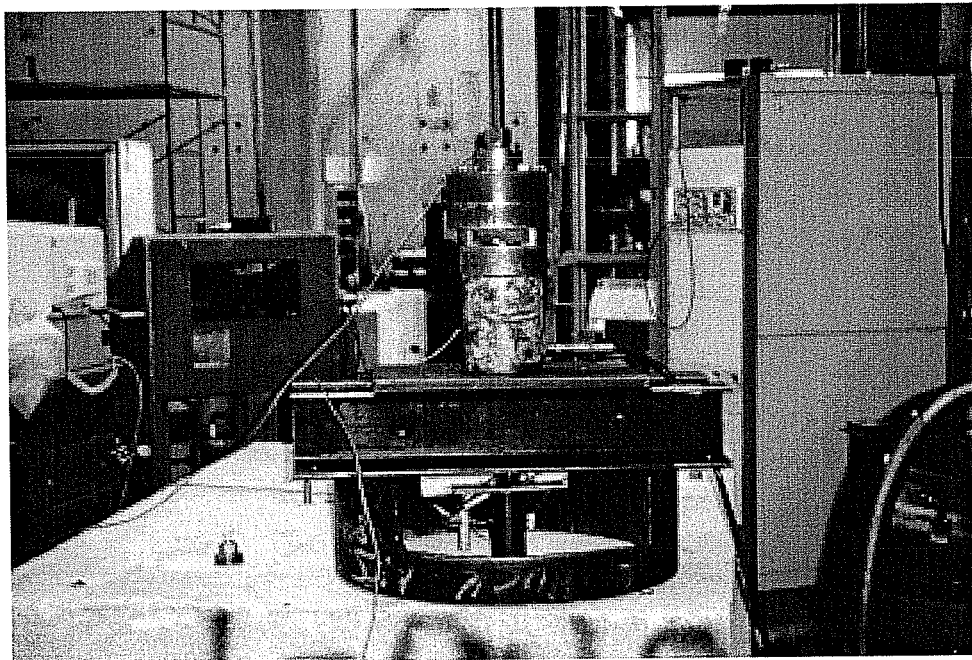
Figure 3.17 Tensile Test Setup

3.6.1.4 Instrumentation for Task 1

Anchor displacement was measured with a linear potentiometer. A metal plate was locked in place with a nut above the loading shoe. Vertical movement of the metal plate was equivalent to the vertical movement of the anchor. The potentiometer was placed against this plate, as shown in Figure 3.18 to measure the movement of the anchor.

Measurement of the crack opening was conducted with two DCDT's one on each side of the anchor, as shown in Figure 3.19. The DCDT's were attached to a steel plate glued to the surface on the concrete and reacted against a steel angle that was also glued to the surface of the concrete on the opposite side of the crack.
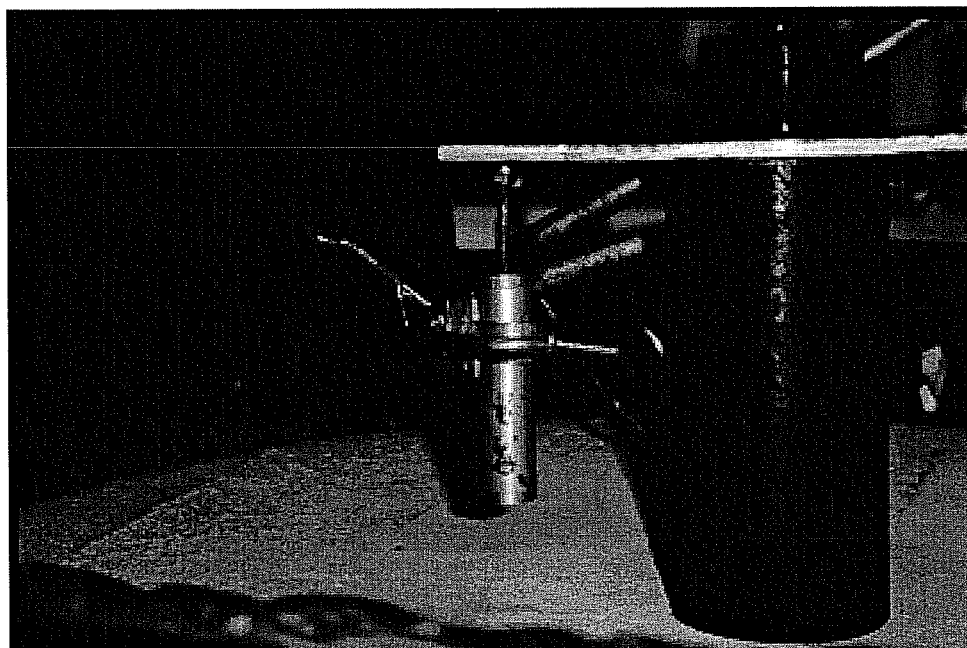
Figure 3.18 View of Linear Potentiometer
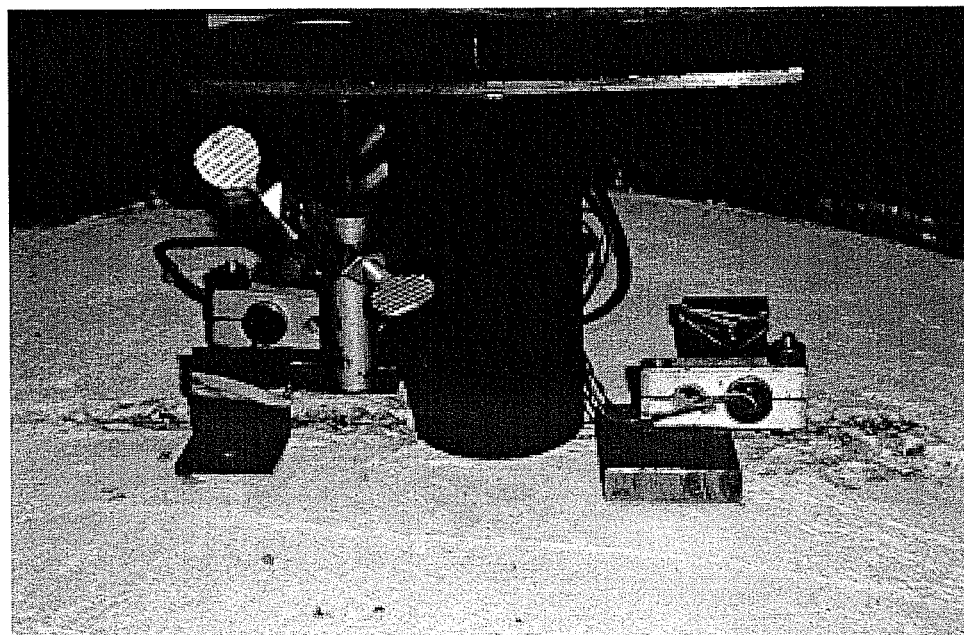
Figure 3.19 View of DCDT's

3.6.1.5 Data Acquisition for Task 1

An amplifier and power supply provided excitation to the load cell. Separate power supplies provided excitation to the linear potentiometer and to the DCDT's. Output signals from the measurement devices were recorded by a Hewlett Packard HP 7090a plotter/data acquisition system. This data was temporarily stored in a buffer until it was downloaded to an IBM-compatible computer and stored in comma-separated value format (CSV). This data was in turn evaluated using a spreadsheet program to convert the voltages to load and displacement values, and to graph the results. Figure 3.20 shows a schematic of this process.
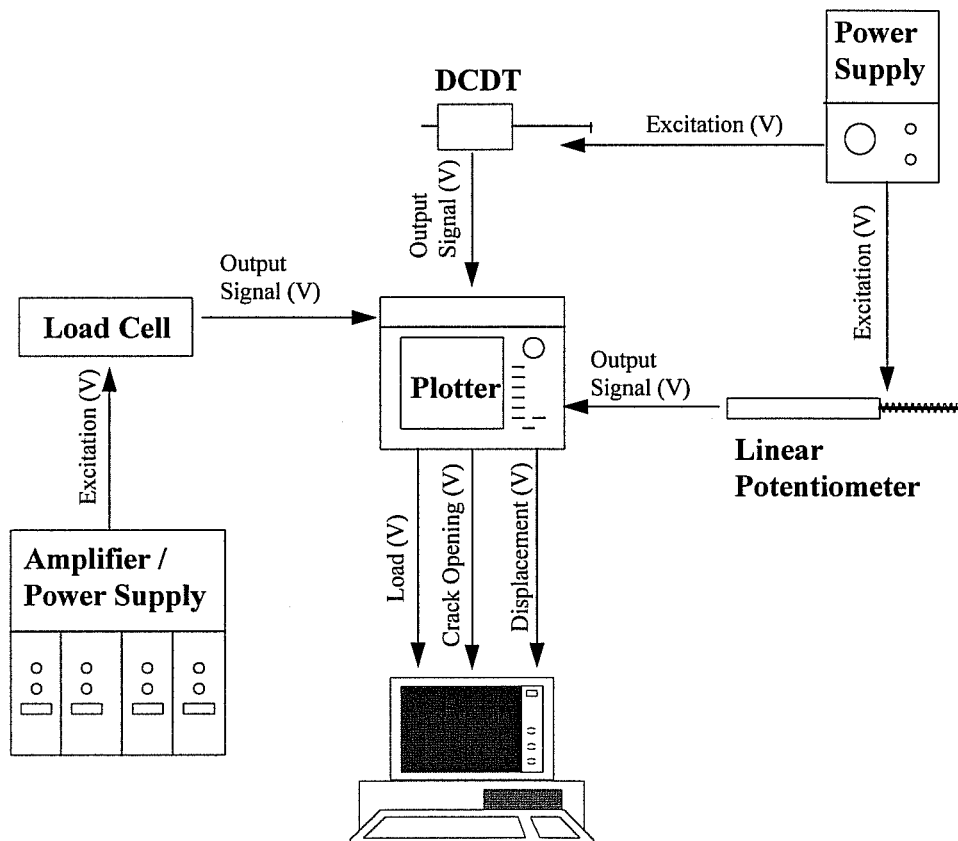
Figure 3.20 Data Acquisition System for Tension Tests

3.6.2 Task 3

3.6.2.1 Crack Initiation for Task 3

The split tubes and wedges were placed in the PVC pipes located on the top and side surfaces of the concrete. The wedges were hit with a sledge hammer to open the crack to a width of 0.3 mm ± 0.02 mm. Small linear potentiometers placed on the top and side surfaces, as shown in Figure 3.21, measured the amount of crack opening. The crack was inspected to ensure that it ran through the anchor.
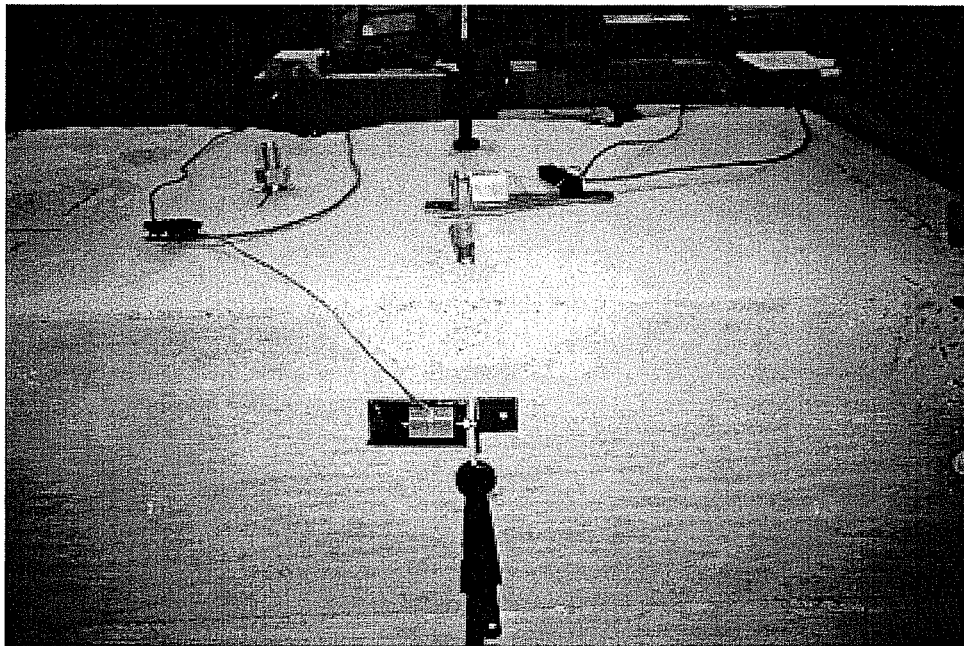
Figure 3.21 Location of Small Potentiometers to Measure Crack Opening

3.6.2.2 Anchor Installation for Task 3

Expansion Anchor II and Undercut Anchor 1 were installed according to manufacturers' instructions. After installation the anchors were torqued to the value specified by the manufacturer. The Cast-in-Place Anchor was torqued to the same value as Undercut Anchor 1. After 5 to 10 minutes, the torque was released and the anchor was re-torqued to half the original torque to simulate the loss of preload that occurs with time.

3.6.2.3 Loading Equipment for Task 3

A reaction frame was constructed of steel I-sections, rectangular tubes, and channels as shown in Figure 3.22. Loading plates for the single- and double-anchor tests shown in Figures 3.23 and 3.24 were placed over the anchors prior to applying torque to the anchor. The loading plates were designed so that the line of action of the applied shear force coincided with the surface of the concrete. Between the loading plate and the concrete surface a 1/32 inch (0.8 mm) Teflon sheet was placed to reduce the friction between the loading plate and the concrete surface. A 1-1/4" (31.8 mm) rod passed through a 100-kip (450-kN) load cell, a centerhole ram, the back-to-back channels of the test frame, and threaded into the loading plate as shown in Figure 3.25.
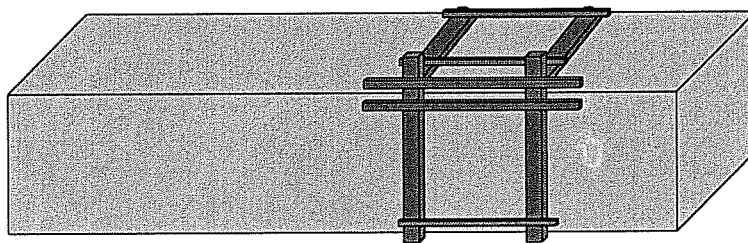
Figure 3.22 Shear Test Frame
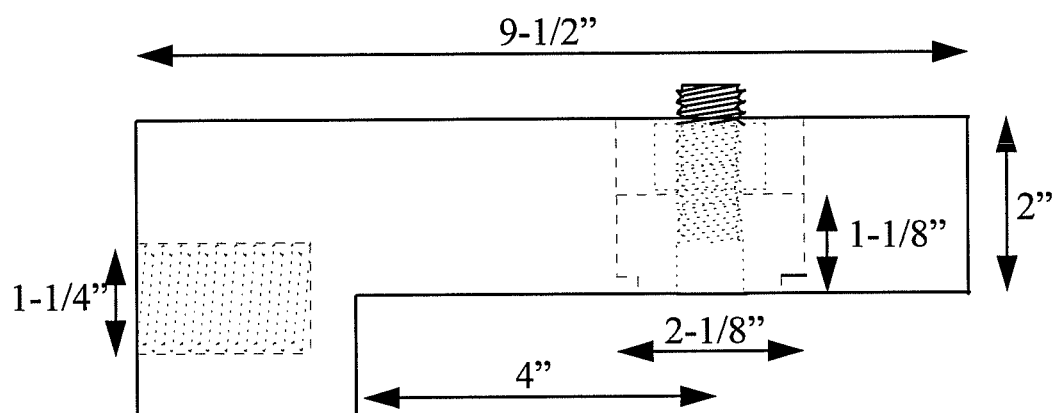
Figure 3.23 Single-Anchor Loading Plate
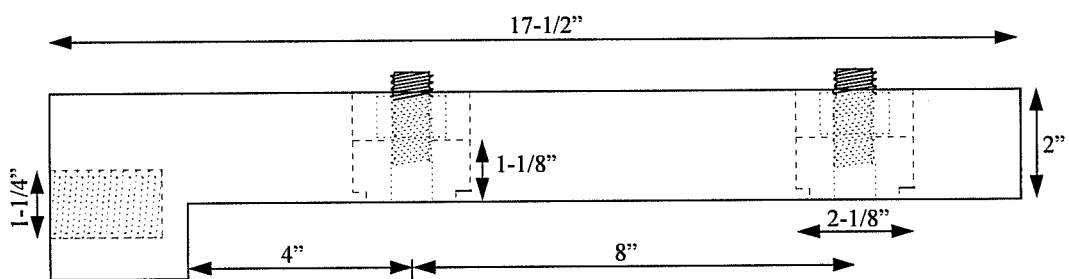
Figure 3.24 Double-Anchor Loading Plate
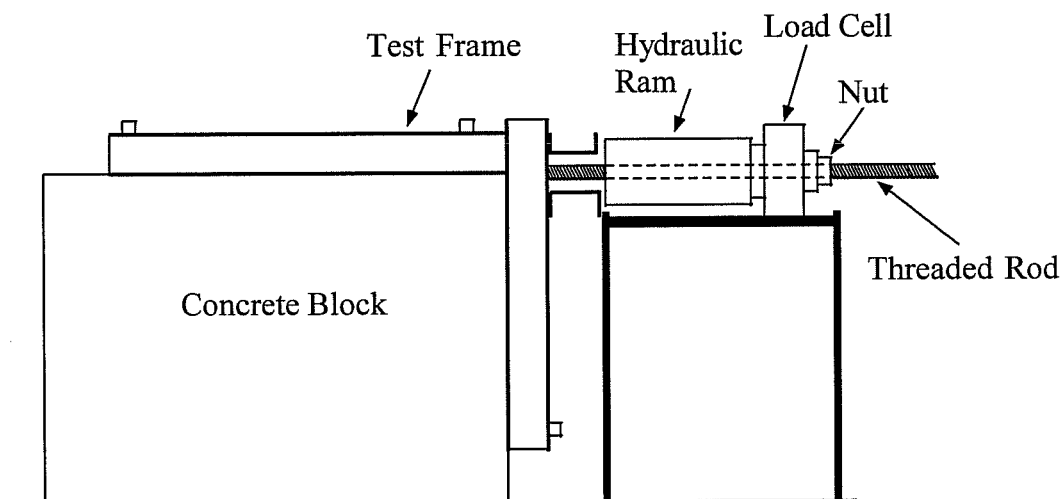
Figure 3.25 Shear Test Setup

For static tests, a 60-ton (534-kN) centerhole hydraulic ram controlled by an electric pump applied load to the anchor. Dynamic single-anchor tests were conducted with a 60-ton (534-kN) Enerpac double-action hydraulic centerhole ram. Double-anchor dynamic tests were conducted with a 100-ton (890-kN) ram. Oil was supplied to the ram through an electric pump, a line tamer, and a servo-valve controlled by an MTS micro-console servo-controller and function generator. Figure 3.26 shows the shear test setup.
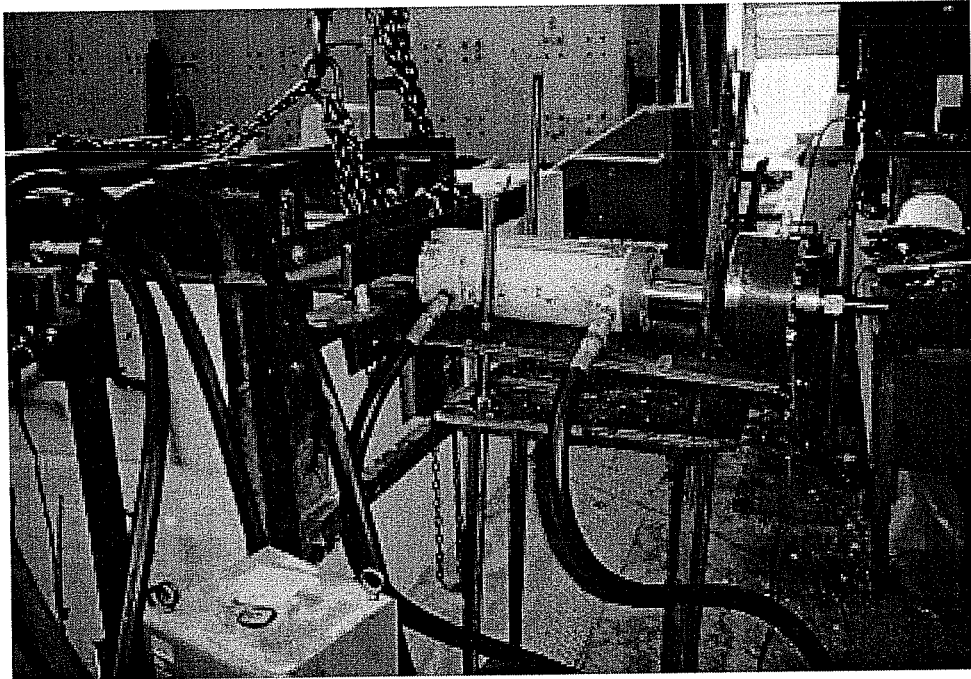
Figure 3.26 Shear Test Setup

3.6.2.4 Instrumentation for Task 3

Anchor displacement was measured with a 2-inch (50-mm) linear potentiometer placed in line with the anchor, against the loading plate, as shown in Figure 3.27. The forward movement of the loading plate was essentially equivalent to the horizontal displacement of the anchor.

The crack opening was measured by 1-inch (25-mm) linear potentiometers placed on the top and side surfaces of the concrete. The linear potentiometers were connected to steel plates which were glued to the concrete, and reacted against steel angles glued to the concrete on the opposite side of the crack.
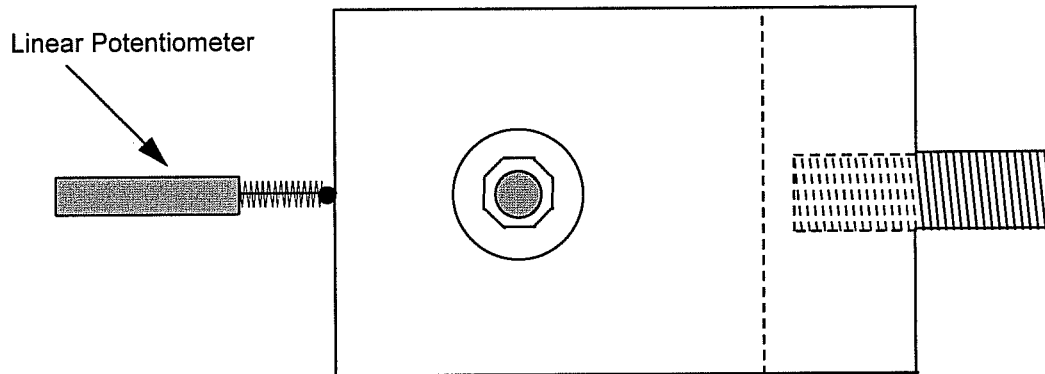
Figure 3.27   Location of Linear Potentiometer for Shear Tests

3.6.2.5   Data Acquisition for Task 3

Excitation was provided to the load cell through an amplifier and a power supply. Another power supply provided excitation to the linear potentiometers. Output signals from the measurement devices were recorded by a Hewlett Packard HP 7090a plotter/data acquisition system. This data was temporarily stored in a buffer until it was downloaded to an IBM-compatible computer and stored in comma-separated value format (CSV). This data was in turn evaluated using a spreadsheet program to convert the voltages to load and displacement values, and to graph the results. Figure 3.28 shows a schematic of this process.
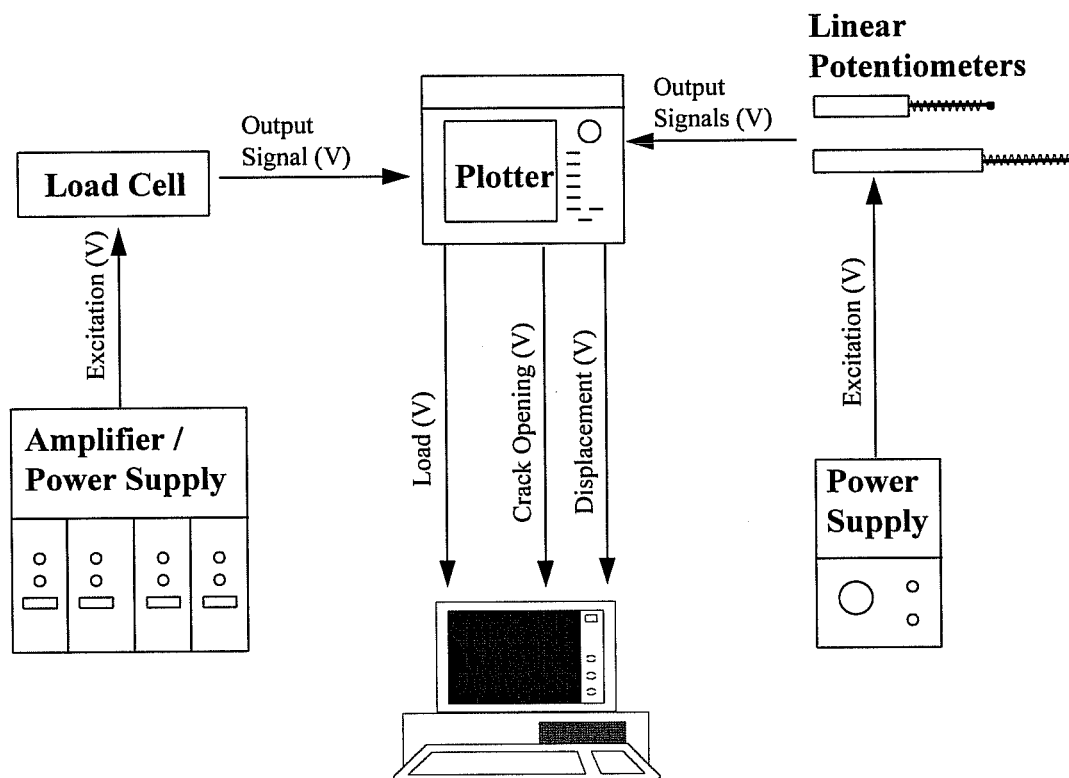
Figure 3.28 Data Acquisition System for Shear Tests

3.7 TEST PROCEDURE

3.7.1 Test Procedure for Task 1

The procedure for Task 1 was as follows:

- For cracked tests, drill holes, insert wedges, set up DCDT's, and form crack;

- Place baseplate over anchor, torque, release and re-torque;

- Place load shoe over baseplate;

- Place reaction ring, ram, and load cell assembly;

- Thread rod into load shoe;

- Set linear potentiometer against plate above load shoe;

- Apply load;

- Transfer data to computer; and

- Analyze data and plot results.

3.7.2 Test Procedure for Task 3

The procedure for Task 3 was as follows:

- For cracked tests, insert wedges, place small linear potentiometers, and form cracks;

- Place Teflon sheet and loading plate over anchor, torque, release, and re-torque;

- Place reaction frame, ram and load cell;

- Thread rod through assembly into the loading plate;

- Set linear potentiometer against loading plate;

- Apply load;

- Transfer data to computer; and

- Analyze data and plot results.

CHAPTER FOUR

TEST RESULTS

4.1 INTRODUCTION

This section presents results from tests conducted as part of Task 1 and Task 3 of the NRC-sponsored research program. For each set of five replicates, the average maximum load and displacement at maximum load are tabulated, along with their coefficients of variation (COV). Since concrete cone breakout failure load depends on the compressive strength of the concrete, all results are normalized by $\sqrt{f_c}$ to 4700-psi (32.4-MPa) concrete, the nominal medium compressive strength used in the test program. Typical load-displacement curves are shown for each set of tests. For tests conducted in cracked concrete the average maximum additional crack opening at concrete failure and the coefficient of variation is noted, and curves of the additional crack opening for increasing load are shown. Detailed load-displacement curves, showing each test conducted in a set of replicates, along with actual concrete compressive strength, the failure loads, displacement at maximum load, and additional crack opening, are located in the Appendix.

4.2 TASK 1 RESULTS

The results from Task 1 testing conducted for this thesis are presented in this section. In Chapter Five, these results are compared with previous Task 1 results presented in [Rodriguez 1995] to assess the effect of aggregate hardness on anchor behavior, to compare the behavior of cast-in-place anchors with post-installed anchors, and to evaluate the effect of anchor type on additional crack opening.

4.2.1 Results of Series 1-9

The purpose of Series 1-9 was to test the most common anchors from previous Task 1 testing under static loading in concrete with granite aggregate to determine the effect of aggregate hardness on anchor behavior. Expansion Anchor II and Undercut Anchor 1 with a 3/4-inch (19-mm) diameter were tested at a 4-inch (100-mm) embedment. Table 4.1 displays the average maximum load and displacement at maximum load for each anchor. Figure 4.1 shows typical load-displacement curves for each anchor.

In one case, the concrete began to fracture, but before the entire concrete breakout cone formed, Expansion Anchor II experienced a pull-through failure. Since this failure occurred at a large displacement after a significant portion of the concrete breakout cone had formed, the load-displacement curve is similar to the cases with concrete cone breakout failures. Undercut Anchor 1 exhibited concrete cone breakout failure for all cases. Figure 4.2 shows a failure cone from an Undercut Anchor 1 test, which is a typical tensile concrete breakout failure cone.

Table 4.1 Average Results for Expansion Anchor II and Undercut Anchor 1 under Static Tensile Loading in Uncracked Concrete with Granite Aggregate

Anchor	Average Maximum Load		COV	Average Displacement at Maximum Load		COV
	kips	(kN)	%	inches	(mm)	%
Expansion Anchor II	15.0	(66.8)	8.5	0.168	(4.27)	26.4
Undercut Anchor 1	26.6	(118)	7.9	0.131	(3.32)	19.8

Typical Load-Displacement Curve - Static Tensile Loading, Uncracked Concrete, Granite Aggregate
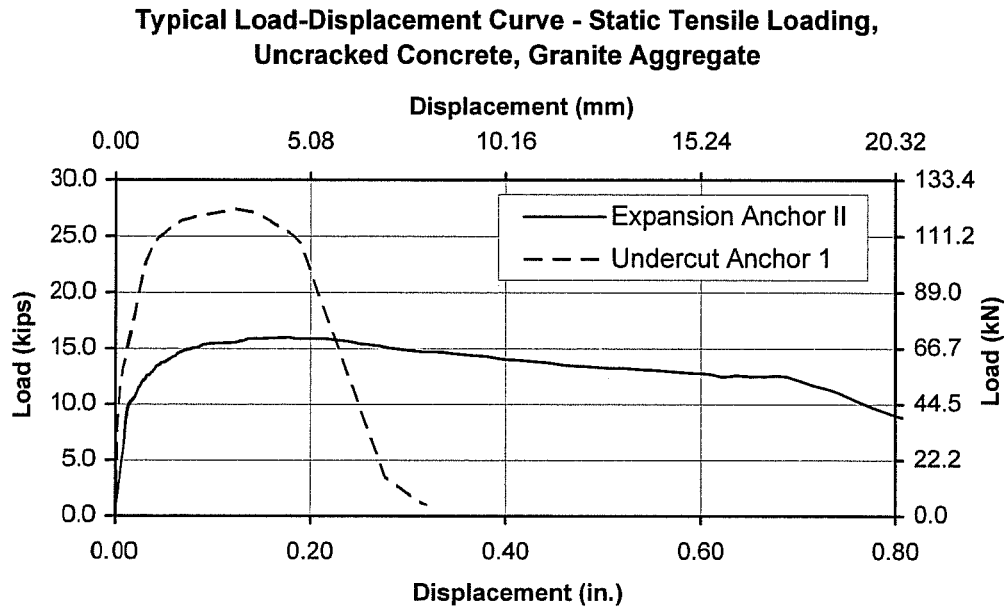
Figure 4.1 Typical Load-Displacement Curve for Expansion Anchor II and Undercut Anchor 1 under Static Tensile Loading in Uncracked Concrete with Granite Aggregate (Tests 9SKG5703 and 9SMG5706)

Figure 4.2 Typical Concrete Breakout Cone for Tension Tests

4.2.2 Results of Series 1-10

Similar to Series 1-9, this series examined the behavior of common anchors from previous Task 1 testing in concrete with granite aggregate to determine the effect of aggregate hardness on anchor behavior. These tests were conducted under dynamic loading. Expansion Anchor II and Undercut Anchor 1 with 3/4-inch (19-mm) diameter were tested at a 4-inch (100-mm) embedment. Table 4.2 displays the average maximum load and displacement at maximum load for each anchor. Figure 4.3 shows typical load-displacement curves for each anchor.

In three tests, Expansion Anchor II experienced a pull-through failure before the full concrete breakout cone had formed. Since the pull-through occurred at large displacements after some fracture of the concrete had occurred, the load-displacement curves for the cases with cone failure and the cases with cone/pull-through failure are similar. Figure 4.4 shows a cone/pull-through failure. All tests with Undercut Anchor 1 exhibited concrete cone breakout failures.

Table 4.2 Average Results for Expansion Anchor II and Undercut Anchor 1 under Dynamic Tensile Loading in Uncracked Concrete with Granite Aggregate

Anchor	Average Maximum Load		COV	Average Displacement at Maximum Load		COV
	kips	(kN)	%	inches	(mm)	%
Expansion Anchor II	17.5	(77.7)	5.1	0.104	(2.63)	33.6
Undercut Anchor 1	28.0	(125)	8.8	0.141	(3.57)	52.8

Typical Load-Displacement Curve - Dynamic Tensile Loading, Uncracked Concrete, Granite Aggregate
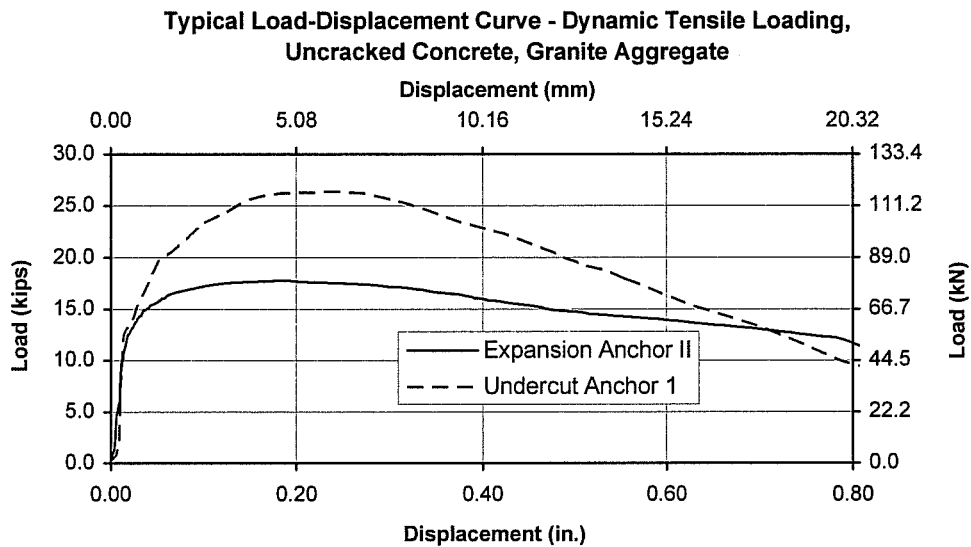
Figure 4.3 Typical Load-Displacement Curve for Expansion Anchor II and Undercut Anchor 1 under Dynamic Tensile Loading in Uncracked Concrete with Granite Aggregate (Tests 10DKG5703 and 10DM5708)
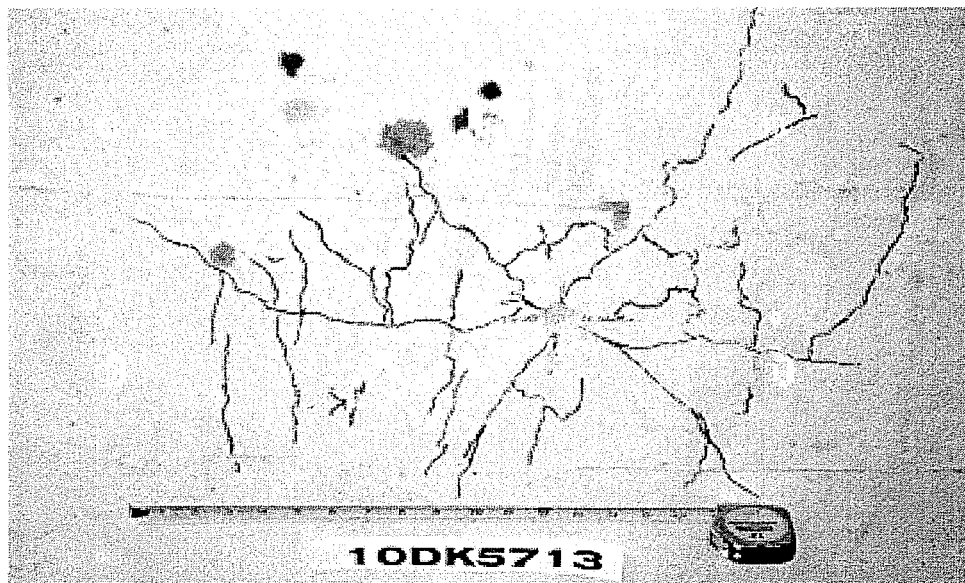
Figure 4.4 Typical Cone Pull-through Failure for Tensile Tests

4.2.3 Results of Series 1-11

Series 1-11 examined the behavior of Cast-in-Place Anchors under static loading in uncracked and cracked concrete. The results from this series are used with previous results from Task 1 to compare the behavior of cast-in-place anchors with post-installed anchors. Cast-in-Place Anchors with a 3/4-inch (19-mm) diameter were tested at an embedment of 4 inches (100 mm). Table 4.3 shows the average results for the tests conducted. Figure 4.5 shows typical load-displacement curves. All anchors had concrete cone breakout failures.

Table 4.3 Average Results for Cast-in-Place Anchor under Static Tensile Loading

Concrete Condition	Average Maximum Load		COV	Average Displacement at Maximum Load		COV
	kips	(kN)	%	inches	(mm)	%
Uncracked	22.8	(102)	4.9	0.047	(1.19)	22.1
Cracked	19.9	(88.3)	4.7	0.051	(1.31)	23.0

Table 4.4 displays the average maximum additional crack opening recorded during the test. The initial crack opening was 0.3 mm. Figure 4.6 shows a curve of the average additional crack opening with increasing load.

Table 4.4 Average Additional Crack Opening for Cast-in-Place Anchor under Static Loading

Average Maximum Additional Crack Opening mm	COV %
0.11	26.8

**Typical Load-Displacement Curve Cast-in-Place Anchor,
Static Tensile Loading, Uncracked and Cracked Concrete**
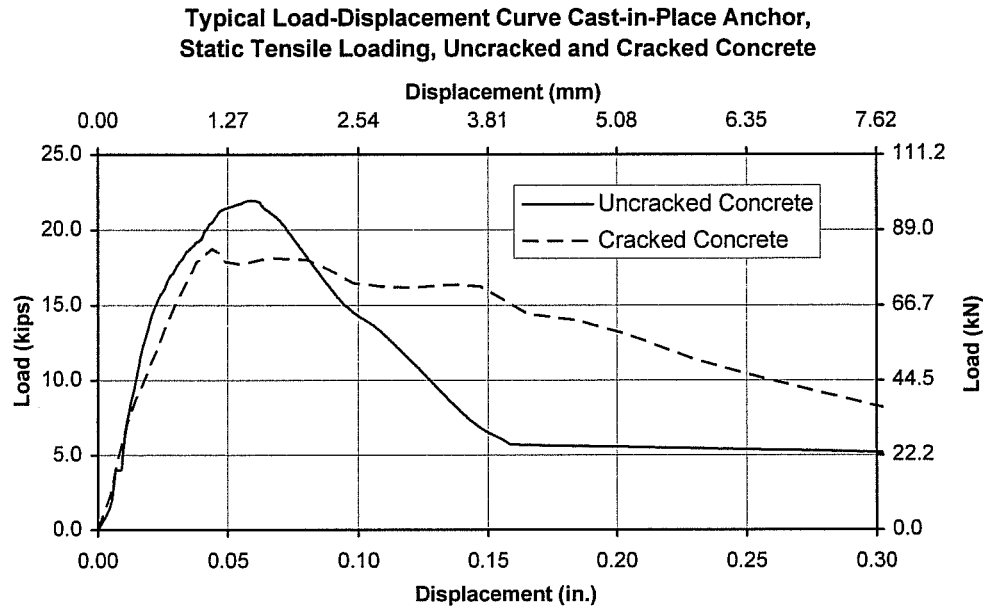
*Figure 4.5 Typical Load-Displacement Curve for Cast-in-Place Anchor under
Static Tensile Loading in Uncracked and Cracked Concrete
(Tests 11SC5705 and 11SC5706)*

**Average Additional Crack Opening vs. Load
Cast-in-Place Anchor, Static Tensile Loading**
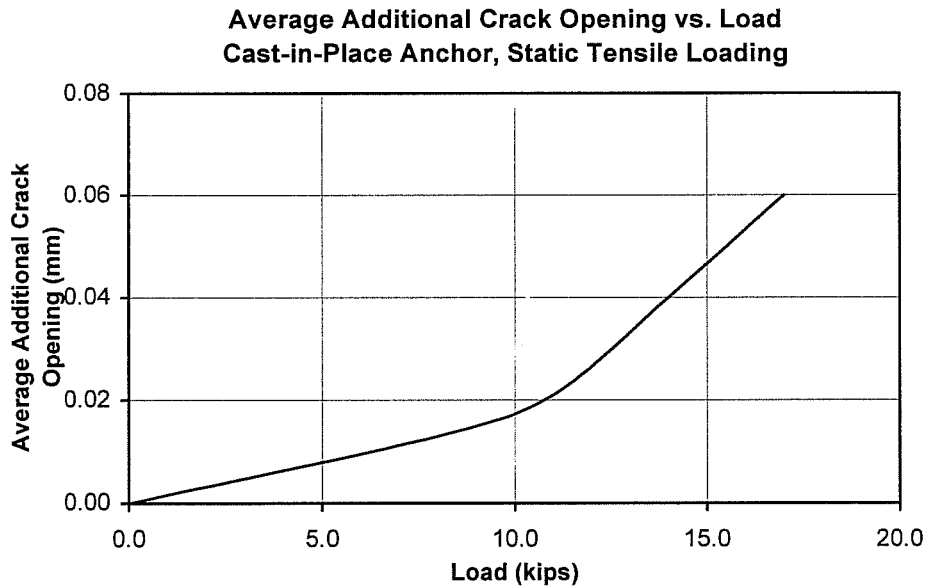
*Figure 4.6 Average Additional Crack Opening vs. Load for Cast-in-Place Anchor
under Static Tensile Loading*

4.2.4 Results of Series 1-12

Series 1-12 is similar to Series 1-11 except that tests were conducted under dynamic loading. These results are combined with previous results from Task 1 to compare the behavior of cast-in-place anchors and post-installed anchors. Table 4.5 displays the average maximum load and displacement at maximum load for the tests conducted in this series. Figure 4.7 shows typical load-displacement curves for the anchors tested in this series. All anchors had concrete cone breakout failures. Figure 4.8 shows a typical concrete breakout failure cone.

In this case, the curve for the anchor in cracked concrete has a maximum load higher than that of the anchor tested in uncracked concrete. This result is due to the fact that under dynamic loading the sheet-metal crack formers, as shown in Chapter Three, Figure 3.6, tore as the anchor failed. The anchor tested in cracked concrete has a higher maximum load due to the load necessary to tear the sheet metal. This increase in load was determined from tensile tests of the sheet metal to be approximately 2.4 kips (11 kN). The average maximum load for anchors in cracked concrete in Table 4.5 was adjusted so that the reported average does not include the additional load.

Table 4.5 Average Results for Cast-in-Place Anchor under Dynamic Tensile Loading

Concrete Condition	Average Maximum Load		COV	Average Displacement at Maximum Load		COV
	kips	(kN)	%	inches	(mm)	%
Uncracked	29.6	(132)	4.7	0.069	(1.75)	14.8
Cracked	28.7	(128)	3.4	0.105	(2.67)	20.7

**Typical Load-Displacement Curve - Cast-in-Place Anchor,
Dynamic Tensile Loading, Uncracked and Cracked Concrete**
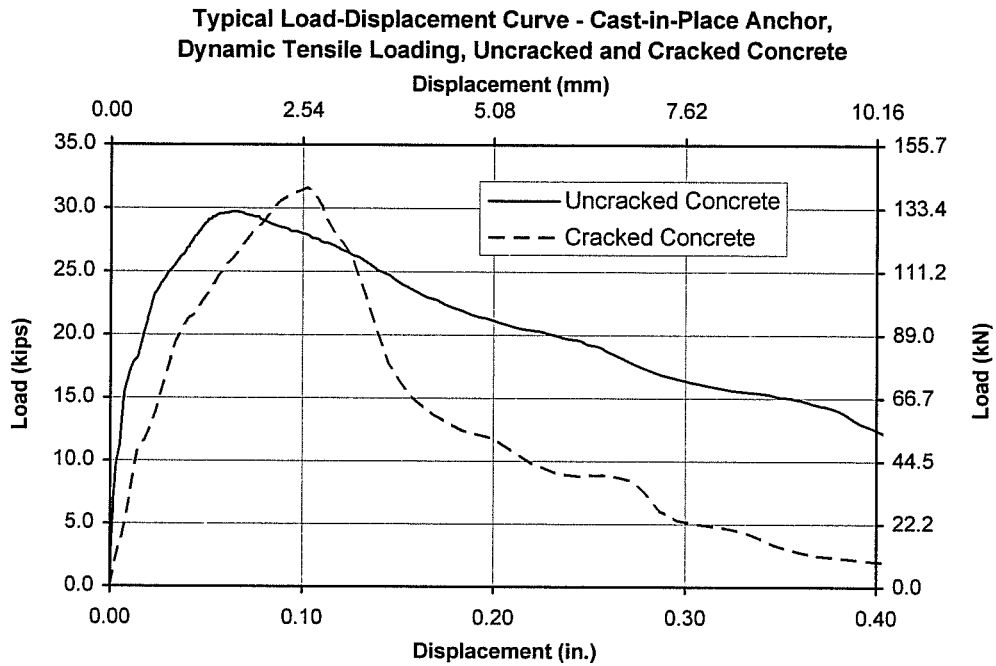
*Figure 4.7 Typical Load-Displacement Curve for Cast-in-Place Anchors under
Dynamic Tensile Loading in Uncracked and Cracked Concrete
(Tests 12DC5705 and 12DC5710)*
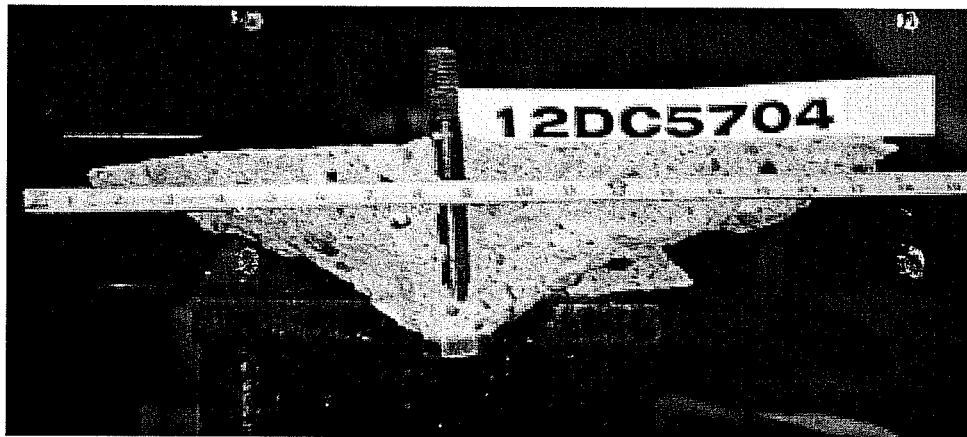
Figure 4.8 Typical Failure Cone for Cast-in-Place Anchors under Tensile Load

Table 4.6 displays the maximum average additional crack opening recorded during the test. Note that the initial crack opening was 0.3 mm. Figure 4.9 shows a curve of the average increase in crack opening with increasing load.

Table 4.6 *Average Additional Crack Opening for Cast-in-Place Anchor under Dynamic Tensile Loading*

Average Maximum Additional Crack Opening mm	COV %
0.13	21.5

Average Additional Crack Opening vs. Load
Cast-in-Place Anchor, Dynamic Tensile Loading
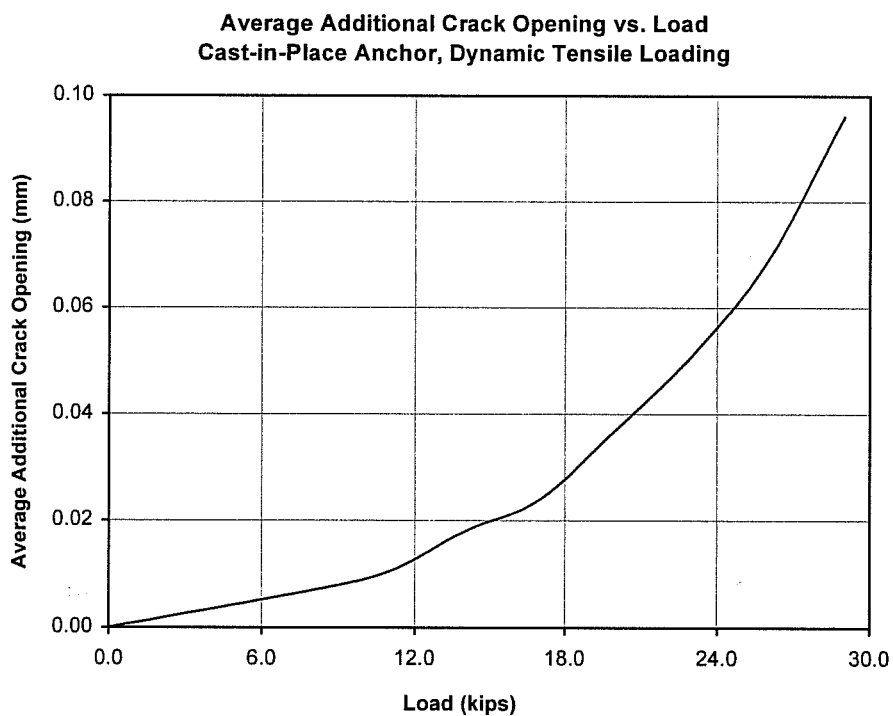
Figure 4.9 *Average Additional Crack Opening vs. Load for Cast-in-Place Anchor under Dynamic Tensile Loading*

4.3 TASK 3 RESULTS

This section describes results obtained from the shear test conducted as part of Task 3 of the research program. These results are intended to provide an understanding of the shear behavior of near-edge anchors, the effect of a hairpin, and the shear behavior of double-anchor connections.

Some tests with hairpins exhibited significant ductility. For consistency, the maximum test displacement was set at 1.2 inches (30.5 mm). For tests which deformed past this limit, the maximum load and corresponding displacement up to 1.2 inches (30.5 mm) was recorded.

4.3.1 Results of Series 3-1

Series 3-1 examined the shear behavior of anchors under static loading in uncracked concrete. Cast-in-Place Anchors were tested with either no hairpin, a close hairpin, or a far hairpin. Expansion Anchor II and Undercut Anchor 1 were tested with a far hairpin. All anchors had a 3/4-inch (19-mm) diameter, and were tested at an edge distance of 4 inches (100 mm) and an embedment of 4 inches (100 mm) in 4700-psi (32.4-MPa) concrete.

For the tests with no hairpin, all failures were by concrete cone breakout. Table 4.7 displays the average results for the five anchors tested. Figure 4.10 shows a typical load-displacement curve. Figure 4.11 portrays a typical failure cone for anchors tested with no hairpin.

Table 4.7 Average Results for Cast-in-Place Single-Anchor Connection under Static Shear Loading in Uncracked Concrete with No Hairpin

	Average Maximum Load		COV	Average Displacement at Maximum Load		COV
	kips	(kN)	%	inches	(mm)	%
Concrete Failure	8.8	(39)	9.6	0.080	(2.03)	80.0
Ultimate Failure	8.8	(39)	9.6	0.080	(2.03)	80.0

Typical Load-Displacement Curve - Cast-in-Place Anchor, Static Shear Loading, Uncracked Concrete, No Hairpin

Figure 4.10 Typical Load Displacement Curve for Cast-in-Place Single-Anchor Connection under Static Shear Loading in Uncracked Concrete with No Hairpin (Test 1SCR5701)

Figure 4.11 Typical Failure Cone for Cast-in-Place Single-Anchor Connection
with No Hairpin Loaded in Shear

With the close hairpin in place, the anchor continued to resist load after concrete cone breakout. The test continued until the anchor either fractured at a large displacement, or deformed to such an extent that its load carrying capacity was reduced. Table 4.8 summarizes the maximum load and displacement at maximum load recorded at concrete failure and at ultimate failure. Figure 4.12 shows a typical load-displacement curve.

Table 4.8 Average Results for Cast-in-Place Single-Anchor Connection under Static
Shear Loading in Uncracked Concrete with Close Hairpin

	Average Maximum Load		COV	Average Displacement at Maximum Load		COV
	kips	(kN)	%	inches	(mm)	%
Concrete Failure	12.6	(55.9)	11.4	0.100	(2.55)	31.0
Ultimate Failure	22.9	(102)	16.1	1.072	(27.2)	19.4

Table 4.9 Average Results for Cast-in-Place Single-Anchor Connection under Static
Shear Loading in Uncracked Concrete with Far Hairpin

	Average Maximum Load		COV	Average Displacement at Maximum Load		COV
	kips	(kN)	%	inches	(mm)	%
Concrete Failure	12.0	(53.4)	7.7	0.104	(2.63)	38.8
Ultimate Failure	17.3	(76.9)	14.3	0.713	(18.1)	53.1

**Typical Load-Displacement Curve - Cast-in-Place Anchor,
Static Shear Loading, Uncracked Concrete, Far Hairpin**

*Figure 4.13 Typical Load-Displacement Curve for Cast-in-Place Single-Anchor
Connection under Static Shear Loading in Uncracked Concrete with Far Hairpin
(Test 1SCR5713)*

The far hairpin allowed Expansion Anchor II to continue to deform after concrete cone breakout occurred. Two of the anchors fractured, and the others deformed with some pull-out until their load-carrying capacity was reduced. Table 4.10 summarizes the maximum load and displacement at maximum load obtained at concrete failure and at ultimate failure. Figure 4.14 shows a typical load-displacement curve.

Table 4.10 Average Results for Expansion Anchor II Single-Anchor Connection under Static Shear Loading in Uncracked Concrete with Far Hairpin

	Average Maximum Load		COV	Average Displacement at Maximum Load		COV
	kips	(kN)	%	inches	(mm)	%
Concrete Failure	7.9	(35)	13.0	0.228	(5.79)	20.5
Ultimate Failure	8.6	(38)	13.3	0.636	(16.2)	24.9

Typical Load-Displacement Curve - Expansion Anchor II, Static Shear Loading, Uncracked Concrete, Far Hairpin

Figure 4.14 Typical Load-Displacement Curve for Expansion Anchor II Single-Anchor Connection under Static Shear Loading in Uncracked Concrete with Far Hairpin (Test 1SKR5718)

Undercut Anchor 1 with a far hairpin also continued to carry load after the concrete cone breakout failure. As the anchor deformed, the concrete between the hairpin and the anchor was crushed. The failure mode was a gradual reduction in capacity at large displacements; none of the anchors fractured. In three of the five cases the concrete cracked as the torque was applied. Once cracking was noticed the torque was stopped. The anchor was then retorqued to half of the torque at which the crack started. Table 4.11 highlights the maximum load and displacement at maximum load recorded at concrete failure and at ultimate failure. Figure 4.15 shows a typical load-displacement curve.

Table 4.11 Average Results for Undercut Anchor 1 Single-Anchor Connection under Static Loading in Uncracked Concrete with Far Hairpin

| | Average Maximum Load | | COV | Average Displacement at Maximum Load | | COV |
	kips	(kN)	%	inches	(mm)	%
Concrete Failure	9.2	(41)	3.0	0.205	(5.20)	13.4
Ultimate Failure	14.8	(65.7)	16.8	0.450	(11.4)	20.0

Figure 4.15 Typical Load-Displacement Curve for Undercut Anchor 1 Single-Anchor Connection under Static Shear Loading in Uncracked Concrete with Far Hairpin (Test 1SMR5725)

4.3.2 Results of Series 3-2

Series 3-2 examined the shear behavior of anchors under dynamic loading in uncracked concrete. Cast-in-Place Anchors were tested with either no hairpin, a close hairpin, or a far hairpin. Expansion Anchor II and Undercut Anchor 1 were tested with a far hairpin. All anchors had a 3/4-inch (19-mm) diameter and were tested at an edge distance of 4 inches (100 mm) and an embedment of 4 inches (100 mm) in 4700-psi (32.4-MPa) concrete.

All of the anchors with no hairpin failed by concrete cone breakout. Table 4.12 displays the average results for these tests. Figure 4.16 shows a typical load-displacement curve.

Table 4.12 Average Results for Cast-in-Place Single-Anchor Connection under Dynamic Shear Loading in Uncracked Concrete with No Hairpin

	Average Maximum Load		COV	Average Displacement at Maximum Load		COV
	kips	(kN)	%	inches	(mm)	%
Concrete Failure	11.2	(49.9)	15.6	0.068	(1.72)	25.3
Ultimate Failure	11.2	(49.9)	15.6	0.068	(1.72)	25.3

**Typical Load-Displacement Curve – Cast-in-Place Anchor,
Dynamic Shear Loading, Uncracked Concrete, No Hairpin**

*Figure 4.16 Typical Load-Displacement Curve for Cast-in-Place Single-Anchor
Connection under Dynamic Shear Loading in Uncracked Concrete with No Hairpin
(Test 2DCR5704)*

Tests conducted with a close hairpin showed significant ductility. After concrete cone breakout, the anchor continued to carry load until it fractured at a large displacement, or deformed until its load-carrying capacity was reduced. Table 4.13 summarizes the maximum load and displacement at concrete cone breakout and at ultimate failure. Figure 4.17 shows a typical load-displacement curve.

*Table 4.13 Average Results for Cast-in-Place Single-Anchor Connection under
Dynamic Shear Loading in Uncracked Concrete with Close Hairpin*

	Average Maximum Load		COV	Average Displacement at Maximum Load		COV
	kips	(kN)	%	inches	(mm)	%
Concrete Failure	15.2	(67.4)	13.5	0.087	(2.21)	67.1
Ultimate Failure	21.4	(95.0)	13.8	0.975	(24.8)	32.4

**Typical Load-Displacement Curve - Cast-in-Place Anchor,
Dynamic Shear Loading, Uncracked Concrete, Close Hairpin**

*Figure 4.17 Typical Load-Displacement Curve for Cast-in-Place Single-Anchor
Connection under Dynamic Shear Loading in Uncracked Concrete with Close Hairpin
(Test 2DCR5706)*

The far hairpin also enhanced the behavior of near-edge Cast-in-Place Anchors. After the concrete cone breakout, the anchor continued to carry load and to displace, crushing the concrete between the anchor and the hairpin. Failure occurred due to a drop in load-carrying capacity at large displacements. Table 4.14 displays the average maximum load and displacement at maximum load. Figure 4.18 shows a typical load-displacement curve.

Table 4.14 Average Results for Cast-in-Place Single-Anchor Connection under Dynamic Shear Loading in Uncracked Concrete with Far Hairpin

	Average Maximum Load		COV	Average Displacement at Maximum Load		COV
	kips	(kN)	%	inches	(mm)	%
Concrete Failure	13.9	(61.8)	26.0	0.113	(2.86)	21.8
Ultimate Failure	18.0	(80.1)	28.4	0.893	(22.7)	32.6

Typical Load-Displacement Curve - Cast-in-Place Anchor, Dynamic Shear Loading, Uncracked Concrete, Far Hairpin

Figure 4.18 Typical Load-Displacement Curve for Cast-in-Place Single-Anchor Connection under Dynamic Shear Loading in Uncracked Concrete with Far Hairpin (Test 2DCR5715)

The far hairpin allowed the Expansion Anchor II to continue to deform after concrete cone breakout; however, little additional load was carried by the anchor. Four of the anchors fractured, and the other anchor failed due to a decrease in load-carrying capacity at large displacements. The anchors fractured just above the collar, below the surface of the concrete and the height of the hairpin. Table 4.15 displays the maximum load and displacement at maximum load for concrete cone breakout and ultimate failure. Note that the maximum load is approximately the same for both cases. Figure 4.19 shows a typical load-displacement curve. Figure 4.20 shows two tested Expansion Anchors, one which fractured and one which did not.

Table 4.15 Average Results for Expansion Anchor II Single-Anchor Connection under Dynamic Shear Loading in Uncracked Concrete with Far Hairpin

| | Average Maximum Load | | COV | Average Displacement at Maximum Load | | COV |
	kips	(kN)	%	inches	(mm)	%
Concrete Failure	9.6	(43)	9.1	0.265	(6.73)	28.0
Ultimate Failure	9.8	(44)	9.6	0.501	(12.7)	70.4

**Typical Load-Displacement Curve - Expansion Anchor II,
Dynamic Shear Loading, Uncracked Concrete, Far Hairpin**
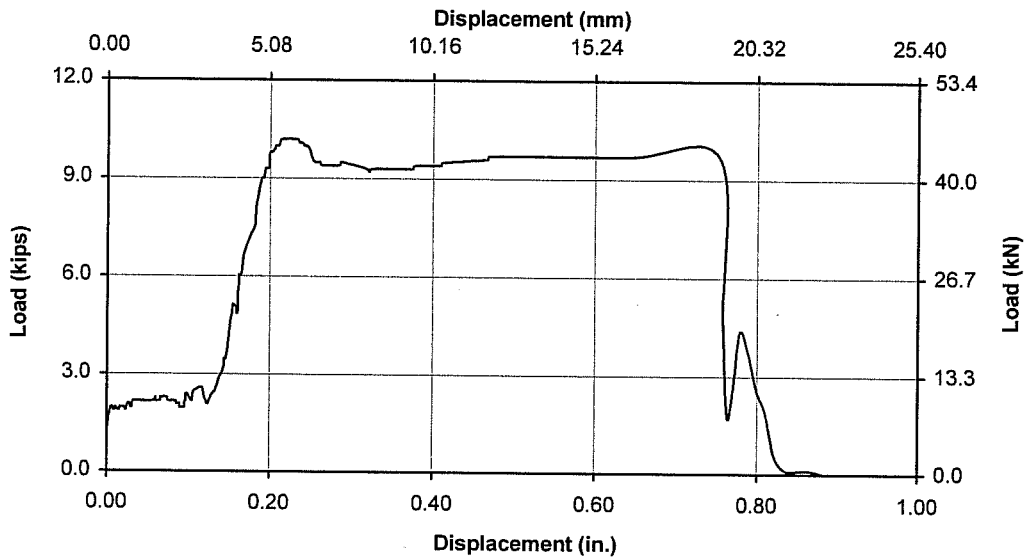
*Figure 4.19 Typical Load-Displacement Curve for Expansion Anchor II Single-Anchor
Connection under Dynamic Shear Loading in Uncracked Concrete with Far Hairpin
(Test 2DKR5718)*

Figure 4.20 Deformation of Expansion Anchor II Loaded in Shear

Undercut Anchor 1 with a far hairpin continued to gain load-carrying capacity and to displace after concrete cone breakout. One of the anchors fractured at a large displacement. The others failed due to a decrease in load-carrying capacity at large displacements. Essentially all of the concrete between the anchor and the hairpin was crushed. Table 4.16 summarizes the results for maximum load and displacement at maximum load. Figure 4.21 shows a typical load-displacement curve. Figure 4.22 shows an anchor after testing; notice the crushed concrete between the anchor and the hairpin.

Table 4.16 Average Results for Undercut Anchor 1 under Dynamic Loading in Uncracked Concrete with Far Hairpin

	Average Maximum Load		COV	Average Displacement at Maximum Load		COV
	kips	(kN)	%	inches	(mm)	%
Concrete Failure	10.3	(45.8)	12.0	0.181	(4.60)	14.7
Ultimate Failure	15.1	(67.0)	7.4	0.481	(12.2)	9.0
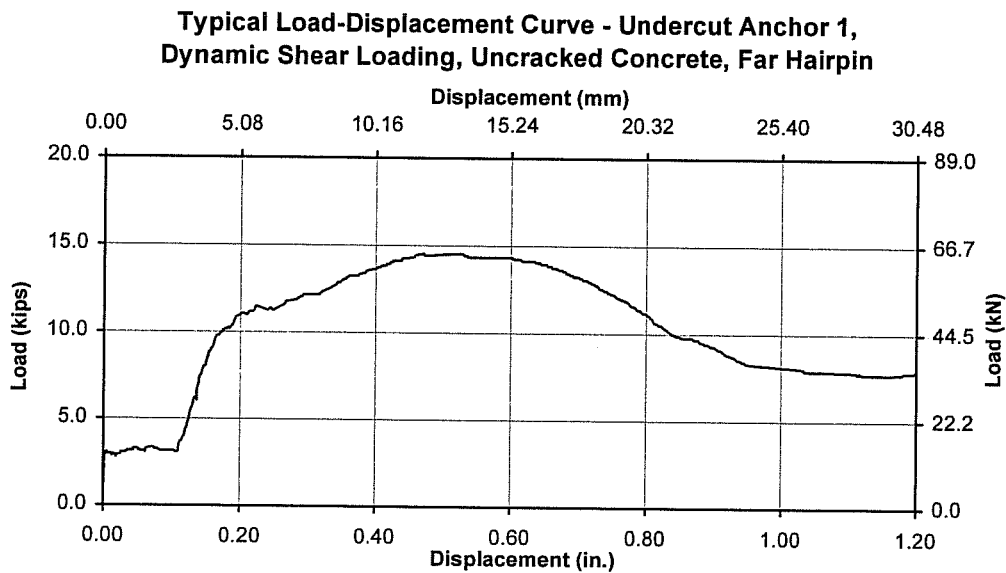
Figure 4.21 *Typical Load-Displacement Curve for Undercut Anchor 1 Single-Anchor Connection under Dynamic Shear Loading in Uncracked Concrete with Far Hairpin (Test 2DMR5723)*
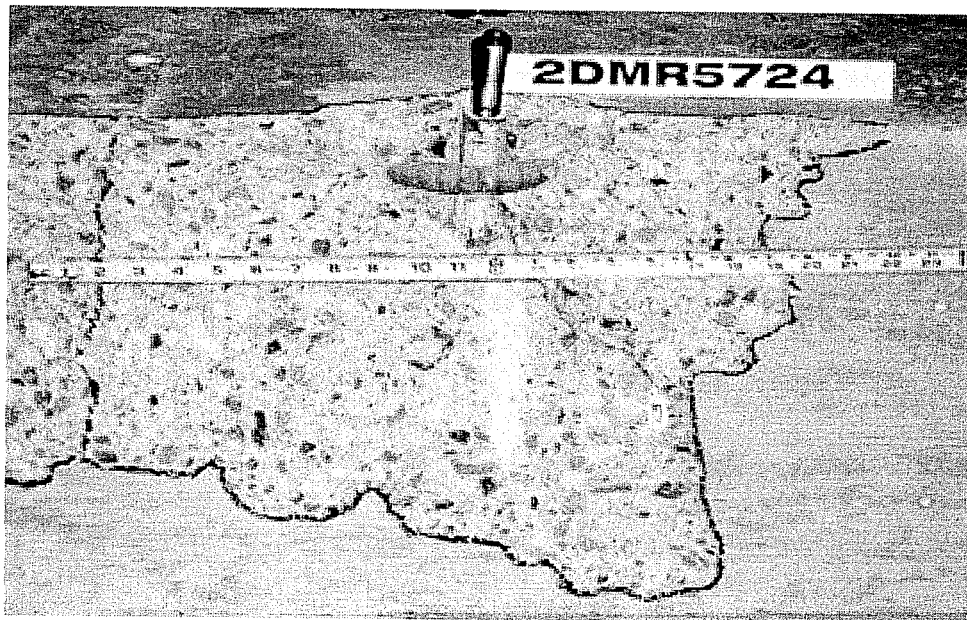
Figure 4.22 *Typical Failure of Undercut Anchor 1 Single-Anchor Connection under Dynamic Shear Loading with a Far Hairpin*

4.3.3 Results of Series 3-3

Series 3-3 investigated the shear behavior of Cast-in-Place Anchors under static loading in concrete with a 0.3-mm initial crack width. Cast-in-Place Anchors with a 3/4-inch (19-mm) diameter were tested at an edge distance of 4 inches (100 mm) and an embedment of 4 inches (100 mm) with either no hairpin, a close hairpin, or a far hairpin, in 4700-psi (32.4-MPa) concrete.

The anchors tested with no hairpin failed by concrete cone breakout. Table 4.17 summarizes the maximum load and displacement at maximum load. Table 4.18 displays the average maximum additional crack opening recorded during the test. Measurements were taken on the side and the top of the specimen. Figure 4.23 shows a typical load-displacement curve.

Table 4.17 Average Results for Cast-in-Place Single-Anchor Connection under Static Shear Loading in Cracked Concrete with No Hairpin

	Average Maximum Load		COV	Average Displacement at Maximum Load		COV
	kips	(kN)	%	inches	(mm)	%
Concrete Failure	7.2	(32)	11.1	0.075	(1.92)	33.9
Ultimate Failure	7.2	(32)	11.1	0.075	(1.92)	33.9

Table 4.18 Average Additional Crack Opening up to Concrete Failure for Cast-in-Place Single-Anchor Connection under Static Shear Loading with No Hairpin

Average Maximum Additional Crack Opening			
Side mm	COV %	Top mm	COV %
0.05	48.3	0.01	70.7

**Typical Load-Displacement Curve - Cast-in-Place Anchor,
Static Shear Loading, Cracked Concrete, No Hairpin**

*Figure 4.23 Typical Load-Displacement Curve for Cast-in-Place Single-Anchor
Connection under Static Shear Loading in Cracked Concrete with No Hairpin
(Test 3SCR5703)*

All of the anchors tested with the close hairpin continued to carry additional load
and to displace after concrete cone breakout. The anchors failed due to a decrease in
load-carrying capacity at large displacements. Table 4.19 highlights the average
maximum load and displacement at maximum load recorded at concrete failure and at
ultimate failure. Table 4.20 displays the maximum additional crack opening recorded up
to concrete failure. Figure 4.24 shows a typical load-displacement curve. Figure 4.25
portrays a typical failure; notice the deformation of the anchor around the hairpin.

Table 4.19 Average Results for Cast-in-Place Single-Anchor Connection under Static Shear Loading in Cracked Concrete with Close Hairpin

	Average Maximum Load		COV %	Average Displacement at Maximum Load		COV %
	kips	(kN)		inches	(mm)	
Concrete Failure	9.6	(43)	11.5	0.063	(1.60)	20.5
Ultimate Failure	22.1	(98.1)	4.4	0.986	(25.0)	19.9

Table 4.20 Average Additional Crack Opening up to Concrete Failure for Cast-in-Place Single-Anchor Connection under Static Shear Loading with Close Hairpin

Average Maximum Additional Crack Opening			
Side mm	COV %	Top mm	COV %
0.09	71.0	0.03	69.9

Typical Load-Displacement Curve - Cast-in-Place Anchor, Static Shear Loading, Cracked Concrete, Close Hairpin

Figure 4.24 Typical Load-Displacement Curve for Cast-in-Place Single-Anchor Connection under Static Shear Loading in Cracked Concrete with Close Hairpin (Test 3SCR5708)
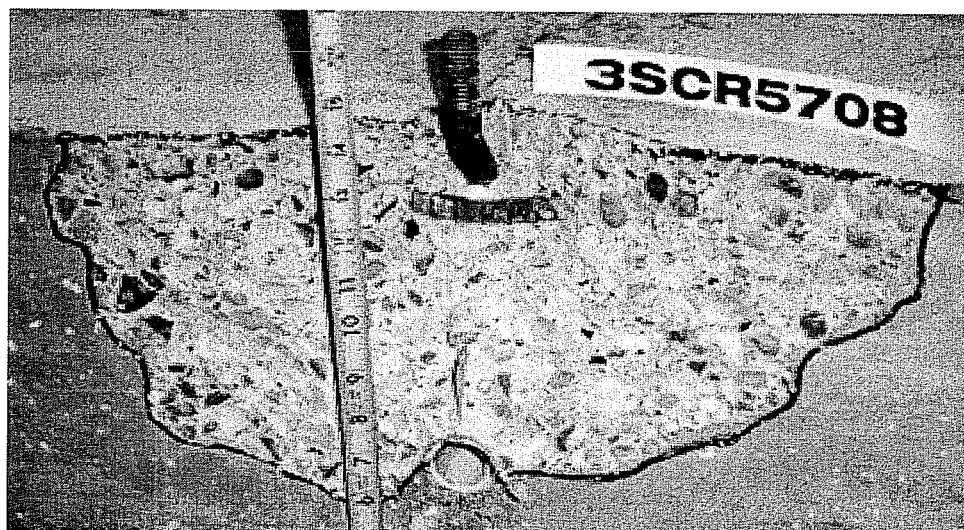
Figure 4.25 Typical Failure Cone for Cast-in-Place Single-Anchor Connection with Close Hairpin Loaded in Shear

Anchors tested with the far hairpin also exhibited enhanced performance. Failure was due to a drop in load-carrying capacity at large displacements. Table 4.21 displays the average results for maximum load and displacement at maximum load. Table 4.22 displays the average maximum additional crack opening up to concrete failure. Figure 4.26 shows a typical load-displacement curve.

Table 4.21 Average Results for Cast-in-Place Single-Anchor Connection under Static Shear Loading in Cracked Concrete with Far Hairpin

	Average Maximum Load		COV	Average Displacement at Maximum Load		COV
	kips	(kN)	%	inches	(mm)	%
Concrete Failure	10.8	(47.9)	15.8	0.145	(3.69)	47.7
Ultimate Failure	16.1	(71.8)	9.7	0.897	(22.8)	22.0

Table 4.22 Average Additional Crack Opening up to Concrete Failure for Cast-in-Place Single-Anchor Connection under Static Shear Loading with Far Hairpin

Average Maximum Additional Crack Opening			
Side mm	COV %	Top mm	COV %
0.13	60.3	0.02	24.9

Typical Load-Displacement Curve - Cast-in-Place Anchor, Static Shear Loading, Cracked Concrete, Far Hairpin
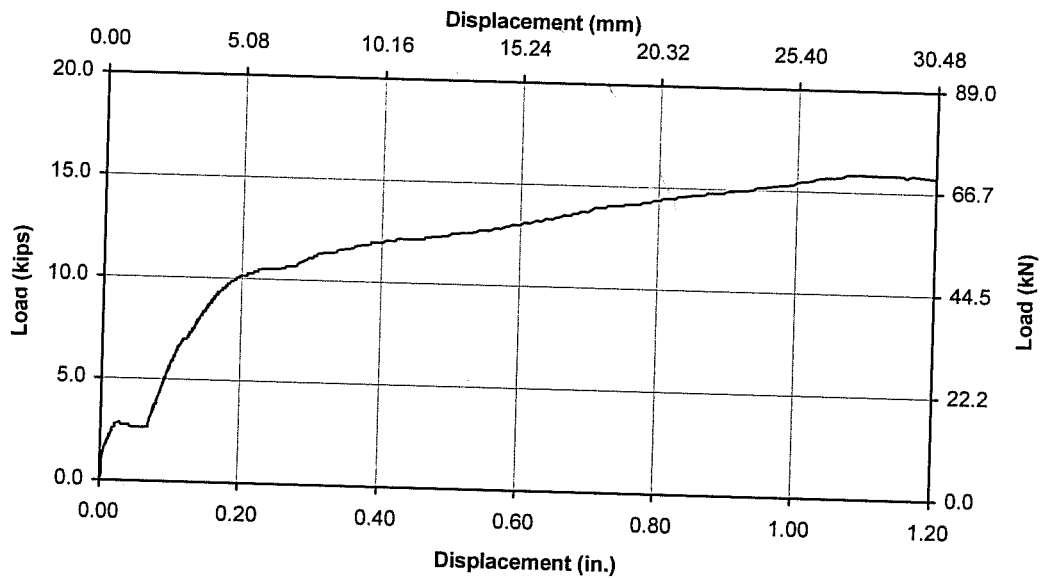
Figure 4.26 Typical Load-Displacement Curve for Cast-in-Place Single-Anchor Connection under Static Shear Loading in Cracked Concrete with Far Hairpin (Test 3SCR5712)

Figure 4.27 shows the average additional side crack opening with increasing load for each of the three cases examined. The top crack that was measured behind the anchor did not open significantly and therefore is not included in the curve.

Average Additional Crack Opening vs. Load
Single-Anchor Connection, Static Shear Loading
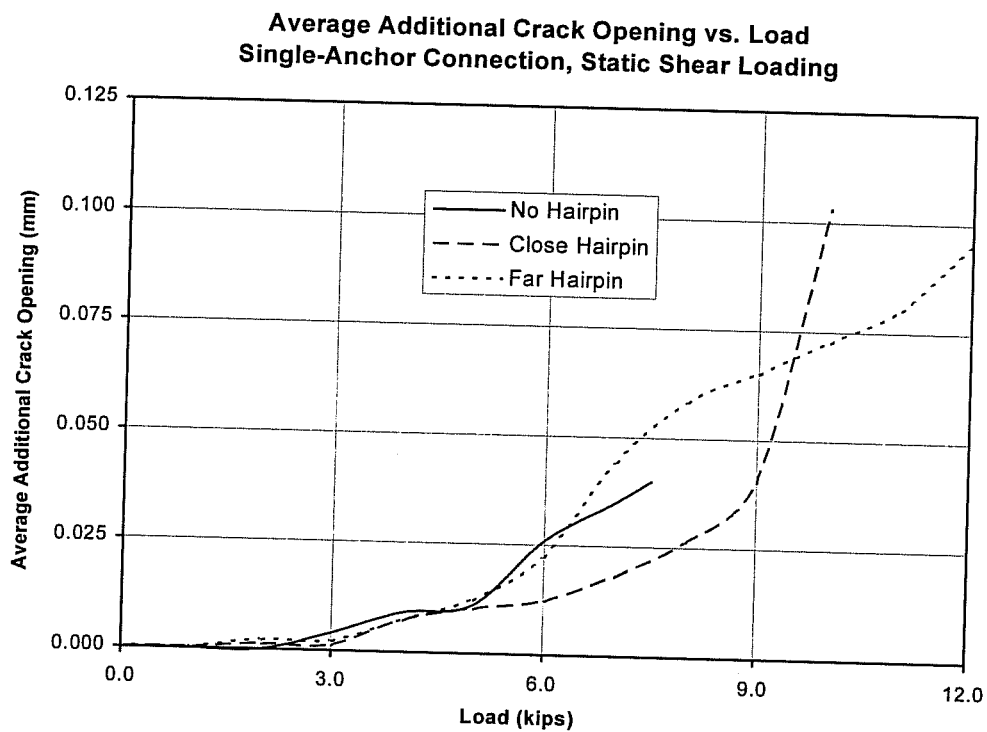
Figure 4.27 Average Additional Side Crack Opening vs. Load for Cast-in-Place Single-Anchor Connection under Static Shear Loading

4.3.4 Results of Series 3-4

Series 3-4 examined the shear behavior of Cast-in-Place Anchors under dynamic loading in concrete with a 0.3-mm initial crack width. Cast-in-Place Anchors with a 3/4-inch (19-mm) diameter were tested at a 4-inch (100-mm) edge distance and a 4-inch (100-mm) embedment with either no hairpin, a close hairpin, or a far hairpin in 4700-psi (32.4-MPa) concrete.

All tests with no hairpin exhibited concrete cone breakout failure. Table 4.23 highlights the maximum load and displacement at maximum load. Table 4.24 summarizes the average maximum additional crack opening. Figure 4.28 shows a typical load-displacement curve.

Table 4.23 Average Results for Cast-in-Place Single-Anchor Connection under Dynamic Shear Loading in Cracked Concrete with No Hairpin

	Average Maximum Load		COV %	Average Displacement at Maximum Load		COV %
	kips	(kN)		inches	(mm)	
Concrete Failure	10.4	(46.1)	20.0	0.114	(2.89)	23.6
Ultimate Failure	10.4	(46.1)	20.0	0.114	(2.89)	23.6

Table 4.24 Average Additional Crack Opening up to Concrete Failure for Cast-in-Place Single-Anchor Connection under Dynamic Shear Loading with No Hairpin

Average Maximum Additional Crack Opening			
Side mm	COV %	Top mm	COV %
0.17	44.8	0.02	86.4

**Typical Load-Displacement Curve - Cast-in-Place Anchor,
Dynamic Shear Loading, Cracked Concrete, No Hairpin**
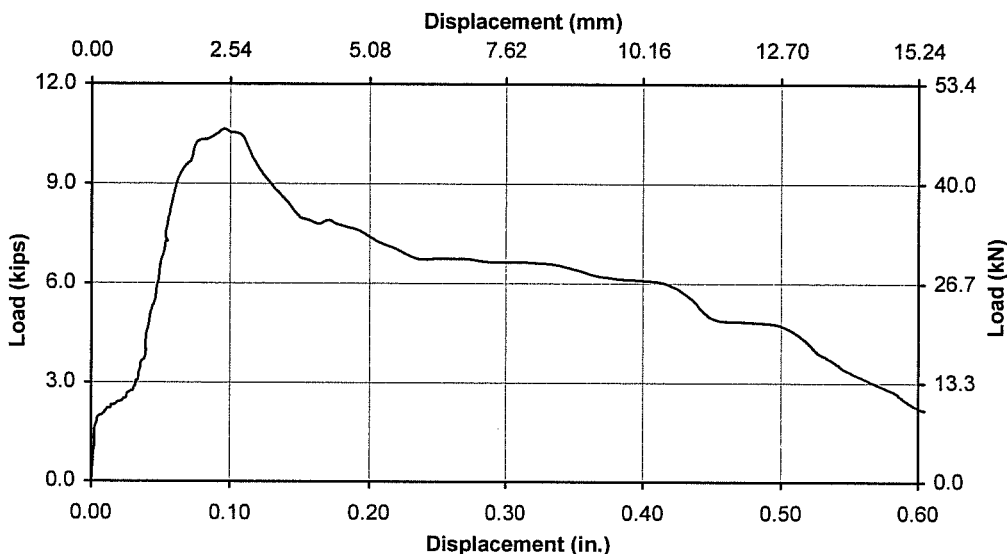
*Figure 4.28 Typical Load-Displacement Curve for Cast-in-Place Single-Anchor
Connection under Dynamic Shear Loading in Cracked Concrete with No Hairpin
(Test 4DCR5704)*

Cast-in-Place Anchors with a close hairpin exhibited enhanced performance.
Ultimate failure occurred due to a decrease in load-carrying capacity at large
displacements. Table 4.25 summarizes the maximum load and displacement at
maximum load. Table 4.26 highlights the maximum additional crack opening up to
concrete failure. Figure 4.29 shows a typical load-displacement curve.

*Table 4.25 Average Results for Cast-in-Place Single-Anchor Connection under
Dynamic Shear Loading in Cracked Concrete with Close Hairpin*

	Average Maximum Load		COV	Average Displacement at Maximum Load		COV
	kips	(kN)	%	inches	(mm)	%
Concrete Failure	14.7	(65.5)	12.4	0.066	(1.68)	39.6
Ultimate Failure	24.1	(107)	15.8	1.08	(27.4)	15.9

Table 4.26 Average Additional Crack Opening up to Concrete Failure for Cast-in-Place Single-Anchor Connection under Dynamic Shear Loading with Close Hairpin

Average Maximum Additional Crack Opening			
Side mm	COV %	Top mm	COV %
0.12	54.1	0.02	49.8

Typical Load-Displacement Curve - Cast-in-Place Anchor, Dynamic Shear Loading, Cracked Concrete, Close Hairpin
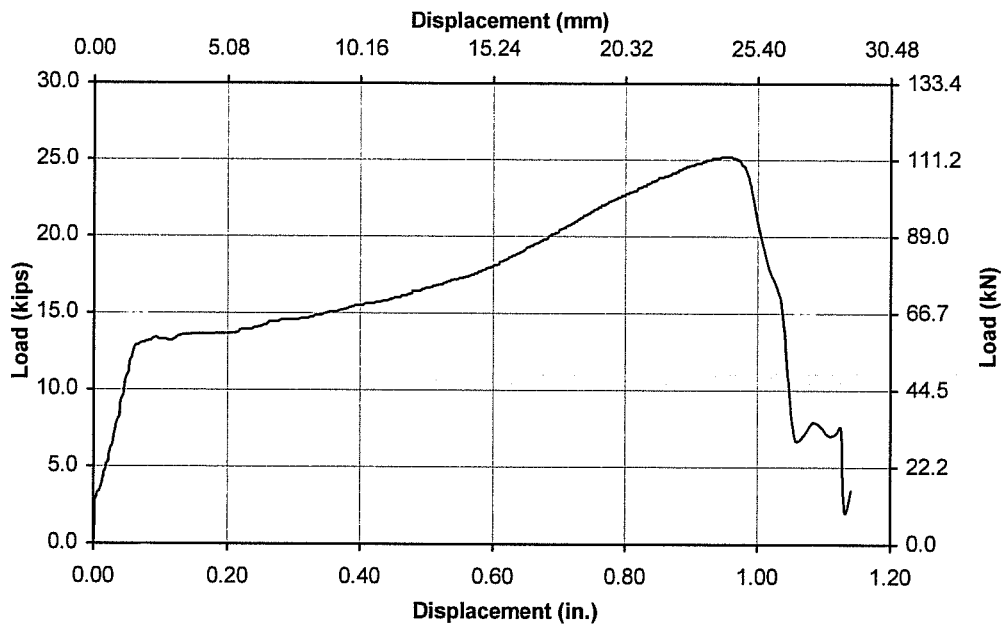
Figure 4.29 Typical Load-Displacement Curve for Cast-in-Place Single-Anchor Connection under Dynamic Shear Loading in Cracked Concrete with Close Hairpin (Test 4DCR5707)

Anchors with a far hairpin carried little additional load after concrete cone breakout; however, the load was sustained for a significant displacement. Table 4.27 highlights the maximum load and displacement at maximum load. Table 4.28 displays the additional crack opening up to concrete failure. Figure 4.30 shows a typical load-displacement curve. Figure 4.31 shows a failure cone for Cast-in-Place Anchors with far hairpins. Notice that the concrete between the anchor and the hairpin was crushed during the test.

Table 4.27 Average Results for Cast-in-Place Single-Anchor Connection under Dynamic Shear Loading in Cracked Concrete with Far Hairpin

	Average Maximum Load		COV	Average Displacement at Maximum Load		COV
	kips	(kN)	%	inches	(mm)	%
Concrete Failure	15.6	(69.2)	17.1	0.162	(4.10)	26.2
Ultimate Failure	18.0	(80.1)	9.0	0.852	(21.7)	58.0

Table 4.28 Average Additional Crack Opening up to Concrete Failure for Cast-in-Place Single-Anchor Connection under Dynamic Shear Loading with Far Hairpin

Average Maximum Additional Crack Opening			
Side mm	COV %	Top mm	COV %
0.11	56.0	0.02	84.1

Typical Load-Displacement Curve - Cast-in-Place Anchor,
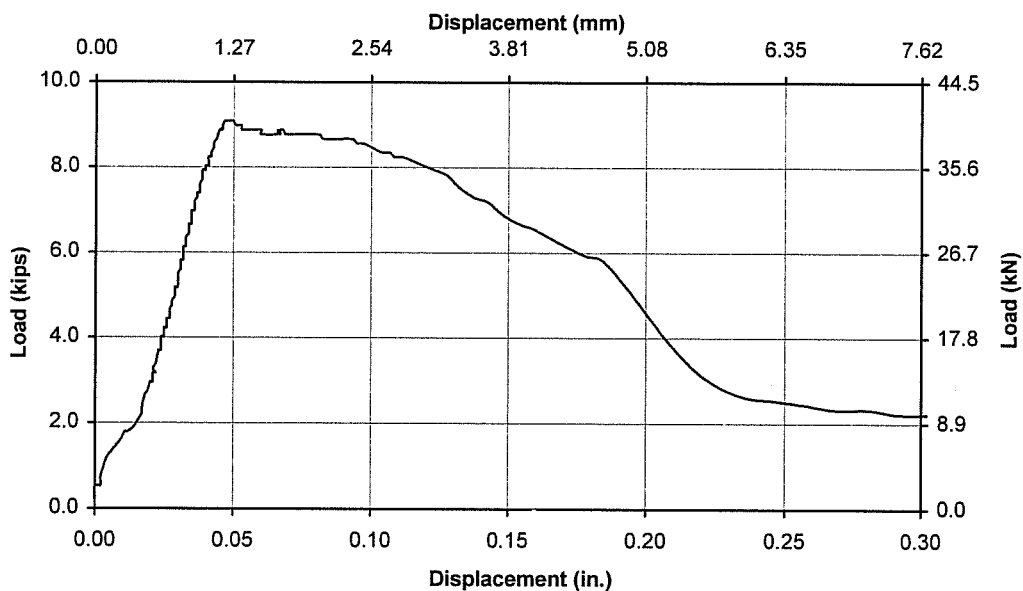Static Shear Loading, Cracked Concrete, Far Hairpin
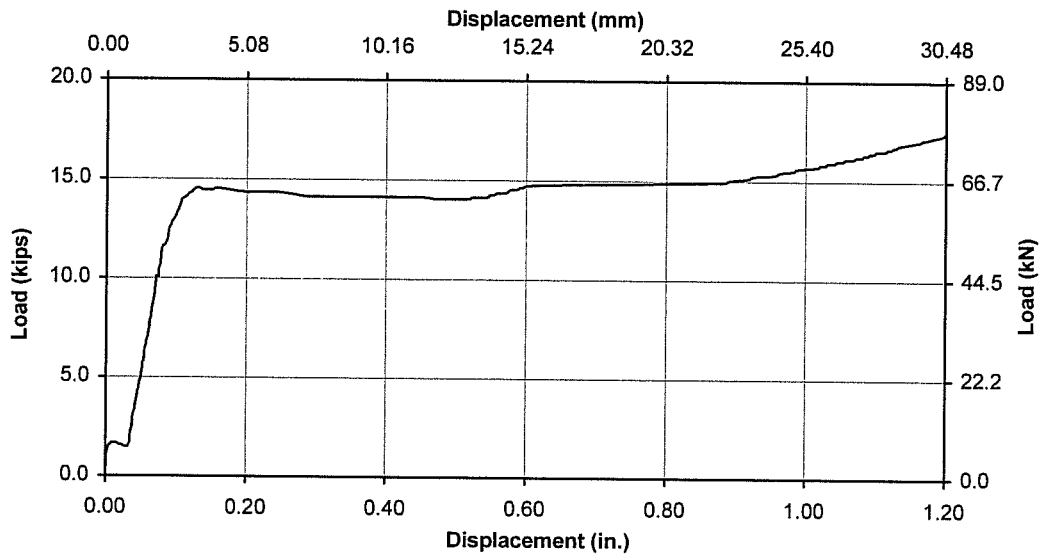
Figure 4.30 Typical Load-Displacement Curve for Cast-in-Place Single-Anchor Connection under Dynamic Shear Loading in Cracked Concrete with Far Hairpin (Test 4DCR5713)
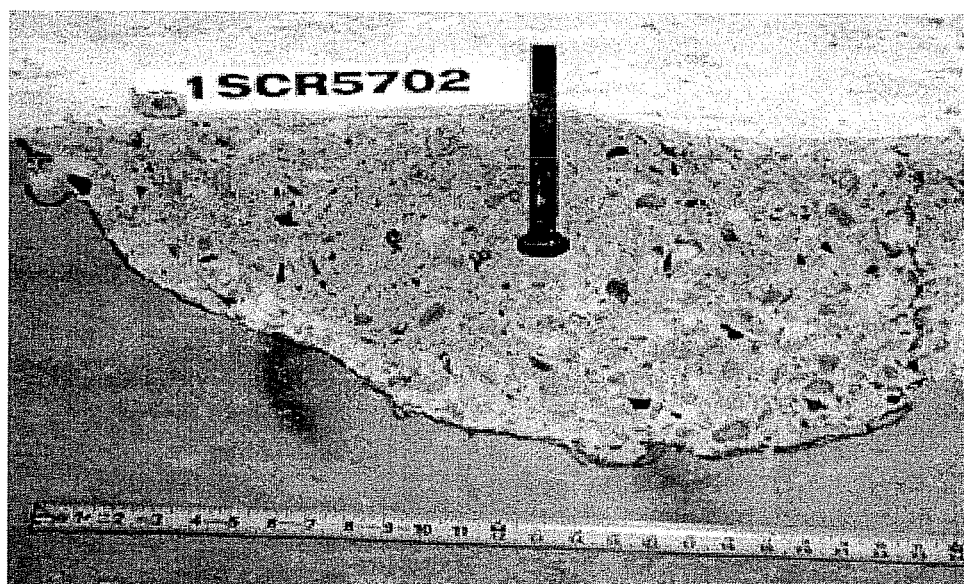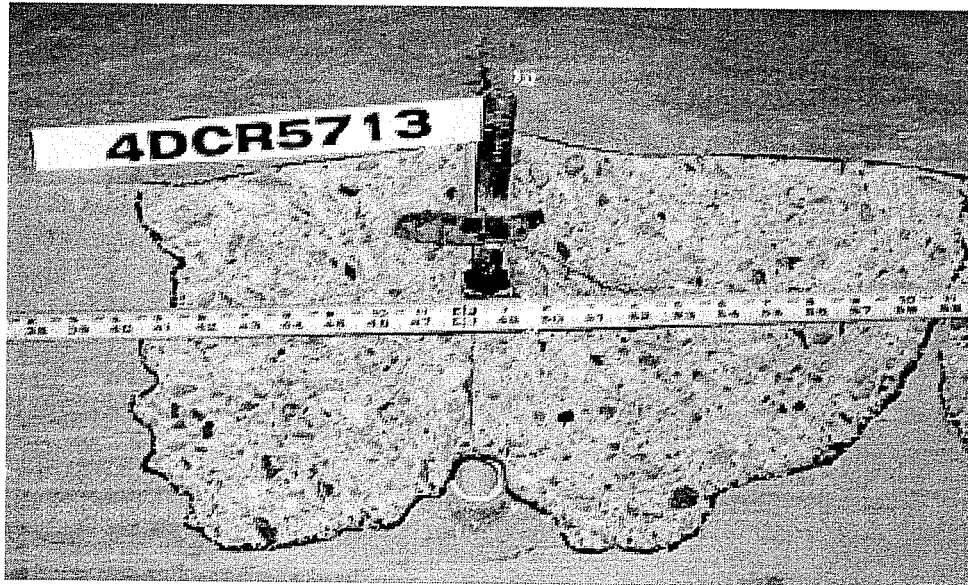

Figure 4.31 Typical Failure Cone for Cast-in-Place Single-Anchor Connection with Far Hairpin Loaded in Shear

Figure 4.32 shows the average additional side crack opening with increasing load. As noted earlier, the top crack opening is insignificant compared to the side crack opening and is therefore not portrayed in the curve.

Average Additional Crack Opening vs. Load
Single-Anchor Connection, Dynamic Shear Loading
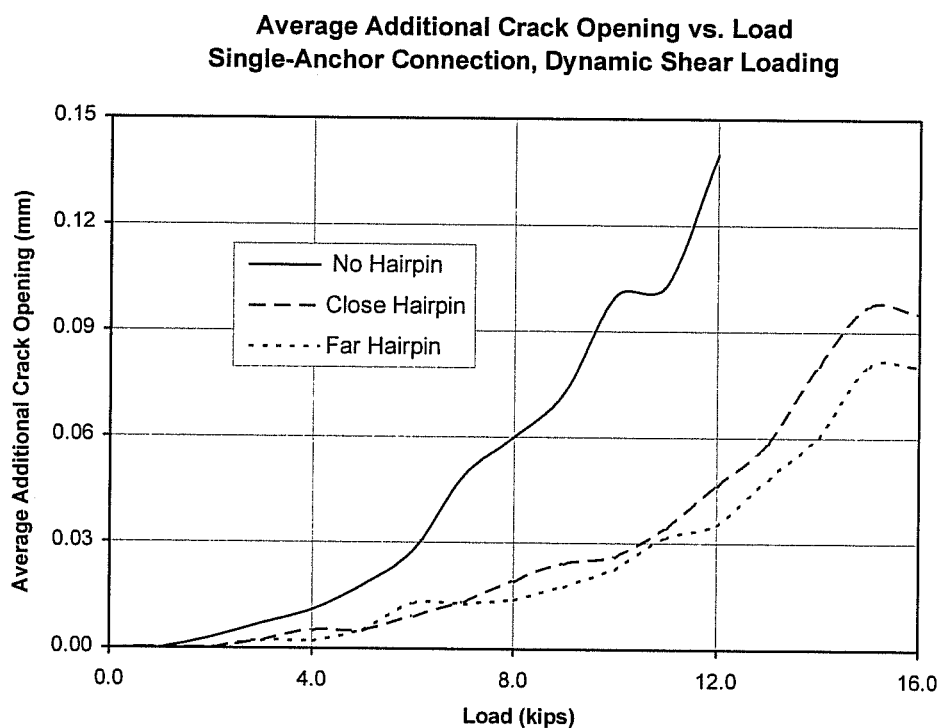
Figure 4.32 Average Additional Side Crack Opening vs. Load for Cast-in-Place Single-Anchor Connection under Dynamic Shear Loading

4.3.5 Results of Series 3-5

Series 3-5 examined double-anchor connections under static loading in uncracked concrete. The anchors were located on a line perpendicular to the free edge at 4-inch (100-mm) and 12-inch (300-mm) edge distances. Cast-in-Place Anchors with 3/4-inch (19-mm) diameters were tested at a 4-inch (100-mm) embedment with either no hairpin or a close hairpin in 4700-psi (32.4-MPa) concrete.

Anchors with no hairpin transferred load to the back anchor when concrete cone breakout occurred. Ultimate failure occurred when the back anchor fractured. In one case, shown in Figure 4.34, the back anchor had a pryout failure. The pryout failure occurred at such a high load that there is no distinction in the load-displacement curves between the anchors that fractured and the anchor that experienced a pryout failure. Table 4.29 summarizes the average maximum load and displacement at maximum load at concrete failure and at ultimate failure. Figure 4.33 shows a typical load-displacement curve.

Table 4.29 Average Results for Cast-in-Place Double-Anchor Connection under Static Shear Loading in Uncracked Concrete with No Hairpin

	Average Maximum Load		COV	Average Displacement at Maximum Load		COV
	kips	(kN)	%	inches	(mm)	%
Concrete Failure	27.1	(121)	9.4	0.152	(3.86)	32.9
Ultimate Failure	37.6	(167)	4.3	0.723	(18.4)	3.6

**Typical Load-Displacement Curve - Cast-in-Place Anchors,
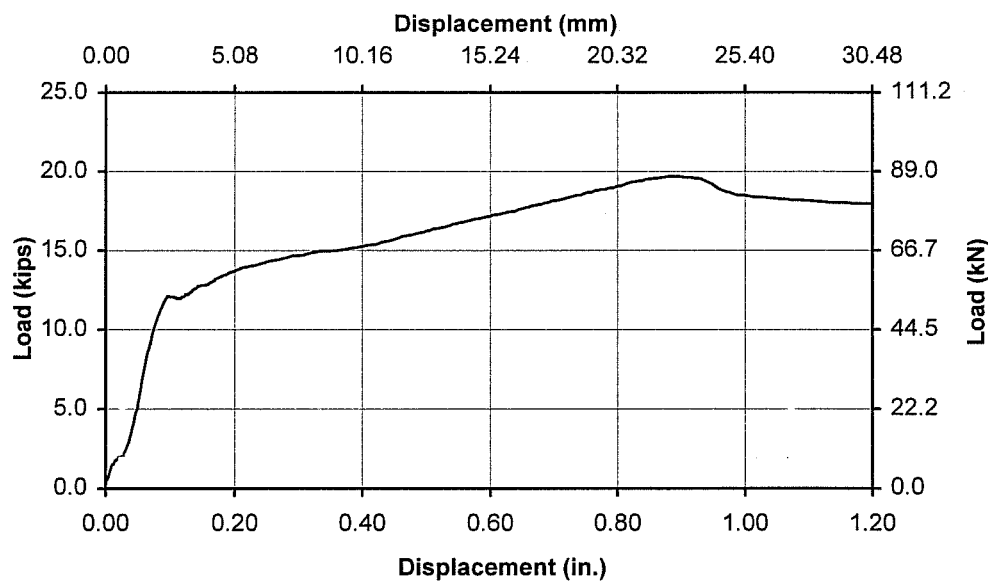Static Shear Loading, Uncracked Concrete, No Hairpin**
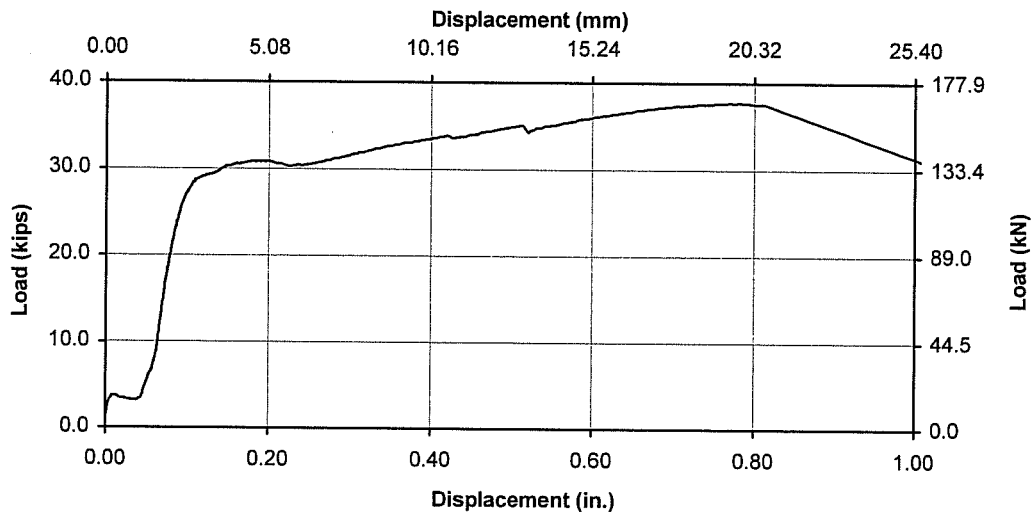
*Figure 4.33 Typical Load-Displacement Curve for Cast-in-Place Double-Anchor
Connection under Static Shear Loading in Uncracked Concrete with No Hairpin
(Test 5SCR5703)*
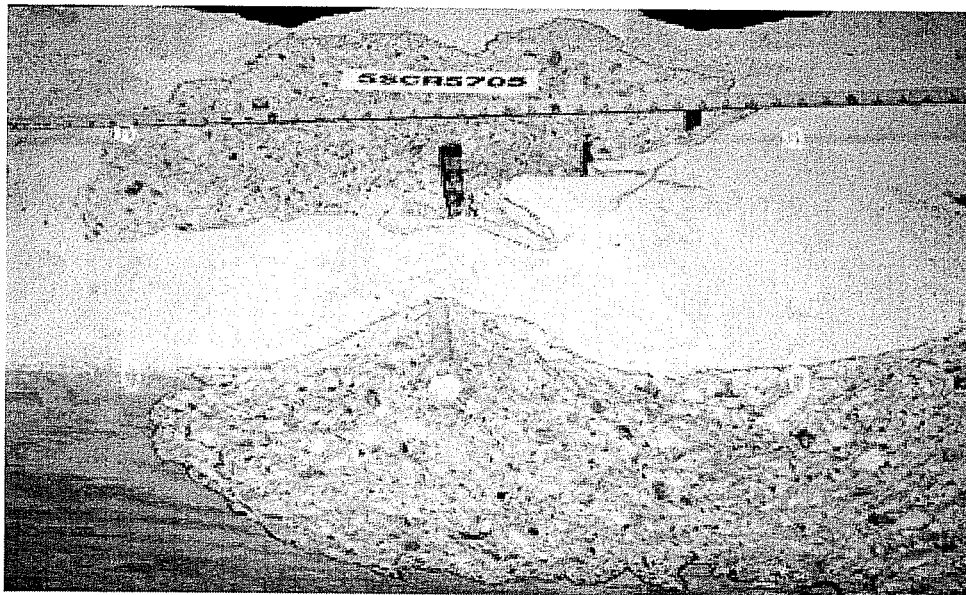
*Figure 4.34 Cone Failure of Front Anchor and Pryout Failure of Back
Anchor for Double-Anchor Connection with No Hairpin Loaded in Shear*

Table 4.30 highlights the results for double-anchor tests with a close hairpin. After concrete cone breakout, some load is carried by the front anchor, but most of the load is transferred to the back anchor. Ultimate failure is governed by the back anchor. In two of the five cases the back anchor had a pryout failure at a high load. One of these cases also showed a crack from the back anchor extending forward toward the free edge, and the front anchor fractured. For the other cases, the back anchor fractured and the front anchor remained in place, although it had little remaining load-carrying capacity. Despite the different failure modes, each of the five cases had similar load-displacement curves. Figure 4.35 shows a typical load-displacement curve.

Table 4.30 Average Results for Cast-in-Place Double-Anchor Connection under Static Shear Loading in Uncracked Concrete with Close Hairpin

	Average Maximum Load		COV	Average Displacement at Maximum Load		COV
	kips	(kN)	%	inches	(mm)	%
Concrete Failure	34.6	(154)	6.8	0.178	(4.53)	16.7
Ultimate Failure	48.8	(217)	13.7	0.738	(18.8)	17.9

98

Typical Load-Displacement Curve - Cast-in-Place Anchors, Static Shear Loading, Uncracked Concrete, Close Hairpin
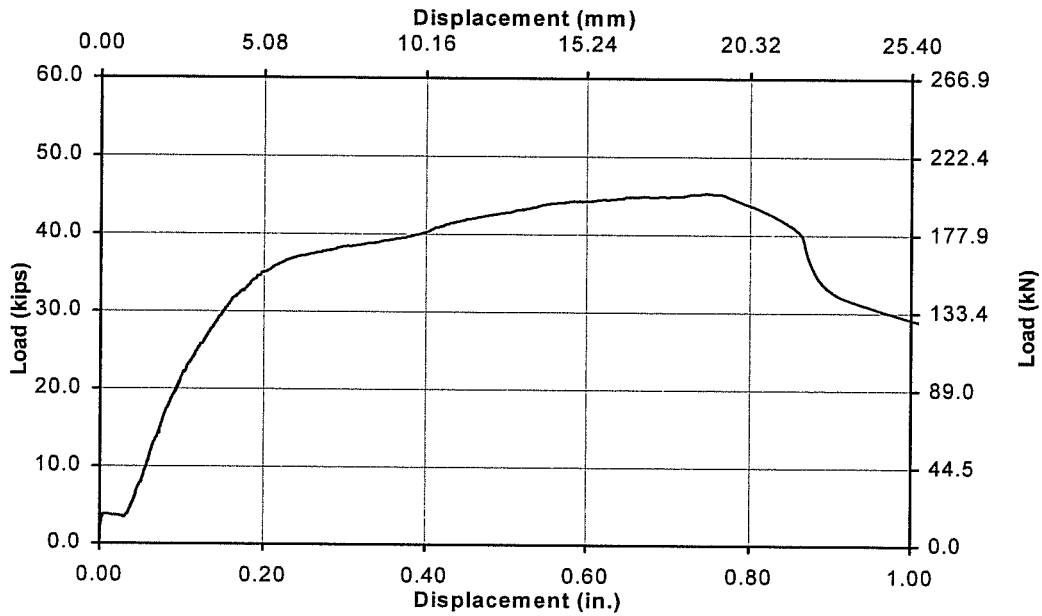
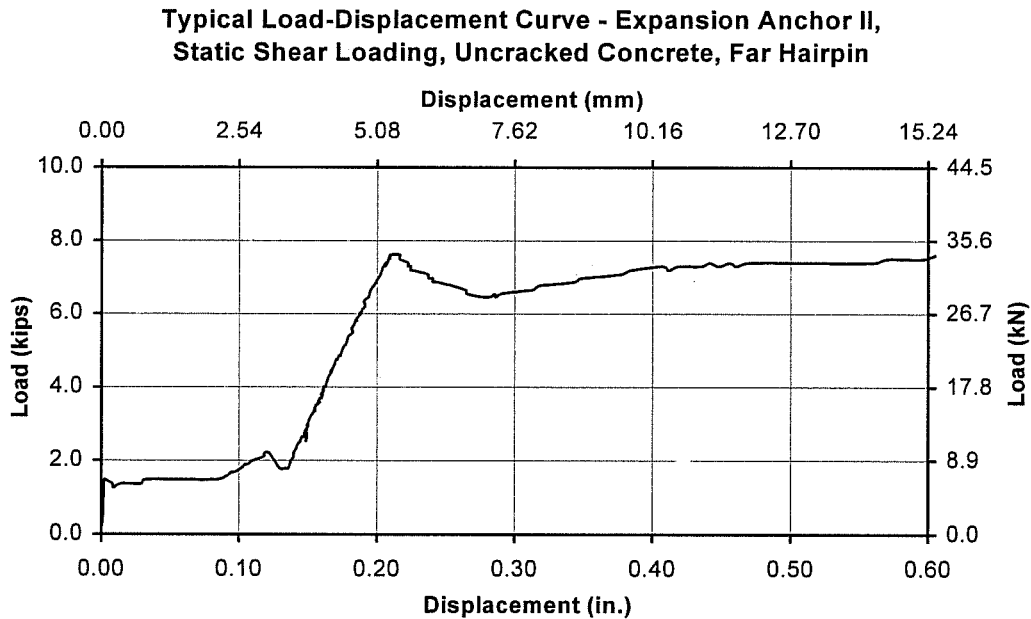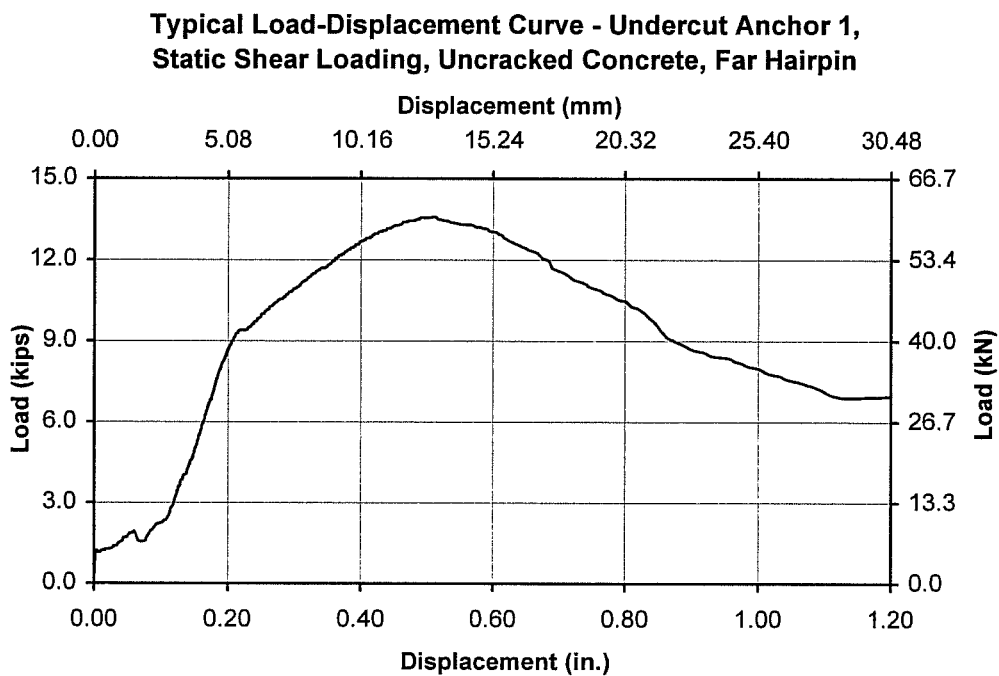*Figure 4.35 Typical Load-Displacement Curve for Cast-in-Place Double-Anchor Connection under Static Shear Loading in Uncracked Concrete with Close Hairpin (Test 5SCR5709)*

4.3.6 Results of Series 3-6

Series 3-6 examined the behavior of double-anchor connections under dynamic loading in uncracked concrete. Cast-in-Place Anchors were located in a line perpendicular to the free edge at edge distances of 4 inches (100 mm) and 12 inches (300 mm). Anchors with 3/4-inch (19-mm) diameter were tested at a 4-inch (100-mm) embedment with either no hairpin or a close hairpin in 4700 psi (32.4-MPa) concrete.

Connections with no hairpin transferred load to the back anchor when concrete cone breakout occurred. Ultimate failure was governed by fracture of the back anchor. Table 4.31 summarizes the average maximum load and displacement at maximum load recorded at concrete failure and at ultimate failure. Figure 4.36 shows a typical load-displacement curve.

Table 4.31 Average Results for Cast-in-Place Double-Anchor Connection under Dynamic Shear Loading in Uncracked Concrete with No Hairpin

	Average Maximum Load		COV %	Average Displacement at Maximum Load		COV %
	kips	(kN)		inches	(mm)	
Concrete Failure	26.0	(116)	2.8	0.110	(2.79)	18.8
Ultimate Failure	37.3	(166)	8.2	0.637	(16.2)	23.3

**Typical Load-Displacement Curve - Cast-in-Place Anchors,
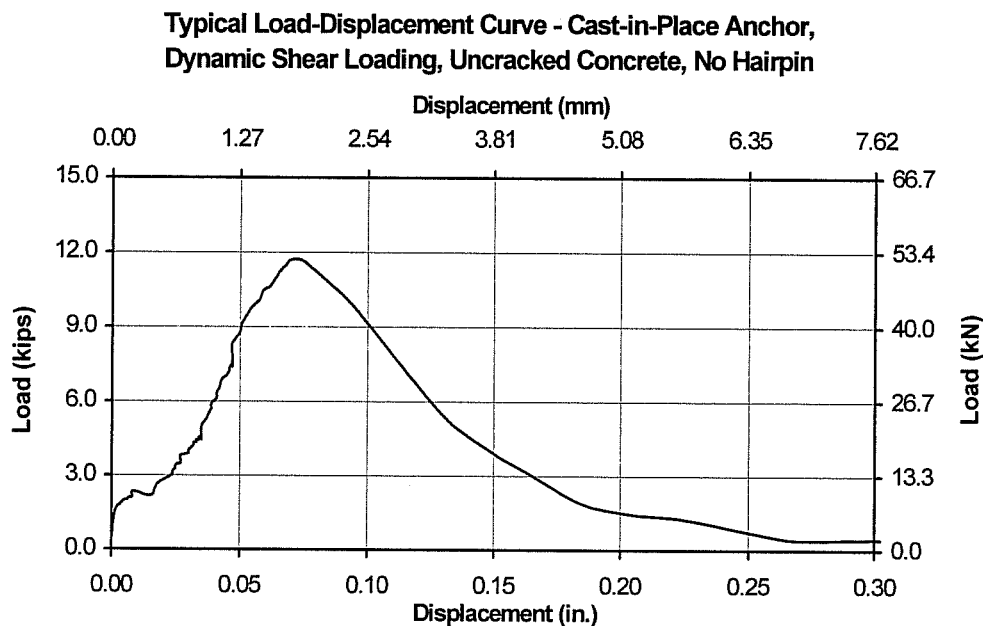Dynamic Shear Loading, Uncracked Concrete, No Hairpin**
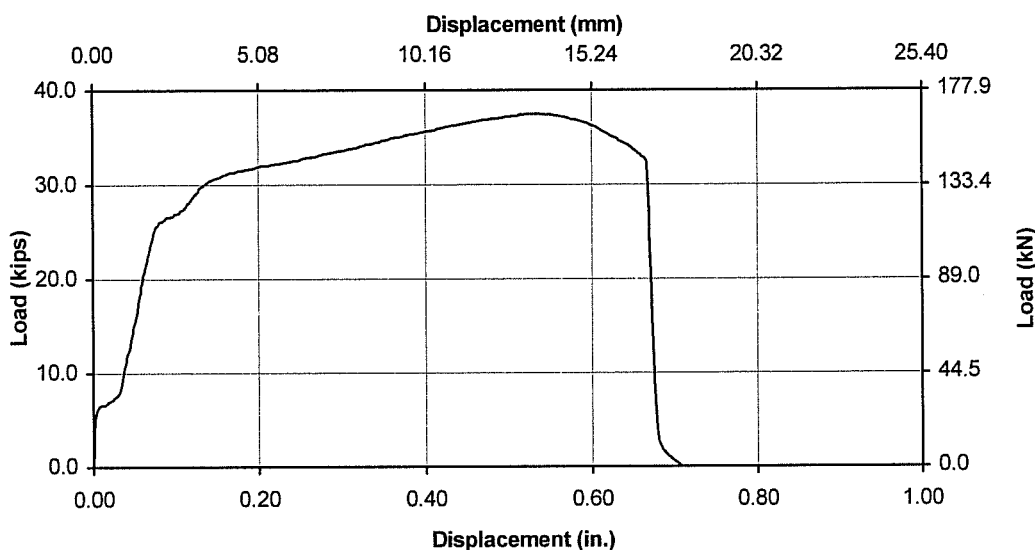
*Figure 4.36 Typical Load-Displacement Curve for Cast-in-Place Double Anchor
Connection under Dynamic Shear Loading in Uncracked Concrete with No Hairpin
(Test 6DCR5705)*

Table 4.32 displays the results for double-anchor connections with a close hairpin under dynamic loading. After the concrete in front of the first anchor failed, most of the load was transferred to the back anchor. Ultimate failure was governed by the response of the back anchor. In two of the cases the equipment could not apply enough load to fracture the anchors; however, both the front and back anchors were significant yielded and fracture was imminent. In the other three cases both anchors fractured. Figure 4.37 shows a typical load-displacement curve. Figure 4.38 shows a test in which both anchors fractured. Figure 4.39 shows the back anchor of a test in which the anchors yielded. Notice the extent of yielding and the spalling of concrete in front of the anchor.

Table 4.32 Average Results for Cast-in-Place Double-Anchor Connection under Dynamic Loading in Uncracked Concrete with Close Hairpin

| | Average Maximum Load | | COV | Average Displacement at Maximum Load | | COV |
	kips	(kN)	%	inches	(mm)	%
Concrete Failure	38.4	(171)	3.4	0.171	(4.35)	13.0
Ultimate Failure	54.0	(240)	9.9	0.693	(17.6)	16.8

Typical Load-Displacement Curve - Cast-in-Place Anchors, Dynamic Shear Loading, Uncracked Concrete, Close Hairpin
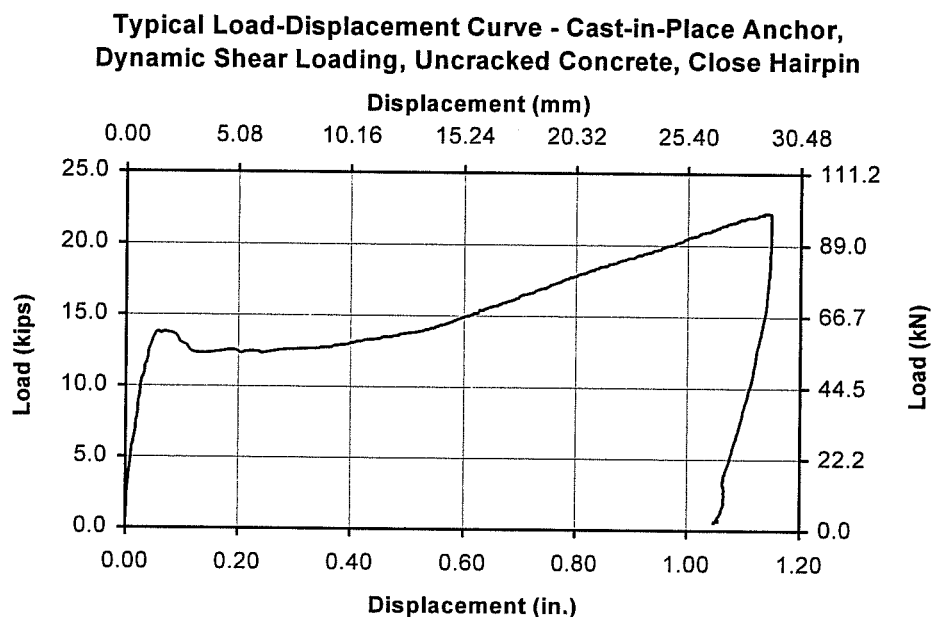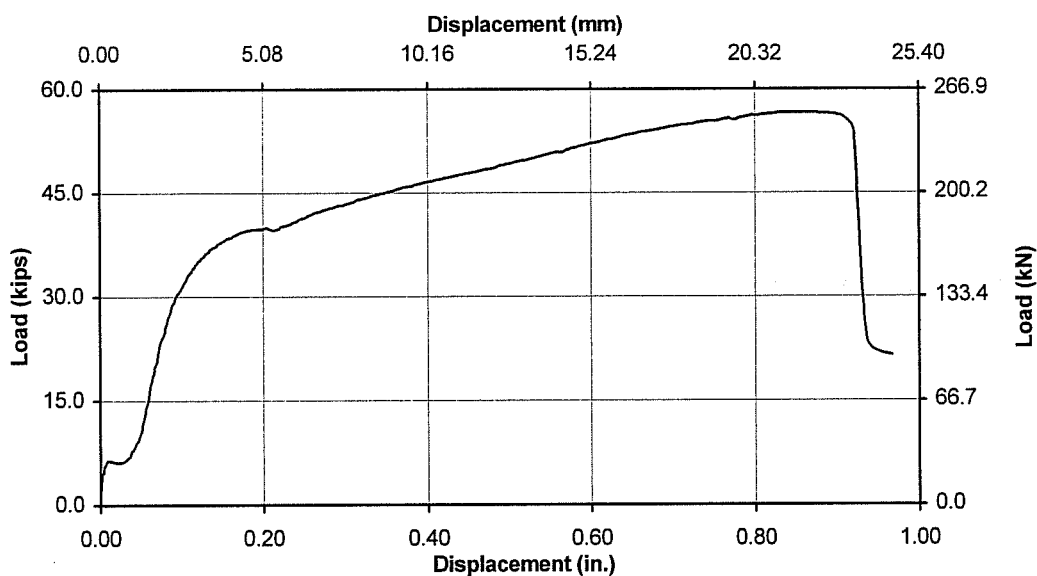

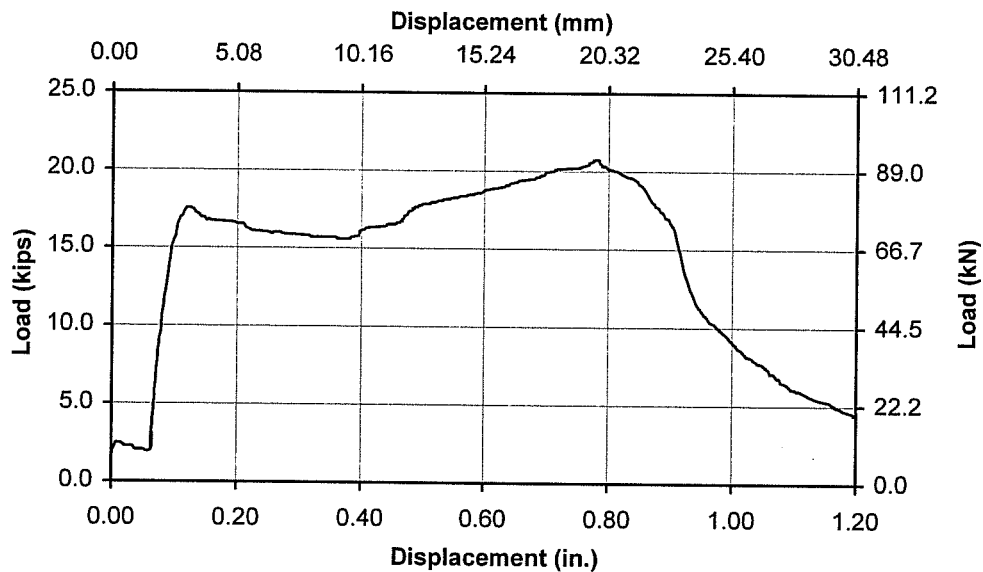*Figure 4.37 Typical Load-Displacement Curve for Cast-in-Place Double-Anchor Connection under Dynamic Shear Loading in Uncracked Concrete with Close Hairpin (Test 6DCR5708)*
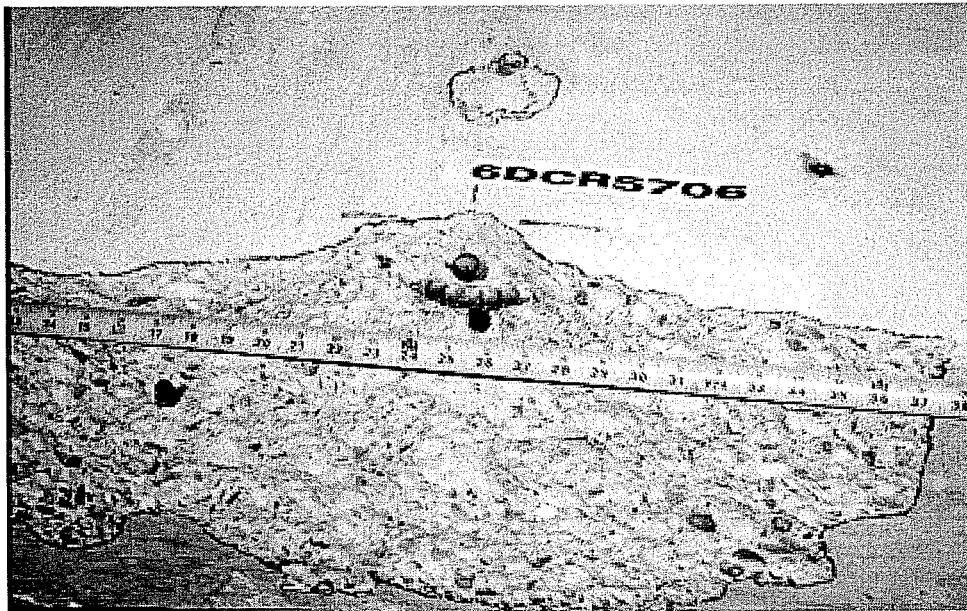
Figure 4.38 Fracture of Front and Back Anchors for Double-Anchor Connection under Dynamic Shear Loading

Figure 4.39 Yielding of Back Anchor and Spalling of Concrete for Double-Anchor Connection under Dynamic Shear Loading

4.3.7 Results of Series 3-7

Series 3-7 examined the behavior of double-anchor connections under static loading in concrete with a 0.3-mm initial crack width. Anchors were located in a line perpendicular to the edge at distances of 4 inches (100 mm) and 12 inches (300 mm). Cast-in-Place Anchors with a 3/4-inch (19-mm) diameter, and a 4-inch (100-mm) embedment, were tested with either no hairpin or a close hairpin in 4700-psi (32.4-MPa) concrete.

Anchors with no hairpin transferred all of the load to the back anchor at concrete cone breakout. Ultimate failure was governed by the back anchor. In four of the five cases the back anchor had a brittle pryout failure. In a few cases the back anchor also started to form a crack toward the front edge, as shown in Figure 4.41. In one case the back anchor fractured. Table 4.33 summarizes the average maximum load and displacement at maximum load. Table 4.34 displays the average additional crack opening up to concrete failure. Figure 4.40 shows a typical load-displacement curve.

Table 4.33 Average Results for Cast-in-Place Double-Anchor Connection under Static Shear Loading in Cracked Concrete with No Hairpin

	Average Maximum Load		COV	Average Displacement at Maximum Load		COV
	kips	(kN)	%	inches	(mm)	%
Concrete Failure	28.0	(124)	14.6	0.176	(4.48)	16.0
Ultimate Failure	35.1	(156)	8.2	0.638	(16.2)	38.8

Table 4.34 Average Additional Crack Opening for Cast-in-Place Double-Anchor
Connection under Static Shear Loading with No Hairpin

Average Maximum Additional Crack Opening			
Side mm	COV %	Top mm	COV %
0.17	27.4	0.06	26.5

**Typical Load-Displacement Curve - Cast-in-Place Anchors,
Static Shear Loading, Cracked Concrete, No Hairpin**
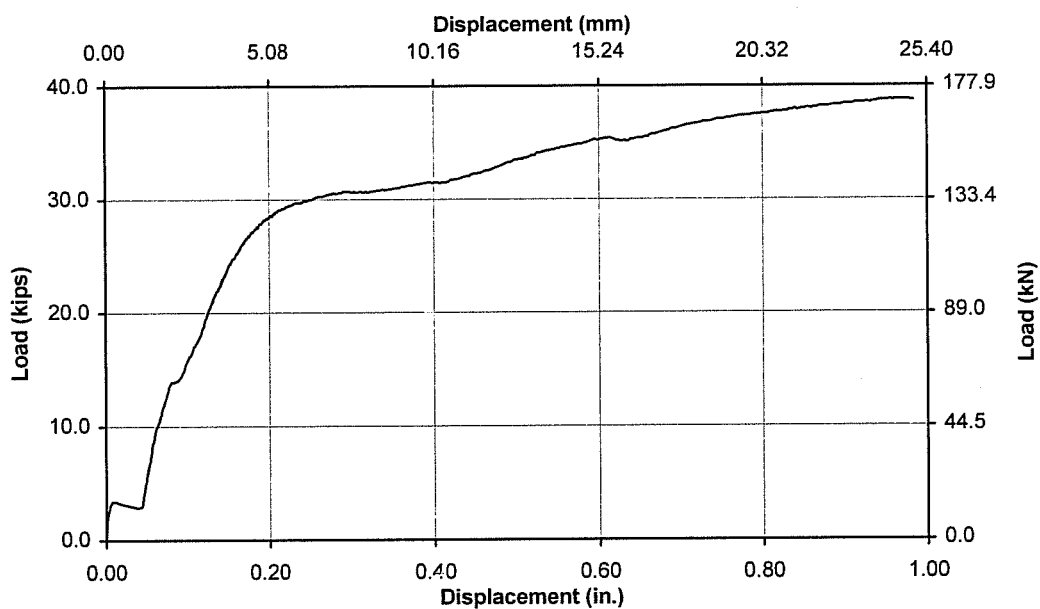
Figure 4.40 Typical Load-Displacement Curve for Cast-in-Place Double-Anchor
Connection under Static Shear Loading in Cracked Concrete with No Hairpin
(Test 7SCR5705)
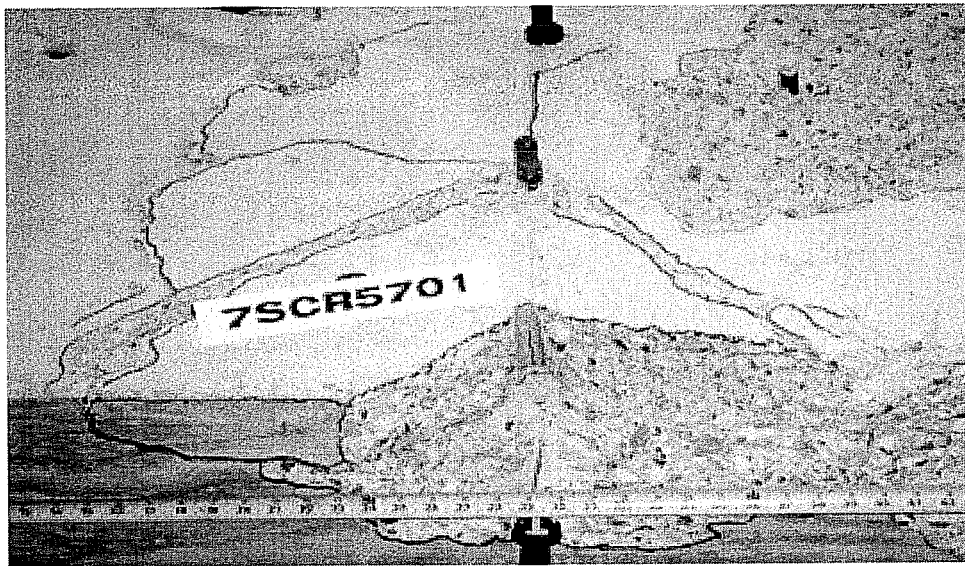
Figure 4.41 Cone Failure of Front Anchor with No Hairpin, Yielding and Pryout of Back Anchor, Along with Cracking toward Free Edge under Static Shear Loading

Anchors with a close hairpin were governed by the behavior of the back anchor. In four of the cases the back anchor fractured. For three of those cases the front anchor remained in place but had little remaining load-carrying capacity, as shown in Figure 4.43. In one case the back anchor exhibited a brittle pryout failure. Table 4.35 summarizes the load and displacement results. Table 4.36 highlights the additional crack opening up to concrete failure. Figure 4.42 shows a typical load-displacement curve.

Table 4.35 Average Results for Cast-in-Place Single-Anchor Connection under Static Shear Loading in Cracked Concrete with Close Hairpin

	Average Maximum Load		COV	Average Displacement at Maximum Load		COV
	kips	(kN)	%	inches	(mm)	%
Concrete Failure	35.1	(156.2)	12.9	0.172	(4.37)	31.8
Ultimate Failure	51.5	(229.2)	11.9	0.712	(18.1)	28.9

Table 4.36 Average Additional Crack Opening for Cast-in-Place Double-Anchor Connection under Static Shear Loading with Close Hairpin

Average Maximum Additional Crack Opening			
Side mm	COV %	Top mm	COV %
0.17	21.6	0.04	0.0

Typical Load-Displacement Curve - Cast-in-Place Anchors, Static Shear Loading, Cracked Concrete, Close Hairpin
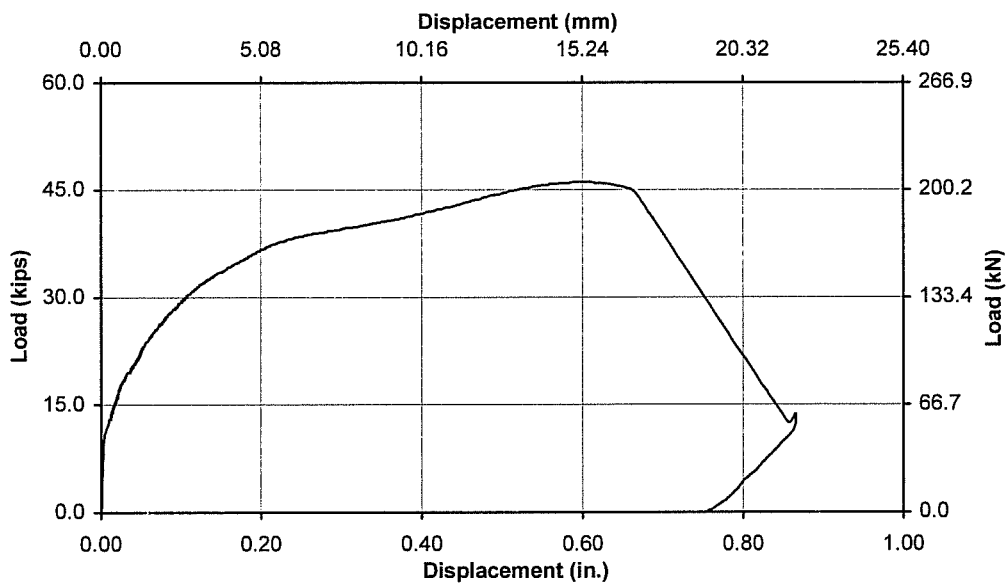
Figure 4.42 Typical Load-Displacement Curve for Cast-in-Place Double-Anchor Connection under Static Shear Loading in Cracked Concrete with Close Hairpin (Test 7SCR5710)

107
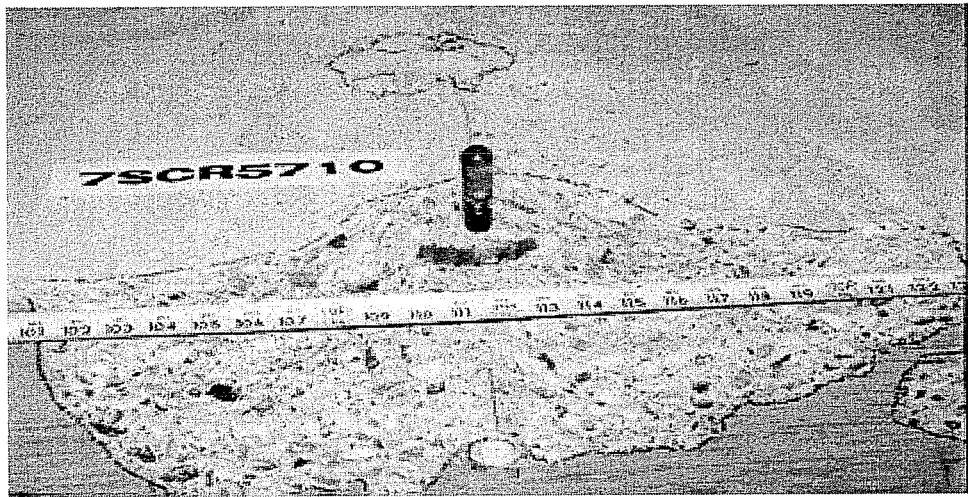
Figure 4.43 Cone Failure Followed by Deformation of Front Anchor with Close Hairpin and Fracture of Back Anchor for Double-Anchor Connection under Static Shear Loading

Figure 4.44 shows the average additional side crack opening with increasing load for both cases in this series. The top crack opening is not portrayed.
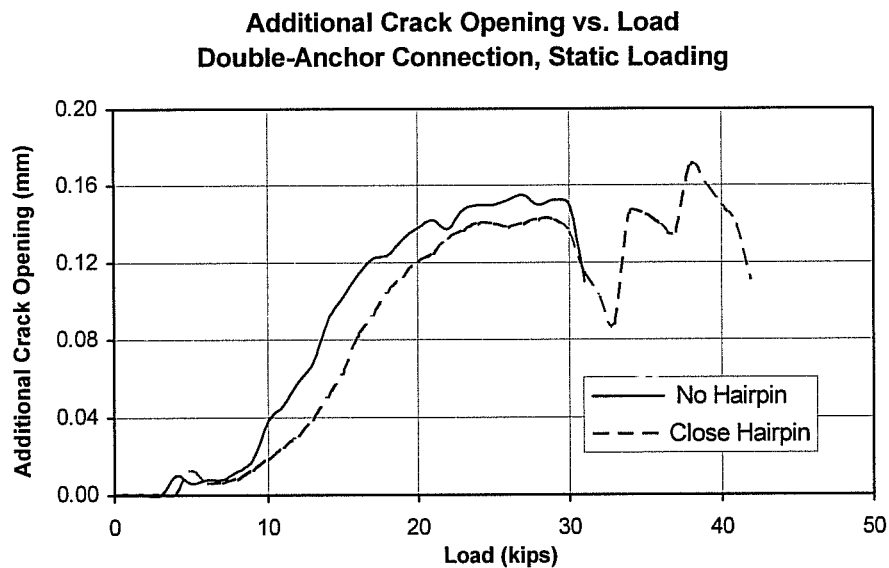
Figure 4.44 Average Additional Side Crack Opening vs. Load for Cast-in-Place Double-Anchor Connection under Static Shear Loading

4.3.8 Results of Series 3-8

Series 3-8 examined the shear behavior of double-anchor connections under dynamic loading in concrete with a 0.3-mm initial crack width. Anchors were located in a line perpendicular to the side with edge distances of 4 inches (100 mm) and 12 inches (300 mm). Cast-in-Place Anchors with a 3/4-inch (19-mm) diameter and an embedment of 4 inches (100 mm) were tested with either no hairpin or a close hairpin in 4700-psi (32.4-MPa) concrete.

Anchors with no hairpin transferred all load to the back anchor at concrete failure. Ultimate failure was governed by the response of the back anchor, which fractured in all cases. In one case a crack had started to propagate from the back anchor toward the free edge. Table 4.37 displays the load and displacement results. Table 4.38 highlights the average maximum additional crack opening up to concrete failure. Figure 4.45 shows a typical load-displacement curve.

Table 4.37 Average Results for Cast-in-Place Double-Anchor Connection under Dynamic Shear Loading in Cracked Concrete with No Hairpin

	Average Maximum Load		COV	Average Displacement at Maximum Load		COV
	kips	(kN)	%	inches	(mm)	%
Concrete Failure	27.1	(120)	1.9	0.163	(4.13)	39.1
Ultimate Failure	34.4	(153)	10.5	0.555	(14.1)	29.6

Table 4.38 Average Additional Crack Opening up to Concrete Failure for Cast-in-Place Double-Anchor Connection under Dynamic Shear Loading with No Hairpin

Average Maximum Additional Crack Opening			
Side mm	COV %	Top mm	COV %
0.22	12.3	0.04	11.8

Typical Load-Displacement Curve - Cast-in-Place Anchors, Dynamic Shear Loading, Cracked Concrete, No Hairpin
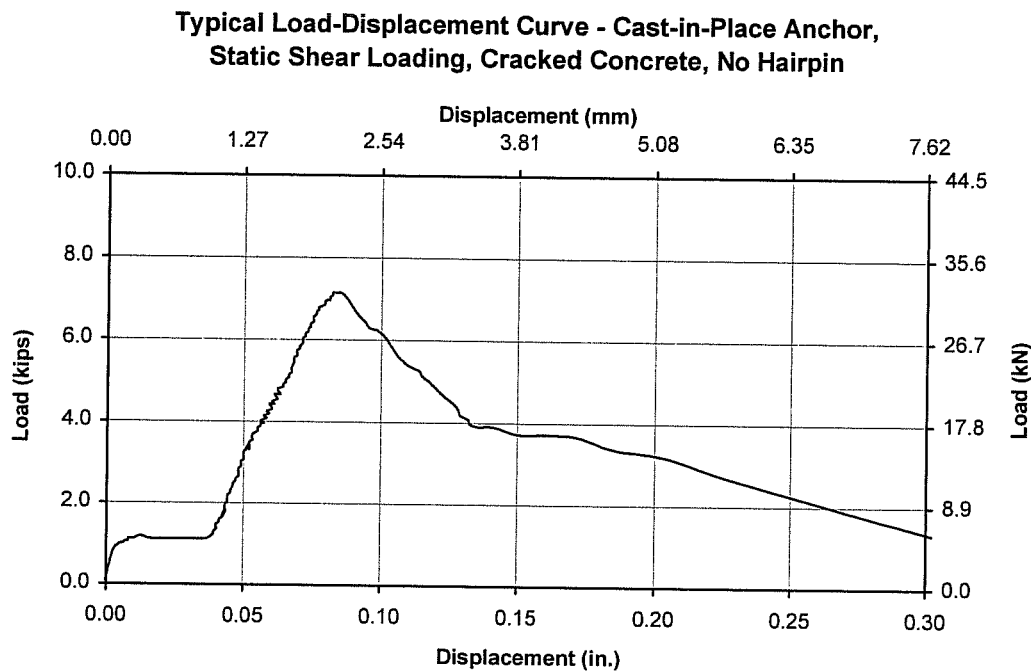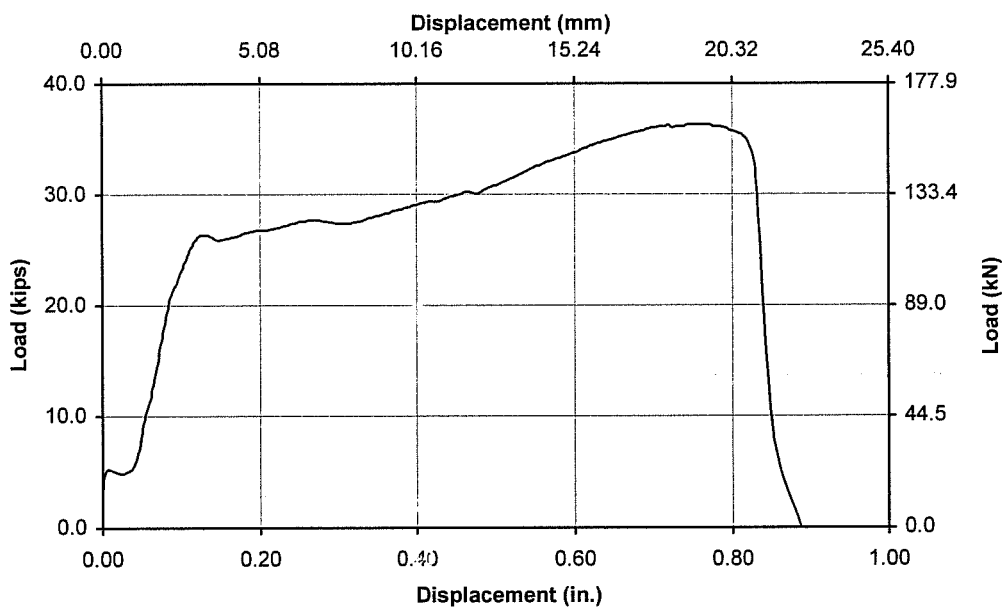

Figure 4.45 Typical Load-Displacement Curve for Cast-in-Place Double-Anchor Connection under Dynamic Shear Loading in Cracked Concrete with No Hairpin (Test 8DCR5702)

Connections with a close hairpin were also governed by the back anchor. In three cases both anchors fractured. In two cases the anchors were significantly yielded and were on the verge of fracture when the loading equipment reached its maximum capacity. Table 4.39 highlights the load and displacement results for the anchors. Table 4.40 summarizes the additional crack opening up to concrete failure. Figure 4.46 shows a typical load-displacement curve.

Table 4.39 Average Results for Cast-in-Place Double-Anchor Connection under Dynamic Shear Loading in Cracked Concrete with Close Hairpin

	Average Maximum Load		COV %	Average Displacement at Maximum Load		COV %
	kips	(kN)		inches	(mm)	
Concrete Failure	35.0	(156)	3.0	0.174	(4.42)	24.1
Ultimate Failure	53.1	(236)	5.7	0.708	(18.0)	16.0

Table 4.40 Average Additional Crack Opening up to Concrete Failure for Cast-in-Place Double-Anchor Connection under Dynamic Shear Loading with Close Hairpin

Average Maximum Additional Crack Opening			
Side mm	COV %	Top mm	COV %
0.18	12.5	0.04	42.1

**Typical Load-Displacement Curve - Cast-in-Place Anchors,
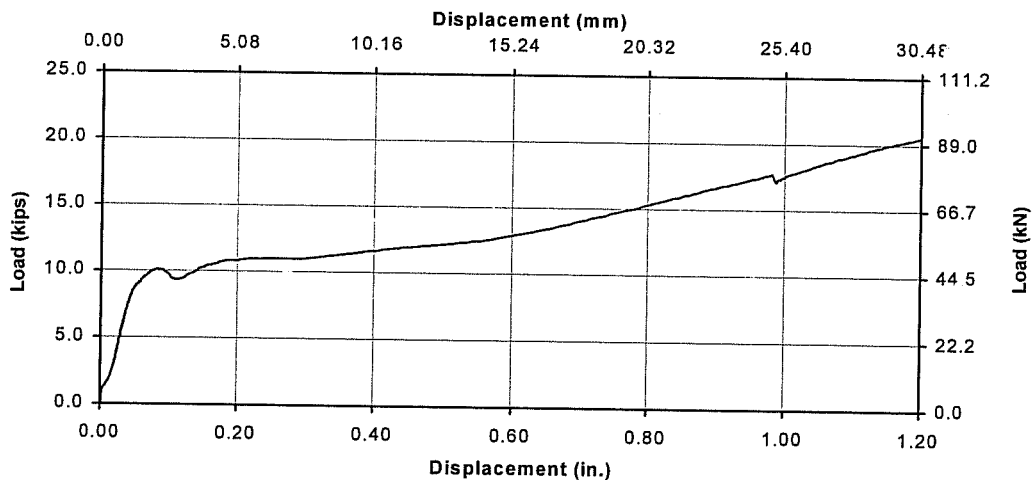Dynamic Shear Loading, Cracked Concrete, Close Hairpin**
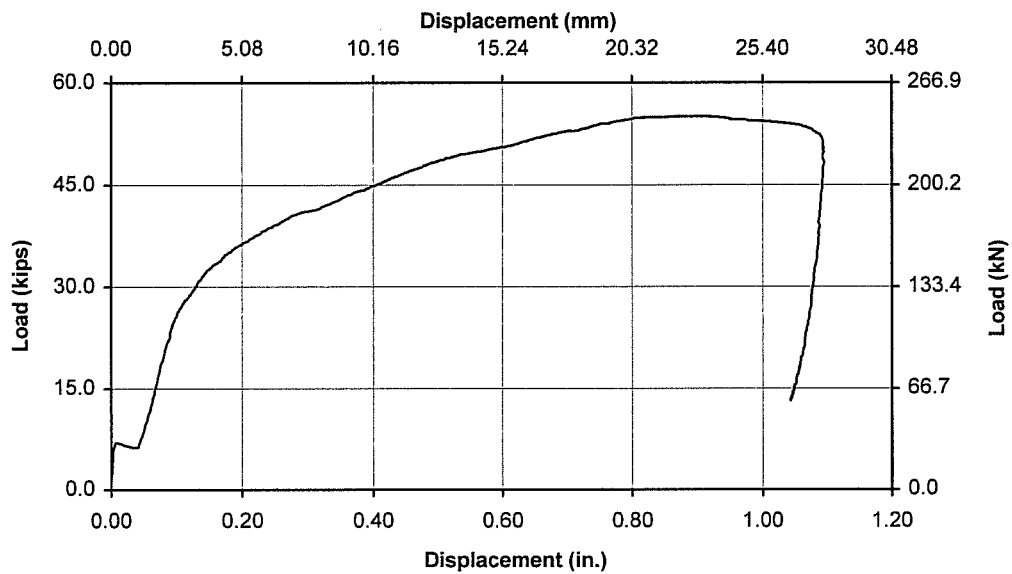
*Figure 4.46 Typical Load-Displacement Curve for Cast-in-Place Double-Anchor
Connection under Dynamic Shear Loading in Cracked Concrete with Close Hairpin
(Test 8DCR5706)*

Figure 4.47 shows the average additional side crack opening with increasing load up to concrete failure. The top crack opening is not shown.

Additional Crack Opening vs. Load
Double-Anchor Connection, Dynamic Shear Loading
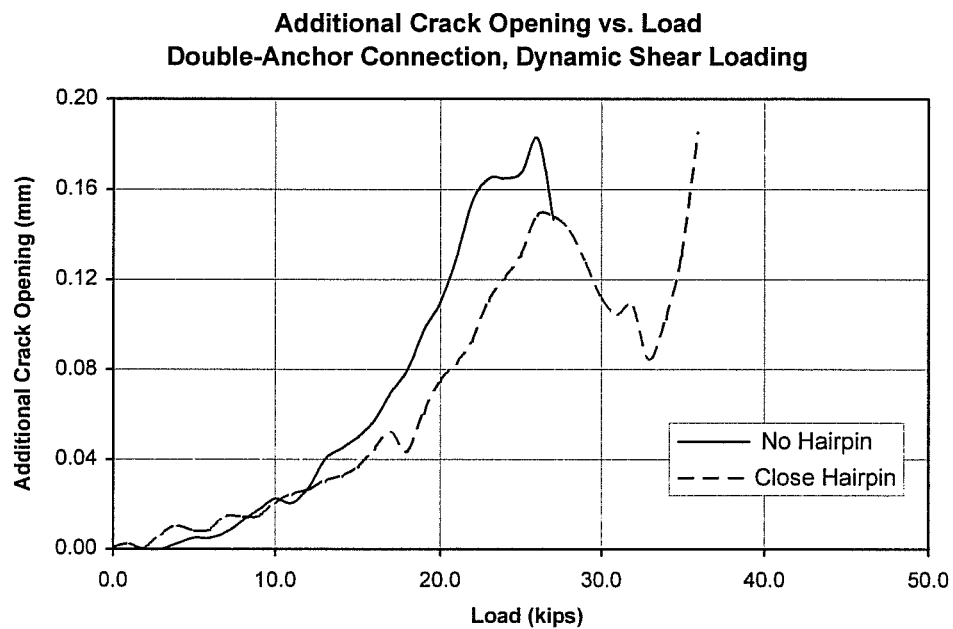
Figure 4.47 Average Additional Side Crack Opening vs. Load for Cast-in-Place Double-Anchor Connection under Dynamic Shear Loading

CHAPTER FIVE

DISCUSSION OF TEST RESULTS

5.1 INTRODUCTION

This chapter discusses the results presented in Chapter Four. Tensile test results are presented in terms of the normalized tensile capacity, k_{nc}, to facilitate comparison among different anchor types, embedments and concrete strengths:

$$k_{nc} = \frac{P_n}{h_{ef}^{1.5} \sqrt{f_c}} \qquad (5\text{-}1)$$

k_{nc} = normalization factor for tensile capacity

P_n = measured tensile capacity, lbs

h_{ef} = effective embedment, inches

f_c = tested concrete compressive strength, psi

For shear tests, the maximum loads and displacements are presented. In addition, to show the effects of loading rate and cracked concrete, results are normalized by the capacity under static loading in uncracked concrete. To show the effect of the hairpin, results are normalized by the capacity with no hairpin.

In some figures, abbreviations are used to refer to the different anchor types. Cast-in-Place Anchors are designated by CIP. The Undercut Anchors used in tests performed by the author are referred to as UC1. Expansion Anchor II is referred to as EAII. A second Undercut Anchor tested by [Rodriguez 1995] is referred to as UC2. The Sleeve Anchor tested by [Rodriguez 1995] is referred to as Sleeve.

5.2 BEHAVIOR OF EXPANSION ANCHORS TESTED IN SERIES 1-9 AND 1-10

This section discusses the significance of the results from Expansion Anchor II tests in Series 1-9 and 1-10. Comparisons are made with Expansion Anchor II tests reported in [Rodriguez 1995], in order to draw conclusions about the effect of aggregate hardness on the behavior of expansion anchors.

5.2.1 Effect of Aggregate Hardness on Tensile Capacity of Expansion Anchor II

As shown in Figure 5.1, under static and dynamic loading, tensile capacities are approximately uniform for Expansion Anchor II embedded in otherwise identical concrete made with the three different aggregates. Peak load appears to decrease slightly with increasing aggregate hardness for static loading, but to increase slightly with increasing aggregate hardness under dynamic loading. However, in all cases the percentage change in capacity is less than the coefficient of variation (about 5%) within each group of 5 replicates. Therefore, anchor tensile capacity is judged not to be significantly affected by aggregate hardness.

As noted in [Rodriguez 1995], dynamic loading increases the tendency for pull-out and pull-through failure of expansion anchors. This general tendency is attributed to a decrease in the coefficient of friction between the wedge and the concrete, and between the mandrel and the wedge, under dynamic as compared to static loading. In concrete made with limestone or river gravel aggregate, dynamic tests with pull-through or cone failure modes had a lower capacity than static tests with cone failure modes [Rodriguez 1995]. In granite, however, three dynamic tests failed by combined pull-through/cone breakout, with capacities larger than for static tests with cone breakout. While dynamic and static tensile capacities are approximately the same in river gravel and limestone, the dynamic capacity is more than 15% higher than the static capacity in granite. This indicates that aggregate hardness does have some effect on the ratio between dynamic and static tensile capacity. This is believed to be due to an increase in friction between the clip and the concrete, and a decrease in friction between the mandrel and the clip.
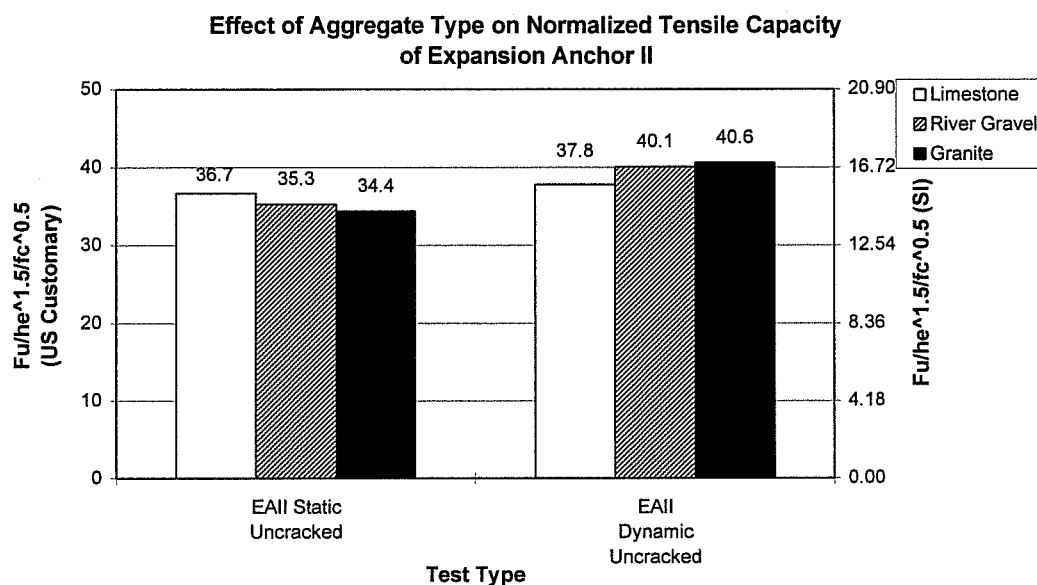
Figure 5.1 Effect of Aggregate Type on Normalized Tensile Capacity of Expansion Anchor II

5.2.2 Effect of Aggregate Hardness on Peak-Load Displacement of Expansion Anchor II Loaded in Tension

Aggregate hardness appears to have no significant effect on the displacement at peak load of Expansion Anchor II under static loading, as shown in Figure 5.2. However, displacement under dynamic loading in granite-aggregate concrete is significantly lower than in concrete made with limestone or river gravel aggregate, and also lower than the static displacement in granite. Under static loading in granite, the clip slipped down the mandrel approximately 1/4 inch (6 mm), indicating slight pull-through before the eventual cone failure. The hardness of the granite aggregate apparently increases the friction coefficient between the clip and the concrete, thus increasing the tendency for pull-through failure under dynamic loading. Three of the five dynamic tensile tests in granite had combined pull-through/cone failure. Due to the low peak-load displacements associated with these tests, it can be assumed that the anchor did not pull through the cone until after the maximum load had been reached.

Dynamic tests in granite with cone failures did not show any pull-through. Although dynamic loading decreases the coefficient of friction between the mandrel and the clip, the use of granite aggregate increases the normal force between the mandrel and the clip, thus reducing pull-through. Therefore, the hardness of the aggregate reduced the displacement of the anchor. This behavior is believed to explain why the peak-load dynamic displacement in granite is lower than the peak-load static displacement.
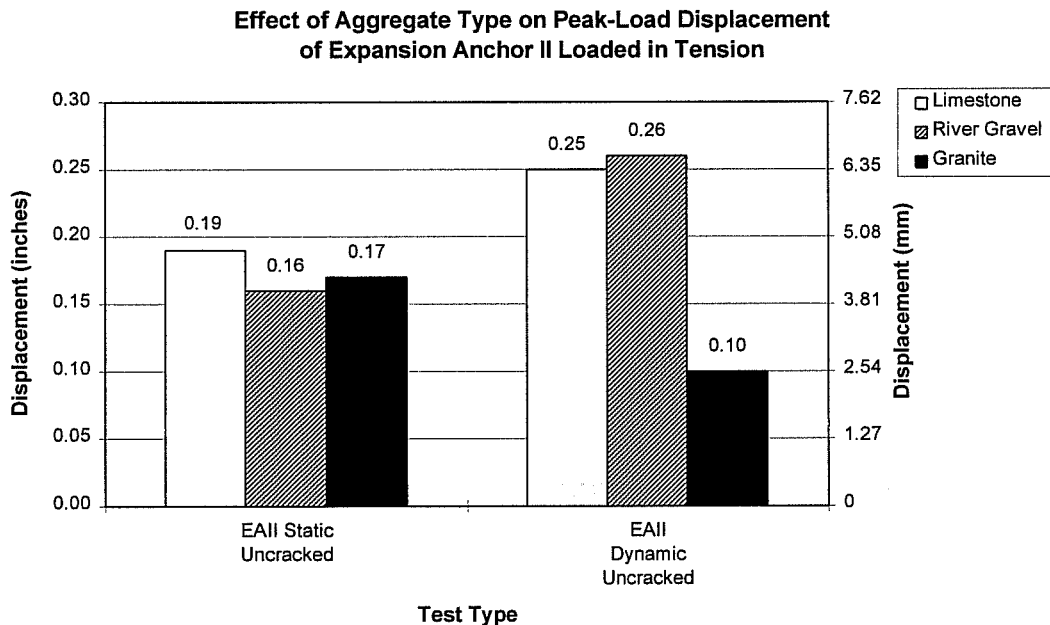
Figure 5.2 Effect of Aggregate Type on Peak-Load Displacement of
Expansion Anchor II Loaded in Tension

5.2.3 Effect of Aggregate Type on Normalization Coefficient for Tensile Capacity of Expansion Anchor II

Table 5.1 summarizes the normalization coefficient in terms of the CC Method, using U.S. customary units. A normalization coefficient of 35 is appropriate for Expansion Anchor II under static loading in all aggregates tested, and also for Expansion Anchor II under dynamic loading in concrete with limestone or river gravel aggregate. The normalization coefficient can be increased by a factor of about 1.15, to about 40, for dynamic loading in concrete with granite aggregate.

Table 5.1 Normalization Coefficient for Expansion Anchor II
in Uncracked Concrete Loaded in Tension

Aggregate Type	Load Type	
	Static	Dynamic
Limestone	35	35
River Gravel	35	35
Granite	35	40

5.3 BEHAVIOR OF UNDERCUT ANCHORS TESTED IN SERIES 1-9 AND 1-10

This section discusses the behavior of Undercut Anchors tested in granite-aggregate concrete in Series 1-9 and 1-10. Comparisons are made with tests conducted by [Rodriguez 1995] on the same anchor in concrete with limestone and river gravel aggregate to asses the effect of aggregate hardness.

5.3.1 Effect of Aggregate Hardness on Tensile Capacity of Undercut Anchor 1

Figure 5.3 shows that under static loading, increasing aggregate hardness increases the tensile capacity of Undercut Anchor 1. Tensile capacity in concrete with granite aggregate is significantly higher than in concrete with limestone or river gravel. In all cases, the failure surface propagates along the interface between the cement paste and the aggregate, rather than through the aggregate. It is believed that the rough angular surface of the granite, as contrasted with the smooth surface of the limestone and the river gravel, allows a better bond between the aggregate and the paste, resulting in higher interface strengths and therefore higher cone breakout loads. Under dynamic loading, aggregate hardness does not seem to affect tensile capacity. It is possible that the increase in the strength of the aggregate-paste interface due to the surface roughness of the aggregate is about the same as the increase in the strength of the paste itself due to the dynamic loading rate.

For concrete made with limestone or river gravel aggregate, dynamic tensile capacity is about 20% greater than static capacity. In concrete made with granite aggregate, the static and dynamic tensile capacities are essentially the same. Apparently, the increase in static capacity due to the difficulty of initiating crack propagation in granite aggregate is similar to the increase in dynamic capacity due to the time required to initiate crack propagation.

**Effect of Aggregate Type on Normalized Tensile Capacity
of Undercut Anchor 1**
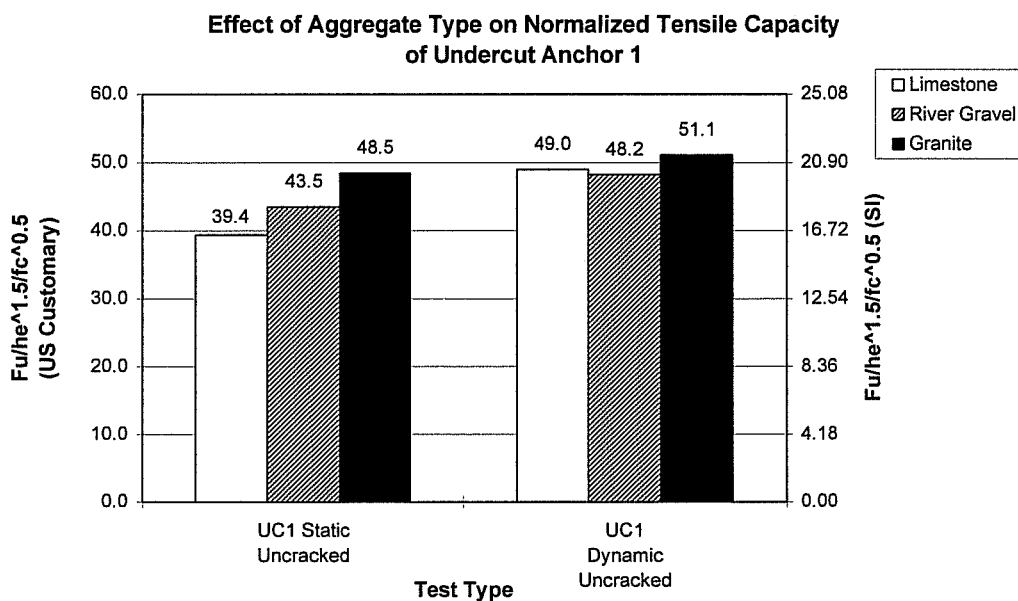
*Figure 5.3 Effect of Aggregate Type on Normalized Tensile Capacity
of Undercut Anchor 1*

5.3.2 Effect of Aggregate Hardness on Peak-Load Displacement of Undercut Anchor 1 Loaded in Tension

As shown in Figure 5.4, static displacement of Undercut Anchor 1 at peak load is apparently independent of aggregate hardness. The decrease in dynamic displacement in granite appears to be significant. This could be due to some higher local strength or stiffness of the granite-aggregate concrete resulting in a smaller zone of local crushing. However, the coefficient of variation in peak-load displacement ranges from 23% to 53% for these tests, reducing the significance of this difference.

**Effect of Aggregate Type on Peak-Load Displacement
of Undercut Anchor 1 Loaded in Tension**
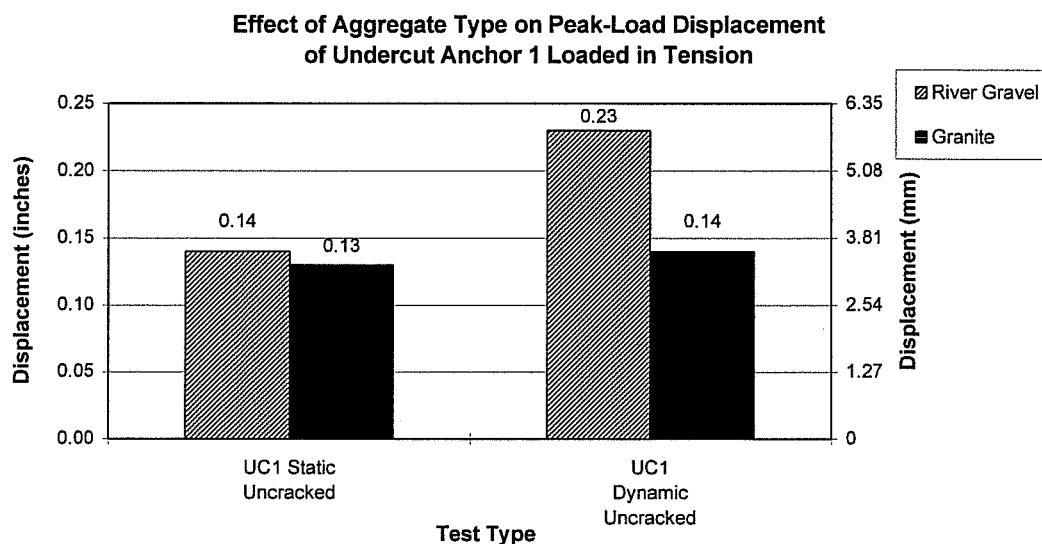
*Figure 5.4 Effect of Aggregate Type on Peak-Load Displacement
of Undercut Anchor 1 Loaded in Tension*

5.3.3 Effect of Aggregate Type on Normalization Coefficient for Tensile Capacity of Undercut Anchor 1

Table 5.2 summarizes the tensile capacity normalized in terms of the CC Method using U.S. customary units. In concrete made with limestone or river gravel aggregate, a normalization coefficient of about 41 is appropriate for Undercut Anchor 1 under static loading. This coefficient increases by a factor of 1.17, to about 48, under dynamic loading. In concrete made with granite aggregate, a suitable normalization coefficient for Undercut Anchor 1 is about 48, under dynamic as well as static loading.

*Table 5.2 Normalization Coefficient for Undercut Anchor 1 in
Uncracked Concrete Loaded in Tension*

Aggregate Type	Load Type	
	Static	Dynamic
Limestone	41	48
River Gravel	41	48
Granite	48	48

5.4 BEHAVIOR OF CAST-IN-PLACE ANCHORS TESTED IN SERIES 1-11 AND 1-12

This section evaluates the tensile behavior of cast-in-place anchors as compared to that of post-installed anchors. Series 1-11 and 1-12 examined cast-in-place anchors under static and dynamic loading in uncracked and cracked concrete. Comparisons are made with Undercut Anchor 1 tested by the author, as well as with Undercut Anchor 1, Undercut Anchor 2, and Sleeve Anchor test results reported in [Rodriguez 1995].

5.4.1 Normalized Tensile Capacity of Cast-in-Place versus Post-Installed Anchors in Uncracked Concrete

Figures 5.5, 5.6 and 5.7 show the normalized tensile capacity of Cast-in-Place Anchor, Undercut Anchor 1, Undercut Anchor 2 and Sleeve Anchor. In uncracked concrete made with limestone or river gravel aggregate, the static tensile capacity of Cast-in-Place Anchors is comparable to that of Undercut Anchor 1, Undercut Anchor 2, and Sleeve Anchors. In uncracked concrete made with limestone or river gravel aggregate, the dynamic capacity of Cast-in-Place Anchors is significantly greater than that of Undercut Anchor 1, and comparable to that of Undercut Anchor 2 and the Sleeve Anchor.

In uncracked concrete, with the exception that the Cast-in-Place Anchor's dynamic capacity exceeds that of Undercut Anchor 1, the tensile capacity of the Cast-in-Place Anchor is comparable to that of Undercut and Sleeve Anchors for both types of loading.
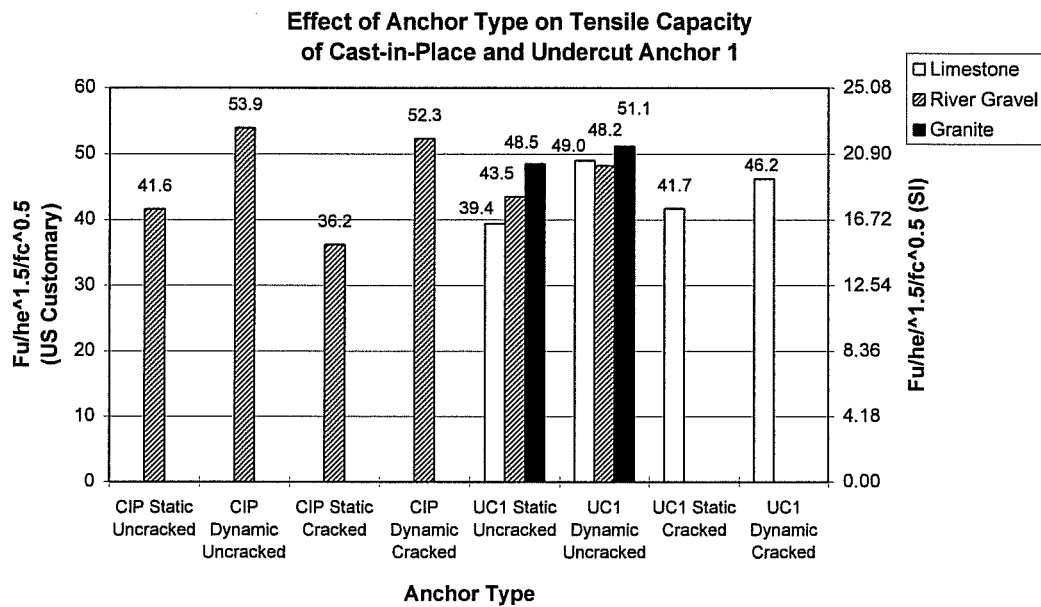
Figure 5.5 Effect of Anchor Type on Normalized Tensile Capacity of Cast-in-Place Anchor and Undercut Anchor 1
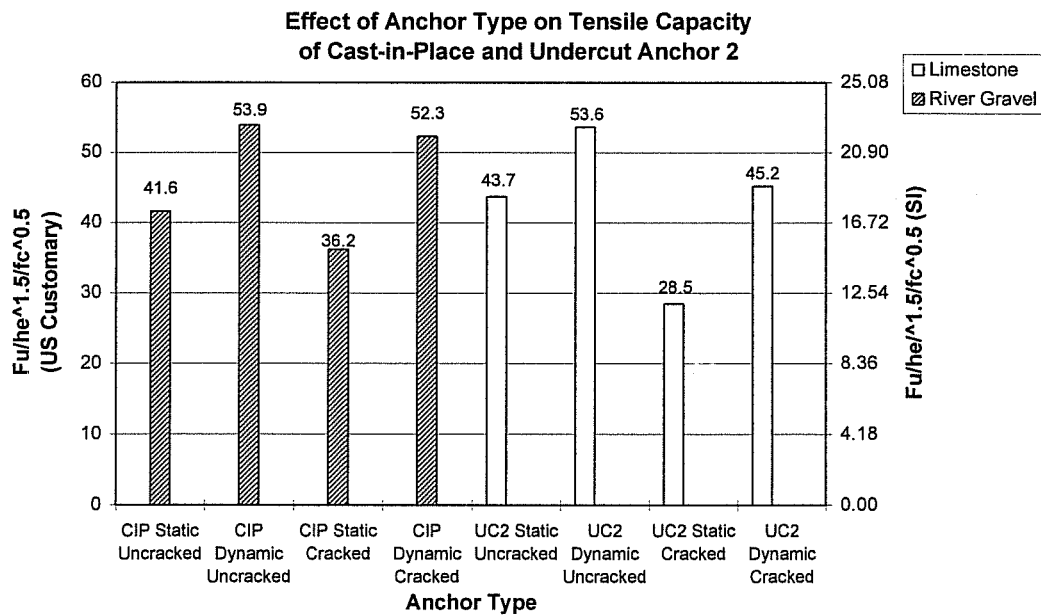
Figure 5.6 Effect of Anchor Type on Normalized Tensile Capacity of Cast-in-Place Anchor and Undercut Anchor 2

**Effect of Anchor Type on Tensile Capacity
of Cast-in-Place and Sleeve Anchor**
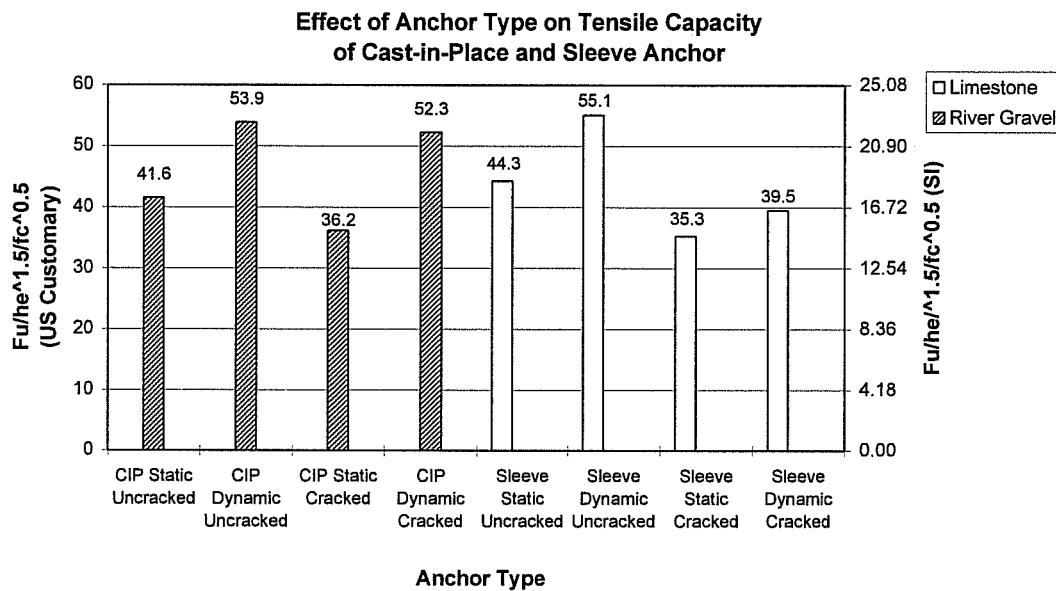
*Figure 5.7 Effect of Anchor Type on Normalized Tensile Capacity of Cast-in-Place
Anchor and Sleeve Anchor*

5.4.2 Effect of Loading Rate on Cast-in-Place versus Post-Installed Anchors Loaded in Tension

In uncracked concrete with limestone or river gravel aggregate, the dynamic tensile capacity of Cast-in-Place, Undercut, and Sleeve Anchors significantly exceeds their static tensile capacity, as shown in Figures 5.5, 5.6, and 5.7. The increases in capacity are as follows: Cast-in-Place, 27%; Undercut Anchor 1 (limestone), 24%; Undercut Anchor 1 (river gravel), 13%; Undercut Anchor 2, 23%; and Sleeve, 24%. In cracked concrete, the dynamic capacity of the Cast-in-Place Anchor and Undercut Anchor 2 is more than 50% higher than the static capacity; there is no significant increase for the Undercut Anchor 1 and the Sleeve Anchor.

5.4.3 Effect of Cracked Concrete on Normalized Tensile Capacities of Cast-in-Place and Post-Installed Anchors

As shown in Figures 5.5, 5.6, and 5.7, the tensile capacity of an anchor in cracked concrete is usually lower than in uncracked concrete. Under static loading, all post-installed anchors except Undercut Anchor 1 have significant reductions in tensile capacity: Cast-in-Place, 15%; Undercut Anchor 1, no significant reduction; Undercut Anchor 2, 35%; and Sleeve, 20%. Under dynamic loading, Cast-in-Place and Undercut Anchor 1 have small reductions in capacity, 3% and 9% respectively. Undercut Anchor 2 and Sleeve Anchor have more significant reductions in capacity, 16% and 28% respectively. Other researchers have found cast-in-place and undercut anchors to have a 25% reduction in tensile capacity under static loading in concrete with a 0.3-mm to 0.4-mm crack width [Eligehausen and Balogh 1995]. However, those tests did not compare otherwise identical anchors in cracked versus uncracked concrete, as in the tests reported here.

The Cast-in-Place Anchor exhibits unusual behavior with respect to the other anchors. In cracked concrete, its static capacity is significantly lower than that of Undercut Anchor 1, significantly higher than that of Undercut Anchor 2, and comparable to that of the Sleeve Anchor. In cracked concrete, the dynamic capacity of Cast-in-Place Anchors is significantly higher than that of Undercut Anchor 1, Undercut Anchor 2, and Sleeve Anchor. Apparently the Cast-in-Place Anchor under dynamic loading is not significantly affected by cracked concrete.

5.4.4 Peak-Load Displacement of Cast-in-Place versus Post-Installed Anchors Loaded in Tension

Figures 5.8, 5.9, and 5.10, show the peak-load displacement of Cast-in-Place Anchor, Undercut Anchor 1, Undercut Anchor 2, and Sleeve Anchor. For all test cases, the displacement at maximum load for the Cast-in-Place Anchor is significantly lower than that of Undercut Anchor 1. In uncracked concrete under static and dynamic loading, the displacement of Cast-in-Place Anchor is significantly lower than the

displacement of Undercut Anchor 2 and Sleeve Anchor. In cracked concrete under static loading, high coefficients of variation for the Undercut Anchor 2 and Sleeve Anchor make it difficult to draw firm conclusions about peak-load displacements. In cracked concrete under dynamic loading, an opposing trend is observed. The displacement of the Cast-in-Place Anchor is larger than that of Undercut Anchor 2 and Sleeve Anchors. For most cases it is evident that the Cast-in-Place Anchor undergoes smaller displacements than the other anchors.
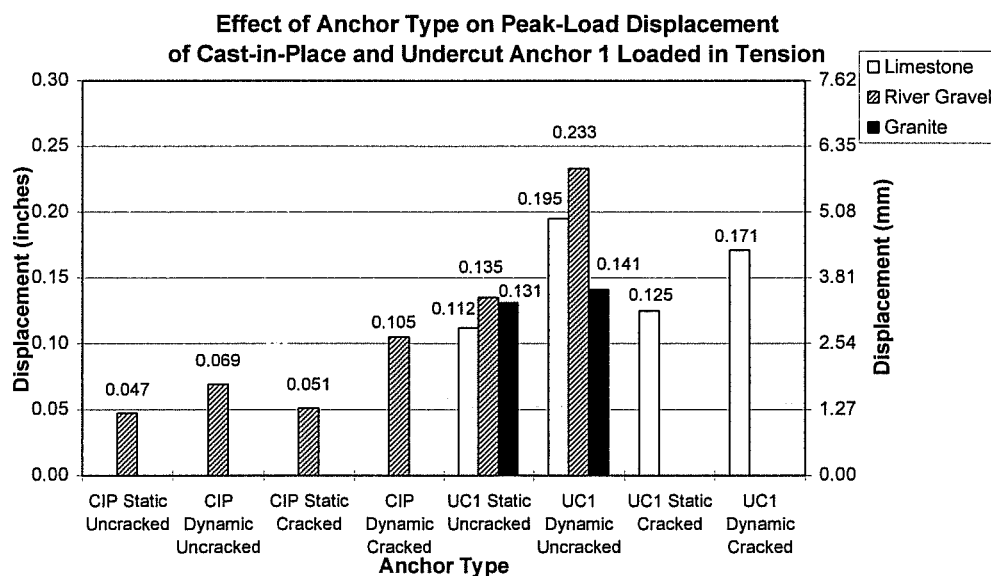
Figure 5.8   Effect of Anchor Type on Peak-Load Displacement of Cast-in-Place Anchor and Undercut Anchor 1 Loaded in Tension

126

**Effect of Anchor Type on Peak-Load Displacement
of Cast-in-Place and Undercut Anchor 2 Loaded in Tension**
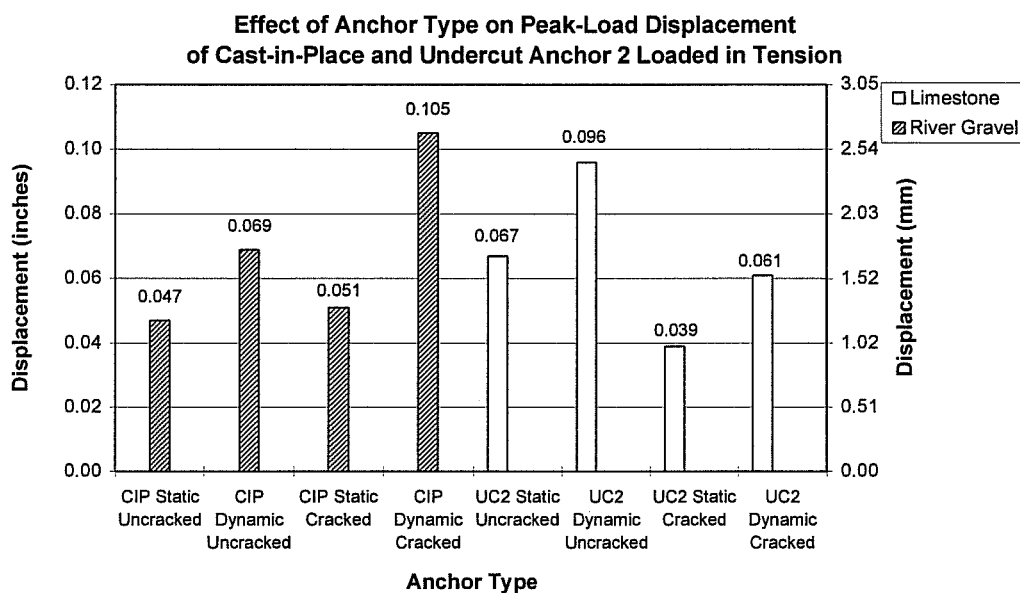
*Figure 5.9 Effect of Anchor Type on Peak-Load Displacement of Cast-in-Place
Anchor and Undercut Anchor 2 Loaded in Tension*

**Effect of Anchor Type on Peak-Load Displacement
of Cast-in-Place and Sleeve Anchor Loaded in Tension**
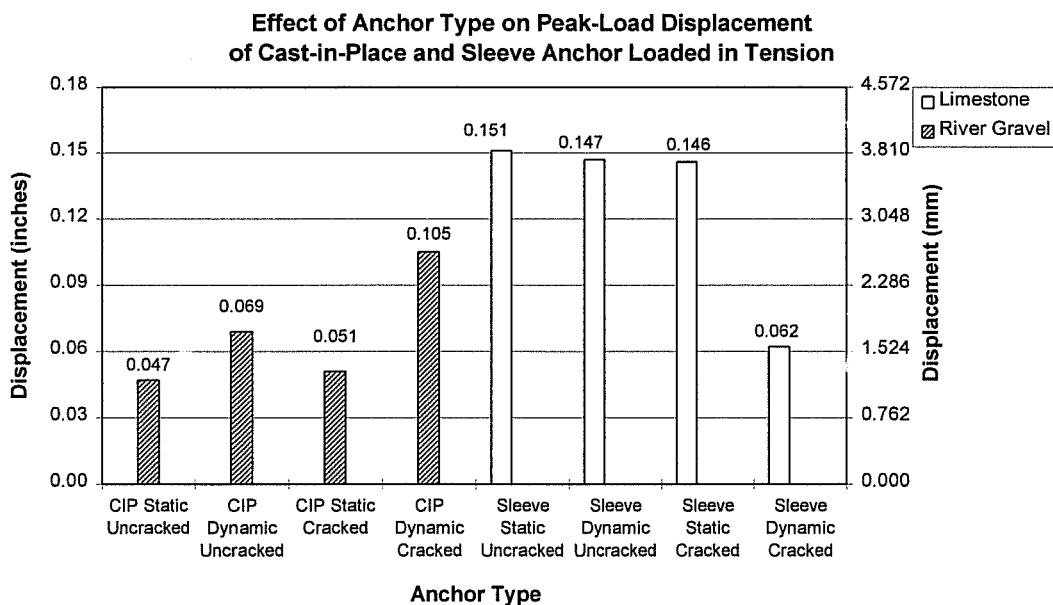
*Figure 5.10 Effect of Anchor Type on Peak-Load Displacement of Cast-in-Place
Anchor and Sleeve Anchor Loaded in Tension*

5.4.5 Effect of Loading Rate on Peak-Load Displacement of Cast-in-Place and Post-Installed Anchors Loaded in Tension

Figures 5.8, 5.9 and 5.10, show that peak-load displacements under dynamic loading are larger than under static loading in cracked and uncracked concrete for all anchors except the Sleeve Anchor. This result is expected since the dynamic capacity is larger than the static capacity. The Sleeve Anchor had coefficients of variation of about 50%, which make the changes in peak-load displacement difficult to interpret.

5.4.6 Effect of Cracked Concrete on Peak-Load Displacement of Cast-in-Place and Post-Installed Anchors Loaded in Tension

As shown in Figures 5.8, 5.9 and 5.10, peak-load displacements are not significantly altered when concrete is cracked. Only the Cast-in-Place Anchor under dynamic loading showed an increase in peak-load displacement in cracked as opposed to uncracked concrete. The coefficients of variation for peak-load displacements are about 20%.

5.4.7 Normalization Coefficient for Cast-in-Place and Post-Installed Anchors

Table 5.3 shows the normalization coefficient in terms of the CC Method, using U.S. customary units. In uncracked concrete, under static loading, a normalization coefficient of 41 is appropriate for the Cast-in-Place, Undercut, and Sleeve Anchors tested. Under dynamic loading, the coefficient can be increased by 20%, to 50. In cracked concrete, the capacity of Cast-in-Place Anchor should be reduced by about 15%, to 35, for static loading; for dynamic loading no reduction should be taken. The capacity of Undercut Anchor 1 in cracked concrete should conservatively be reduced by about 5%. The capacity of Undercut Anchor 2 and Sleeve Anchor should be reduced by about 20% in cracked concrete.

Table 5.3 Normalization Coefficient for Cast-in-Place and Post-Installed Anchors Loaded in Tension

Anchor	Test Type			
	Static Uncracked	Dynamic Uncracked	Static Cracked	Dynamic Cracked
Cast-in-Place Anchor	41	50	35	50
Undercut Anchor 1	41	50	39	47
Undercut Anchor 2	41	50	33	39
Sleeve Anchor	41	50	33	39

5.5 EFFECT OF ANCHOR TYPE ON ADDITIONAL CRACK OPENING FOR TENSILE TESTS

To relate the tensile failure loads and tensile load-displacement behavior of anchors in cracked concrete, to the crack opening behavior of each anchor type, Figures 5.11 and 5.12 show the average additional crack opening values for each set of 5 replicates for various values of load. The original crack width in all cases was 0.3 mm.

As shown in Figure 5.11, Expansion Anchor II, when loaded statically, consistently had the greatest amount of additional crack opening at a given load. The Cast-in-Place Anchor and the Sleeve Anchor consistently had the least. However, the anchors with the least amount of additional crack opening did not have the highest failure load. Note that in Figure 5.11, the highest failure load and highest total additional crack opening corresponded to Undercut Anchor 1. Additional crack opening is believed to be a valid indicator of the splitting force exerted by the anchor. However, for a given crack width, the capacity of the anchor depends strongly on the anchor geometry and internal stiffness characteristics.

Under dynamic loading, as shown in Figure 5.12, Expansion Anchor II again shows the greatest additional crack opening at a given load, and this behavior characteristic correlates well with its failure at relatively low loads. In this case, the Cast-in-Place Anchor generally showed the least additional crack opening at a given load. Once more, the Undercut Anchor 1 showed relatively large additional crack widths, indicating high splitting forces, but also the highest capacity.

Finally, comparison of Figures 5.11 and 5.12 shows that the additional crack opening behavior of anchors differs for dynamic versus static loading. Under static loading, Expansion Anchor II consistently showed the most additional crack opening at a given load, followed by Undercut Anchor 1. Under dynamic loading, although Expansion Anchor II again showed the most additional crack opening at a given load, it was followed by the Sleeve Anchor.

Additional Crack Opening versus Static Tensile Load
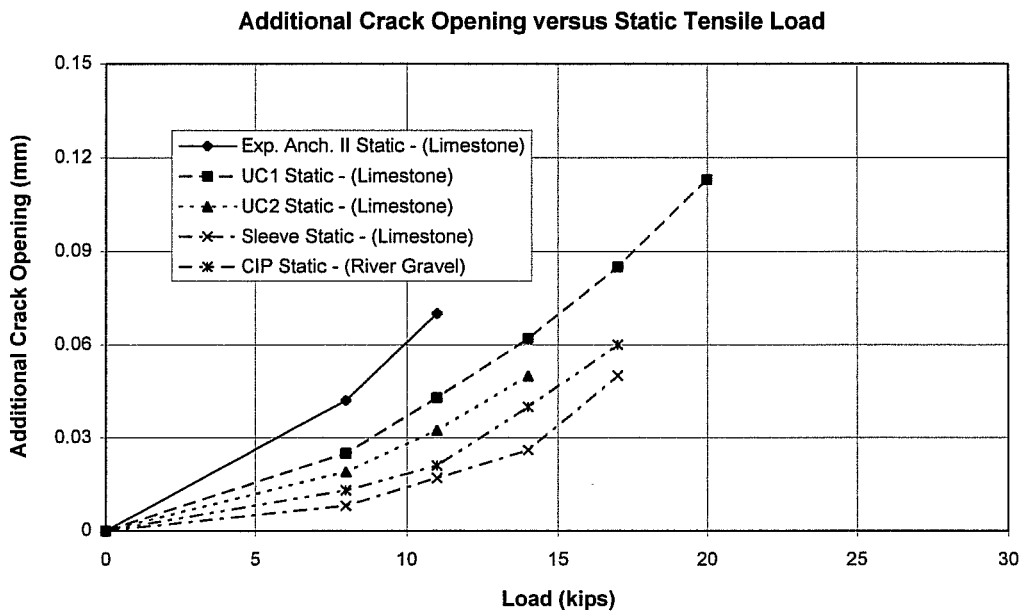
Figure 5.11 Additional Crack Opening versus Tensile Load for Static Loading

Additional Crack Opening versus Dynamic Tensile Load
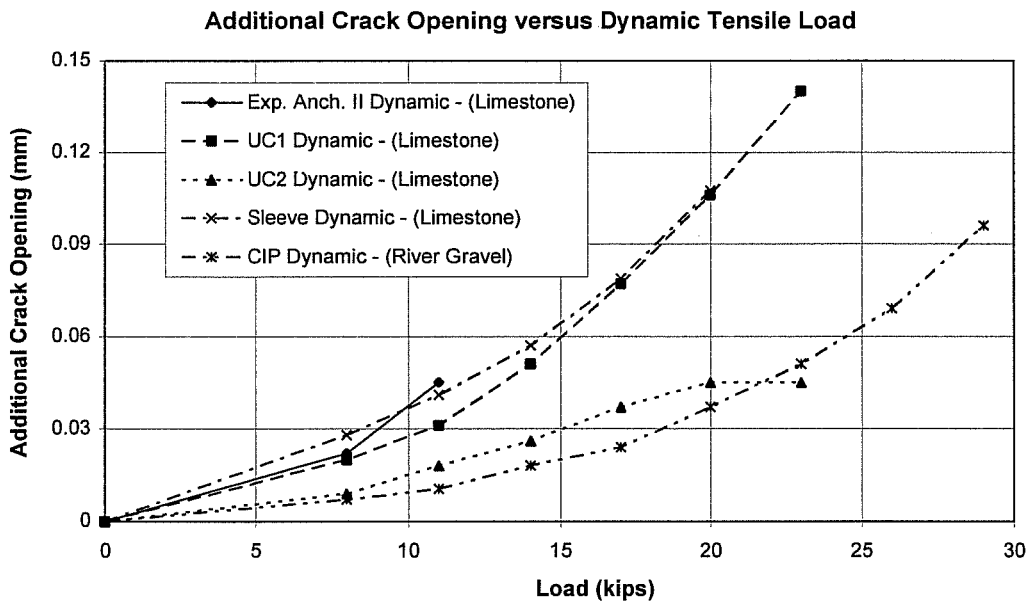
Figure 5.12 Additional Crack Opening versus Tensile Load for Dynamic Loading

5.6 BEHAVIOR OF SINGLE-ANCHOR CONNECTIONS UNDER SHEAR LOADING

This section discusses the behavior of near-edge single-anchor connections under shear loading. The effects of dynamic loading, cracked concrete, and hairpins are evaluated.

5.6.1 Effect of Loading Rate and Cracked Concrete on Concrete Cone Breakout Load of Single-Anchor Connections Loaded in Shear

Figure 5.13 shows the load at concrete cone breakout for Cast-in-Place Anchors loaded in shear. In Figure 5.14 the concrete cone breakout load for single-anchor connections is normalized by the breakout load for anchors under static loading in uncracked concrete, to show the percentage change in capacity for different test conditions. Comparing data for each test type provides an indication of the effect of loading rate and cracked concrete on the concrete cone breakout load.

For all anchors tested, the dynamic capacity exceeds the static capacity. The increase in capacity is approximately 20% for Cast-in-Place Anchors with all hairpin types.

In cracked concrete, the capacity is reduced by approximately 18%, compared with the corresponding uncracked cases. Anchors with far hairpins retain more of their original capacity. This can be attributed to the fact that the concrete between the anchor and the far hairpin is well confined, reducing the effect of cracking. In addition, the reduction in capacity due to cracked concrete is lower for dynamic loading than for static loading. This is due to the fact that the additional crack opening is generally lower under dynamic loading than under static loading.

These observations regarding the effects of cracked concrete and dynamic loading on the concrete cone breakout capacity of anchors loaded in shear, are similar to observations made previously for anchors loaded in tension [Rodriguez 1995].

Effect of Loading Rate and Cracked Concrete on Concrete Cone Breakout Load of Cast-in-Place Anchor Loaded in Shear

Figure 5.13 Effect of Loading Rate and Cracked Concrete on Concrete Cone Breakout Load of Cast-in-Place Single-Anchor Connections Loaded in Shear

Normalized Effect of Loading Rate and Cracked Concrete on Concrete Cone Breakout Loadof Cast-in-Place Anchor Loaded in Shear

Figure 5.14 Normalized Effect of Loading Rate and Cracked Concrete on Concrete Cone Breakout Load of Cast-in-Place Single-Anchor Connections Loaded in Shear

Figure 5.15 shows the load at concrete cone breakout for Expansion Anchor II and Undercut Anchor 1 with no hairpin. In Figure 5.16 the load at concrete cone breakout is normalized by the load in uncracked concrete under static loading, to show the change in capacity for dynamic loading.

The increase in capacity for Expansion Anchor II is 20%, similar to that for Cast-in-Place Anchors. Undercut Anchor 1 has an increase in capacity of only 12%.

The capacity of these post-installed anchors with a far hairpin is lower than the capacity of Cast-in-Place Anchors with a far hairpin. Expansion Anchor II is not as stiff as the Cast-in-Place Anchors. This may partially explain the lower capacity for this anchor. In a few cases, the concrete cracked during installation of Undercut Anchor 1, reducing the capacity of the anchor. In addition, the load transfer mechanism for each anchor type affects the anchor performance.

**Effect of Loading Rate on Concrete Cone Breakout Load of
Expansion Anchor II and Undercut Anchor 1 Loaded in Shear**
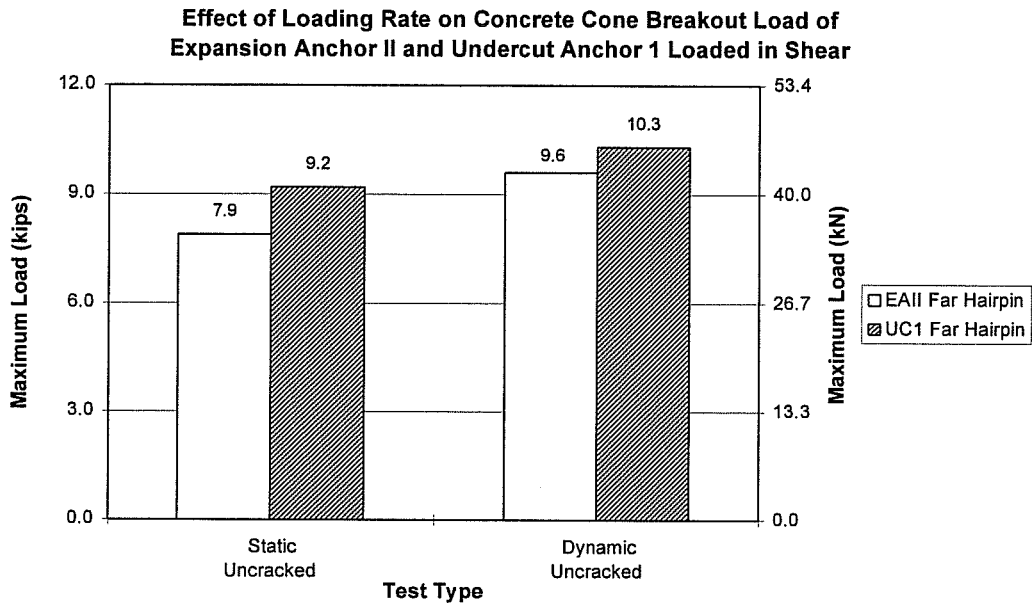
*Figure 5.15 Effect of Loading Rate on Concrete Cone Breakout Load of Expansion
Anchor II and Undercut Anchor 1 Single-Anchor Connections Loaded in Shear*

**Normalized Effect of Loading Rate on Concrete Cone Breakout Load of
Expansion Anchor II and Undercut Anchor 1 Loaded in Shear**
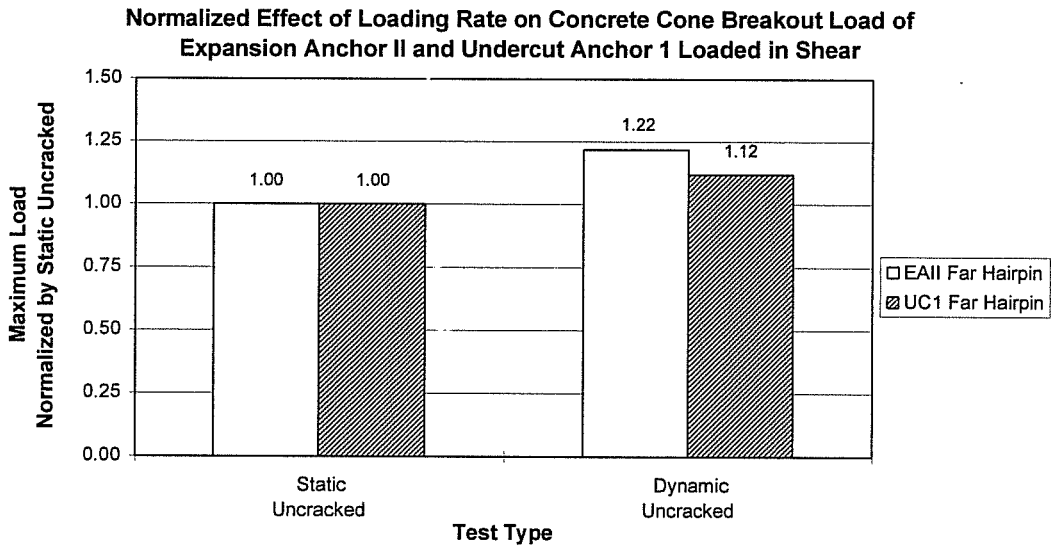
*Figure 5.16 Normalized Effect of Loading Rate on Concrete Cone Breakout Load of
Expansion Anchor II and Undercut Anchor 1 Single-Anchor Connections
Loaded in Shear*

5.6.2 Effect of Loading Rate and Cracked Concrete on Ultimate Failure Load of Single-Anchor Connections Loaded in Shear

Figure 5.17 shows the ultimate capacity for Cast-in-Place single-anchor connections loaded in shear. Figure 5.18 presents the ultimate capacity normalized by the static uncracked capacity to show the percentage change in capacity due to dynamic loading and cracked concrete. The ultimate load is the highest load recorded up to a maximum displacement of 1.2 inches (30 mm).

Ultimate failure of Cast-in-Place single-anchor connections with no hairpin occurred at concrete cone breakout. The conclusions for the effect of loading rate and cracked concrete are the same as discussed in Section 5.6.1.

Connections with hairpins withstood significant additional load after concrete cone breakout. The ultimate load is approximately the same for each test type. Anchors restrained by a hairpin bent around the hairpin until the anchor displaced more than 1.2 inches (30 mm), or until load carrying capacity was reduced because the anchor either fractured, or deformed to such an extent that the capacity decreased. Load capacity at ultimate failure is a function of the steel of the anchor bolt, rather than of the concrete strength; therefore, ultimate failure occurs at approximately the same load regardless of loading rate and cracked concrete.

**Effect of Loading Rate and Cracked Concrete on
Ultimate Load of Cast-in-Place Anchor Loaded in Shear**

*Figure 5.17 Effect of Loading Rate and Cracked Concrete on Ultimate Load of
Cast-in-Place Single-Anchor Connections Loaded in Shear*

**Normalized Effect of Loading Rate and Cracked Concrete on Ultimate
Load of Cast-in-Place Anchor Loaded in Shear**

*Figure 5.18 Normalized Effect of Loading Rate and Cracked Concrete on Ultimate
Load of Cast-in-Place Single-Anchor Connections Loaded in Shear*

The ultimate load of Expansion Anchor II and Undercut Anchor 1 with a far hairpin is shown in Figure 5.19. Figure 5.20 displays the maximum load normalized by the capacity under static loading in uncracked concrete to show the percentage change in capacity due to dynamic loading.

The dynamic capacity of Expansion Anchor II is 14% higher than the static capacity. This is related to the fact that under static loading the anchor tended to pull-out as it displaced. However, under dynamic loading the anchor did not pull-out and eventually failed due to fracture of the anchor.

For Undercut Anchor 1 the ultimate capacity under dynamic loading is essentially equal to the ultimate capacity under static loading. Under static and dynamic loading almost all of the anchors showed a decrease in load-carrying capacity after significant displacement. Only one anchor fractured under dynamic loading. Similar to Cast-in-Place Anchors with hairpins, the ultimate failure of Undercut Anchor 1 is a function of the behavior of the steel of the anchor and is therefore not significantly affected by loading rate.

The ultimate capacity of these post-installed anchors with a far hairpin is lower than the ultimate capacity of Cast-in-Place Anchors with a far hairpin. As mentioned in the previous section this is partially due to the lower stiffness of Expansion Anchor II, cracking at installation of Undercut Anchor 1, and differences in the load transfer mechanism of each anchor.

138
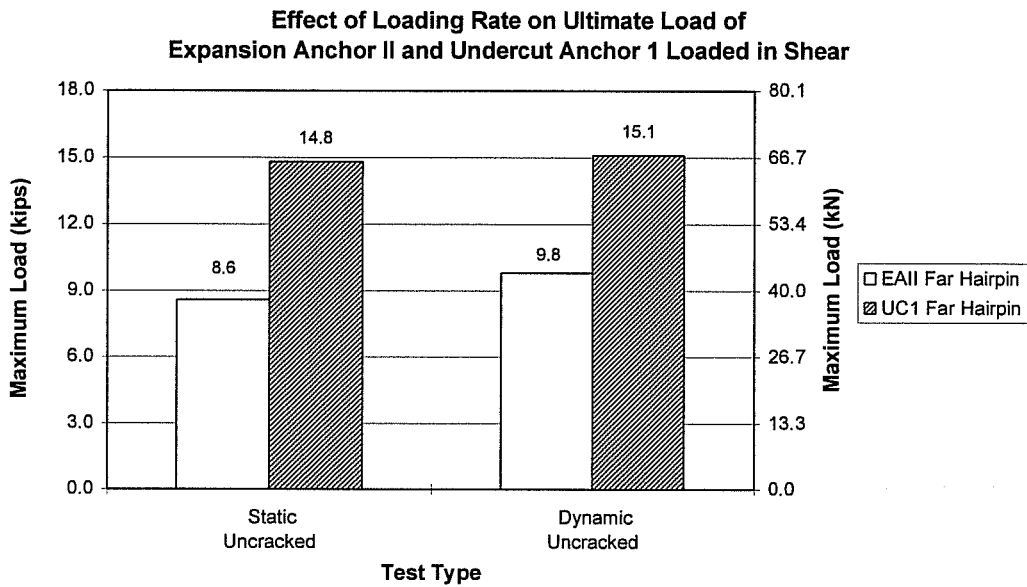
Figure 5.19 Effect of Loading Rate on Ultimate Load of Expansion Anchor II and Undercut Anchor 1 Single-Anchor Connections Loaded in Shear
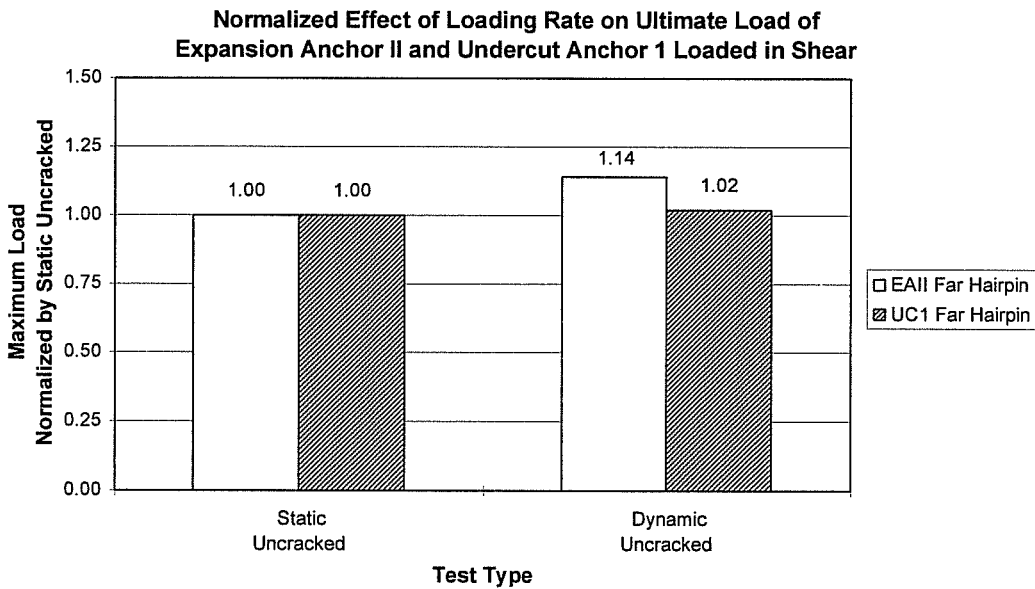
Figure 5.20 Normalized Effect of Loading Rate on Ultimate Load of Expansion Anchor II and Undercut Anchor 1 Single-Anchor Connections Loaded in Shear

5.6.3 Effect of Hairpin on Concrete Cone Breakout Load of Single-Anchor Connections Loaded in Shear

To evaluate the effect of the hairpin, concrete cone breakout loads for each test type with a hairpin were normalized by the corresponding breakout capacities with no hairpin. This provides a way to evaluate how each hairpin configuration affects the load capacity. Figure 5.21 shows the normalized concrete cone breakout capacities for Cast-in-Place Anchors. Actual Concrete cone breakout capacities are shown in Figure 5.13.

The close hairpin increases the load capacity at concrete cone breakout by approximately 37% for all test conditions. The concrete cone breakout load for anchors with a far hairpin increases 30% in uncracked concrete and 50% in cracked concrete. The large increase in capacity for the far hairpin in cracked concrete is related to the fact that the hairpin, in addition to confining the concrete between the hairpin and the anchor, is also effective in reducing the crack opening, thus increasing the load at concrete cone breakout.
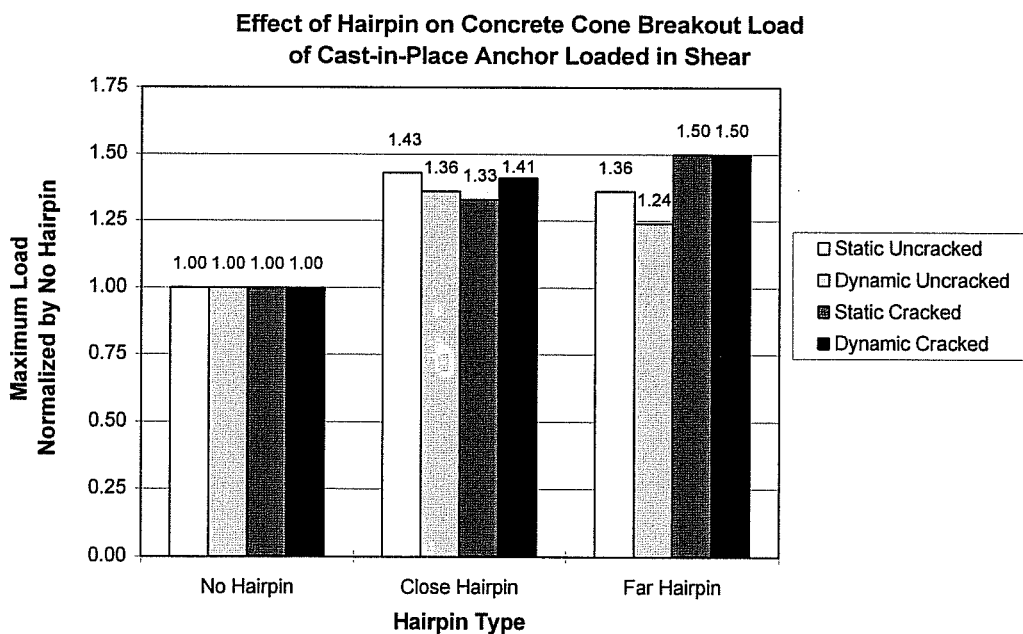
Figure 5.21 Effect of Hairpin on Concrete Cone Breakout Load of Cast-in-Place Single-Anchor Connections Loaded in Shear

5.6.4 Effect of Hairpin on Ultimate Failure Load of Single-Anchor Connections Loaded in Shear

Figure 5.22 shows the ultimate capacity of Cast-in-Place Anchors for each test type, normalized by the ultimate capacity for that test type with no hairpin. Actual ultimate load capacities are shown in Figure 5.17.

The hairpin substantially increases the load-carrying capacity of near-edge single-anchor connections. The increase in capacity is greater for static loading than for dynamic loading, and greater for cracked concrete than for uncracked concrete. Close hairpins increase the ultimate load-carrying capacity 1.9 to 3.0 times. Far hairpins increase the ultimate load-carrying capacity by about 1.6 to 2.2 times, slightly less than the increase for close hairpins.

As mentioned in Section 5.7.2, the ultimate capacity of anchors loaded in shear and restrained by a hairpin is essentially constant. The effect of the hairpin varies because the capacities with no hairpin vary with respect to loading rate and cracked concrete.

**Effect of Hairpin on Ultimate Load
of Cast-in-Place Anchor Loaded in Shear**
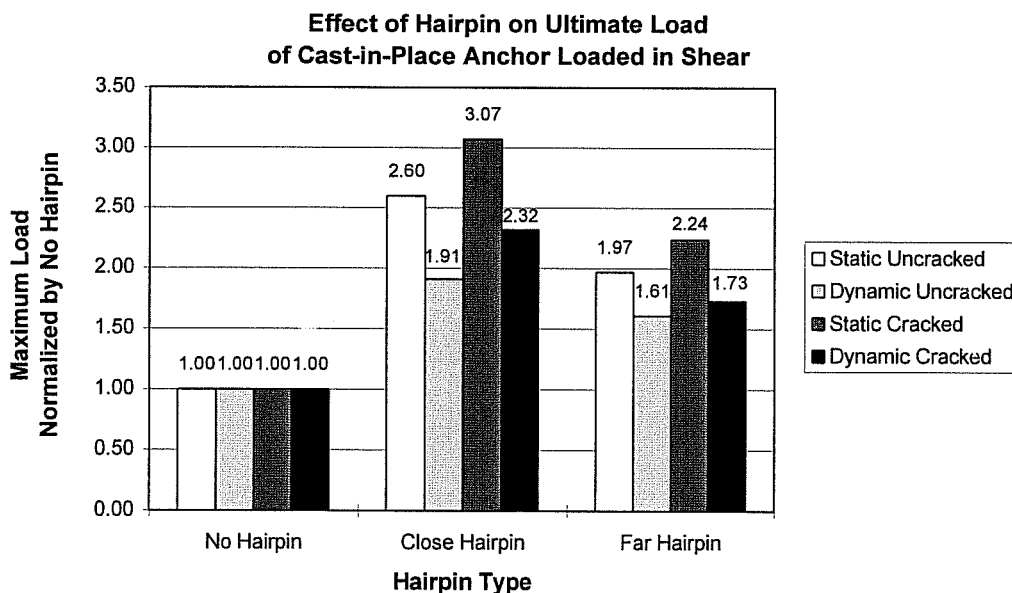
Figure 5.22 Effect of Hairpin on Ultimate Load of Cast-in-Place Single-Anchor Connections Loaded in Shear

5.6.5 Effect of Loading Rate and Cracked Concrete on Displacement at Concrete Cone Breakout of Single-Anchor Connections Loaded in Shear

Figure 5.23 shows the displacements at concrete cone breakout for tests with Cast-in-Place Anchors. It is difficult to draw firm conclusions with respect to displacements because the coefficient of variation for these tests ranged from 13% to 80%, with an average of 38%.

Displacement is directly related to load; larger failure loads should have correspondingly larger displacements. As mentioned in Section 5.6.1, the concrete cone breakout load for anchors with no hairpin, increases approximately 20% under dynamic loading and decreases 15% in cracked concrete. The displacements follow this trend with the exception that in uncracked concrete the displacement under dynamic loading is lower than the displacement under static loading.

The largest displacement for Cast-in-Place Anchors with a close hairpin is in the static uncracked case. Although the load at concrete cone breakout for anchors with a close hairpin is larger than that for anchors with no hairpin, the displacement in cracked concrete for anchors with a close hairpin is less than that for anchors with no hairpin.

Tests with the far hairpin have higher displacements than tests with no hairpin due to the larger concrete cone breakout load. The trend for the far hairpin tests is that displacement increases slightly under dynamic loading and increases significantly in cracked concrete, opposite to the trend for the close hairpin.

Figure 5.24 shows the displacement at concrete cone breakout for Expansion Anchor II and Undercut Anchor 1. Under dynamic loading, the displacement of Expansion Anchor II increases while the displacement of Undercut Anchor 1 decreases. It was difficult to determine the load and displacement at concrete cone breakout for Undercut Anchor 1 since about half of the tests showed no load drop nor sharp change in curvature; however, the displacement should have been larger under dynamic loading.

Effect of Loading Rate and Cracked Concrete on Displacement at Concrete Cone Breakout of Cast-in-Place Anchor Loaded in Shear

Legend: □ No Hairpin, ▨ Close Hairpin, ■ Far Hairpin

Values: CIP Static Uncracked: 0.080, 0.100, 0.104; CIP Dynamic Uncracked: 0.068, 0.087, 0.113; CIP Static Cracked: 0.075, 0.063, 0.145; CIP Dynamic Cracked: 0.114, 0.066, 0.162
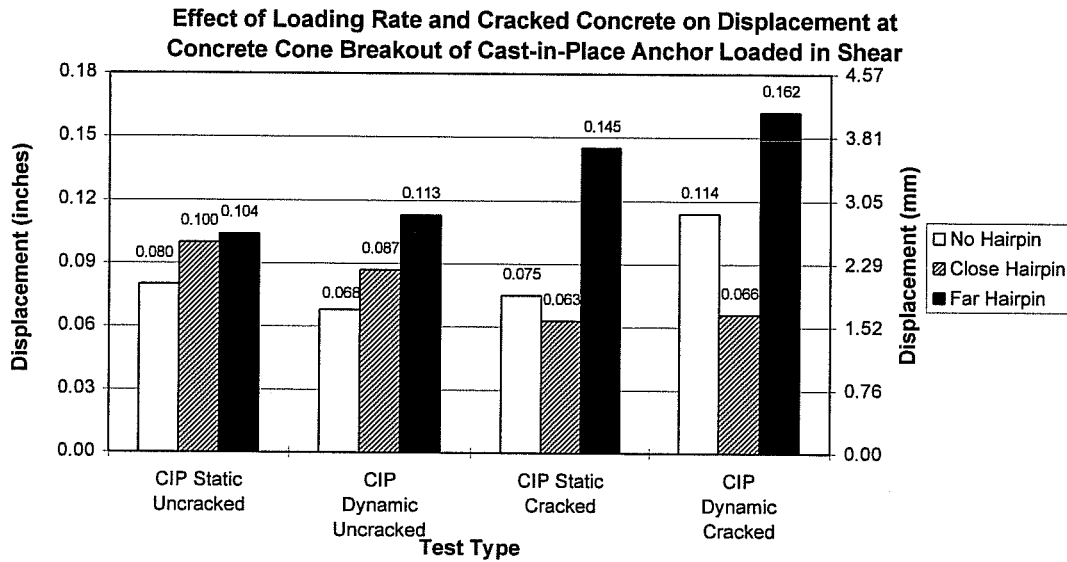
Figure 5.23 Effect of Loading Rate and Cracked Concrete on Displacement at Concrete Cone Breakout of Cast-in-Place Single-Anchor Connections Loaded in Shear

Effect of Loading Rate on Displacement at Concrete Cone Breakout of Expansion Anchor II and Undercut Anchor 1 Loaded in Shear

Legend: □ EAII Far Hairpin, ▨ UC1 Far Hairpin

Values: Static Uncracked: 0.228, 0.205; Dynamic Uncracked: 0.265, 0.181
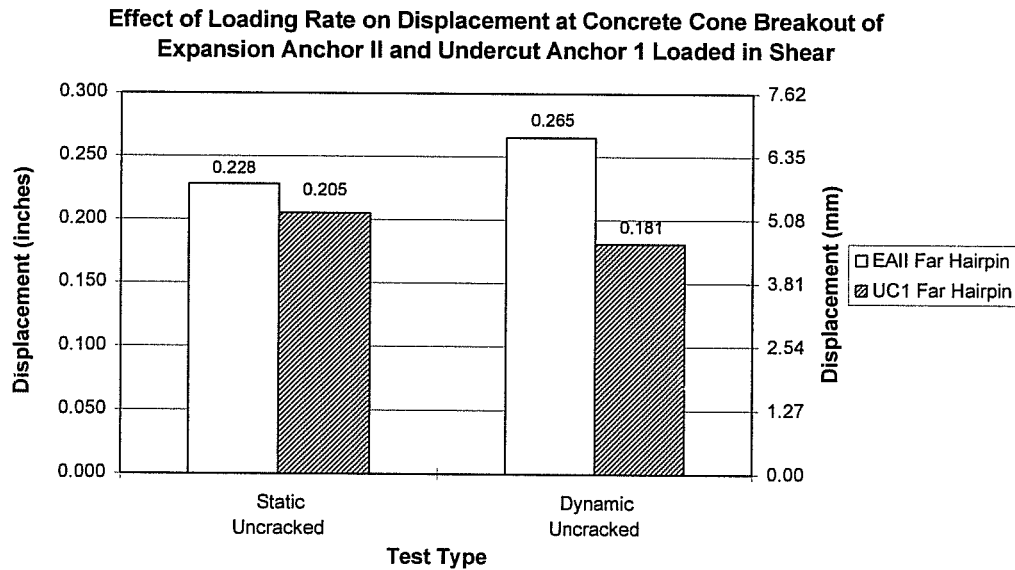
Figure 5.24 Effect of Loading Rate on Displacement at Concrete Cone Breakout of Expansion Anchor II and Undercut Anchor 1 Single-Anchor Connections Loaded in Shear

5.6.6 Effect of Loading Rate and Cracked Concrete on Displacement at Ultimate Failure of Single Anchor Connections Loaded in Shear

Figure 5.25 shows the displacement at ultimate load for Cast-in-Place Anchors. Ultimate load is determined as the maximum load up to a displacement of 1.2 inches (30 mm). Again, it is difficult to draw firm conclusions from the displacement data because the coefficient of variation for each set of tests ranged from 16% to 80% with an average of 35%. However, hairpins dramatically increase the displacement at failure.

Tests with no hairpin fail at concrete cone breakout. Therefore the conclusions for displacement at ultimate are the same as for displacement at concrete cone breakout discussed in Section 5.6.5.

The displacement at ultimate load for anchors with a close hairpin is directly related to the ultimate load. Anchors with higher failure loads have higher displacements. Since the failure load for anchors with a close hairpin was not significantly affected by loading rate and cracked concrete, the displacements are also not significantly affected.

The displacement of anchors with a far hairpin is also directly proportional to the failure load. The test condition which resulted in the highest failure load has the highest displacement.

Figure 5.26 shows the displacement at ultimate failure for Expansion Anchor II and Undercut Anchor 1. Expansion Anchor II shows a decrease of approximately 20% in displacement for dynamic loading as compared with static loading, partially due to the fact that under dynamic loading Expansion Anchor II was more likely to fracture. Also, the coefficient of variation under dynamic loading was large, 70%. Undercut Anchor 1 has approximately the same displacement under static loading and dynamic loading This is because the ultimate load for Undercut Anchor 1 is approximately the same for static and dynamic loading..

Effect of Loading Rate and Cracked Concrete on Displacement at Ultimate Load of Cast-in-Place Anchor Loaded in Shear
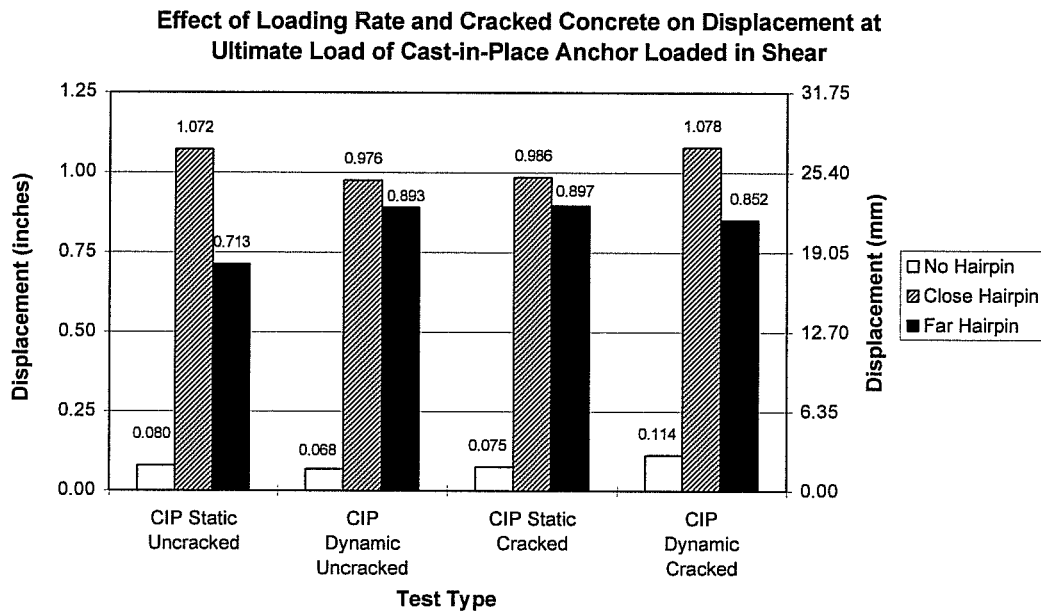
Figure 5.25 Effect of Loading Rate and Cracked Concrete on Displacement at Ultimate Load of Cast-in-Place Single-Anchor Connections Loaded in Shear

Effect of Loading Rate on Displacement at Ultimate Load of Expansion Anchor II and Undercut Anchor 1 Loaded in Shear
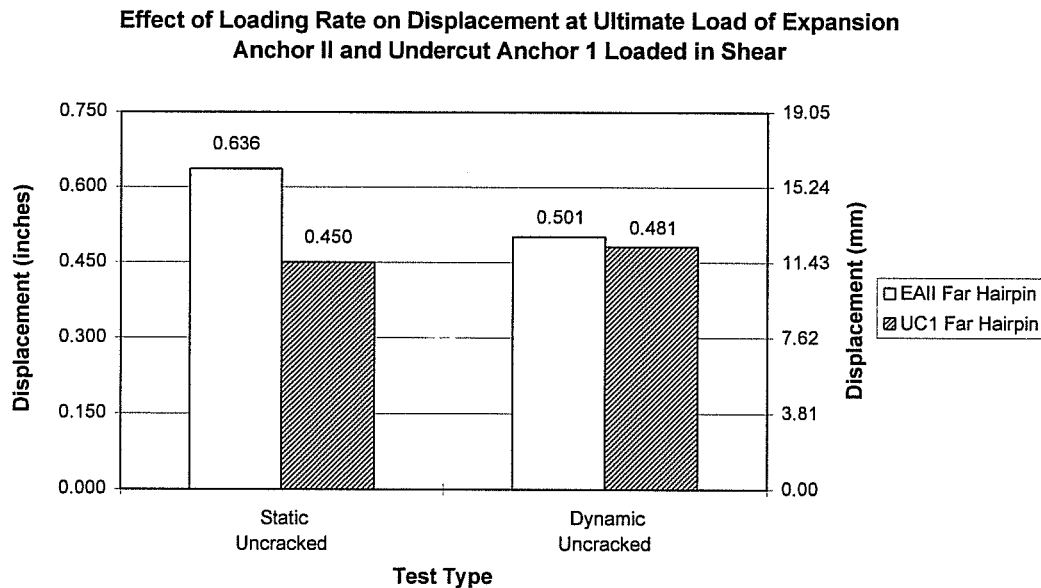
Figure 5.26 Effect of Loading Rate on Displacement at Ultimate Load of Expansion Anchor II and Undercut Anchor 1 Single-Anchor Connections

5.6.7 Effect of Hairpin on Displacement at Ultimate Failure of Single-Anchor Connections Loaded in Shear

As shown in Figure 5.27, the use of hairpins significantly increases the failure displacement of near-edge anchors loaded in shear. The close hairpin increases the displacement at ultimate load between 9.5 and 14.3 times. The far hairpin increases the displacement at ultimate load by about 7.5 to 13.1 times. For both hairpin types, the largest increase in failure displacement occurs for dynamic loading in uncracked concrete, and the smallest increase in failure displacement occurs for dynamic loading in cracked concrete.z

Effect of Hairpin on Displacement at Ultimate Load of Cast-in-Place Anchor Loaded in Shear
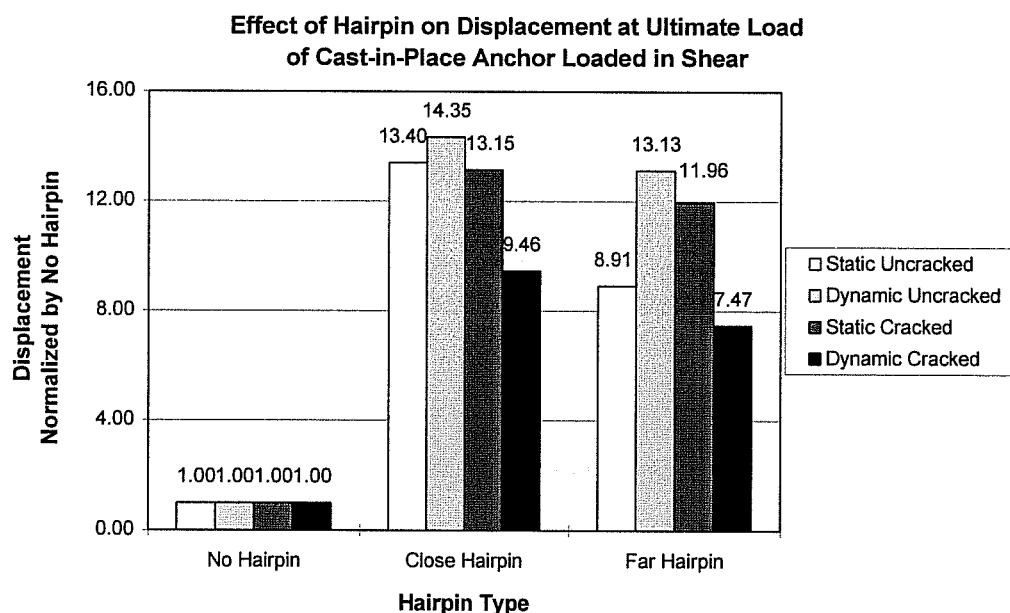
Figure 5.27 Effect of Hairpin on Displacement at Ultimate Load of Cast-in-Place Single-Anchor Connections Loaded in Shear

5.6.8 Normalization Coefficient for Near-Edge Single-Anchor Connections Loaded in Shear

The CC Method, presented in Chapter Two, uses a coefficient of 13 in its equation to predict the shear capacity of near-edge anchors with concrete cone breakout failures. This coefficient is presented as 13 in the literature; however, the conversion from SI units (in which the coefficient is 1.0) to U.S. customary units actually results in a coefficient of 12. Test results for Cast-in-Place Anchors with no hairpin were normalized to determine the coefficient for the design equation that would produce the test results. These coefficients are shown in Figure 5.28. Since tests with a hairpin do not fail by concrete cone breakout, the normalization coefficients based on the CC Method are not useful indicators of behavior. The effect of the hairpin is presented in terms of a multiple of the capacity with no hairpin.

Normalization Coefficient for Cast-in-Place Single-Anchor Connections with No Hairpin Loaded in Shear
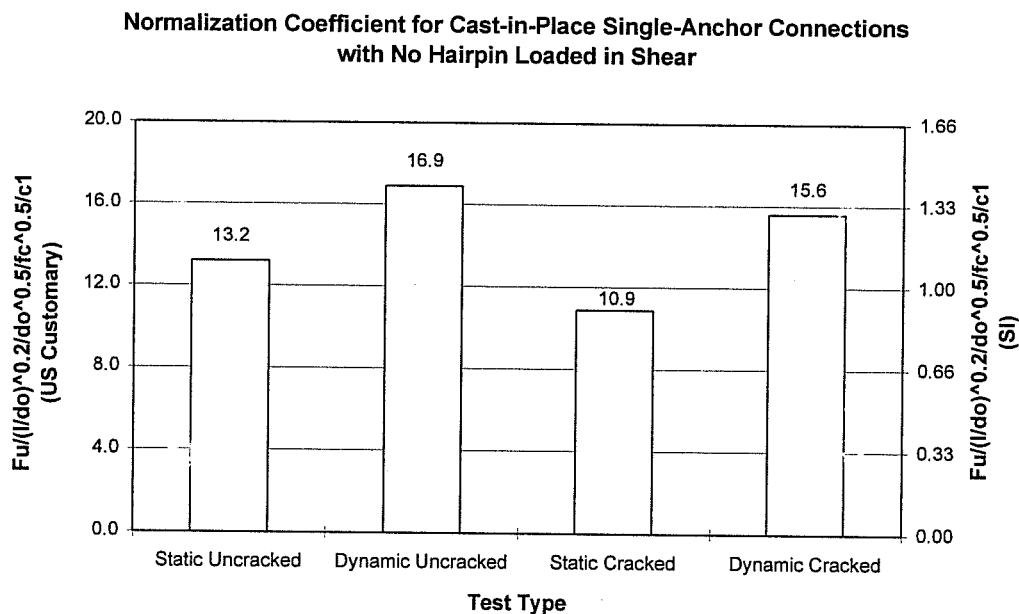
Figure 5.28 Normalization Coefficient for Near-Edge Cast-in-Place Single-Anchor Connections with No Hairpin Loaded in Shear

As shown in Figure 5.28, the static uncracked case is close to the theoretical equation. For anchors under dynamic loading the normalized coefficient can be increased approximately 20%, to 17. A reduction of 15% should be used to account for the change in capacity in cracked concrete.

Ideally, the use of a hairpin should transform the behavior of a near-edge anchor to that of an anchor with no reductions in capacity due to edge effects. In reality, a hairpin with a 1.5-inch (38-mm) concrete cover cannot transform the behavior of a near-edge anchor to that of a far-edge anchor, due to the flexibility of the hairpin and of the anchor. The hairpin can yield and deform, reducing the capacity of the anchor. The anchor flexibility affects the capacity of the connection in two ways: first, after the concrete fails, the anchor bends around a close hairpin until the anchor steel fractures under combined shear and bending; second, for a close or far hairpin the anchor displacement can be so large that the load-carrying capacity is reduced. In this test program, the ultimate capacity of anchors restrained by a hairpin was limited by fracture of the anchor as it deformed around the hairpin, or by large displacement of the anchor. The hairpin was designed so that its strength would not govern the connection capacity. Results for anchors restrained with a hairpin were compared to those for anchors with no hairpin to provide a guideline for estimating the effect of the hairpin for this test program.

For anchors with a hairpin, the concrete cone breakout capacity can be predicted by increasing the capacity determined from the CC Method by a factor of 1.35 To estimate the ultimate capacity of anchors with hairpins, the concrete cone capacity for near-edge anchors can be factored by 2.6 for close hairpins and 2.0 for far hairpins. At ultimate failure, no adjustment should be made for the effects of dynamic loading or cracked concrete, since ultimate failure is a function of steel behavior. These results are specific for this test program.

5.7 BEHAVIOR OF DOUBLE-ANCHOR CONNECTIONS UNDER SHEAR LOADING

Single-anchor connections consisted of a 3/4-inch (19-mm) diameter anchor with an embedment of 4 inches (100 mm) and an edge distance of 4 inches (100 mm). Double-anchor connections were tested with the same anchor diameter and embedment. The front anchor of the double-anchor connection was located at an edge distance of 4 inches (100 mm), the same edge distance as the single-anchor connections. The back anchor of the double-anchor connection was located at a 12-inch (300-mm) edge distance. The spacing between the two anchors was 8 inches (200 mm), twice the embedment.

The objective of the double-anchor tests was to compare single- and double-anchor tests and thereby obtain an indication of the extent of load sharing as well as the interaction of the two anchors. To achieve this objective, a conceptual model was developed and compared with actual test results.

The model hypothesizes that the two anchors are far enough from each other that each behaves individually, and the response of the double-anchor connection is therefore equal to the sum of the responses of each anchor. The model assumes that a rigid baseplate is used so that the displacements of the two anchors are equal to each other and to the displacement of the baseplate. This hypothesis was evaluated by testing a single anchor located in the position of the back anchor of the double-anchor connection. For each test condition, the response of this anchor was added to the response of a single near-edge anchor and compared with the response of a double-anchor connection. Figure 5.29 shows the load-displacement behavior of the back anchor.

**Cast-in-Place Anchor, Static Shear Loading,
Uncracked Concrete, Edge Distance 12 in.**
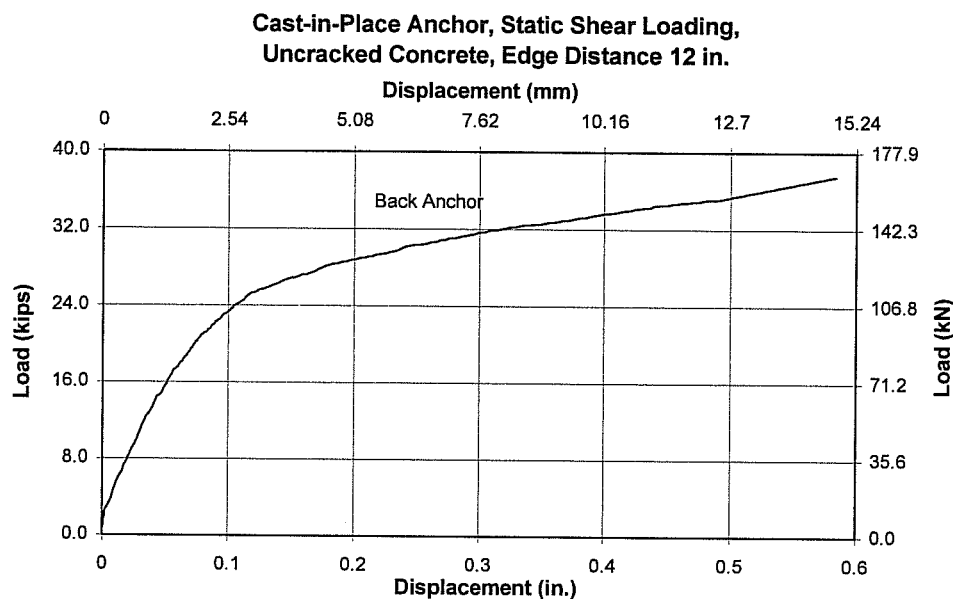
Displacement (mm)

Figure 5.29 Shear Load-Displacement Response of Back Anchor

Figure 5.30 shows the load-displacement results from (A) shear tests on a single near-edge anchor, (B) shear tests on a single back anchor, (C) the summation of those two single anchor tests, and (D) shear tests on a double-anchor connection. All are for anchors under static loading with a close hairpin in uncracked concrete. The summation (C) of the curves for the single-anchor behavior and the back anchor behavior is generally close to (D) the curve for the double-anchor connection. The curve for the double-anchor connection is shifted to the right slightly compared to the curve for the summation of the two anchors because the baseplate slipped during the double-anchor test. In all cases, the results for the summation of the responses of the near-edge single-anchor connection and the back anchor are quite close to the response of the double-anchor connections. Slight differences exist due to differences in slip of the baseplate; however, as seen in Figure 5.30, the curves have the same slope, and the change in curvature (which is used to determine the concrete cone breakout load) occurs at essentially the same load. Similar figures which evaluate the double-anchor model for other test cases are located in the Appendix.

**Evaluation of Double-Anchor Model for Anchors Loaded in Shear
Static Loading, Close Hairpin, Uncracked Concrete**

Displacement (mm)
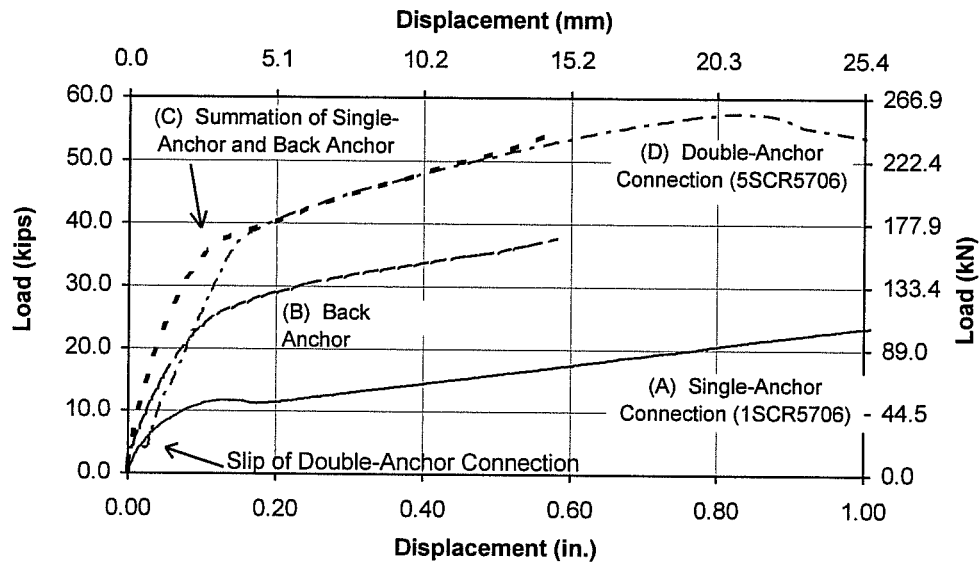
*Figure 5.30 Evaluation of Double-Anchor Model for Anchors Loaded in Shear for
the Case of Static Loading, Close Hairpin, Uncracked Concrete*

It can be confidently concluded that for 3/4-inch (19-mm) diameter anchors spaced at 8 inches (200 mm), the shear behavior of a connection with two anchors will be equal to the summation of the behavior of each individual anchor. For anchors located closer to each other than 8 inches (200 mm) and diameters greater than 3/4 inch (19 mm), this conclusion may not hold.

5.7.1 Effect of Loading Rate and Cracked Concrete on Concrete Cone Breakout Load of Double-Anchor Connections Loaded in Shear

Figure 5.31 shows the load at concrete cone breakout for Cast-in-Place double-anchor connections. In Figure 5.32 the concrete cone breakout load is normalized by the capacity under static loading in uncracked concrete, to show the percentage change due to dynamic loading and cracked concrete.

For all test types the concrete cone breakout load was higher for anchors with a close hairpin. This is because the concrete cone breakout load for the single near-edge anchor is higher with a close hairpin, as discussed in Section 5.6.3.

The effect of loading rate and cracked concrete is less significant for double-anchor connections. The concrete cone breakout load of the front anchor is affected by loading rate and cracked concrete. Dynamic loading increases the tensile strength of the concrete, increasing the cone breakout load. Cracked concrete interrupts the tension ring at the surface of the concrete, reducing the concrete cone breakout load. At concrete cone breakout the back anchor is still elastic. The stiffness of the elastic portion of the curve is not significantly affected by dynamic loading and cracked concrete. Since the back anchor dominates the capacity of the connection, the effect of a hairpin, dynamic loading, and cracked concrete on concrete cone breakout is less dramatic for double-anchor connections than for single-anchor ones. The effect of the hairpin in described in more detail in Section 5.7.3.

152

**Effect of Loading Rate and Cracked Concrete on Concrete Cone
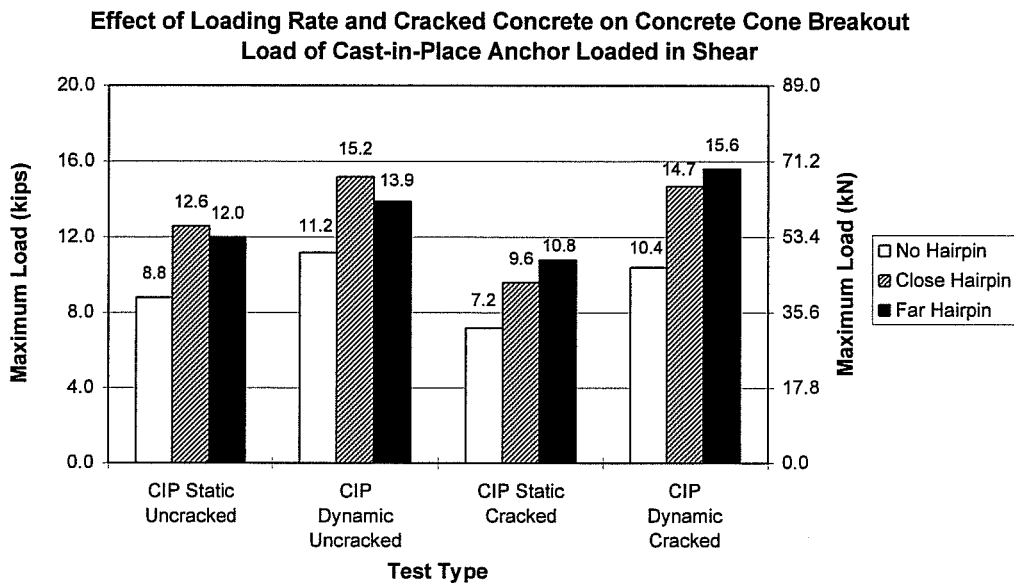Breakout Load of Cast-in-Place Anchors Loaded in Shear**
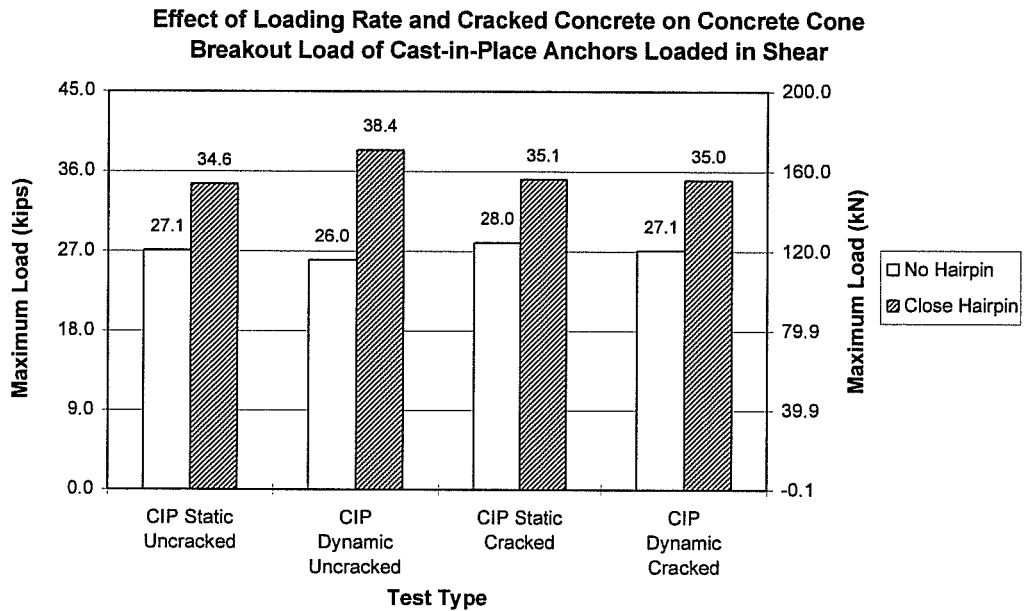
*Figure 5.31 Effect of Loading Rate and Cracked Concrete on Concrete Cone
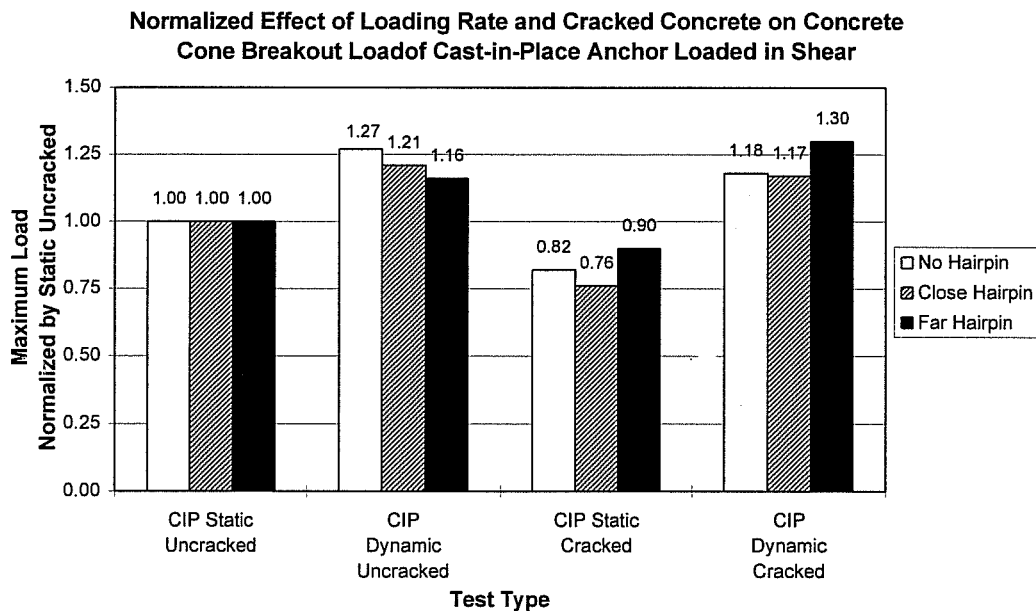Breakout Load of Cast-in-Place Double-Anchor Connections Loaded in Shear*

**Normalized Effect of Loading Rate and Cracked Concrete on Concrete
Cone Breakout Load of Cast-in-Place Anchors Loaded in Shear**
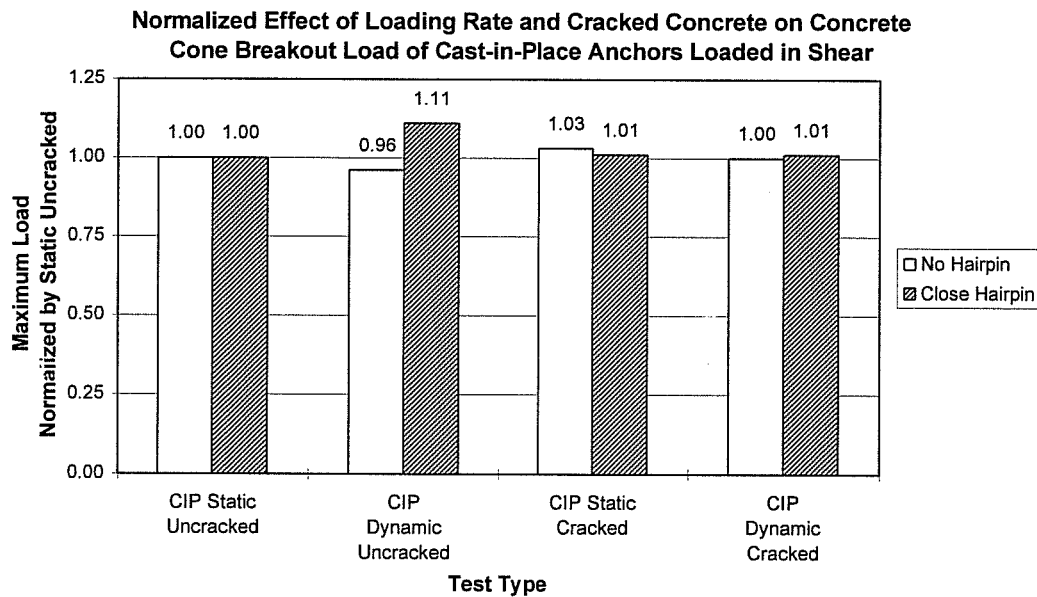
*Figure 5.32 Normalized Effect of Loading Rate and Cracked Concrete on Concrete
Cone Breakout of Cast-in-Place Double-Anchor Connections Loaded in Shear*

5.7.2 Effect of Loading Rate on Ultimate Failure of Double-Anchor Connections Loaded in Shear

Figure 5.33 shows the ultimate capacity of Cast-in-Place double-anchor connections. In Figure 5.34 the ultimate capacity is normalized by the capacity under static loading in uncracked concrete to show the percentage change in capacity due to dynamic loading and cracked concrete.

The ultimate capacity of anchors with a close hairpin is approximately 15 kips (67 kN) larger than the capacity of connections with no hairpin. This is because at the displacement at which the back anchor fails, single-anchor connections with a close hairpin carry approximately 15 kips (67 kN). Single-anchor connections with no hairpin carry no load after concrete cone breakout.

Ultimate failure occurs due to either fracture or pryout of the back anchor. Pryout failure occurred only under static loading, and most often in cracked concrete. Pryout occurred after some yielding of the anchor; therefore, the maximum load for anchors which failed by pryout was not necessarily lower than the maximum load for anchors that failed by fracture. For all tests, the change in capacity is within the coefficient of variation, therefore at ultimate the effect of dynamic loading and cracked concrete is not significant.

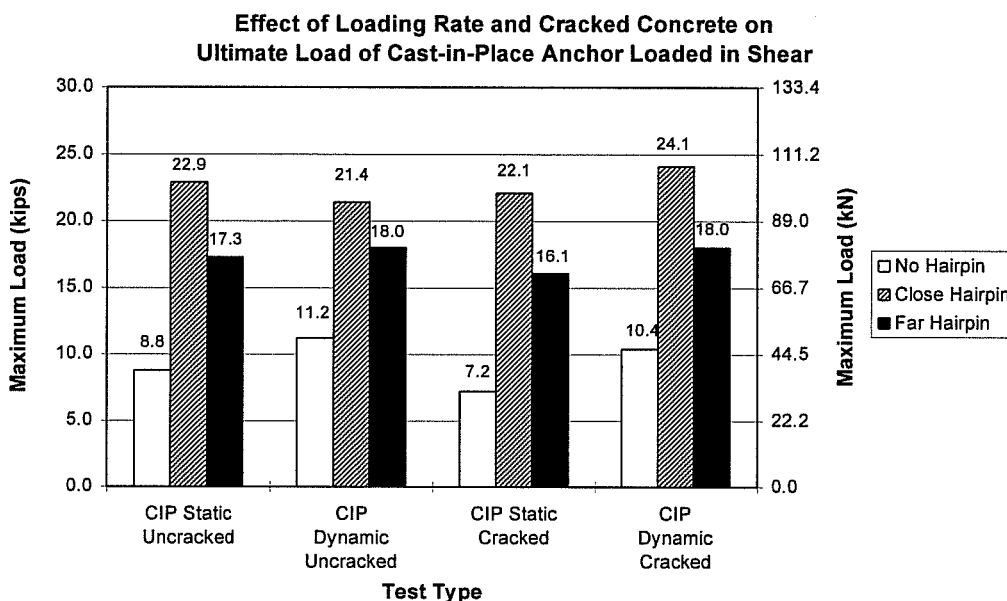**Effect of Loading Rate and Cracked Concrete on Ultimate Load of Cast-in-Place Anchors Loaded in Shear**
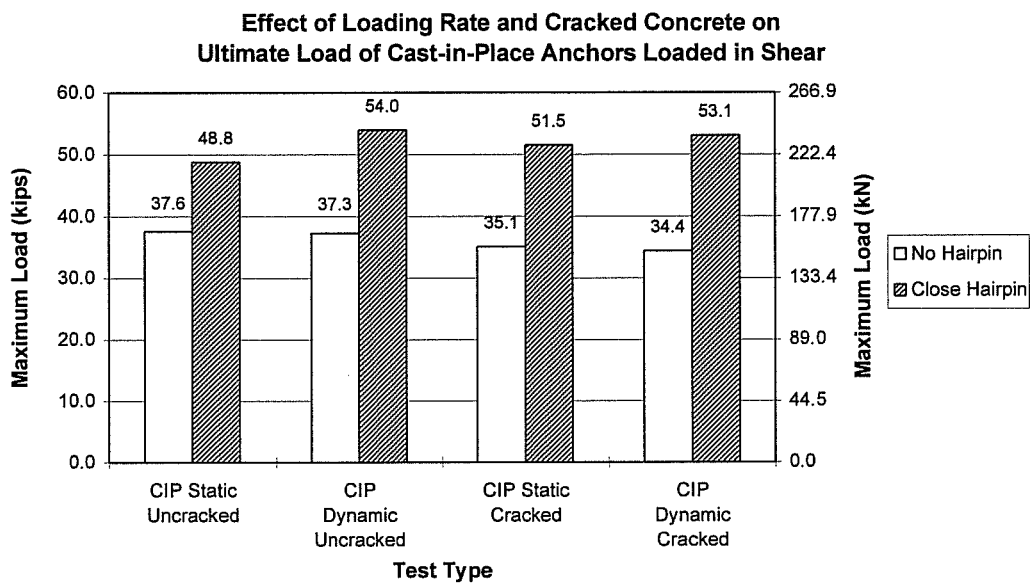
Figure 5.33 Effect of Loading Rate and Cracked Concrete on Ultimate Load of Cast-in-Place Double-Anchor Connections Loaded in Shear

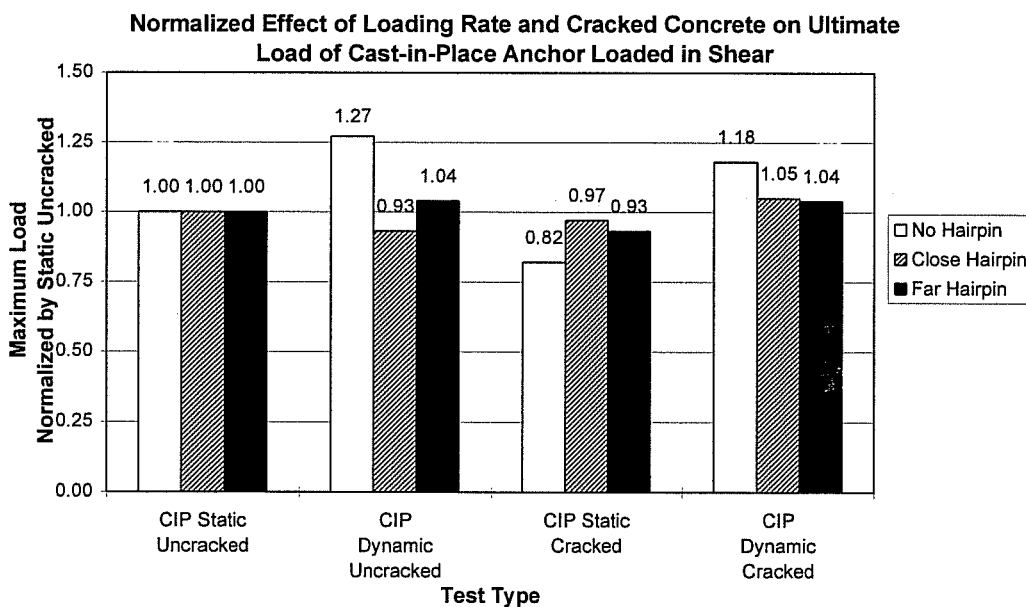**Normalized Effect of Loading Rate and Concrete Condition on Ultimate Load of Cast-in-Place Anchors Loaded in Shear**
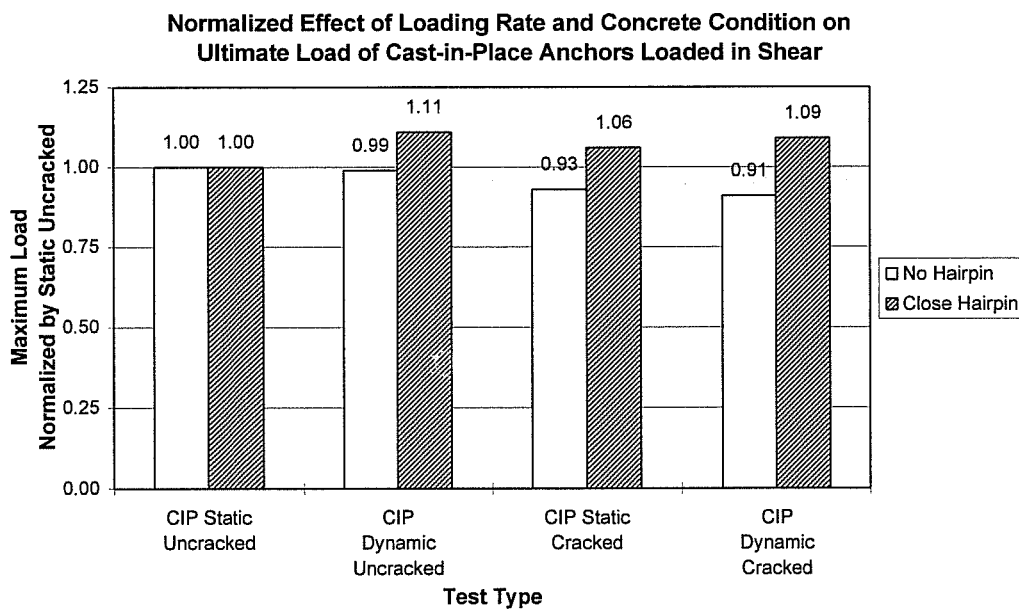
Figure 5.34 Normalized Effect of Loading Rate and Cracked Concrete on Ultimate Load of Cast-in-Place Double-Anchor Connections Loaded in Shear

5.7.3 Effect of Hairpin on Concrete Cone Breakout Load of Double-Anchor Connections Loaded in Shear

Figure 5.35 shows the effect of a close hairpin on the concrete cone breakout load of Cast-in-Place double-anchor connections. As mentioned in Section 5.7.1, the hairpin increases the concrete cone breakout load of the front anchor, thus increasing the concrete cone breakout load for the double-anchor connection.

Effect of Hairpin on Concrete Cone Breakout Load of Cast-in-Place Anchors Loaded in Shear
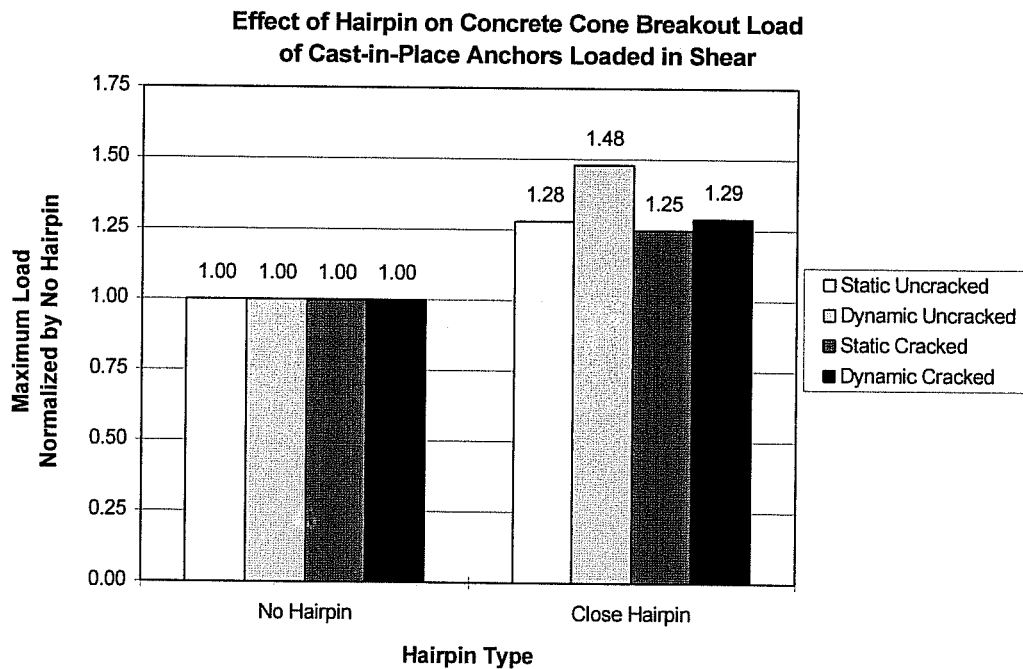
Figure 5.35 Effect of Hairpin on Concrete Cone Breakout Load of Cast-in-Place Double-Anchor Connections Loaded in Shear

5.7.4 Effect of Hairpin on Ultimate Failure Load of Double-Anchor Connections Loaded in Shear

Close hairpins increase the ultimate capacity of double-anchor connections as shown in Figure 5.36. As mentioned in Section 5.7.2, the increase in capacity occurs because the close hairpin enables the front anchor to carry a load of approximately 15 kips (67 kN) after concrete cone breakout.

**Effect of Hairpin on Ultimate Load
of Cast-in-Place Anchors Loaded in Shear**
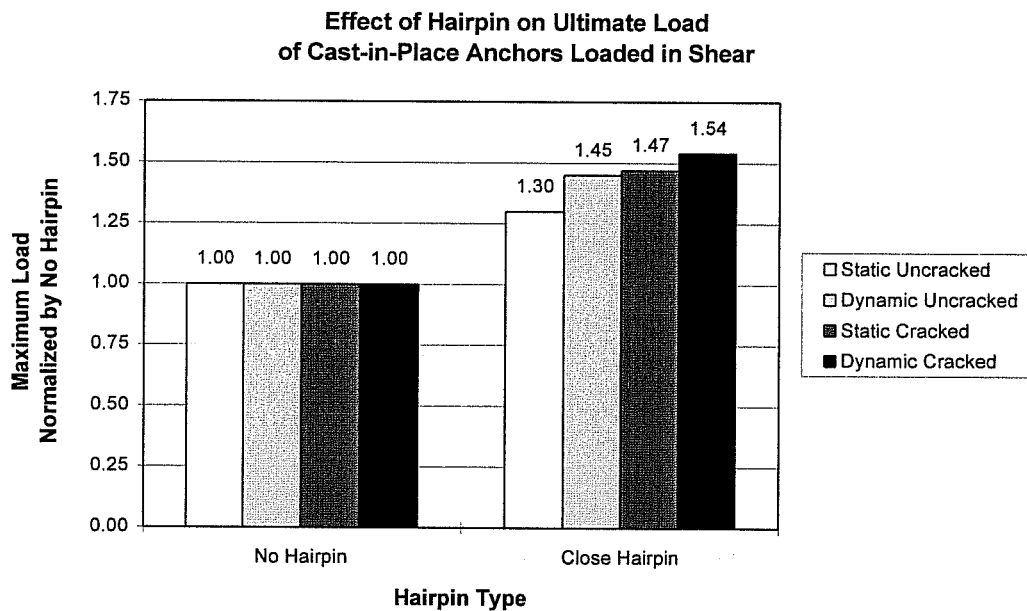
*Figure 5.36 Effect of Hairpin on Ultimate Load of Cast-in-Place
Double-Anchor Connections Loaded in Shear*

5.7.5 Effect of Loading Rate and Cracked Concrete on Displacement at Concrete Cone Breakout of Double-Anchor Connections Loaded in Shear

Figure 5.37 shows the effect of loading rate and cracked concrete on the displacement at concrete cone breakout of Cast-in-Place double-anchor connections. It is difficult to draw firm conclusions from displacement results because the coefficient of variation ranges from 16% to 39% with an average of 24%. For all tests with a close hairpin the displacements are essentially the same. For no hairpin, the displacements are directly related to the load at concrete cone breakout. These displacements are slightly higher than the displacements at concrete cone breakout for single-anchor connections. This is most likely due to differences in slip of the baseplate.

Effect of Loading Rate and Cracked Concrete on Displacement at Concrete Cone Breakout of Cast-in-Place Anchors Loaded in Shear
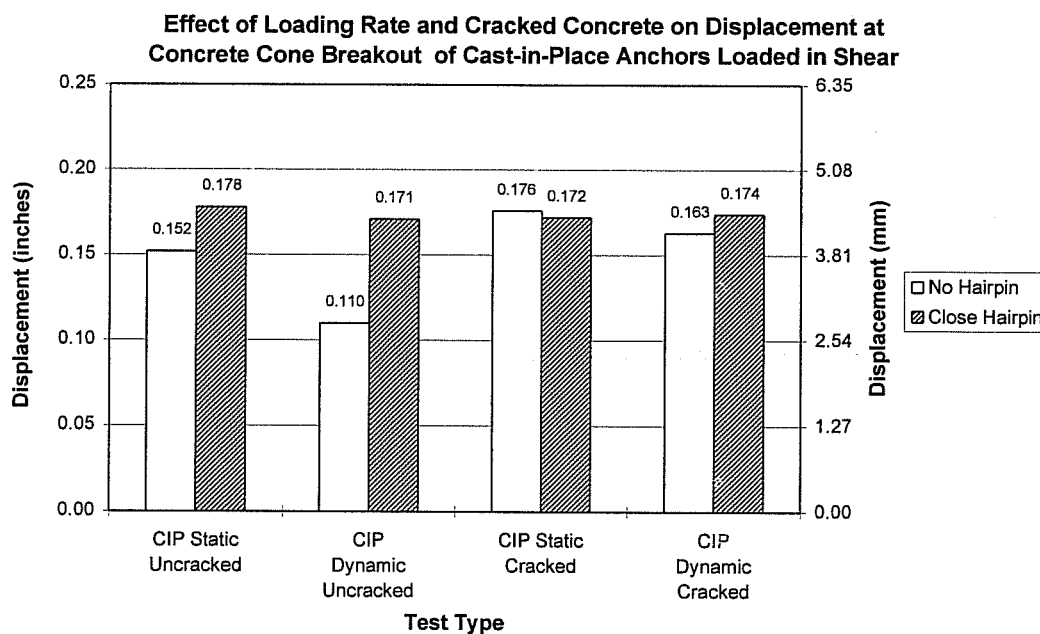
Figure 5.37 Effect of Loading Rate and Cracked Concrete on Displacement at Concrete Cone Breakout of Cast-in-Place Double-Anchor Connections Loaded in Shear

5.7.6 Effect of Loading Rate and Cracked Concrete on Displacement at Ultimate Failure of Double-Anchor Connections Loaded in Shear

Figure 5.38 shows the effect of loading rate and cracked concrete on the displacement at ultimate load of Cast-in-Place double-anchor connections. The coefficient of variation ranges from 9% to 39% with an average of 23%. Anchors with a close hairpin have essentially the same displacement in all cases. With no hairpin, the displacements are directly related to the load at ultimate failure. The displacements at ultimate are lower for double-anchor connections than for single-anchor connections with hairpins because the single anchor can undergo significant deformation around the hairpin, whereas the double-anchor connection fails when the back anchor fractures. The back anchor is less ductile than the front anchor because it is restrained by the concrete, whereas the front anchor is restrained by the hairpin located 1.5 inches (38 mm) from the concrete surface.

Effect of Loading Rate and Cracked Concrete on Displacement at Ultimate Load of Cast-in-Place Anchors Loaded in Shear
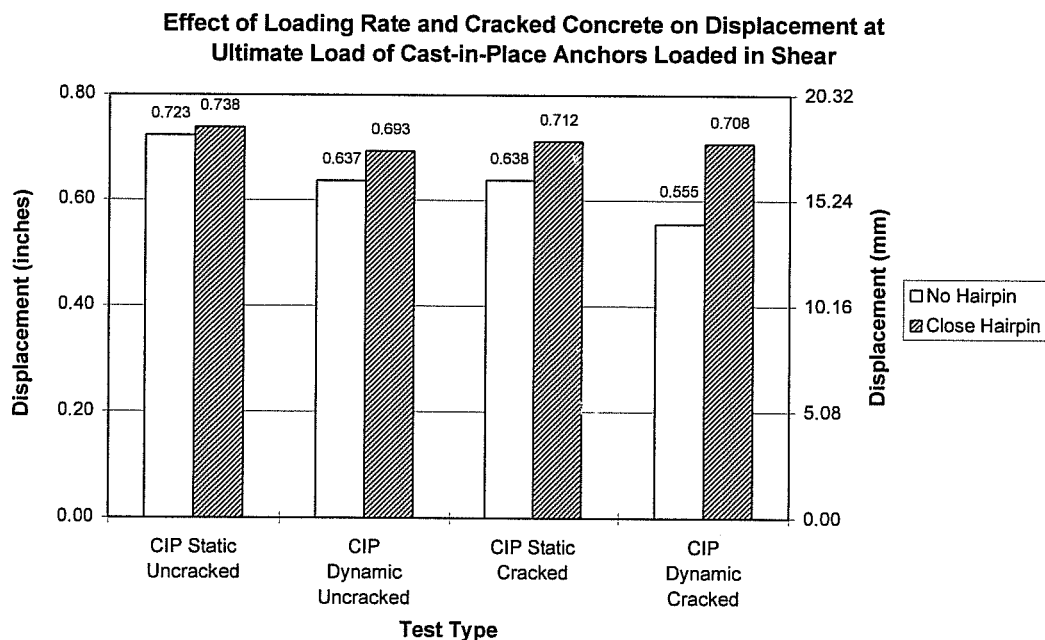
Figure 5.38 Effect of Loading Rate and Cracked Concrete on Displacement at Ultimate Load of Cast-in-Place Double-Anchor Connections Loaded in Shear

5.7.7 Normalization Coefficient for Cast-in-Place Double-Anchor Connections Loaded in Shear

The ultimate capacity of the double-anchor connections tested were not governed by concrete cone breakout, like near-edge single-anchor connections. Therefore, it is not useful to normalize the failure loads with respect to the concrete cone breakout capacity of a single near-edge anchor. Instead, the behavior is best represented by superimposing the load-displacement response of each anchor in the connection, provided that the anchors are separated enough so that they do not influence each other.

CHAPTER SIX

SUMMARY, CONCLUSIONS and RECOMMENDATIONS

6.1 SUMMARY

The U.S. Nuclear Regulatory Commission (NRC) is sponsoring a multi-year research program at The University of Texas at Austin to assess the seismic performance of anchorages used to connect mechanical and electrical equipment to concrete structures. The research includes the study of single anchors under tensile loading, single near-edge anchors loaded in shear, double-anchor connections loaded in shear, and multiple-anchor connections loaded in shear and moment.

This thesis addresses part of the NRC-sponsored research program. Results for single anchors under tensile loading are presented first and compared to results presented in [Rodriguez 1995]. The purpose of these tests was to evaluate the effect of aggregate hardness on the tensile behavior of post-installed anchors, to compare the tensile behavior of cast-in-place anchors to that of heavy-duty post-installed anchors, and to evaluate the effect of anchor type on the additional crack opening for tensile tests. Results for near-edge single anchor connections and double-anchor connections loaded in shear are also presented. Shear behavior of single near-edge anchors is evaluated. In addition, the behavior of double-anchor connections is evaluated and compared to the behavior of near-edge single-anchor connections.

6.2 CONCLUSIONS REGARDING THE EFFECT OF AGGREGATE HARDNESS ON TENSILE CAPACITY OF EXPANSION AND UNDERCUT ANCHORS

1. Aggregate hardness does not significantly affect static or dynamic tensile capacity of Expansion Anchor II in concrete made with limestone or river gravel aggregate. However, the use of granite aggregate produces a slight beneficial change in the ratio of dynamic to static capacity. In concrete made with granite aggregate, dynamic tensile capacity is about 15% higher than the static capacity.

   In concrete made with limestone or river gravel aggregate, dynamic loading increases the tendency for pull-out and pull-through failure, and reduces the tensile capacity of expansion anchors in general, including Expansion Anchor II. The increase in dynamic tensile capacity in granite aggregate occurs because harder aggregate evidently decreases the tendency for pull-out failure and leads to cone failures with higher capacities, due to the higher tensile strength of concrete at high strain rates.

2. Aggregate hardness does affect the static tensile capacity of Undercut Anchor 1. Static tensile capacity of Undercut Anchor 1 in concrete made with granite aggregate is about 23% and 12% higher than in concrete made with limestone or river gravel aggregate, respectively. Unlike behavior in concrete made with limestone or river gravel aggregate, dynamic tensile capacity of Undercut Anchor 1 in concrete made with granite aggregate is about equal to the static capacity.

3. Under static loading, aggregate hardness appears to have no significant effect on the peak-load displacement of Expansion Anchor II. Under dynamic loading, however, peak-load displacement of Expansion Anchor II is significantly lower in concrete with granite aggregate than with limestone or river gravel aggregate. This is probably due to lower pull-out.

4. Aggregate hardness appears to have no significant effect on the static or dynamic peak-load displacement of Undercut Anchor 1.

5. In terms of the CC Method, and using U.S. customary units, a normalization coefficient of 35 is appropriate for Expansion Anchor II under static loading in all aggregates tested, and also for Expansion Anchor II under dynamic loading in concrete with limestone or river gravel aggregate. The normalization coefficient can be increased by a factor of about 1.15, to about 40, for dynamic loading in concrete with granite aggregate. This conclusion refers only to evaluation of the data presented here, and is not intended as a design recommendation.

6. In concrete made with limestone or river gravel aggregate, a normalization coefficient of approximately 41 is appropriate for Undercut Anchor 1 under static loading. This coefficient increases by a factor of 1.17, to about 48, under dynamic loading. In concrete made with granite aggregate, a suitable normalization coefficient for Undercut Anchor 1 is about 48, for dynamic as well as static loading. This conclusion refers only to evaluation of the data presented here, and is not intended as a design recommendation.

6.3 CONCLUSIONS REGARDING THE TENSILE BEHAVIOR OF CAST-IN-PLACE ANCHORS AS COMPARED TO UNDERCUT AND SLEEVE ANCHORS

1. In uncracked concrete made with limestone or river gravel aggregate, the static tensile capacity of Cast-in-Place Anchors is comparable to that of Undercut Anchor 1, Undercut Anchor 2, and Sleeve Anchor. In uncracked concrete made with limestone or river gravel aggregate, the dynamic capacity of Cast-in-Place Anchors is significantly greater than that of Undercut Anchor 1, and comparable to that of Undercut Anchor 2 and Sleeve Anchor.

2. The tensile capacity of an anchor in cracked concrete is usually lower than in uncracked concrete. Under static loading, all post-installed anchors except Undercut Anchor 1 have significant reductions in tensile capacity. The capacity reductions are as follows: Cast-in-Place Anchor, 15%; Undercut Anchor 1, no significant reduction; Undercut Anchor 2, 35%; and Sleeve Anchor 20%. Under dynamic loading both Undercut Anchor 1 and the Cast-in-Place Anchor have no significant reduction in tensile capacity. The capacity reductions are as follows: Cast-in-Place, no significant reduction; Undercut Anchor 1, no significant reduction; Undercut Anchor 2, 16%; and Sleeve Anchor, 28%.

3. In uncracked concrete with limestone or river gravel aggregate, the dynamic tensile capacity of Cast-in-Place, Undercut, and Sleeve Anchors significantly exceeds their static tensile capacity. The increases in capacity are as follows: Cast-in-Place Anchor, 27%; Undercut Anchor 1 (limestone aggregate), 24%; Undercut Anchor 1 (river gravel aggregate), 13%; Undercut Anchor 2, 23%; Sleeve Anchor, 24%; In cracked concrete, the dynamic capacity of Cast-in-Place Anchor and Undercut Anchor 2 is more than 50% higher than the static capacity; there is no significant increase for Undercut Anchor 1 and Sleeve Anchor.

4. For all test cases, the displacement at maximum load for the Cast-in-Place Anchor is significantly lower than that of Undercut Anchor 1. In uncracked concrete under static and dynamic loading, the displacement of Cast-in-Place Anchor is significantly lower than the displacement of Undercut Anchor 2 and Sleeve Anchor. In cracked concrete under static loading, high coefficients of variation for the Sleeve Anchor and Undercut Anchor 2 make it difficult to draw firm conclusions about peak-load displacements. In cracked concrete under dynamic loading, an opposing

trend is observed. The displacement of the Cast-in-Place Anchor is larger than that of Undercut Anchor 2 and Sleeve Anchor. For most cases it is evident that the Cast-in-Place Anchor undergoes smaller displacements than the other anchors.

5. Peak-Load displacements are not significantly altered by the presence of 0.3 mm cracks. Only the Cast-in-Place Anchor under dynamic loading showed an increase in peak-load displacement in cracked concrete.

6. Peak-load displacements under dynamic loading are larger than under static loading in cracked and uncracked concrete for all anchors except the Sleeve Anchor.

7. In terms of the CC Method, and using U.S. customary units, a normalization coefficient of 41 is appropriate for Cast-in-Place, Undercut, and Sleeve Anchors in uncracked concrete under static loading. Under dynamic loading the coefficient can be increased by about 20% (to 50) for all anchors. In cracked concrete the Cast-in-Place anchor should be reduced by about 15% (to about 35) for static loading; for dynamic loading no reduction should be taken. Undercut Anchors should be reduced about 30% (to 35) for static loading, and about 15% (to 42) for dynamic loading in cracked concrete. Sleeve Anchors should be reduced about 20% (to 33) for static loading in cracked concrete, and about 20% (to 39) for dynamic loading in cracked concrete. This conclusion refers only to evaluation of the data presented here, and is not intended as a design recommendation.

6.4 Conclusions Regarding the Effect of Anchor Type on Additional Crack Opening for Tensile Tests

1. Additional crack opening is a valid indicator of the splitting force exerted by an anchor. However, for a given crack width, the capacity of the anchor depends strongly on the anchor geometry and the internal stiffness characteristics. The least amount of crack opening does not necessarily result in the highest failure loads. Expansion Anchor II exhibits the greatest additional crack opening, but fails at low loads. Undercut Anchor 1 has large additional crack opening, indicating high splitting forces, but also as the highest capacity. Additional crack opening behavior differs for static and dynamic loading.

6.5 Conclusions Regarding the Behavior of Single Near-Edge Anchors Loaded in Shear

1. Cast-in-Place Anchors show an increase in concrete cone breakout capacity of 20% under dynamic loading, and a decrease in breakout capacity of 18% in cracked concrete, compared to their static capacity in uncracked concrete. Cast-in-Place Anchors with far hairpins (1-1/4 in. or 32 mm clear from the anchor) have a lower reduction in concrete cone breakout capacity due to cracked concrete, because the concrete between the anchor and the hairpin is well confined, reducing the effect of cracking. In addition, the reduction for cracked concrete is lower for dynamic loading than for static loading because in general, the additional crack opening is lower for dynamic loading than for static loading.

2. Expansion Anchor II behaves similarly to Cast-in-Place Anchors with respect to concrete cone breakout under dynamic loading. Undercut Anchor 1 has the lowest increase in concrete cone breakout capacity under dynamic loading, 12%. This is partly due to concrete cracking during installation of the anchor.

3. The concrete cone breakout capacity of Expansion Anchor II and of Undercut Anchor 1 was lower than that of the Cast-in-Place Anchor. This is due to the lower

stiffness of Expansion Anchor II, to cracking of the concrete during installation of Undercut Anchor 1, and to differences in the load-transfer mechanism for the different anchor types.

4. The ultimate failure load, taken as the ultimate load up to a displacement of 1.2 inches (30 mm), of Cast-in-Place Anchors with close hairpins (placed directly against the anchor) is larger than that of Cast-in-Place Anchors with far hairpins (1-1/4 in. or 32 mm clear from the anchor). Dynamic loading and cracked concrete have essentially no effect on the ultimate failure load of Cast-in-Place Anchors with hairpins because the failure is related to the behavior of the steel, not to the fracture of the concrete.

5. Expansion Anchor II has an increase in ultimate capacity of 14% under dynamic loading as compared to static. This is due to the fact that under static loading the anchor tended to pull out as it displaced, whereas under dynamic loading, the anchor did not pull out and failed by fracture. Undercut Anchor 1 showed no significant change in ultimate capacity due to dynamic loading, because ultimate failure was governed by steel.

6. The ultimate capacity of Expansion Anchor II and of Undercut Anchor 1 was lower than that of the Cast-in-Place Anchor. This is due to the lower stiffness of Expansion Anchor II, to cracking of the concrete during installation of Undercut Anchor 1, and to differences in the load-transfer mechanism for the different anchor types.

7. The hairpin confines the concrete around the anchor and reduces the additional crack opening, thus increasing the concrete cone breakout load of Cast-in-Place Anchors. For anchors with a close hairpin the increase over the no-hairpin case is 37%.

Anchors with a far hairpin have an increase of 30% in uncracked concrete and an increase of 50% in cracked concrete.

8. At ultimate, the close hairpin increases the capacity of Cast-in-Place Anchors under static loading in uncracked concrete by a factor of 2.6. The far hairpin increases the capacity under static loading in uncracked concrete by a factor of 2.0. The ultimate capacity of Cast-in-Place Anchors with hairpins is not affected by dynamic loading or cracked concrete.

9. The displacement at concrete cone breakout of Cast-in-Place Anchors with no hairpin is essentially directly related to load. Tests with higher failure loads have higher displacements, except for the tests under dynamic loading in uncracked concrete. For anchors with a close hairpin, the largest displacement is under static loading in uncracked concrete. The displacement decreases for dynamic loading and cracked concrete. Anchors with a far hairpin show an opposing trend. The largest displacement is for dynamic loading in cracked concrete. Displacements decrease for static loading and uncracked concrete. It is difficult to draw firm conclusions with respect to displacements because the coefficient of variation for displacements averaged 38% in these tests.

10. The displacement at concrete cone breakout increased due to dynamic loading for Expansion Anchor II, but decreased under dynamic loading for Undercut Anchor 1. Reasons for the later behavior are not known.

11. The displacement at ultimate failure (defined as the displacement corresponding to the maximum load up to a maximum displacement of 1.2 inches, 30 mm) for Cast-in-Place Anchors with hairpins was directly related to the ultimate load. Higher

loads had correspondingly higher displacements. The displacements showed no effect of dynamic loading or cracked concrete since the ultimate load was not affected by these changes.

12. At ultimate failure the displacement of Expansion Anchor II was lower under dynamic loading than static. This could be attributed to fracture of the anchor under dynamic loading at low displacements. However, it is difficult to make a firm conclusion because the coefficient of variation for displacements of Expansion Anchor II under dynamic loading was 70%. Undercut Anchor 1 showed no change in displacement under static and dynamic loading since the ultimate load was not affected by dynamic loading.

13. The hairpin allows the Cast-in-Place Anchor to achieve significant ductility. For anchors with a close hairpin the displacement at ultimate failure is increased by 9.5 to 14.3 times over the ultimate displacement with no hairpin. Anchors with a far hairpin have a slightly lower increase of 7.5 to 13.1 times.

14. In terms of the CC Method, and using U.S. customary units, a normalization coefficient of 13 is appropriate for single near-edge Cast-in-Place Anchors loaded in shear with no hairpin. The coefficient should be increased 20% (to 17) under dynamic loading. A decrease of 15% should be used in cracked concrete. This conclusion refers only to evaluation of the data presented here, and is not intended as a design recommendation.

15. The ultimate capacity of anchors with hairpins is not governed by concrete cone breakout. Therefore, normalization coefficients based on the CC Method are not useful indicators of behavior. Instead, the capacity of an anchor with a hairpin is best represented as a multiple of the capacity with no hairpin. For anchors with a

hairpin, the concrete cone breakout capacity can be predicted by increasing the capacity determined from the CC Method by a factor of 1.35. To estimate the ultimate capacity of anchors with hairpins, the concrete cone capacity for near edge anchors can be factored by 2.6 for close hairpins and 2.0 for far hairpins. At ultimate failure, no adjustment should be made for the effects of dynamic loading and cracked concrete. These results are specific to this test program.

6.6 CONCLUSIONS REGARDING THE BEHAVIOR OF DOUBLE-ANCHOR CONNECTIONS LOADED IN SHEAR

1. The behavior of a double anchor connection consisting of 3/4-inch (19-mm) diameter Cast-in-Place Anchors embedded 4 inches (100 mm) with the front anchor at a 4-inch (100-mm) edge distance and the back anchor at a 12-inch (300-mm) edge distance can be determined by superimposing the load-displacement behaviors of each anchor. This conclusion is specific to this test program and may not hold for larger anchors, smaller embedments, or closer spacing.

2. The effect of loading rate and cracked concrete on the concrete cone breakout load of double-anchor connections is less significant than the effect on single-anchor connections. The capacity of the front anchor increases 20% for dynamic loading and decreases 15% for cracked concrete. The back anchor, however, is not significantly affected by dynamic loading or cracked concrete. Since the behavior of the back anchor dominates the response of the double-anchor connection, the effects of dynamic loading and cracked concrete are decreased.

3. The ultimate load of Cast-in-Place double-anchor connections with a close hairpin is approximately 15 kips (67 kN) larger than the capacity with no hairpin, because at the displacement at which the back anchor fractures, the front anchor with a close

hairpin can carry about 15 kips (67 kN). With no hairpin, the front anchor cannot sustain any load after concrete cone breakout. Since the ultimate failure load of the front and the back anchors is not affected by loading rate and cracked concrete, the behavior of the double-anchor connection is also not affected.

4. The concrete cone breakout load of single-anchor connections is increased with a close hairpin. Therefore, the concrete cone breakout load of the double-anchor connection is increased for connections with a close hairpin.

5. The displacement at concrete cone breakout for double-anchor connections with no hairpin is directly related to the load at concrete cone breakout. At concrete cone breakout the displacement of double-anchor connections with a close hairpin is essentially the same for all test types. The displacement at concrete cone breakout for double-anchor connections is slightly higher than the displacement for single-anchor connections. This is most likely due to differences in slip of the baseplate.

6. The displacement at ultimate failure of double-anchor connections with no hairpin is directly related to ultimate load. For anchors with a close hairpin the displacement at ultimate is approximately the same for each test type. The displacements at ultimate are lower for double-anchor connections than for single-anchor connections with hairpins because the single anchor can undergo significant deformation around the hairpin, whereas the double-anchor connection fails when the back anchor fails by fracture or pryout.

7. The ultimate capacities of the double-anchor connections tested here were not governed by concrete cone breakout. Therefore, it is not useful to normalize these loads by the breakout capacity of a single near-edge anchor. Instead, the behavior is best represented by the summation of the load-displacement response of each anchor in the connection, provided that the anchors are spaced far enough from each other so that the behavior of one anchor does not influence the behavior of the other.

6.7 RECOMMENDATIONS FOR EVALUATION AND DESIGN OF ANCHOR CONNECTIONS

1. The results presented in this thesis can be used for the evaluation of single anchors under tensile loading, single near-edge anchors under shear loading, and double-anchor connections under shear loading. While not in the form of design recommendations, they could be used as a basis for such recommendations.

6.8 RECOMMENDATIONS FOR FUTURE RESEARCH

1. The research presented here evaluates the effect of a 0.3-mm initial crack width on the behavior of anchors loaded in shear and tension. Tests in concrete with larger crack widths would be useful to determine the rate of reduction in capacity with increasing initial crack width.

2. This effect of a cast-in-place hairpin on the behavior of anchors loaded in shear is discussed in this thesis. Many near-edge anchors are not restrained by a hairpin. Further research should be conducted to develop effective post-installed hairpins, and to evaluate the effect of those post-installed hairpins on the behavior of near-edge connections loaded in shear.

3. The front and back anchors of the double-anchor shear connections tested here were spaced at 2 embedments, and did not affect each others' performance. Therefore, the behavior of the double-anchor connection was essentially the superposition of the behavior of each individual anchor. The critical spacing at which two shear anchors begin to affect each other's performance should be determined for different anchor types, diameters, and effective embedments.

4. To achieve more accurate load-displacement curves for shear tests, it would be helpful to measure the position of the anchor shank with respect to the hole in the baseplate. This would allow the load-displacement curves for each anchor to be adjusted for the effect of initial hole tolerance.

5. When conducting shear tests in cracked concrete, it is important to measure the initial crack width to ensure conformance with the desired value. However, because the crack width does not change significantly during testing, it need not be monitored once the crack width has been correctly established.

The conclusions presented are those of the author, and are not to be considered as NRC recommendations or policy.

APPENDIX A

RESULTS FOR TASK 1

Results for Series 1-9

Anchor	Test Number	Loading	Diameter		Effective Embedment h_e		f'_c		Normalized f'_c		Normalized F_u		Displacement		k_{nc}		Failure Mode
			in.	(mm)	in.	(mm)	psi	(MPa)	psi	(MPa)	kips	(kN)	in.	(mm)	US	(SI)	
EAII	9SKG5701	Static	0.75	(19)	3.44	(87.3)	4315	(29.8)	4700	(32.4)	13.4	(59.6)	0.154	(3.91)	30.7	(12.8)	cone
	9SKG5702	Static	0.75	(19)	3.44	(87.3)	4315	(29.8)	4700	(32.4)	14.7	(65.4)	0.232	(5.89)	33.6	(14.1)	cone
	9SKG5703	Static	0.75	(19)	3.44	(87.3)	4315	(29.8)	4700	(32.4)	16.0	(71.2)	0.150	(3.81)	36.6	(15.3)	cone
	9SKG5704	Static	0.75	(19)	3.44	(87.3)	4315	(29.8)	4700	(32.4)	16.6	(73.8)	0.190	(4.83)	38.0	(16.0)	cone/pull-through
	9SKG5705	Static	0.75	(19)	3.44	(87.3)	4315	(29.8)	4700	(32.4)	14.4	(64.1)	0.115	(2.92)	33.0	(13.8)	cone
									Average		15.0	(66.8)	0.168	(4.27)	34.4	(14.4)	
									COV		8.53		26.44		8.52		
UC1	9SMG5706	Static	0.75	(19)	4	(100)	4315	(29.8)	4700	(32.4)	27.3	(121)	0.114	(2.90)	49.8	(20.8)	cone
	9SMG5707	Static	0.75	(19)	4	(100)	4315	(29.8)	4700	(32.4)	23.1	(103)	0.126	(3.20)	42.1	(17.6)	cone
	9SMG5708	Static	0.75	(19)	4	(100)	4315	(29.8)	4700	(32.4)	26.7	(119)	0.152	(3.86)	48.7	(20.4)	cone
	9SMG5709	Static	0.75	(19)	4	(100)	4315	(29.8)	4700	(32.4)	28.7	(128)	0.100	(2.54)	52.3	(21.9)	cone
	9SMG5710	Static	0.75	(19)	4	(100)	4315	(29.8)	4700	(32.4)	27.3	(121)	0.162	(4.11)	49.8	(20.8)	cone
									Average		26.6	(118)	0.131	(3.32)	48.5	(20.3)	
									COV		7.89		19.78		7.90		
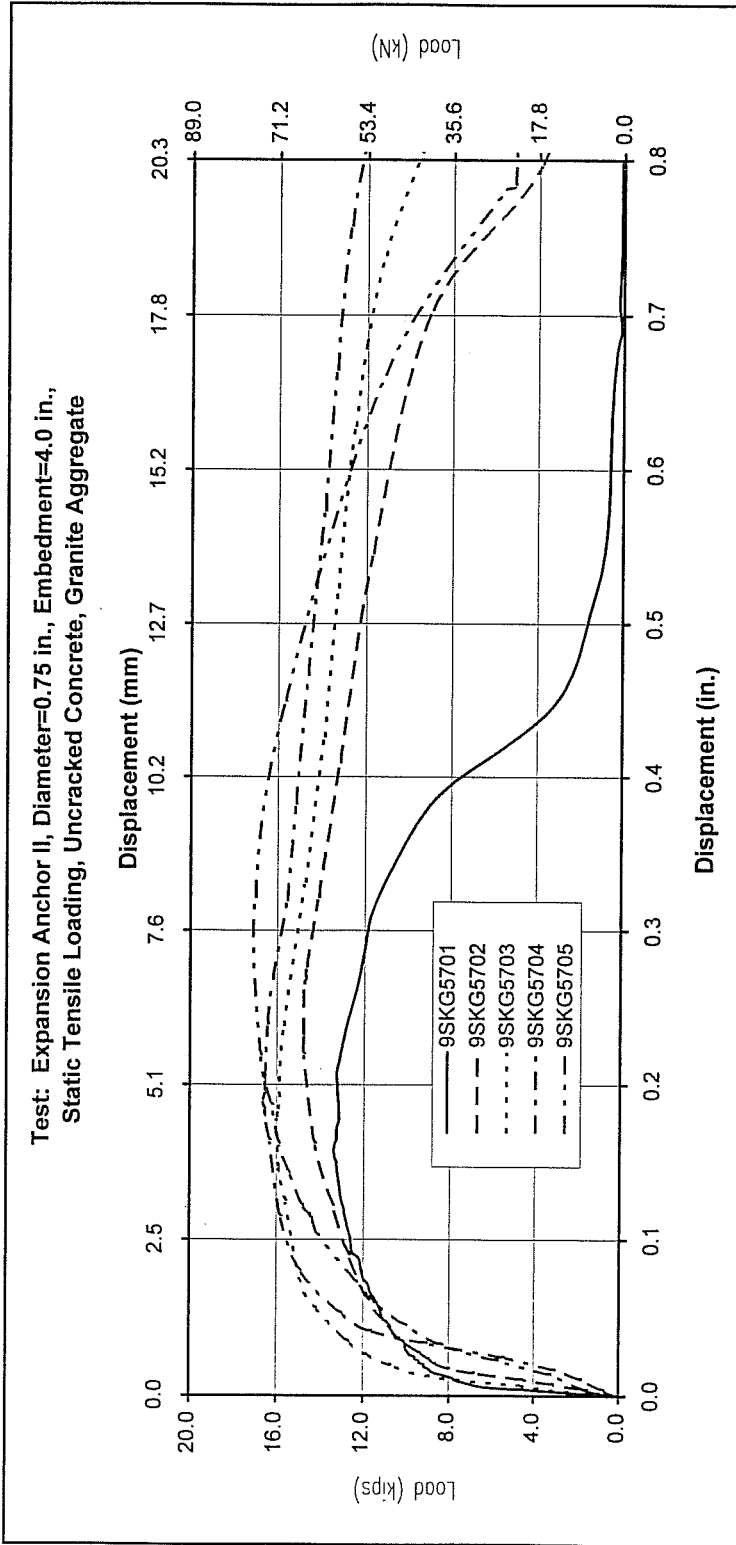
Test: Expansion Anchor II, Diameter=0.75 in., Embedment=4.0 in., Static Tensile Loading, Uncracked Concrete, Granite Aggregate

Test Name	Date	Loading	Effective Embedment h_e		f_c	Normalized f_c	Normalized Maximum Load		Displacement at Maximum Load		k_{nc}	Failure Mode
			inches	(mm)	psi	psi	kips	(kN)	inches	(mm)	US	
9SKG5701	6/16/95	Static	3.44	(87.3)	4315	4700	13.4	(59.6)	0.154	(3.91)	30.7	Cone
9SKG5702	6/16/95	Static	3.44	(87.3)	4315	4700	14.7	(65.4)	0.232	(5.89)	33.6	Cone
9SKG5703	6/19/95	Static	3.44	(87.3)	4315	4700	16.0	(71.2)	0.150	(3.81)	36.6	Cone
9SKG5704	6/19/95	Static	3.44	(87.3)	4315	4700	16.6	(73.8)	0.190	(4.83)	38.0	Cone/Pull-through
9SKG5705	6/19/95	Static	3.44	(87.3)	4315	4700	14.4	(64.1)	0.115	(2.92)	33.0	Cone
						Average	15.0	(66.8)	0.168	(4.27)	34.4	

Test: Undercut Anchor 1, Diameter=0.75 in., Embedment=4.0 in., Static Tensile Loading, Uncracked Concrete, Granite Aggregate

Load (kips) / Load (kN) vs. Displacement (in.) / Displacement (mm)

Legend: 9SMG5706, 9SMG5707, 9SMG5708, 9SMG5709, 9SMG5710
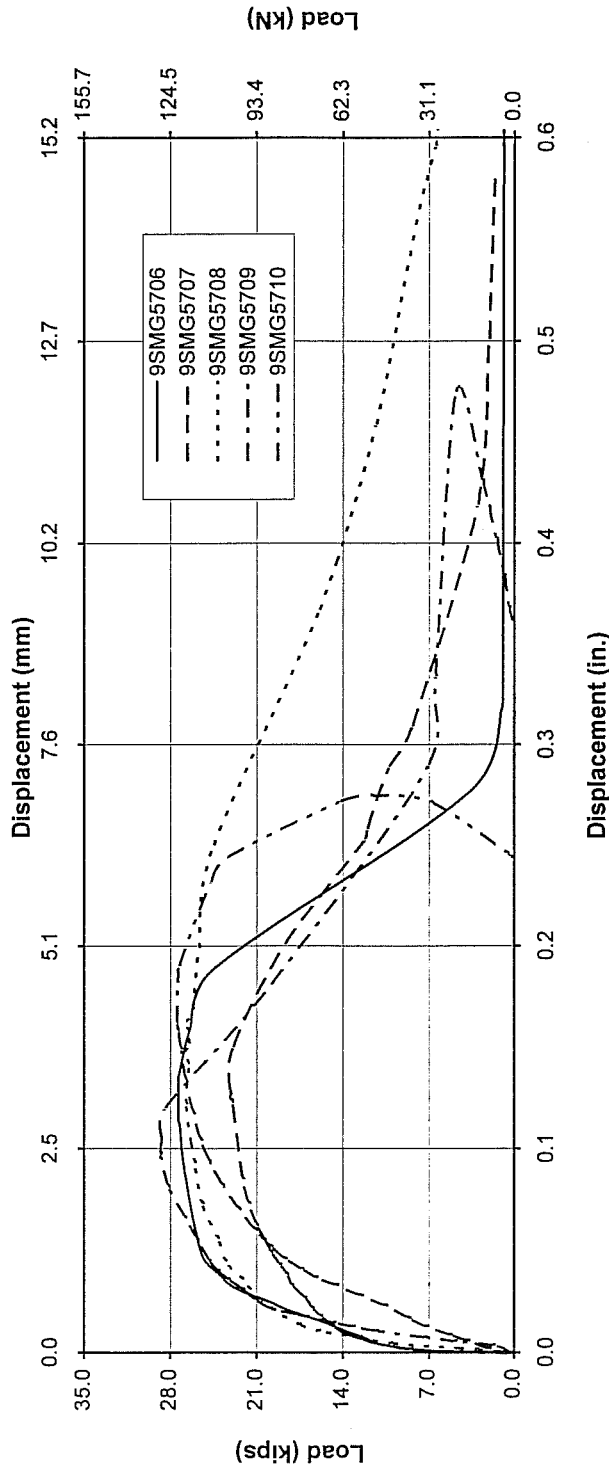
Test Name	Date	Loading	Effective Embedment h_e inches	(mm)	f_c psi	Normalized f_c psi	Normalized Maximum Load kips	(kN)	Displacement at Maximum Load inches	(mm)	k_{nc} US	Failure Mode
9SMG5706	6/20/95	Static	4	(100)	4315	4700	27.3	(121)	0.114	(2.90)	49.8	Cone
9SMG5707	6/20/95	Static	4	(100)	4315	4700	23.1	(103)	0.126	(3.20)	42.1	Cone
9SMG5708	6/20/95	Static	4	(100)	4315	4700	26.7	(119)	0.152	(3.86)	48.7	Cone
9SMG5709	6/20/95	Static	4	(100)	4315	4700	28.7	(128)	0.100	(2.54)	52.3	Cone
9SMG5710	6/20/95	Static	4	(100)	4315	4700	27.3	(121)	0.162	(4.11)	49.8	Cone
						Average	26.6	(118)	0.131	(3.32)	48.5	

Results for Series 1-10

Anchor	Test Number	Loading	Diameter in.	(mm)	Effective Embedment he in.	(mm)	fc psi	(MPa)	Normalized fc psi	(MPa)	Normalized Fu kips	(kN)	Displacement in.	(mm)	knc US	(SI)	Failure Mode
EAll	10DK5705	Dynamic	0.75	(19)	3.44	(87.3)	4315	(29.8)	4700	(32.4)	16.4	(72.9)	0.116	(2.95)	37.5	(15.7)	cone
	10DK5712	Dynamic	0.75	(19)	3.44	(87.3)	4315	(29.8)	4700	(32.4)	18.0	(80.1)	0.074	(1.88)	41.2	(17.3)	cone/pull-through
	10DK5713	Dynamic	0.75	(19)	3.44	(87.3)	4315	(29.8)	4700	(32.4)	16.7	(74.3)	0.112	(2.84)	38.2	(16.0)	cone/pull-through
	10DK5714	Dynamic	0.75	(19)	3.44	(87.3)	4315	(29.8)	4700	(32.4)	17.7	(78.7)	0.151	(3.84)	40.5	(17.0)	cone
	10DK5715	Dynamic	0.75	(19)	3.44	(87.3)	4315	(29.8)	4700	(32.4)	18.5	(82.3)	0.065	(1.65)	42.3	(17.7)	cone/pull-through
									Average		17.5	(77.7)	0.104	(2.63)	39.9	(16.7)	
									COV		5.07		33.57		5.08		
UC1	10DM5706	Dynamic	0.75	(19)	4	(100)	4315	(29.8)	4700	(32.4)	30.3	(135)	0.144	(3.66)	55.3	(23.1)	cone
	10DM5707	Dynamic	0.75	(19)	4	(100)	4315	(29.8)	4700	(32.4)	28.8	(128)	0.221	(5.61)	52.5	(22.0)	cone
	10DM5708	Dynamic	0.75	(19)	4	(100)	4315	(29.8)	4700	(32.4)	26.4	(117)	0.200	(5.08)	48.1	(20.1)	cone
	10DM5709	Dynamic	0.75	(19)	4	(100)	4315	(29.8)	4700	(32.4)	24.6	(109)	0.099	(2.51)	44.9	(18.8)	cone
	10DM5710	Dynamic	0.75	(19)	4	(100)	4315	(29.8)	4700	(32.4)	30.0	(133)	0.039	(0.99)	54.7	(22.9)	cone
									Average		28.0	(125)	0.141	(3.57)	51.1	(21.4)	
									COV		8.75		52.82		8.75		

Test: Expansion Anchor II, Diameter=0.75 in., Embedment=4.0 in.,
Dynamic Tensile Loading, Uncracked Concrete, Granite Aggregate

Test Name	Date	Loading	Effective Embedment h_e inches	(mm)	f'_c psi	Normalized f'_c psi	Normalized Maximum Load kips	(kN)	Displacement at Maximum Load inches	(mm)	k_{nc} US	Failure Mode
10DK5705	6/21/95	Dynamic	3.44	(87.3)	4315	4700	16.4	(72.9)	0.116	(2.95)	37.5	Cone
10DK5712	6/21/95	Dynamic	3.44	(87.3)	4315	4700	18.0	(80.1)	0.074	(1.88)	41.2	Cone/Pull-through
10DK5713	6/21/95	Dynamic	3.44	(87.3)	4315	4700	16.7	(74.3)	0.112	(2.84)	38.2	Cone/Pull-through
10DK5714	6/22/95	Dynamic	3.44	(87.3)	4315	4700	17.7	(78.7)	0.151	(3.84)	40.5	Cone
10DK5715	6/22/95	Dynamic	3.44	(87.3)	4315	4700	18.5	(82.3)	0.065	(1.65)	42.3	Cone/Pull-through
Average							17.5	(77.7)	0.104	(2.63)	40.0	

Test: Undercut Anchor 1, Diameter=0.75 in., Embedment=4.0 in., Static Tensile Loading, Uncracked Concrete, Granite Aggregate

Legend: 10DM5706, 10DM5707, 10DM5708, 10DM5709, 10DM5710

Test Name	Date	Loading	Effective Embedment h_e inches	(mm)	f_c psi	Normalized f_c psi	Normalized Maximum Load kips	(kN)	Displacement at Maximum Load inches	(mm)	k_{nc} US	Failure Mode
10DM5706	6/23/95	Dynamic	4	(100)	4315	4700	30.3	(135)	0.144	(3.66)	55.3	Cone
10DM5707	6/23/95	Dynamic	4	(100)	4315	4700	28.8	(128)	0.221	(5.61)	52.5	Cone
10DM5708	6/23/95	Dynamic	4	(100)	4315	4700	26.4	(117)	0.200	(5.08)	48.1	Cone
10DM5709	6/23/95	Dynamic	4	(100)	4315	4700	24.6	(109)	0.099	(2.51)	44.9	Cone
10DM5710	6/23/95	Dynamic	4	(100)	4315	4700	30.0	(133)	0.039	(0.991)	54.7	Cone
Average							28.0	(125)	0.141	(3.57)	51.1	

Results for Series 1-11

Anchor	Test Number	Loading	Diameter in. (mm)		Effective Embedment h_e in. (mm)		f_c psi (MPa)		Normalized f_c psi (MPa)		Normalized F_u kips (kN)		Displacement in. (mm)		k_nc US (SI)		Additional Crack Opening mm	Failure Mode
CIP	11SC5701	Static	0.75	(19)	4	(100)	4381	(30.2)	4700	(32.4)	24.3	(108)	0.052	(1.32)	44.3	(18.5)		cone
	11SC5702	Static	0.75	(19)	4	(100)	4381	(30.2)	4700	(32.4)	22.2	(98.7)	0.029	(0.74)	40.5	(16.9)		cone
	11SC5703	Static	0.75	(19)	4	(100)	4381	(30.2)	4700	(32.4)	23.8	(106)	0.051	(1.30)	43.4	(18.2)		cone
	11SC5704	Static	0.75	(19)	4	(100)	4381	(30.2)	4700	(32.4)	21.9	(97.4)	0.047	(1.19)	39.9	(16.7)		cone
	11SC5705	Static	0.75	(19)	4	(100)	4381	(30.2)	4700	(32.4)	22.0	(97.9)	0.055	(1.40)	40.1	(16.8)		cone
									Average		22.8	(101.6)	0.047	(1.19)	41.6	(17.4)		
									COV		4.92		22.12		4.94			
CIP	11SC5706	Static	0.75	(19)	4	(100)	4381	(30.2)	4700	(32.4)	18.7	(83.2)	0.043	(1.09)	34.1	(14.3)	0.09	cone
	11SC5707	Static	0.75	(19)	4	(100)	4381	(30.2)	4700	(32.4)	21.0	(93.4)	0.050	(1.27)	38.3	(16.0)	0.14	cone
	11SC5708	Static	0.75	(19)	4	(100)	4381	(30.2)	4700	(32.4)	19.7	(87.6)	0.056	(1.42)	35.9	(15.0)	0.08	cone
	11SC5709	Static	0.75	(19)	4	(100)	4381	(30.2)	4700	(32.4)	20.6	(91.6)	0.069	(1.75)	37.6	(15.8)	0.11	cone
	11SC5710	Static	0.75	(19)	4	(100)	4381	(30.2)	4700	(32.4)	19.3	(85.8)	0.039	(0.99)	35.2	(14.7)	0.15	cone
									Average		19.9	(88.3)	0.051	(1.31)	36.2	(15.2)	0.11	
									COV		4.73		22.96		4.76		26.75	
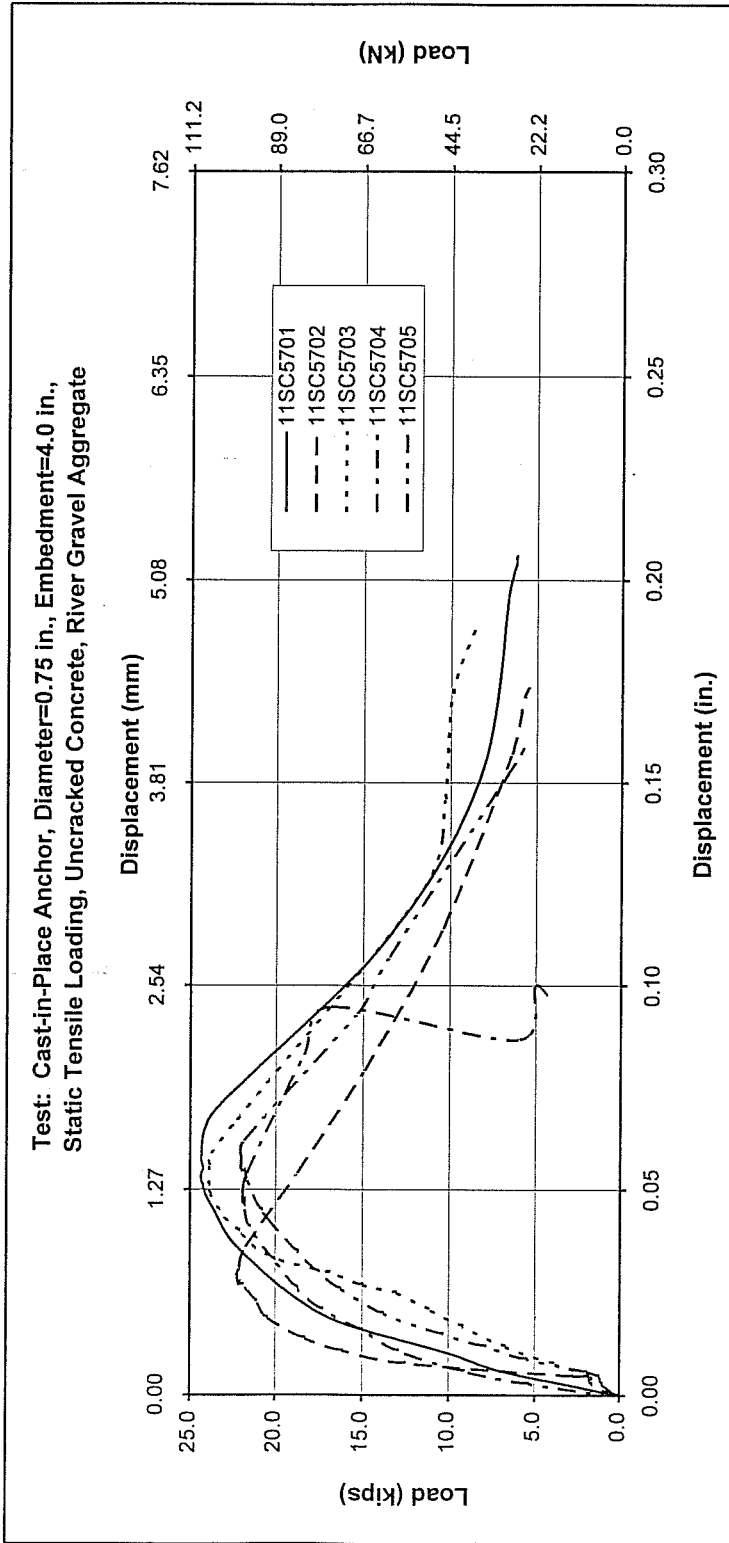
Test: Cast-in-Place Anchor, Diameter=0.75 in., Embedment=4.0 in., Static Tensile Loading, Uncracked Concrete, River Gravel Aggregate

Legend: 11SC5701, 11SC5702, 11SC5703, 11SC5704, 11SC5705

Test Name	Date	Loading	Effective Embedment h_e inches	(mm)	f_c psi	Normalized f_c psi	Normalized Maximum Load kips	(kN)	Displacement at Maximum Load inches	(mm)	k_{nc} US	Failure Mode
11SC5701	6/29/95	Static	4	(100)	4381	4700	24.3	(108)	0.052	(1.32)	44.3	Cone
11SC5702	6/29/95	Static	4	(100)	4381	4700	22.2	(98.7)	0.029	(0.737)	40.5	Cone
11SC5703	6/29/95	Static	4	(100)	4381	4700	23.8	(106)	0.051	(1.30)	43.4	Cone
11SC5704	6/29/95	Static	4	(100)	4381	4700	21.9	(97.4)	0.047	(1.19)	39.9	Cone
11SC5705	6/29/95	Static	4	(100)	4381	4700	22.0	(97.9)	0.055	(1.40)	40.1	Cone
Average							22.8	(102)	0.047	(1.19)	41.6	
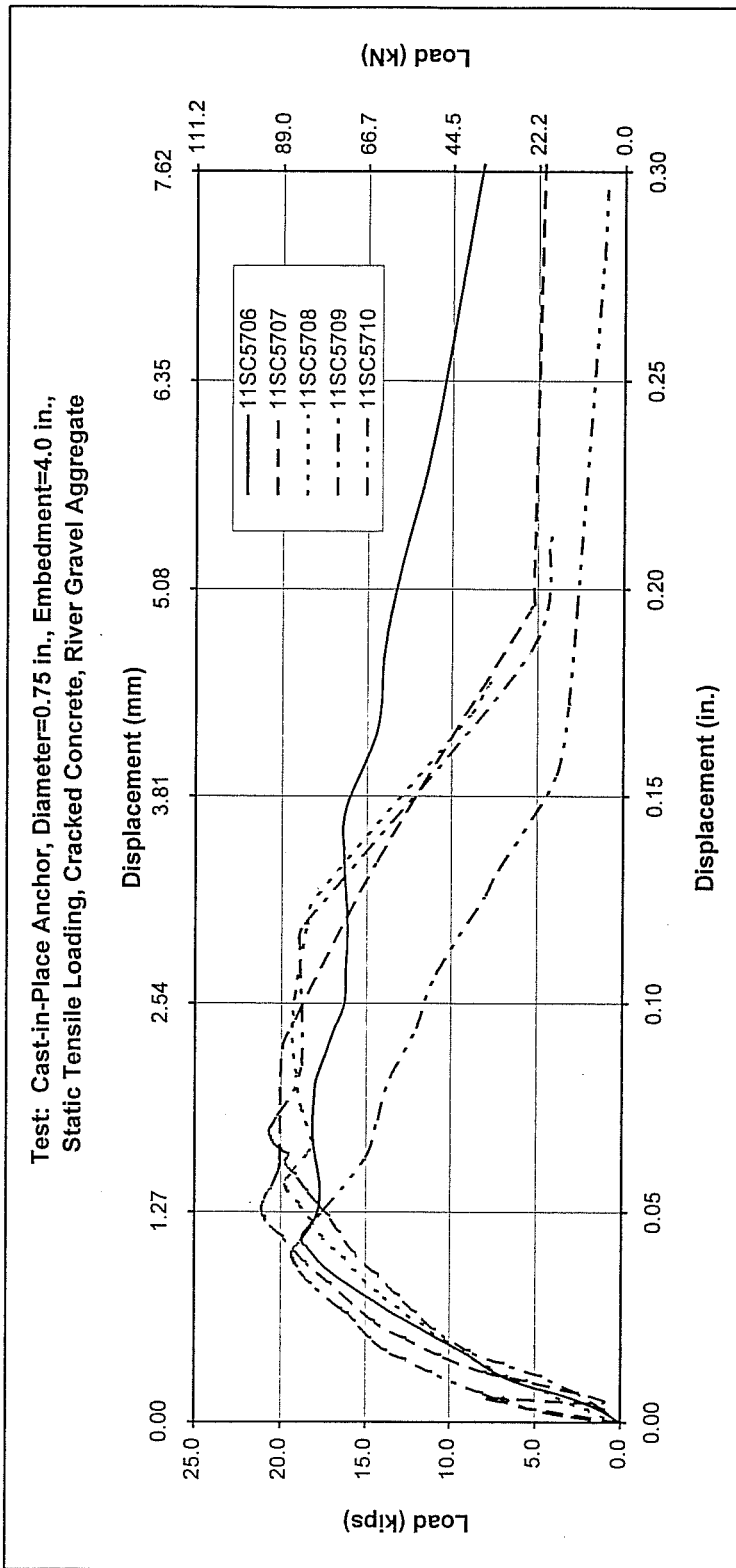
Test: Cast-in-Place Anchor, Diameter=0.75 in., Embedment=4.0 in.,
Static Tensile Loading, Cracked Concrete, River Gravel Aggregate

Test Name	Date	Loading	Effective Embedment h_e		f'_c psi	Normalized f'_c psi	Normalized Maximum Load		Displacement at Maximum Load		k_{nc} US	Additional Crack Opening mm	Failure Mode
			inches	(mm)	psi	psi	kips	(kN)	inches	(mm)	US	mm	
11SCR5706	7/3/95	Static	4	(100)	4381	4700	18.7	(83.2)	0.043	(1.09)	34.1	0.09	Cone
11SCR5707	7/3/95	Static	4	(100)	4381	4700	21.0	(93.4)	0.050	(1.27)	38.3	0.14	Cone
11SCR5708	7/5/95	Static	4	(100)	4381	4700	19.7	(87.6)	0.056	(1.42)	35.9	0.08	Cone
11SCR5709	7/5/95	Static	4	(100)	4381	4700	20.6	(91.6)	0.069	(1.75)	37.6	0.11	Cone
11SCR5710	7/5/95	Static	4	(100)	4381	4700	19.3	(85.8)	0.039	(0.991)	35.2	0.15	Cone
Average							19.9	(88.3)	0.051	(1.31)	36.2	0.11	

183

Results for Series 1-12

Anchor	Test Number	Loading	Diameter in. (mm)		Effective Embedment h_e in. (mm)		f'_c psi (MPa)		Normalized f'_c psi (MPa)		Normalized F_u kips (kN)		Displacement in. (mm)		knc US (SI)		Additional Crack Opening mm	Failure Mode
CIP	12DC5701	Dynamic	0.75	(19)	4	(100)	4381	(30.2)	4700	(32.4)	31.9	(142)	0.068	(1.73)	58.2	(24.3)		cone
	12DC5702	Dynamic	0.75	(19)	4	(100)	4381	(30.2)	4700	(32.4)	28.5	(127)	0.069	(1.75)	52.0	(21.8)		cone
	12DC5703	Dynamic	0.75	(19)	4	(100)	4381	(30.2)	4700	(32.4)	29.3	(130)	0.086	(2.18)	53.4	(22.4)		cone
	12DC5704	Dynamic	0.75	(19)	4	(100)	4381	(30.2)	4700	(32.4)	28.5	(127)	0.060	(1.52)	52.0	(21.8)		cone
	12DC5705	Dynamic	0.75	(19)	4	(100)	4381	(30.2)	4700	(32.4)	29.7	(132)	0.062	(1.57)	54.2	(22.7)		cone
									Average		29.6	(132)	0.069	(1.75)	54.0	(22.6)		
									COV		4.723		14.85		4.73			
CIP	12DC5707	Dynamic	0.75	(19)	4	(100)	4244	(29.3)	4700	(32.4)	31.7	(141)	0.107	(2.72)	57.8	(24.2)	0.15	cone
	12DC5708	Dynamic	0.75	(19)	4	(100)	4244	(29.3)	4700	(32.4)	31.1	(138)	0.130	(3.30)	56.7	(23.7)	0.09	cone
	12DC5709	Dynamic	0.75	(19)	4	(100)	4244	(29.3)	4700	(32.4)	31.7	(141)	0.114	(2.90)	57.8	(24.2)	0.15	cone
	12DC5710	Dynamic	0.75	(19)	4	(100)	4244	(29.3)	4700	(32.4)	31.6	(141)	0.102	(2.59)	57.6	(24.1)	0.12	cone
	12DC5712	Dynamic	0.75	(19)	4	(100)	4244	(29.3)	4700	(32.4)	29.2	(130)	0.071	(1.80)	53.2	(22.3)	0.16	cone
									Average		31.1	(138)	0.105	(2.66)	56.6	(23.7)	0.13	
									COV		3.44		20.66		3.47		21.50	
											28.7	(128)	0.105	(2.66)	56.6	(23.7)		

Average edited to remove effect of sheet metal cracking

Test: Cast-in-Place Anchor, Diameter=0.75 in., Embedment=4.0 in.,
Dynamic Tensile Loading, Uncracked Concrete, River Gravel Aggregate

Test Name	Date	Loading	Effective Embedment h_e		f'_c	Normalized f'_c	Normalized Maximum Load		Displacement at Maximum Load		k_{nc}	Failure Mode
			inches	(mm)	psi	psi	kips	(kN)	inches	(mm)	US	
12DC5701	6/27/95	Dynamic	4	(100)	4381	4700	31.9	(142)	0.068	(1.73)	58.2	Cone
12DC5702	6/27/95	Dynamic	4	(100)	4381	4700	28.5	(127)	0.069	(1.75)	52.0	Cone
12DC5703	6/27/95	Dynamic	4	(100)	4381	4700	29.3	(130)	0.086	(2.18)	53.4	Cone
12DC5704	6/27/95	Dynamic	4	(100)	4381	4700	28.5	(127)	0.060	(1.52)	52.0	Cone
12DC5705	6/27/95	Dynamic	4	(100)	4381	4700	29.7	(132)	0.062	(1.57)	54.2	Cone
						Average	29.6	(132)	0.069	(1.75)	53.9	

185

Test: Cast-in-Place Anchor, Diameter=0.75 in., Embedment=4.0 in.,
Dynamic Tensile Loading, Cracked Concrete, River Gravel Aggregate
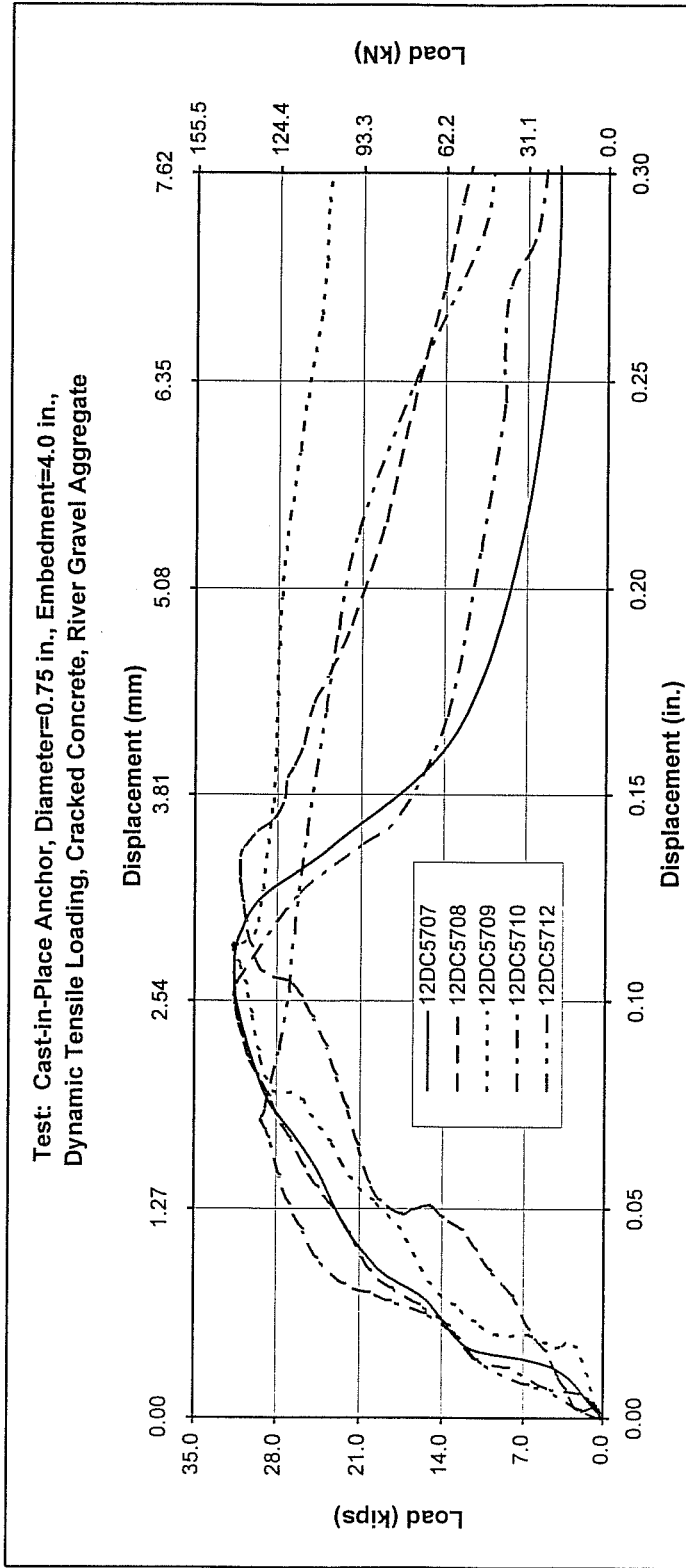
Maximum Load includes 2.4 kips (61 kN) to tear the sheet metal. Anchor capacity is 2.4 kips (61 kN) lower than the capacity shown in the graph.

Test Name	Date	Loading	Effective Embedment h_e inches	(mm)	f_c psi	Normalized f_c psi	Normalized Maximum Load kips	(kN)	Displacement at Maximum Load inches	(mm)	k_{nc} US	Additional Crack Opening mm	Failure Mode
12DC5707	8/30/95	Dynamic	4	(100)	4244	4700	31.7	(141)	0.107	(2.72)	57.8	0.15	Cone
12DC5708	8/30/95	Dynamic	4	(100)	4244	4700	31.1	(138)	0.130	(3.30)	56.7	0.09	Cone
12DC5709	8/30/95	Dynamic	4	(100)	4244	4700	31.7	(141)	0.114	(2.90)	57.8	0.15	Cone
12DC5710	8/30/95	Dynamic	4	(100)	4244	4700	31.6	(141)	0.102	(2.59)	57.6	0.12	Cone
12DC5712	9/1/95	Dynamic	4	(100)	4244	4700	29.2	(130)	0.071	(1.80)	53.2	0.16	Cone
Average							31.1	(138)	0.105	(2.66)	56.6	0.13	

APPENDIX B

RESULTS FOR TASK 3

Results for Cast-in-Place Anchors Testes in Series 3-1

Anchor	Test Number	Loading	Diameter in. (mm)	Effective Embedment h_e in. (mm)	Edge Distance in. (mm)	f_c psi (MPa)	Concrete Cone Breakout Normalized f_c psi (MPa)	Concrete Cone Breakout Normalized F_u kips (kN)	Concrete Cone Breakout Displacement in. (mm)	Ultimate Failure Normalized F_u kips (kN)	Ultimate Failure Displacement in. (mm)	Failure Mode
CIP No Hairpin	1SCR5701	Static	0.75 (19)	4 (100)	4 (100)	4210 (29.0)	4700 (32.4)	9.1 (40)	0.047 (1.19)	9.1 (40.5)	0.047 (1.19)	cone
	1SCR5702	Static	0.75 (19)	4 (100)	4 (100)	4210 (29.0)	4700 (32.4)	8.4 (37)	0.072 (1.83)	8.4 (37.4)	0.072 (1.83)	cone
	1SCR5703	Static	0.75 (19)	4 (100)	4 (100)	4210 (29.0)	4700 (32.4)	7.5 (33)	0.19 (4.83)	7.5 (33.4)	0.19 (4.83)	cone
	1SCR5704	Static	0.75 (19)	4 (100)	4 (100)	4210 (29.0)	4700 (32.4)	9.7 (43)	0.028 (0.71)	9.7 (43.1)	0.028 (0.71)	cone
	1SCR5705	Static	0.75 (19)	4 (100)	4 (100)	4210 (29.0)	4700 (32.4)	9.1 (40)	0.062 (1.57)	9.1 (40.5)	0.062 (1.57)	cone
							Average	8.8 (39)	0.080 (2.03)	8.8 (39.0)	0.080 (2.03)	
							COV	9.61	79.95	9.61	79.95	
CIP Close Hairpin	1SCR5706	Static	0.75 (19)	4 (100)	4 (100)	4210 (29.0)	4700 (32.4)	11.8 (52.5)	0.128 (3.25)	25.4 (113)	1.20 (30.4)	fracture
	1SCR5707	Static	0.75 (19)	4 (100)	4 (100)	4210 (29.0)	4700 (32.4)	14.0 (62.3)	0.080 (2.03)	24.7 (110)	1.04 (26.4)	fracture
	1SCR5708	Static	0.75 (19)	4 (100)	4 (100)	4210 (29.0)	4700 (32.4)	10.5 (46.7)	0.056 (1.42)	26.1 (116)	0.72 (18.3)	cone/disp.
	1SCR5709	Static	0.75 (19)	4 (100)	4 (100)	4210 (29.0)	4700 (32.4)	12.8 (56.9)	0.124 (3.15)	17.2 (76.5)	1.20 (30.5)	cone/disp.
	1SCR5710	Static	0.75 (19)	4 (100)	4 (100)	4210 (29.0)	4700 (32.4)	13.7 (60.9)	0.113 (2.87)	21.3 (94.7)	1.20 (30.5)	cone/disp.
							Average	12.6 (55.9)	0.100 (2.55)	22.94 (102)	1.07 (27.2)	
							COV	11.44	31.02	16.13	19.36	
CIP Far Hairpin	1SCR5711	Static	0.75 (19)	4 (100)	4 (100)	4635 (32.0)	4700 (32.4)	11.3 (50.3)	0.059 (1.50)	17.1 (76.1)	0.961 (24.4)	fracture
	1SCR5712	Static	0.75 (19)	4 (100)	4 (100)	4635 (32.0)	4700 (32.4)	13.2 (58.7)	0.074 (1.88)	13.2 (58.7)	0.074 (1.88)	cone/disp.
	1SCR5713	Static	0.75 (19)	4 (100)	4 (100)	4635 (32.0)	4700 (32.4)	12.1 (53.8)	0.096 (2.44)	19.7 (87.6)	0.878 (22.3)	cone/disp.
	1SCR5714	Static	0.75 (19)	4 (100)	4 (100)	4635 (32.0)	4700 (32.4)	10.9 (48.5)	0.154 (3.91)	18.5 (82.3)	0.988 (25.1)	cone/disp.
	1SCR5715	Static	0.75 (19)	4 (100)	4 (100)	4635 (32.0)	4700 (32.4)	12.5 (55.6)	0.135 (3.43)	17.9 (79.6)	0.666 (16.9)	cone/disp.
							Average	12.0 (53.4)	0.104 (2.63)	17.28 (76.9)	0.713 (18.1)	
							COV	7.68	38.76	14.30	53.14	

Test: Cast-in-Place Anchor, Diameter=0.75 in., Embedment=4.0 in., Edge Distance=4.0 in.,
No Hairpin, Static Shear Loading, Uncracked Concrete, River Gravel Aggregate

V_{CC} = Theoretical Concrete Cracking Load

Test Name	Date	f'_c psi	Normalized f'_c psi	At Concrete Failure						At Ultimate Failure						Failure Mode
				Normalized Maximum Load		Displacement at Maximum Load				Normalized Maximum Load		Displacement at Maximum Load				
				kips	(kN)	inches	(mm)			kips	(kN)	inches	(mm)			
1SCR5701	2/28/96	4210	4700	9.1	(40)	0.047	(1.19)			9.1	(40)	0.047	(1.19)			Cone
1SCR5702	2/29/96	4210	4700	8.4	(37)	0.072	(1.83)			8.4	(37)	0.072	(1.83)			Cone
1SCR5703	2/29/96	4210	4700	7.5	(33)	0.190	(4.83)			7.5	(33)	0.190	(4.83)			Cone
1SCR5704	2/29/96	4210	4700	9.7	(43)	0.028	(0.71)			9.7	(43)	0.028	(0.71)			Cone
1SCR5705	2/29/96	4210	4700	9.1	(40)	0.062	(1.57)			9.1	(40)	0.062	(1.57)			Cone
	Average			8.8	(39)	0.080	(2.03)			8.8	(39)	0.080	(2.03)			

189

Test: Cast-in-Place Anchor, Diameter=0.75 in., Embedment=4.0 in., Edge Distance=4.0 in., Close Hairpin, Static Shear Loading, Uncracked Concrete, River Gravel Aggregate

V_{CC} = Theoretical Concrete Cracking Load
V_H = Ultimate Shear Capacity of Hairpin

Test Name	Date	f'c psi	Normalized f'c psi	At Concrete Failure Normalized Maximum Load kips	(kN)	Displacement at Maximum Load inches	(mm)	At Ultimate Failure Normalized Maximum Load kips	(kN)	Displacement at Maximum Load inches	(mm)	Failure Mode
1SCR5706	2/28/96	4210	4700	11.8	(52.5)	0.128	(3.25)	25.4	(113)	1.20	(30.4)	Fracture
1SCR5707	2/28/96	4210	4700	14.0	(62.3)	0.080	(2.03)	24.7	(110)	1.04	(26.4)	Fracture
1SCR5708	2/28/96	4210	4700	10.5	(46.7)	0.056	(1.42)	26.1	(116)	0.722	(18.3)	Cone / Displacement
1SCR5709	10/23/95	4635	4700	12.8	(56.9)	0.124	(3.15)	17.2	(76.5)	1.20	(30.5)	Cone / Displacement
1SCR5710	10/23/95	4635	4700	13.7	(60.9)	0.113	(2.87)	21.3	(94.7)	1.20	(30.5)	Cone / Displacement
Average				12.6	(55.9)	0.100	(2.55)	22.9	(102)	1.07	(27.2)	

Test: Cast-in-Place Anchor, Diameter=0.75 in., Embedment=4.0 in., Edge Distance=4.0 in., Far Hairpin, Static Shear Loading, Uncracked Concrete, River Gravel Aggregate

Legend: 1SCR5711, 1SCR5712, 1SCR5713, 1SCR5714, 1SCR5715

V_{CC} = Theoretical Concrete Cracking Load
V_H = Ultimate Shear Capacity of Hairpin

Test Name	Date	f_c psi	Normalized f_c psi	At Concrete Failure Normalized Maximum Load kips (kN)	Displacement at Maximum Load inches (mm)	At Ultimate Failure Normalized Maximum Load kips (kN)	Displacement at Maximum Load inches (mm)	Failure Mode
1SCR5711	10/20/95	4635	4700	11.3 (50.3)	0.059 (1.50)	17.1 (76.1)	0.961 (24.4)	Fracture
1SCR5712	10/23/95	4635	4700	13.2 (58.7)	0.074 (1.88)	13.2 (58.7)	0.074 (1.9)	Cone / Displacement
1SCR5713	10/25/95	4635	4700	12.1 (53.8)	0.096 (2.44)	19.7 (87.6)	0.878 (22.3)	Cone / Displacement
1SCR5714	10/30/95	4635	4700	10.9 (48.5)	0.154 (3.91)	18.5 (82.3)	0.988 (25.1)	Cone / Displacement
1SCR5715	10/30/95	4635	4700	12.5 (55.6)	0.135 (3.43)	17.9 (79.6)	0.666 (16.9)	Cone / Displacement
Average				12.0 (53.4)	0.104 (2.63)	17.3 (76.9)	0.713 (18.1)	

Results for Post-Installed Anchors Tested in Series 3-1

Anchor	Test Number	Loading	Diameter in.	(mm)	Effective Embedment h_e in.	(mm)	Edge Distance in.	(mm)	f_c psi	(MPa)	Normalized f_c psi	(MPa)	Concrete Cone Breakout Normalized F_u kips	(kN)	Displacement in.	(mm)	Ultimate Failure Normalized F_u kips	(kN)	Displacement in.	(mm)	Failure Mode
EAll	1SKR5716	Static	0.75	(19)	3.44	(87.3)	4	(100)	4740	(32.7)	4700	(32.4)	8.4	(37)	0.308	(7.82)	10.2	(45.4)	0.391	(9.93)	cone/disp.
Far	1SKR5717	Static	0.75	(19)	3.44	(87.3)	4	(100)	4210	(29.0)	4700	(32.4)	8.4	(37)	0.222	(5.64)	9.0	(40)	0.641	(16.3)	partial fracture
Hairpin	1SKR5718	Static	0.75	(19)	3.44	(87.3)	4	(100)	4210	(29.0)	4700	(32.4)	7.7	(34)	0.211	(5.36)	7.9	(35)	0.681	(17.3)	cone/disp.
	1SKR5719	Static	0.75	(19)	3.44	(87.3)	4	(100)	4210	(29.0)	4700	(32.4)	8.8	(39)	0.214	(5.44)	8.9	(40)	0.831	(21.1)	cone/disp.
	1SKR5720	Static	0.75	(19)	3.44	(87.3)	4	(100)	4210	(29.0)	4700	(32.4)	6.2	(28)	0.185	(4.70)	7.2	(32)	0.638	(16.2)	Fracture
											Average		7.9	(35)	0.228	(5.79)	8.6	(38)	0.636	(16.2)	
											COV		13.03		20.54		13.26		24.86		
UC1	1SMR5721	Static	0.75	(19)	4	(100)	4	(100)	4635	(32.0)	4700	(32.4)	9.3	(41)	0.222	(5.64)	15.7	(69.8)	0.475	(12.1)	cone/disp.
Far	1SMR5722	Static	0.75	(19)	4	(100)	4	(100)	4635	(32.0)	4700	(32.4)					18.3	(81.4)	0.357	(9.07)	cone/disp.
Hairpin	1SMR5723	Static	0.75	(19)	4	(100)	4	(100)	4740	(32.7)	4700	(32.4)	8.9	(40)	0.173	(4.39)	11.6	(51.6)	0.568	(14.4)	cone/disp.
	1SMR5724	Static	0.75	(19)	4	(100)	4	(100)	4740	(32.7)	4700	(32.4)					14.7	(65.4)	0.362	(9.19)	cone/disp.
	1SMR5725	Static	0.75	(19)	4	(100)	4	(100)	4740	(32.7)	4700	(32.4)	9.5	(42)	0.219	(5.56)	13.6	(60.5)	0.488	(12.4)	cone/disp.
											Average		9.2	(41)	0.205	(5.20)	14.8	(65.7)	0.450	(11.4)	
											COV		3.31		13.42		16.83		20.00		

Test: Expansion Anchor II, Diameter=0.75 in., Embedment=4.0 in., Edge Distance=4.0 in., Far Hairpin, Static Shear Loading, Uncracked Concrete, River Gravel Aggregate

V_{CC} = Theoretical Concrete Cracking Load

Test Name	Date	f'_c psi	Normalized f'_c psi	At Concrete Failure				At Ultimate Failure				Failure Mode
				Normalized Maximum Load		Displacement at Maximum Load		Normalized Maximum Load		Displacement at Maximum Load		
				kips	(kN)	inches	(mm)	kips	(kN)	inches	(mm)	
1SKR5716	11/6/95	4740	4700	8.4	(37)	0.308	(7.82)	10.2	(45.4)	0.391	(9.93)	Cone / Displacement
1SKR5717	2/21/96	4210	4700	8.4	(37)	0.222	(5.64)	9.0	(40)	0.641	(16.3)	Partial Fracture
1SKR5718	2/21/96	4210	4700	7.7	(34)	0.211	(5.36)	7.9	(35)	0.681	(17.3)	Cone / Displacement
1SKR5719	2/21/96	4210	4700	8.8	(39)	0.214	(5.44)	8.9	(40)	0.831	(21.1)	Cone / Displacement
1SKR5720	2/21/96	4210	4700	6.2	(28)	0.185	(4.70)	7.2	(32)	0.638	(16.2)	Fracture
Average				7.9	(35)	0.228	(5.79)	8.6	(38)	0.636	(16.2)	

Test: Undercut Anchor 1, Diameter=0.75 in., Embedment=4.0 in., Edge Distance=4.0 in., Far Hairpin, Static Shear Loading, Uncracked Concrete, River Gravel Aggregate

V_{CC} = Theoretical Concrete Cracking Load
V_H = Ultimate Shear Capacity of Hairpin

Test Name	Date	f'_c psi	Normalized f'_c psi	At Concrete Failure				At Ultimate Failure				Failure Mode
				Normalized Maximum Load		Displacement at Maximum Load		Normalized Maximum Load		Displacement at Maximum Load		
				kips	(kN)	inches	(mm)	kips	(kN)	inches	(mm)	
1SMR5721	10/30/95	4635	4700	9.3	(41)	0.222	(5.64)	15.7	(69.8)	0.475	(12.1)	Cone / Displacement
1SMR5722	10/30/95	4635	4700					18.3	(81.4)	0.357	(9.07)	Cone / Displacement
1SMR5723	11/3/95	4740	4700	8.9	(40)	0.173	(4.39)	11.6	(51.6)	0.568	(14.4)	Cone / Displacement
1SMR5724	11/3/95	4740	4700					14.7	(65.4)	0.362	(9.19)	Cone / Displacement
1SMR5725	11/6/95	4740	4700	9.5	(42)	0.219	(5.56)	13.6	(60.5)	0.488	(12.4)	Cone / Displacement
Average				9.2	(41)	0.205	(5.20)	14.8	(65.7)	0.450	(11.4)	

Results for Cast-in-Place Anchors Testes in Series 3-2

Anchor	Test Number	Loading	Diameter in.	Diameter (mm)	Effective Embedment h_e in.	Effective Embedment h_e (mm)	Edge Distance in.	Edge Distance (mm)	f_c psi	f_c (MPa)	Normalized f_c psi	Normalized f_c (MPa)	Concrete Cone Breakout Normalized F_u kips	Concrete Cone Breakout Normalized F_u (kN)	Concrete Cone Breakout Displacement in.	Concrete Cone Breakout Displacement (mm)	Ultimate Failure Normalized F_u kips	Ultimate Failure Normalized F_u (kN)	Ultimate Failure Displacement in.	Ultimate Failure Displacement (mm)	Failure Mode
CIP No Hairpin	2SCR5701	Dynamic	0.75	(19)	4	(100)	4	(100)	4225	(29.1)	4700	(32.4)	13.0	(57.8)	0.057	(1.45)	13.0	(57.8)	0.057	(1.45)	cone
	2SCR5702	Dynamic	0.75	(19)	4	(100)	4	(100)	4225	(29.1)	4700	(32.4)	10.9	(48.5)	0.096	(2.44)	10.9	(48.5)	0.096	(2.44)	cone
	2SCR5703	Dynamic	0.75	(19)	4	(100)	4	(100)	4225	(29.1)	4700	(32.4)	8.4	(37)	0.064	(1.63)	8.4	(37)	0.064	(1.63)	cone
	2SCR5704	Dynamic	0.75	(19)	4	(100)	4	(100)	4225	(29.1)	4700	(32.4)	11.7	(52.0)	0.07	(1.78)	11.7	(52.0)	0.07	(1.78)	cone
	2SCR5705	Dynamic	0.75	(19)	4	(100)	4	(100)	4406	(30.4)	4700	(32.4)	12.1	(53.8)	0.052	(1.32)	12.1	(53.8)	0.052	(1.32)	cone
									Average				11.2	(49.9)	0.068	(1.72)	11.2	(49.9)	0.068	(1.72)	
									COV				15.58		25.34		15.58		25.34		
CIP Close Hairpin	2SCR5706	Dynamic	0.75	(19)	4	(100)	4	(100)	4225	(29.1)	4700	(32.4)	13.8	(61.4)	0.056	(1.42)	22.3	(99)	1.13	(28.7)	cone/disp.
	2SCR5707	Dynamic	0.75	(19)	4	(100)	4	(100)	4225	(29.1)	4700	(32.4)	15.0	(66.7)	0.076	(1.93)	21.1	(94)	0.88	(22.5)	cone/disp.
	2SCR5708	Dynamic	0.75	(19)	4	(100)	4	(100)	4225	(29.1)	4700	(32.4)	18.7	(83.2)	0.087	(2.21)	25.8	(115)	1.20	(30.5)	cone/disp.
	2SCR5709	Dynamic	0.75	(19)	4	(100)	4	(100)	4225	(29.1)	4700	(32.4)	14.6	(64.9)	0.032	(0.81)	19.5	(86.7)	1.20	(30.5)	cone/disp.
	2SCR5710	Dynamic	0.75	(19)	4	(100)	4	(100)	4225	(29.1)	4700	(32.4)	13.7	(60.9)	0.185	(4.70)	18.1	(80.5)	0.46	(11.7)	fracture
									Average				15.2	(67.4)	0.087	(2.21)	21.36	(95)	0.97	(24.8)	
									COV				13.54		67.14		13.80		32.39		
CIP Far Hairpin	2SCR5711	Dynamic	0.75	(19)	4	(100)	4	(100)	4805	(33.1)	4700	(32.4)	17.3	(77.0)	0.088	(2.24)	25.5	(113)	0.566	(14.4)	cone/disp.
	2SCR5712	Dynamic	0.75	(19)	4	(100)	4	(100)	4225	(29.1)	4700	(32.4)	14.0	(62.3)	0.141	(3.58)	14.7	(65.4)	0.718	(18.24)	fracture
	2SCR5713	Dynamic	0.75	(19)	4	(100)	4	(100)	4225	(29.1)	4700	(32.4)	11.1	(49.4)	0.128	(3.25)	16.1	(71.6)	1.200	(30.5)	cone/disp.
	2SCR5714	Dynamic	0.75	(19)	4	(100)	4	(100)	4225	(29.1)	4700	(32.4)	9.5	(42.3)	0.086	(2.18)	12.9	(57.4)	1.200	(30.5)	cone/disp.
	2SCR5715	Dynamic	0.75	(19)	4	(100)	4	(100)	4460	(30.4)	4700	(32.4)	17.6	(78.3)	0.120	(3.05)	20.8	(92.5)	0.779	(19.8)	cone/disp.
									Average				13.9	(61.8)	0.113	(2.86)	18	(80.1)	0.893	(22.7)	
									COV				26.05		21.80		28.41		32.62		

Test: Cast-in-Place Anchor, Diameter=0.75 in., Embedment=4.0 in., Edge Distance=4.0 in., No Hairpin, Dynamic Shear Loading, Uncracked Concrete, River Gravel Aggregate

Load (kN)

Load (kips)

Displacement (mm)

Displacement (in.)

Legend:
- 2DCR5701
- 2DCR5702
- 2DCR5703
- 2DCR5704
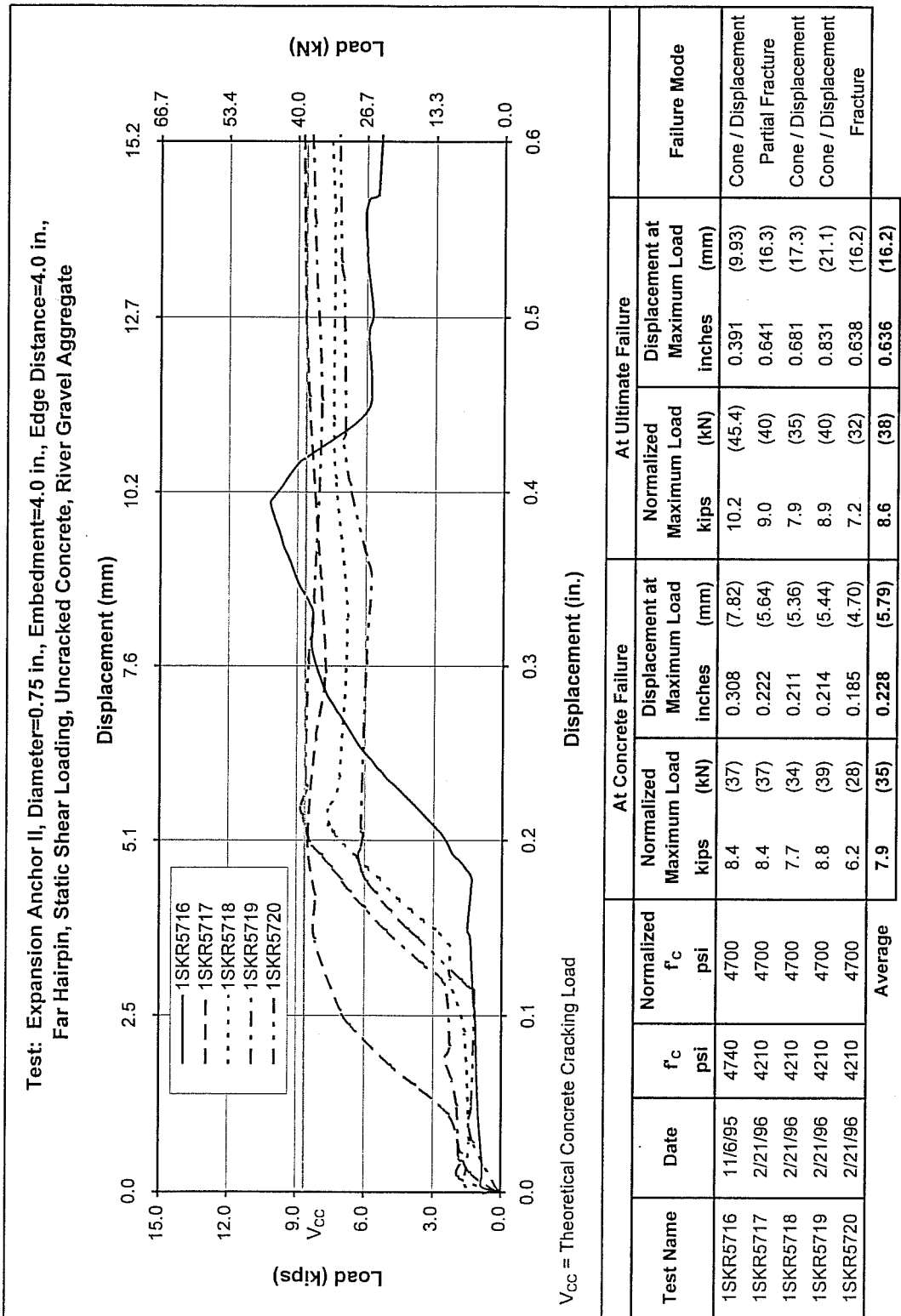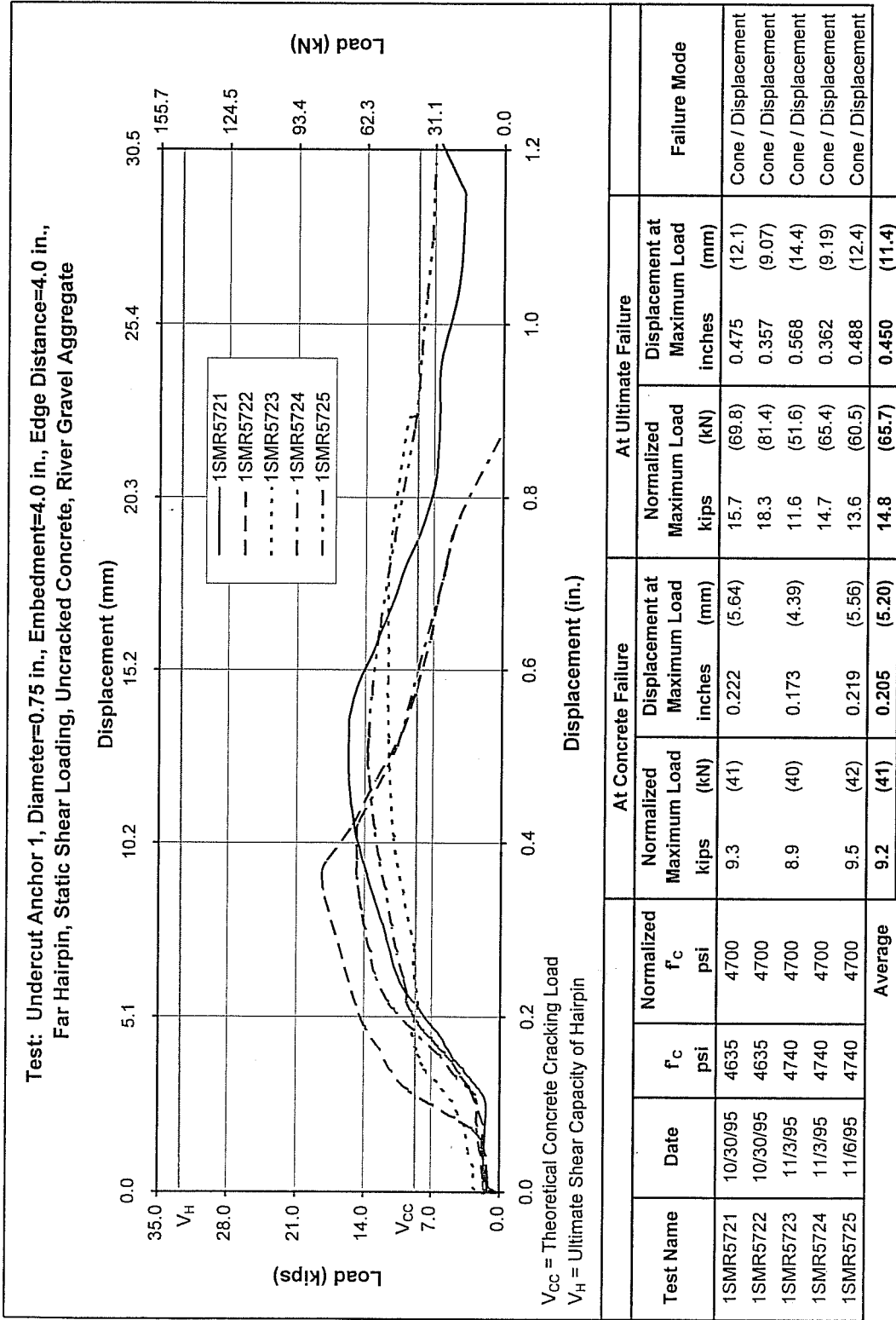- 2DCR5705

V_{CC} = Theoretical Concrete Cracking Load

Test Name	Date	f_C psi	Normalized f_C psi	At Concrete Failure				At Ultimate Failure				Failure Mode
				Normalized Maximum Load kips	(kN)	Displacement at Maximum Load inches	(mm)	Normalized Maximum Load kips	(kN)	Displacement at Maximum Load inches	(mm)	
2DCR5701	3/1/96	4225	4700	13.0	(57.8)	0.057	(1.45)	13.0	(57.8)	0.057	(1.45)	Cone
2DCR5702	3/1/96	4225	4700	10.9	(48.5)	0.096	(2.44)	10.9	(48.5)	0.096	(2.44)	Cone
2DCR5703	3/1/96	4225	4700	8.4	(37)	0.064	(1.63)	8.4	(37)	0.064	(1.63)	Cone
2DCR5704	3/4/96	4225	4700	11.7	(52.0)	0.070	(1.78)	11.7	(52.0)	0.070	(1.78)	Cone
2DCR5705	5/9/96	4406	4700	12.1	(53.8)	0.052	(1.32)	12.1	(53.8)	0.052	(1.32)	Cone
Average				11.2	(49.9)	0.068	(1.72)	11.2	(49.9)	0.068	(1.72)	

Test: Cast-in-Place Anchor, Diameter=0.75 in., Embedment=4.0 in., Edge Distance=4.0 in., Close Hairpin, Dynamic Shear Loading, Uncracked Concrete, River Gravel Aggregate

Legend:
- 2DCR5706
- 2DCR5707
- 2DCR5708
- 2DCR5709
- 2DCR5710

V_{CC} = Theoretical Concrete Cracking Load
V_H = Ultimate Shear Capacity of Hairpin

Test Name	Date	f_c psi	Normalized f_c psi	At Concrete Failure				At Ultimate Failure				Failure Mode
				Normalized Maximum Load		Displacement at Maximum Load		Normalized Maximum Load		Displacement at Maximum Load		
				kips	(kN)	inches	(mm)	kips	(kN)	inches	(mm)	
2DCR5706	3/11/96	4225	4700	13.8	(61.4)	0.056	(1.42)	22.3	(99.2)	1.13	(28.8)	Cone / Displacement
2DCR5707	3/11/96	4225	4700	15.0	(66.7)	0.076	(1.93)	21.1	(93.9)	0.884	(22.5)	Cone / Displacement
2DCR5708	3/11/96	4225	4700	18.7	(83.2)	0.087	(2.21)	25.8	(115)	1.20	(30.5)	Cone / Displacement
2DCR5709	3/11/96	4225	4700	14.6	(64.9)	0.032	(0.813)	19.5	(86.7)	1.20	(30.5)	Cone / Displacement
2DCR5710	3/14/96	4225	4700	13.7	(60.9)	0.185	(4.70)	18.1	(80.5)	0.460	(11.7)	Fracture
Average				15.2	(67.4)	0.087	(2.21)	21.4	(95.0)	0.976	(24.8)	

Test: Cast-in-Place Anchor, Diameter=0.75 in., Embedment=4.0 in., Edge Distance=4.0 in., Far Hairpin, Dynamic Shear Loading, Uncracked Concrete, River Gravel Aggregate

Legend:
- 2DCR5711
- 2DCR5712
- 2DCR5713
- 2DCR5714
- 2DCR5715

V_{CC} = Theoretical Concrete Cracking Load
V_H = Ultimate Shear Capacity of Hairpin

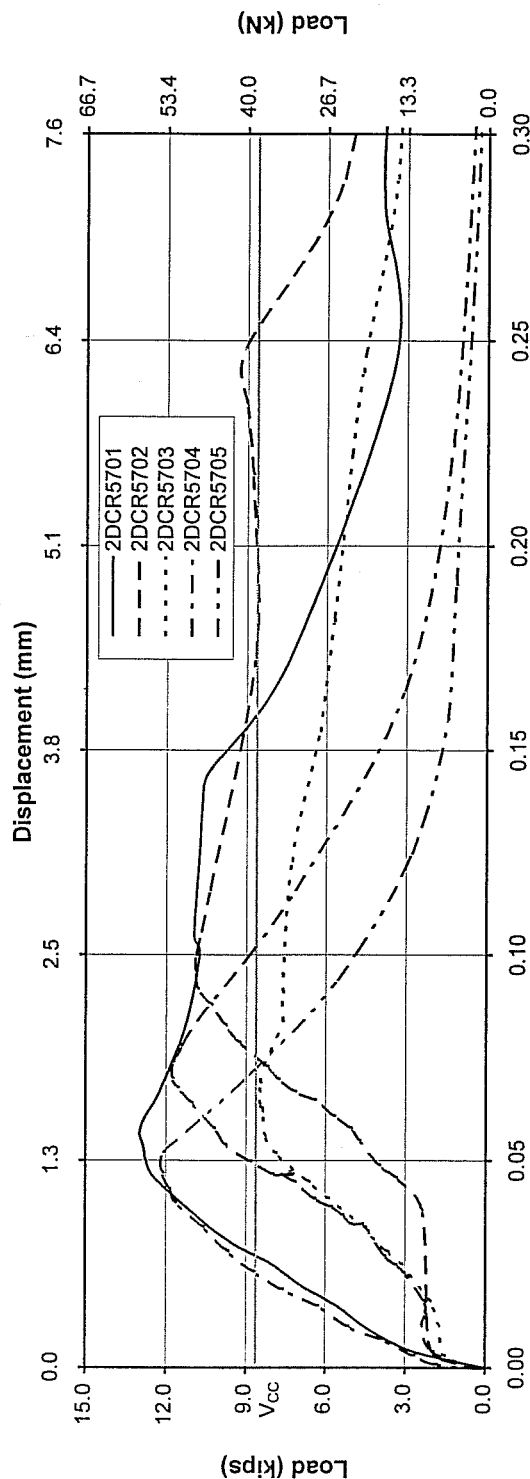| Test Name	Date	f'_c psi	Normalized f'_c psi	At Concrete Failure				At Ultimate Failure				Failure Mode
				Normalized Maximum Load		Displacement at Maximum Load		Normalized Maximum Load		Displacement at Maximum Load		
				kips	(kN)	inches	(mm)	kips	(kN)	inches	(mm)	
2DCR5711	1/23/96	4805	4700	17.3	(77.0)	0.088	(2.24)	25.5	(113)	0.566	(14.4)	Cone / Displacement
2DCR5712	3/14/96	4225	4700	14.0	(62.3)	0.141	(3.58)	14.7	(65.4)	0.718	(18.2)	Fracture
2DCR5713	3/14/96	4225	4700	11.1	(49.4)	0.128	(3.25)	16.1	(71.6)	1.20	(30.5)	Cone / Displacement
2DCR5714	3/14/96	4225	4700	9.5	(42)	0.086	(2.18)	12.9	(57.4)	1.20	(30.5)	Cone / Displacement
2DCR5715	4/17/96	4460	4700	17.6	(78.3)	0.120	(3.05)	20.8	(92.5)	0.779	(19.8)	Cone / Displacement
Average				13.9	(61.8)	0.113	(2.86)	18.0	(80.1)	0.893	(22.7)	

Results for Post-Installed Anchors Tested in Series 3-2

Anchor	Test Number	Loading	Diameter in. (mm)		Effective Embedment h_e in. (mm)		Edge Distance in. (mm)		f'_c psi (MPa)		Normalized f'_c psi (MPa)		Concrete Cone Breakout				Ultimate Failure				Failure Mode
													Normalized F_u kips (kN)		Displacement in. (mm)		Normalized F_u kips (kN)		Displacement in. (mm)		
EAll	2DKR5716	Dynamic	0.75	(19)	3.44	(87.3)	4	(100)	4805	(33.1)	4700	(32.4)	9.9	(44)	0.210	(5.33)	10.2	(45.4)	0.304	(7.72)	fracture
Far	2DKR5717	Dynamic	0.75	(19)	3.44	(87.3)	4	(100)	4805	(33.1)	4700	(32.4)	10.6	(47.1)	0.391	(9.93)	11.0	(48.9)	1.01	(25.6)	fracture
Hairpin	2DKR5718	Dynamic	0.75	(19)	3.44	(87.3)	4	(100)	4805	(33.1)	4700	(32.4)	10.2	(45.4)	0.214	(5.44)	10.2	(45.4)	0.214	(5.44)	fracture
	2DKR5719	Dynamic	0.75	(19)	3.44	(87.3)	4	(100)	4805	(33.1)	4700	(32.4)	8.6	(38)	0.244	(6.20)	8.6	(38)	0.244	(6.20)	cone/disp.
	2DKR5720	Dynamic	0.75	(19)	3.44	(87.3)	4	(100)	4805	(33.1)	4700	(32.4)	8.8	(39)	0.265	(6.73)	9.2	(41)	0.734	(18.6)	Fracture
											Average		9.6	(43)	0.265	(6.73)	9.8	(44)	0.501	(12.7)	
											COV	9.13			27.97				9.58		70.45	
UC1	2DMR5721	Dynamic	0.75	(19)	4	(100)	4	(100)	4805	(33.1)	4700	(32.4)	10.8	(48.0)	0.156	(3.96)	14.3	(63.6)	0.528	(13.4)	cone/disp.
Far	2DMR5722	Dynamic	0.75	(19)	4	(100)	4	(100)	4805	(33.1)	4700	(32.4)	8.6	(38)	0.169	(4.29)	15.3	(68.1)	0.500	(12.7)	cone/disp.
Hairpin	2DMR5723	Dynamic	0.75	(19)	4	(100)	4	(100)	4805	(33.1)	4700	(32.4)	10.3	(45.8)	0.182	(4.62)	14.5	(64.5)	0.471	(12.0)	fracture
	2DMR5724	Dynamic	0.75	(19)	4	(100)	4	(100)	4805	(33.1)	4700	(32.4)					16.9	(75.2)	0.413	(10.5)	cone/disp.
	2DMR5725	Dynamic	0.75	(19)	4	(100)	4	(100)	4805	(33.1)	4700	(32.4)	11.5	(51.2)	0.218	(5.54)	14.3	(63.6)	0.491	(12.5)	cone/disp.
											Average		10.3	(45.8)	0.181	(4.60)	15.06	(67.0)	0.481	(12.2)	
											COV	12.00			14.73				7.36		8.95	

Test: Expansion Anchor II, Diameter=0.75 in., Embedment=4.0 in., Edge Distance=4.0 in., Far Hairpin, Dynamic Shear Loading, Uncracked Concrete, River Gravel Aggregate

V_{CC} = Theoretical Concrete Cracking Load

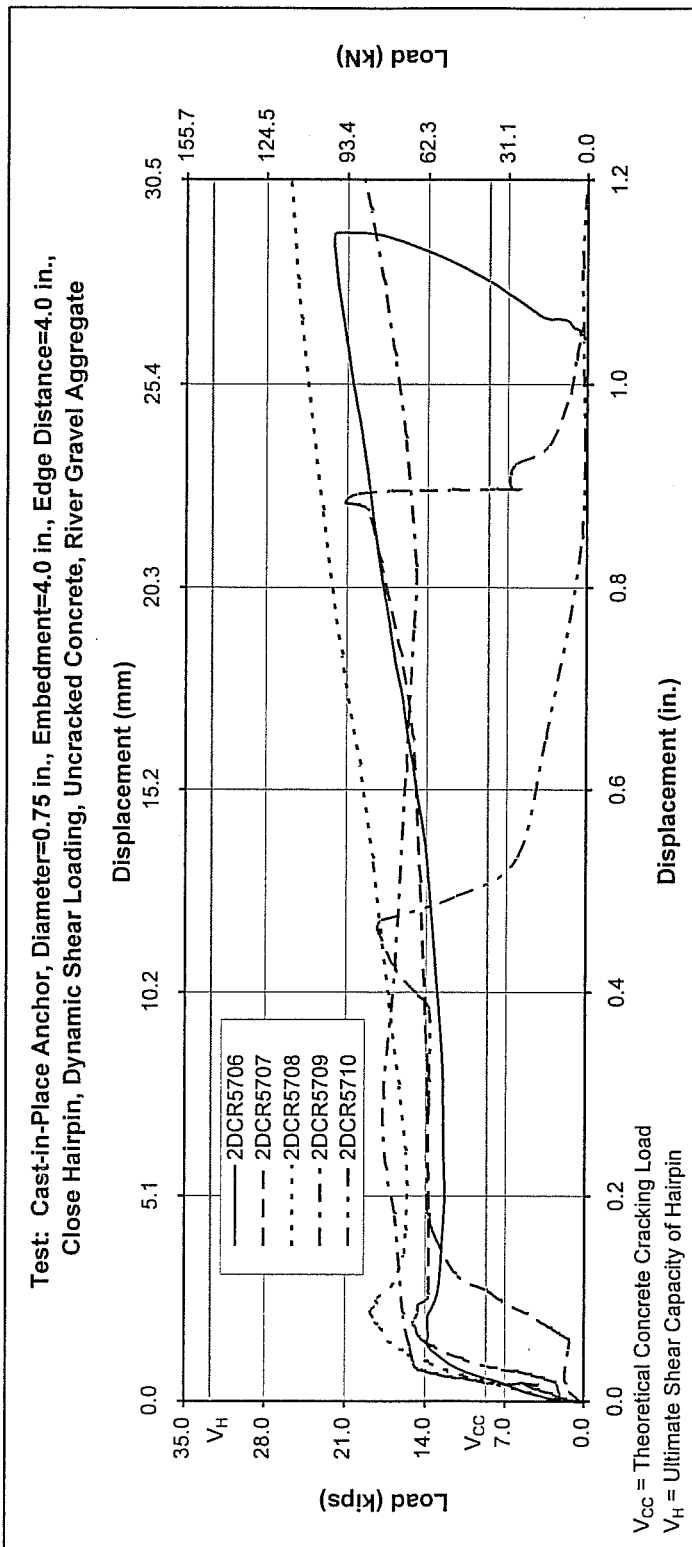| Test Name | Date | f'c psi | Normalized f'c psi | At Concrete Failure | | At Ultimate Failure | | Failure Mode |
				Normalized Maximum Load kips (kN)	Displacement at Maximum Load inches (mm)	Normalized Maximum Load kips (kN)	Displacement at Maximum Load inches (mm)	
2DKR5716	1/24/96	4805	4700	9.9 (44)	0.210 (5.33)	10.2 (45.4)	0.304 (7.72)	Fracture
2DKR5717	1/24/96	4805	4700	10.6 (47.1)	0.391 (9.93)	11.0 (48.9)	1.01 (25.6)	Fracture
2DKR5718	1/24/96	4805	4700	10.2 (45.4)	0.214 (5.44)	10.2 (45.4)	0.214 (5.44)	Fracture
2DKR5719	1/24/96	4805	4700	8.6 (38)	0.244 (6.20)	8.6 (38)	0.244 (6.20)	Cone / Displacement
2DKR5720	1/24/96	4805	4700	8.8 (39)	0.265 (6.73)	9.2 (41)	0.734 (18.6)	Fracture
Average				9.6 (43)	0.265 (6.73)	9.8 (44)	0.501 (12.7)	

Test: Undercut Anchor 1, Diameter=0.75 in., Embedment=4.0 in., Edge Distance=4.0 in., Far Hairpin, Dynamic Shear Loading, Uncracked Concrete, River Gravel Aggregate
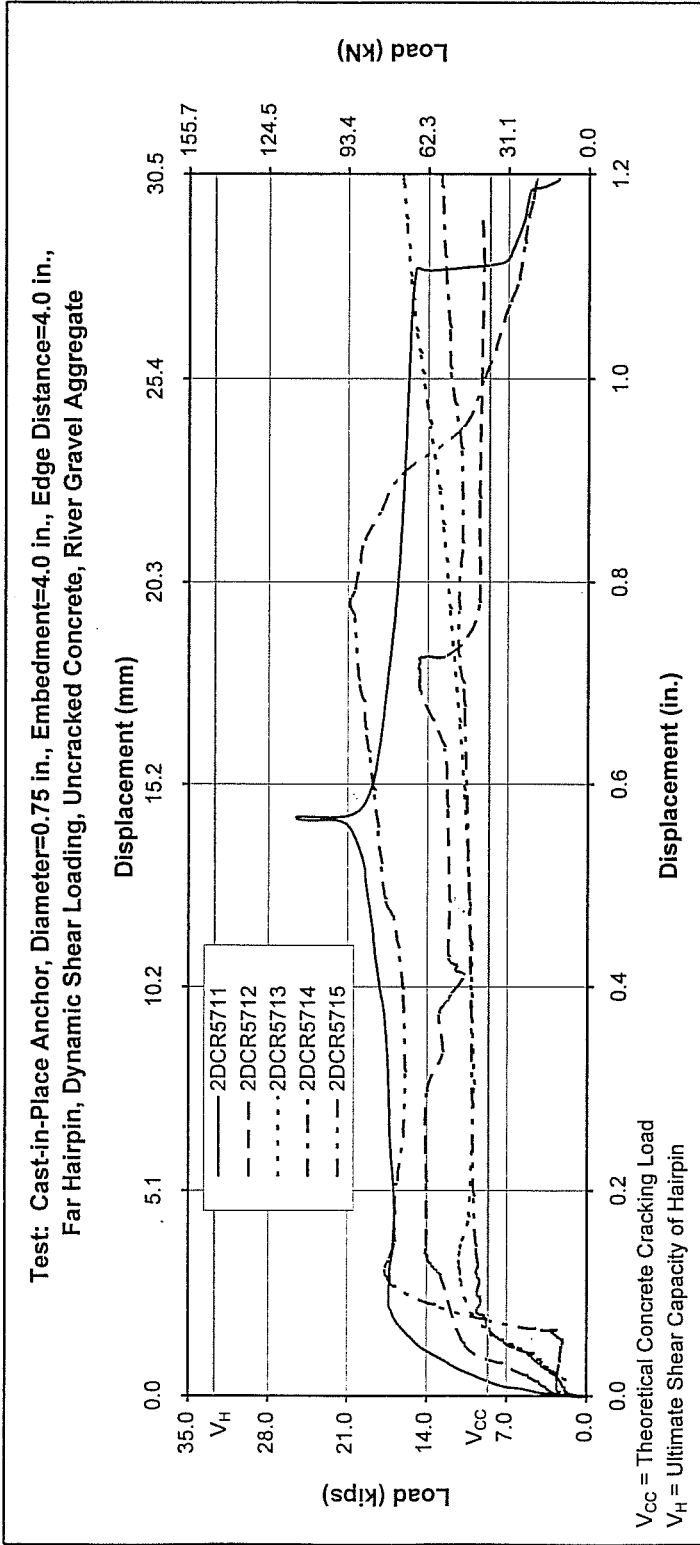

Legend:
- 2DMR5721
- 2DMR5722
- 2DMR5723
- 2DMR5724
- 2DMR5725

V_{CC} = Theoretical Concrete Cracking Load
V_H = Ultimate Shear Capacity of Hairpin

Test Name	Date	f_c psi	Normalized f_c psi	At Concrete Failure			At Ultimate Failure			Failure Mode
				Normalized Maximum Load kips (kN)		Displacement at Maximum Load inches (mm)	Normalized Maximum Load kips (kN)		Displacement at Maximum Load inches (mm)	
2DMR5721	1/25/96	4805	4700	10.8	(48.0)	0.156 (3.96)	14.3	(63.6)	0.528 (13.4)	Cone / Displacement
2DMR5722	1/26/96	4805	4700	8.6	(38)	0.169 (4.29)	15.3	(68.1)	0.500 (12.7)	Cone / Displacement
2DMR5723	1/26/96	4805	4700	10.3	(45.8)	0.182 (4.62)	14.5	(64.5)	0.471 (12.0)	Fracture
2DMR5724	1/26/96	4805	4700	11.5	(51.2)	0.218 (5.54)	16.9	(75.2)	0.413 (10.5)	Cone / Displacement
2DMR5725	1/26/96	4805	4700				14.3	(63.6)	0.491 (12.5)	Cone / Displacement
Average				10.3	(45.8)	0.181 (4.60)	15.1	(67.0)	0.481 (12.2)	

Results for Series 3-3

Anchor	Test Number	Loading	Diameter in. (mm)	Effective Embedment h_e in. (mm)	Edge Distance in. (mm)	f'_c psi (MPa)	Normalized f'_c psi (MPa)	Concrete Cone Breakout Normalized F_u kips (kN)	Displacement in. (mm)	Additional Crack Opening Side mm	Top mm	Ultimate Failure Normalized F_u kips (kN)	Displacement in. (mm)	Failure Mode
CIP	3SCR5701	Static	0.75 (19)	4 (100)	4 (100)	4635 (32.0)	4700 (32.4)	7.5 (33)	0.059 (1.50)	0.03	0.00	7.5 (33)	0.059 (1.50)	cone
No	3SCR5702	Static	0.75 (19)	4 (100)	4 (100)	4635 (32.0)	4700 (32.4)	6.1 (27)	0.075 (1.91)	0.07	0.01	6.1 (27)	0.075 (1.91)	cone
Hairpin	3SCR5703	Static	0.75 (19)	4 (100)	4 (100)	4635 (32.0)	4700 (32.4)	7.2 (32)	0.082 (2.08)	0.05	0.01	7.2 (32)	0.082 (2.08)	cone
	3SCR5704	Static	0.75 (19)	4 (100)	4 (100)	4635 (32.0)	4700 (32.4)	8.3 (37)	0.114 (2.90)	0.09	0.02	8.3 (37)	0.114 (2.90)	cone
	3SCR5705	Static	0.75 (19)	4 (100)	4 (100)	4635 (32.0)	4700 (32.4)	7.0 (31)	0.047 (1.19)	0.03	0.01	7.0 (31)	0.047 (1.19)	cone
							Average	7.2 (32)	0.075 (1.92)	0.05	0.01	7.2 (32)	0.075 (1.92)	
							COV	11.05	33.87	48.29	70.71	11.05	33.87	
CIP	3SCR5706	Static	0.75 (19)	4 (100)	4 (100)	4635 (32.0)	4700 (32.4)	8.6 (38)	0.073 (1.85)	0.03	0.01	22.0 (97.9)	1.08 (27.3)	cone/disp.
Close	3SCR5707	Static	0.75 (19)	4 (100)	4 (100)	4635 (32.0)	4700 (32.4)	10.7 (47.6)	0.051 (1.30)	0.07	0.02	22.7 (101)	1.07 (27.2)	cone/disp.
Hairpin	3SCR5708	Static	0.75 (19)	4 (100)	4 (100)	4740 (32.7)	4700 (32.4)	10.1 (44.9)	0.080 (2.03)	0.16	0.05	20.5 (91.2)	1.20 (30.4)	cone/disp.
	3SCR5709	Static	0.75 (19)	4 (100)	4 (100)	4740 (32.7)	4700 (32.4)	10.3 (45.8)	0.056 (1.42)	0.14	0.04	23.0 (102)	0.696 (17.7)	cone/disp.
	3SCR5710	Static	0.75 (19)	4 (100)	4 (100)	4740 (32.7)	4700 (32.4)	8.2 (36)	0.054 (1.37)	0.03	0.01	22.1 (98.3)	0.888 (22.6)	cone/disp.
							Average	9.6 (43)	0.063 (1.60)	0.09	0.03	22.1 (98.1)	0.986 (25.0)	
							COV	11.56	20.50	71.02	69.87	4.38	19.91	
CIP	3SCR5711	Static	0.75 (19)	4 (100)	4 (100)	4740 (32.7)	4700 (32.4)	10.9 (48.5)	0.201 (5.11)	0.25	0.02	15.7 (69.8)	0.717 (18.2)	cone/disp.
Far	3SCR5712	Static	0.75 (19)	4 (100)	4 (100)	4210 (29.0)	4700 (32.4)	10.6 (47.1)	0.235 (5.97)	0.15	0.02	16.0 (71.2)	1.10 (27.9)	cone/disp.
Hairpin	3SCR5713	Static	0.75 (19)	4 (100)	4 (100)	4210 (29.0)	4700 (32.4)	8.0 (36)	0.100 (2.54)	0.04	0.02	15.5 (68.9)	1.12 (28.3)	cone/disp.
	3SCR5714	Static	0.75 (19)	4 (100)	4 (100)	4210 (29.0)	4700 (32.4)	12.3 (54.7)	0.072 (1.83)	0.09	0.02	18.8 (83.6)	0.829 (21.1)	cone/disp.
	3SCR5715	Static	0.75 (19)	4 (100)	4 (100)	4406 (30.4)	4700 (32.4)	12.1 (53.8)	0.119 (3.02)	0.12	0.01	14.7 (65.4)	0.725 (18.4)	cone/disp.
							Average	10.8 (47.9)	0.145 (3.69)	0.13	0.02	16.1 (71.8)	0.897 (22.8)	
							COV	15.95	47.73	60.32	24.85	9.68	21.99	

Test: Cast-in-Place Anchor, Diameter=0.75 in., Embedment=4.0 in., Edge Distance=4.0 in., No Hairpin, Static Shear Loading, Cracked Concrete, River Gravel Aggregate

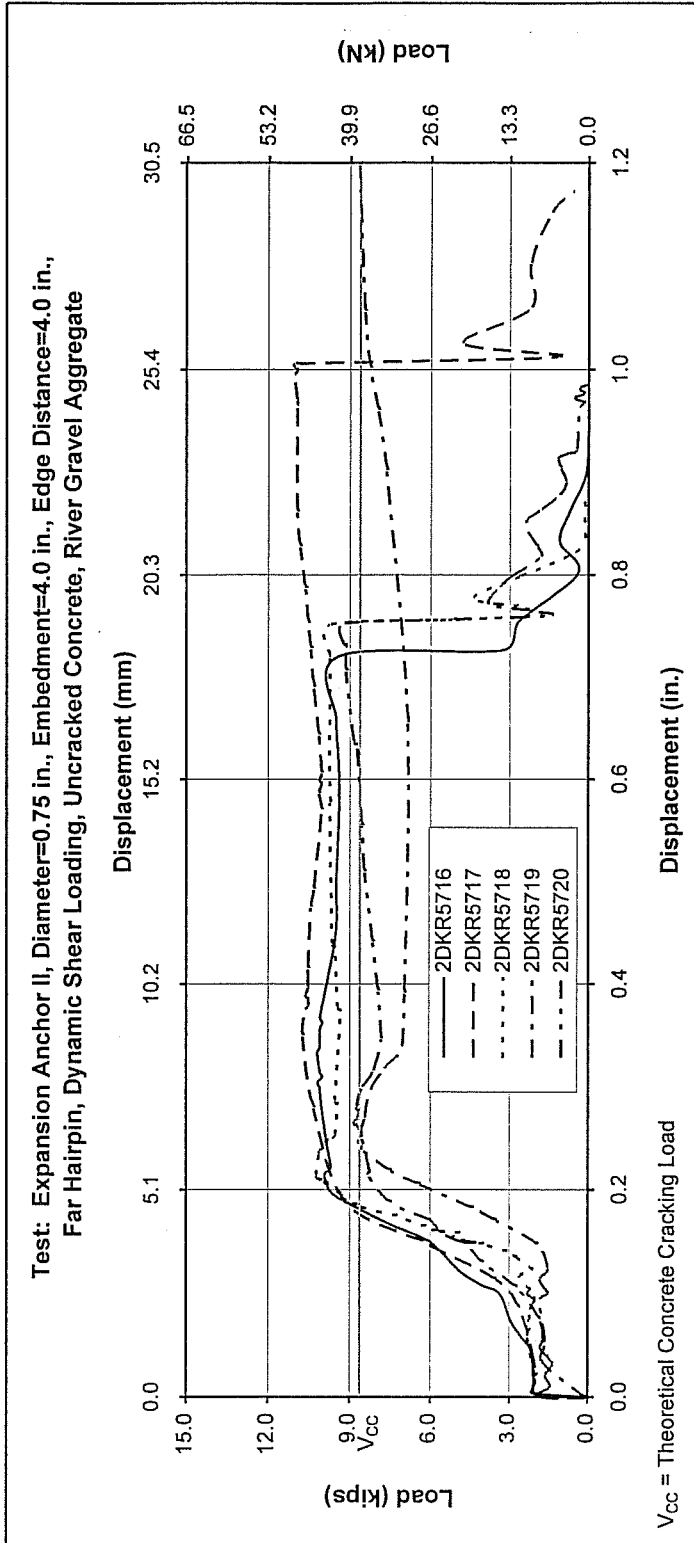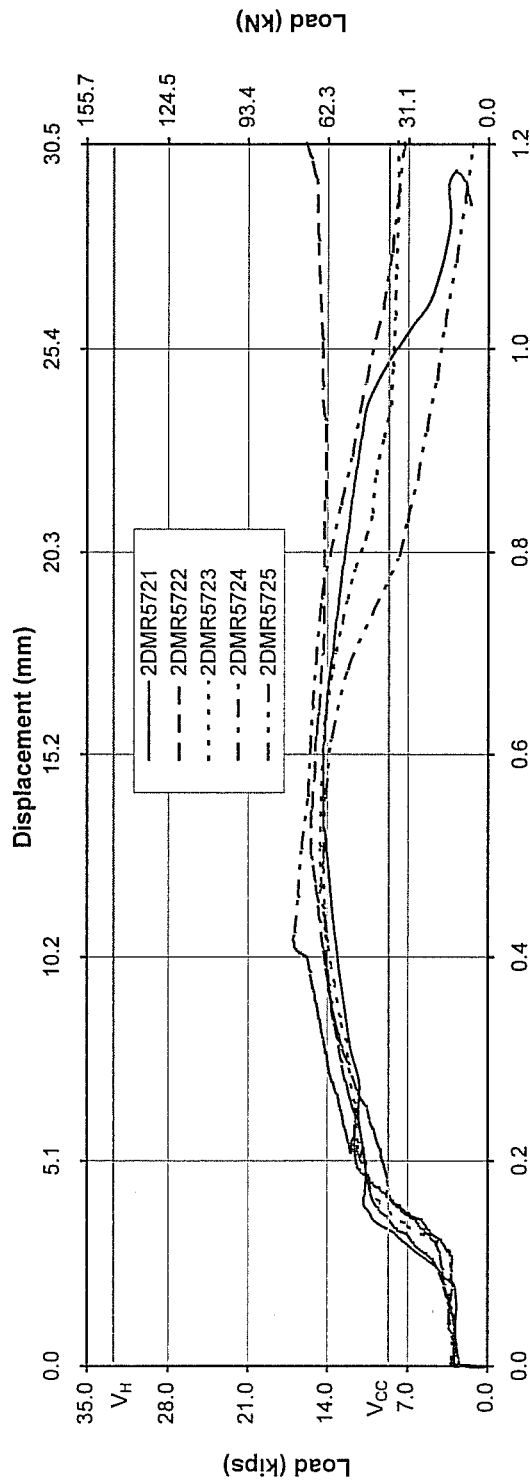V_{CC} = Theoretical Concrete Cracking Load

Test Name	Date	f'c psi	Normalized f'c psi	At Concrete Failure				At Ultimate Failure			
				Normalized Maximum Load		Displacement at Maximum Load		Additional Side Crack Opening	Normalized Maximum Load		Displacement at Maximum Load
				kips	(kN)	inches	(mm)	mm	kips	(kN)	inches	(mm)	Failure Mode
3SCR5701	10/25/95	4635	4700	7.5	(33)	0.059	(1.50)	0.03	7.5	(33)	0.059	(1.50)	Cone
3SCR5702	10/25/95	4635	4700	6.1	(27)	0.075	(1.91)	0.07	6.1	(27)	0.075	(1.91)	Cone
3SCR5703	10/25/95	4635	4700	7.2	(32)	0.082	(2.08)	0.05	7.2	(32)	0.082	(2.08)	Cone
3SCR5704	10/31/95	4635	4700	8.3	(37)	0.114	(2.90)	0.09	8.3	(37)	0.114	(2.90)	Cone
3SCR5705	10/31/95	4635	4700	7.0	(31)	0.047	(1.19)	0.03	7.0	(31)	0.047	(1.19)	Cone
Average				7.2	(32)	0.075	(1.92)	0.05	7.2	(32)	0.075	(1.92)	

Test: Cast-in-Place Anchor, Diameter=0.75 in., Embedment=4.0 in., Edge Distance=4.0 in., Close Hairpin, Static Shear Loading, Cracked Concrete, River Gravel Aggregate

V_{CC} = Theoretical Concrete Cracking Load
V_H = Ultimate Shear Capacity of Hairpin

Test Name	Date	f_c psi	Normalized f_c psi	At Concrete Failure				At Ultimate Failure				Failure Mode
				Normalized Maximum Load kips	(kN)	Displacement at Maximum Load inches	(mm)	Additional Side Crack Opening mm	Normalized Maximum Load kips	(kN)	Displacement at Maximum Load inches	(mm)	
3SCR5706	10/31/95	4635	4700	8.6	(38)	0.073	(1.85)	0.03	22.0	(98)	1.076	(27.33)	Cone / Disp.
3SCR5707	10/31/95	4635	4700	10.7	(48)	0.051	(1.30)	0.07	22.7	(101)	1.072	(27.23)	Cone / Disp.
3SCR5708	11/6/95	4740	4700	10.1	(45)	0.080	(2.03)	0.16	20.5	(91)	1.198	(30.43)	Cone / Disp.
3SCR5709	11/6/95	4740	4700	10.3	(46)	0.056	(1.42)	0.14	23.0	(102)	0.696	(17.68)	Cone / Disp.
3SCR5710	11/8/95	4740	4700	8.2	(36)	0.054	(1.37)	0.03	22.1	(98)	0.888	(22.56)	Cone / Disp.
Average				9.6	(43)	0.063	(1.60)	0.09	22.1	(98)	0.986	(25.04)	

Test: Cast-in-Place Anchor, Diameter=0.75 in., Embedment=4.0 in., Edge Distance=4.0 in., Far Hairpin, Static Shear Loading, Cracked Concrete, River Gravel Aggregate
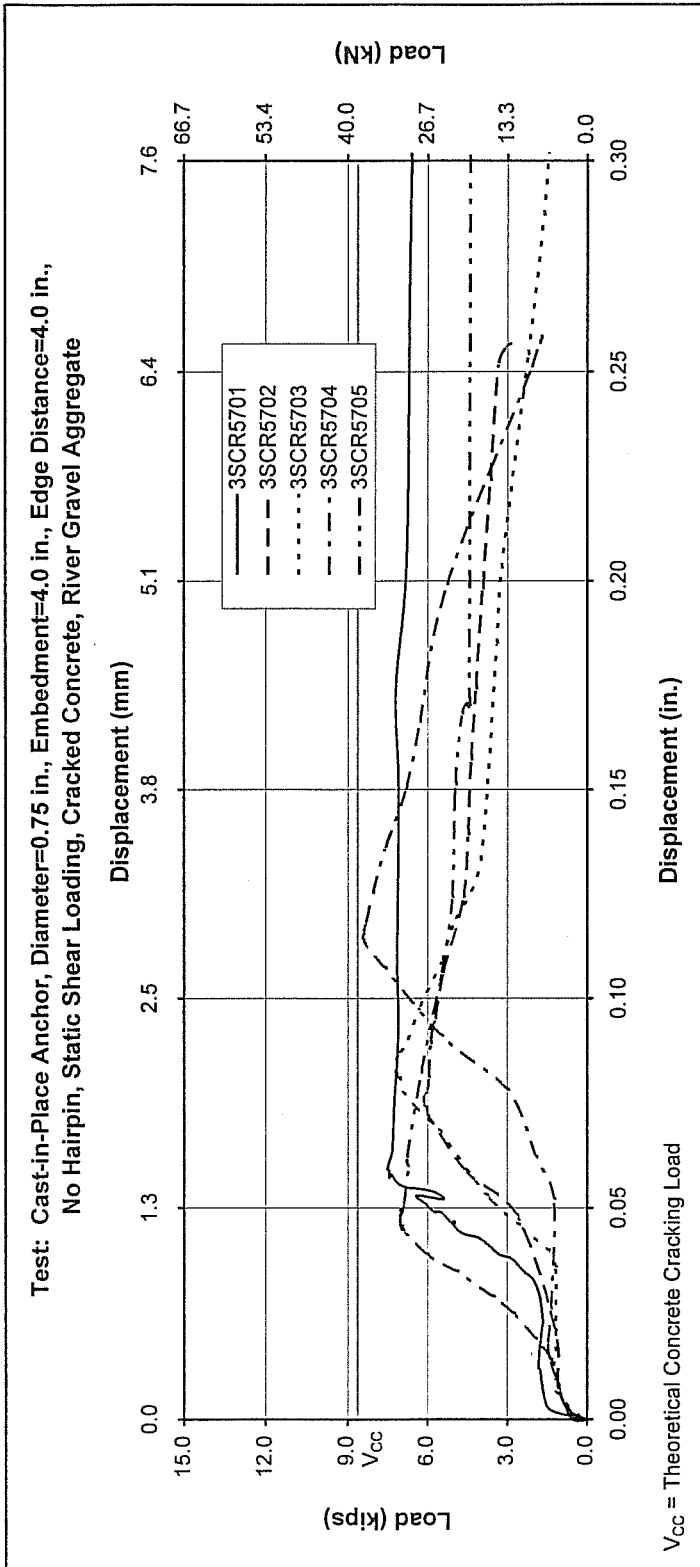

V_{CC} = Theoretical Concrete Cracking Load
V_H = Ultimate Shear Capacity of Hairpin

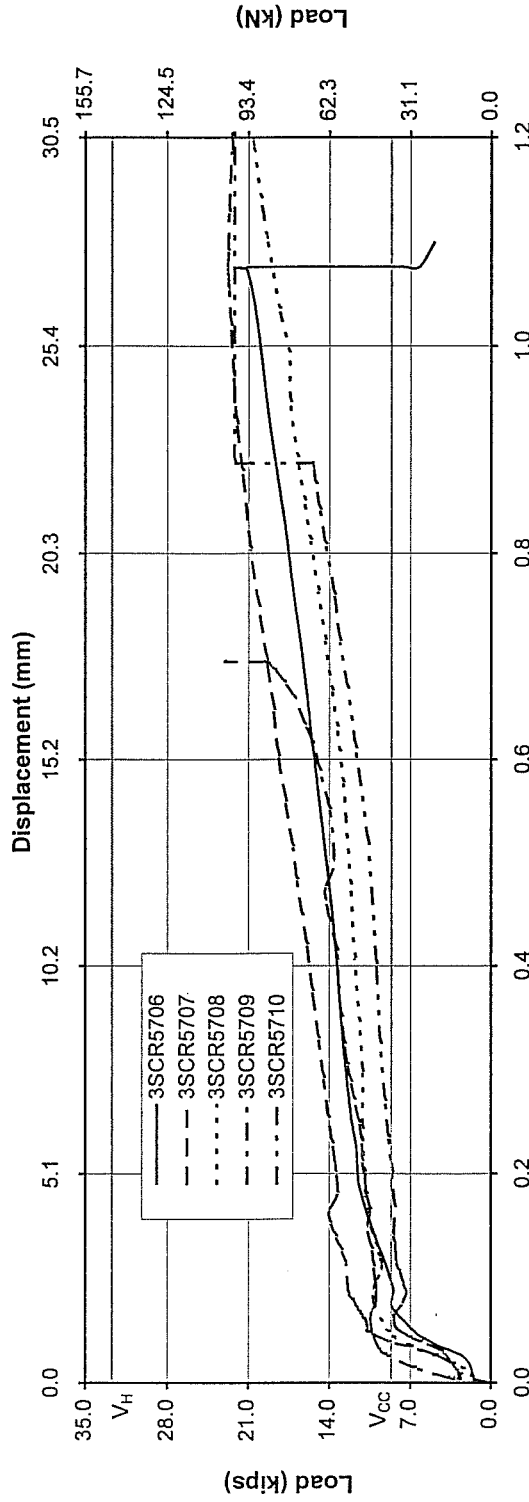| Test Name | Date | f_C psi | Normalized f_C psi | At Concrete Failure | | | At Ultimate Failure | | Failure Mode |
				Normalized Maximum Load kips (kN)	Displacement at Maximum Load inches (mm)	Additional Side Crack Opening mm	Normalized Maximum Load kips (kN)	Displacement at Maximum Load inches (mm)	
3SCR5711	11/8/95	4740	4700	10.9 (48.5)	0.201 (5.11)	0.25	15.7 (69.8)	0.717 (18.2)	Cone / Disp.
3SCR5712	2/23/96	4210	4700	10.6 (47.1)	0.235 (5.97)	0.15	16.0 (71.2)	1.10 (27.9)	Cone / Disp.
3SCR5713	2/26/96	4210	4700	8.0 (35.6)	0.100 (2.54)	0.04	15.5 (68.9)	1.12 (28.3)	Cone / Disp.
3SCR5714	2/26/96	4210	4700	12.3 (54.7)	0.072 (1.83)	0.09	18.8 (83.6)	0.829 (21.1)	Cone / Disp.
3SCR5715	5/9/96	4406	4700	12.1 (53.8)	0.119 (3.02)	0.12	14.7 (65.4)	0.725 (18.4)	Cone / Disp.
Average				10.8 (47.9)	0.145 (3.69)	0.13	16.1 (71.8)	0.897 (22.8)	

Results for Series 3-4

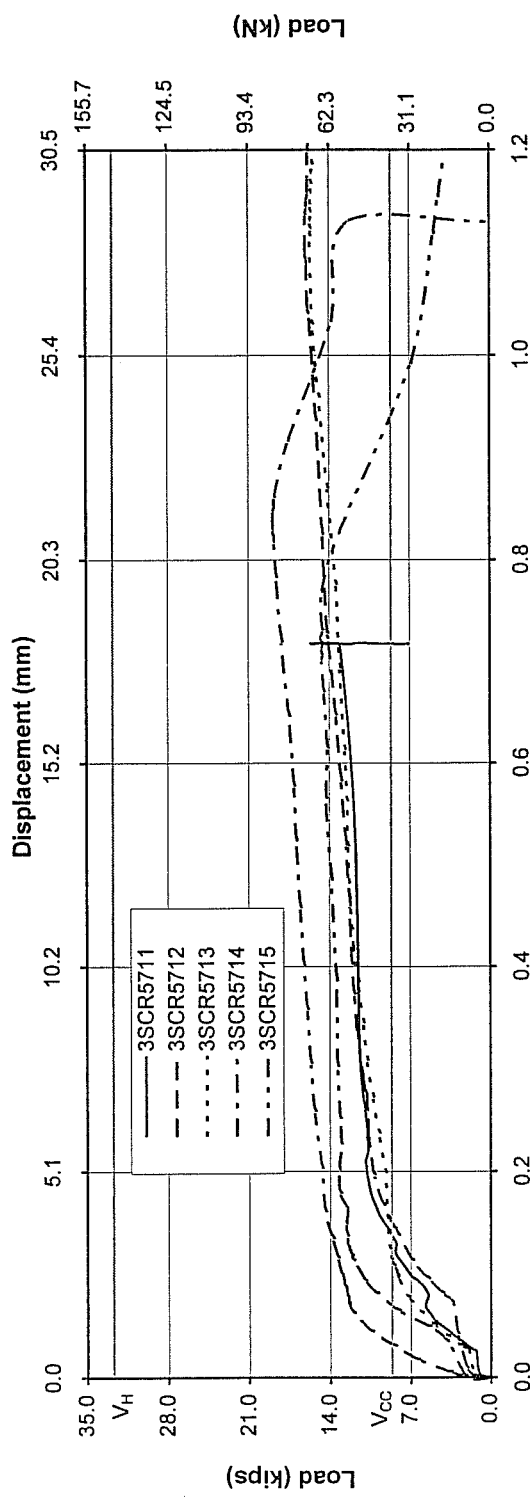| Anchor	Test Number	Loading	Diameter (in.)	(mm)	Effective Embedment h_e (in.)	(mm)	Edge Distance (in.)	(mm)	f_c (psi)	(MPa)	Normalized f_c (psi)	(MPa)	Concrete Cone Breakout — Normalized F_u (kips)	(kN)	Displacement (in.)	(mm)	Additional Crack Opening Side (mm)	Top (mm)	Ultimate Failure — Normalized F_u (kips)	(kN)	Displacement (in.)	(mm)	Failure Mode
CIP No Hairpin	4DCR5701	Dynamic	0.75	(19)	4	(100)	4	(100)	4225	(29.1)	4700	(32.4)	9.8	(44)	0.127	(3.23)	0.09	0.02	9.8	(44)	0.127	(3.23)	cone
	4DCR5702	Dynamic	0.75	(19)	4	(100)	4	(100)	4225	(29.1)	4700	(32.4)	11.0	(48.9)	0.149	(3.78)	0.23	0.01	11.0	(48.9)	0.149	(3.78)	cone
	4DCR5703	Dynamic	0.75	(19)	4	(100)	4	(100)	4225	(29.1)	4700	(32.4)	7.3	(32)	0.117	(2.97)	0.08	0.01	7.3	(32)	0.117	(2.97)	cone
	4DCR5704	Dynamic	0.75	(19)	4	(100)	4	(100)	4225	(29.1)	4700	(32.4)	10.7	(47.6)	0.096	(2.44)	0.21	0.02	10.7	(47.6)	0.096	(2.44)	cone
	4DCR5705	Dynamic	0.75	(19)	4	(100)	4	(100)	4225	(29.1)	4700	(32.4)	13.0	(57.8)	0.080	(2.03)	0.22	0.06	13.0	(57.8)	0.080	(2.03)	cone
											Average		10.4	(46.1)	0.114	(2.89)	0.17	0.02	10.4	(46.1)	0.114	(2.89)	
											COV		20.00		23.59		44.80	86.40	20.00		23.59		
CIP Close Hairpin	4DCR5706	Dynamic	0.75	(19)	4	(100)	4	(100)	4225	(29.1)	4700	(32.4)	15.2	(67.6)	0.090	(2.29)	0.20	0.04	20.6	(91.6)	0.844	(21.4)	cone/disp.
	4DCR5707	Dynamic	0.75	(19)	4	(100)	4	(100)	4225	(29.1)	4700	(32.4)	13.4	(59.6)	0.093	(2.36)	0.13	0.02	25.2	(112)	0.945	(24.0)	cone/disp.
	4DCR5708	Dynamic	0.75	(19)	4	(100)	4	(100)	4225	(29.1)	4700	(32.4)	12.3	(54.7)	0.031	(0.79)	0.04	0.01	29.3	(130)	1.20	(30.5)	cone/disp.
	4DCR5709	Dynamic	0.75	(19)	4	(100)	4	(100)	4225	(29.1)	4700	(32.4)	16.0	(71.2)	0.051	(1.30)	0.07	0.02	20.1	(89)	1.20	(30.5)	cone/disp.
	4DCR5710	Dynamic	0.75	(19)	4	(100)	4	(100)	4225	(29.1)	4700	(32.4)	16.7	(74.3)	0.066	(1.68)	0.15	0.02	25.3	(113)	1.20	(30.5)	cone/disp.
											Average		14.7	(65.5)	0.066	(1.68)	0.12	0.02	24.1	(107)	1.08	(27.4)	
											COV		12.43		39.64		54.06	49.79	15.79		15.87		
CIP Far Hairpin	4DCR5711	Dynamic	0.75	(19)	4	(100)	4	(100)	4800	(33.1)	4700	(32.4)	15.5	(68.9)	0.193	(4.90)	0.16	0.02	18.7	(83.2)	0.517	(13.1)	cone/disp.
	4DCR5712	Dynamic	0.75	(19)	4	(100)	4	(100)	4800	(33.1)	4700	(32.4)	12.4	(55.2)	0.103	(2.62)	0.03	0.01	15.5	(68.9)	1.20	(30.5)	cone/disp.
	4DCR5713	Dynamic	0.75	(19)	4	(100)	4	(100)	4800	(33.1)	4700	(32.4)	14.5	(64.5)	0.157	(3.99)			17.4	(77.4)	1.20	(30.5)	cone/disp.
	4DCR5714	Dynamic	0.75	(19)	4	(100)	4	(100)	4800	(33.1)	4700	(32.4)	15.7	(69.8)	0.211	(5.36)	0.09	0.01	18.7	(83.2)	1.20	(30.5)	cone/disp.
	4DCR5715	Dynamic	0.75	(19)	4	(100)	4	(100)	4225	(29.1)	4700	(32.4)	19.7	(87.6)	0.144	(3.66)	0.15	0.05	19.7	(87.6)	0.144	(3.66)	cone/disp.
											Average		15.6	(69.2)	0.162	(4.10)	0.11	0.02	18.0	(80.1)	0.852	(21.6)	
											COV		17.09		26.24		56.01	84.13	8.99		57.99		

Test: Cast-in-Place Anchor, Diameter=0.75 in., Embedment=4.0 in., Edge Distance=4.0 in., No Hairpin, Dynamic Shear Loading, Cracked Concrete, River Gravel Aggregate

Legend: 4DCR5701, 4DCR5702, 4DCR5703, 4DCR5704, 4DCR5705

Axes: Load (kN), Load (kips), Displacement (mm), Displacement (in.)

V_{CC} = Theoretical Concrete Cracking Load

Test Name	Date	f'c (psi)	Normalized f'c (psi)	At Concrete Failure					At Ultimate Failure				
				Normalized Maximum Load (kips)	(kN)	Displacement at Maximum Load (inches)	(mm)	Additional Side Crack Opening (mm)	Normalized Maximum Load (kips)	(kN)	Displacement at Maximum Load (inches)	(mm)	Failure Mode
4DCR5701	3/4/96	4225	4700	9.8	(44)	0.127	(3.23)	0.09	9.8	(44)	0.127	(3.23)	Cone
4DCR5702	3/7/96	4225	4700	11.0	(48.9)	0.149	(3.78)	0.23	11.0	(48.9)	0.149	(3.78)	Cone
4DCR5703	3/7/96	4225	4700	7.3	(32)	0.117	(2.97)	0.08	7.3	(32)	0.117	(2.97)	Cone
4DCR5704	3/13/96	4225	4700	10.7	(47.6)	0.096	(2.44)	0.21	10.7	(47.6)	0.096	(2.44)	Cone
4DCR5705	3/13/96	4225	4700	13.0	(57.8)	0.080	(2.03)	0.22	13.0	(57.8)	0.080	(2.03)	Cone
Average				10.4	(46.1)	0.114	(2.89)	0.17	10.4	(46.1)	0.114	(2.89)	

207

Test: Cast-in-Place Anchor, Diameter=0.75 in., Embedment=4.0 in., Edge Distance=4.0 in., Close Hairpin, Dynamic Shear Loading, Cracked Concrete, River Gravel Aggregate

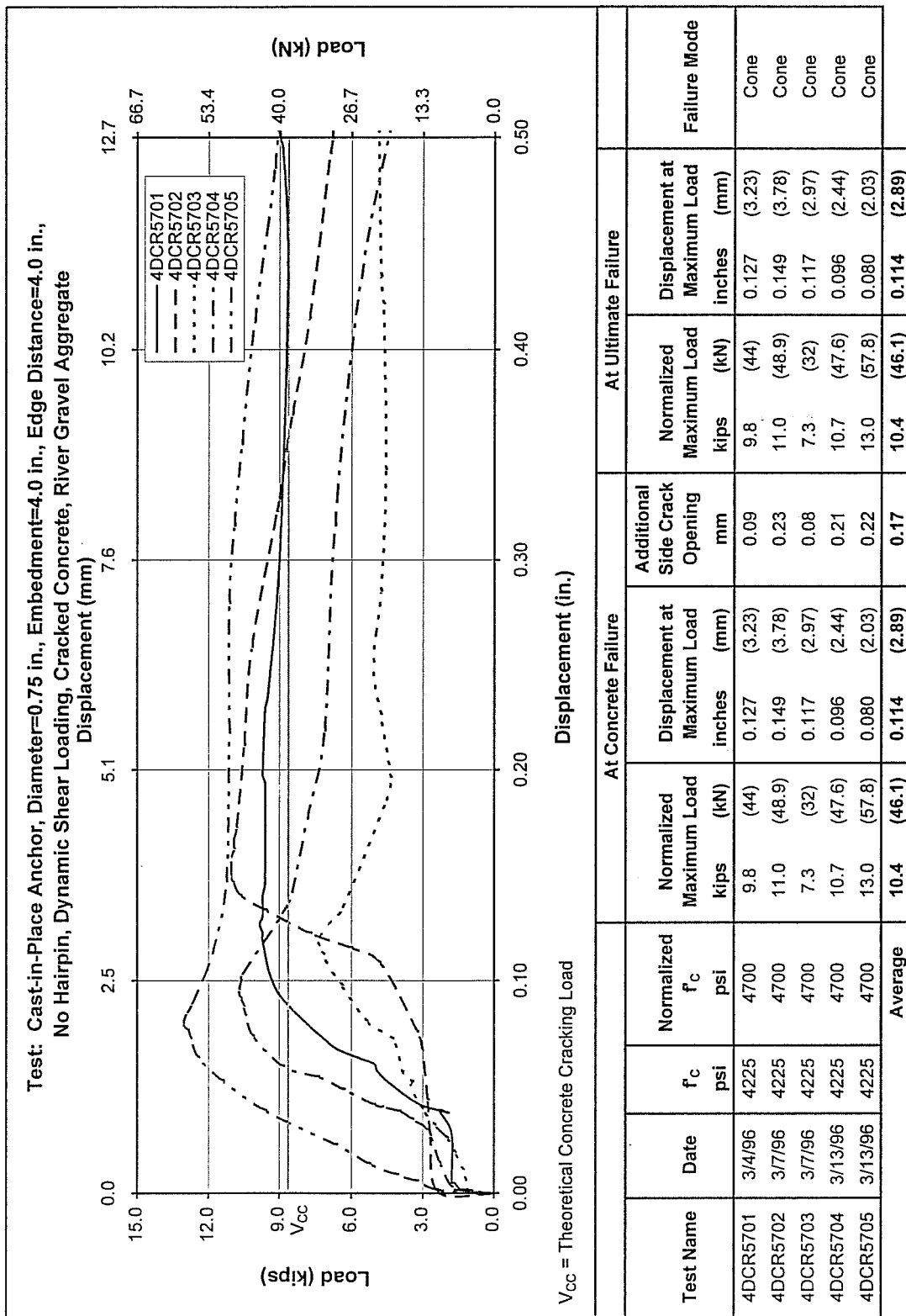Legend: 4DCR5706, 4DCR5707, 4DCR5708, 4DCR5709, 4DCR5710

V_{CC} = Theoretical Concrete Cracking Load
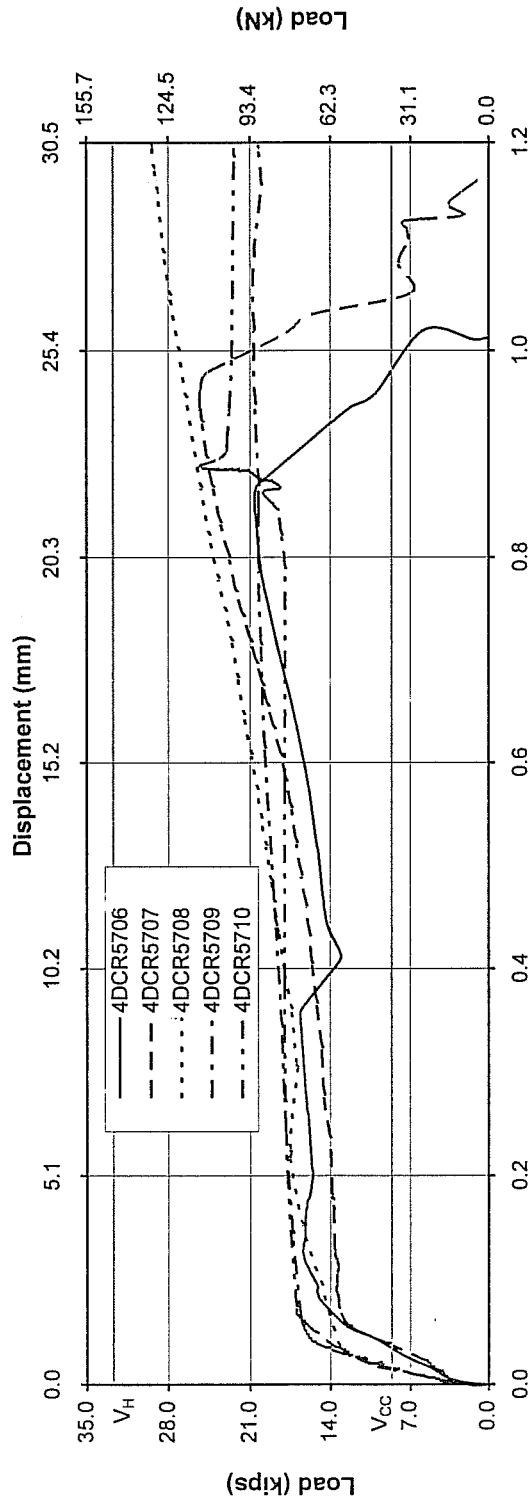V_H = Ultimate Shear Capacity of Hairpin

Test Name	Date	f'_c psi	Normalized f'_c psi	At Concrete Failure					At Ultimate Failure				Failure Mode
				Normalized Maximum Load kips	(kN)	Displacement at Maximum Load inches	(mm)	Additional Side Crack Opening mm	Normalized Maximum Load kips	(kN)	Displacement at Maximum Load inches	(mm)	
4DCR5706	3/13/96	4225	4700	15.2	(67.6)	0.090	(2.29)	0.20	20.6	(91.6)	0.844	(21.4)	Cone / Disp.
4DCR5707	3/13/96	4225	4700	13.4	(59.6)	0.093	(2.36)	0.13	25.2	(112)	0.945	(24.0)	Cone / Disp.
4DCR5708	3/14/96	4225	4700	12.3	(54.7)	0.031	(0.79)	0.04	29.3	(130)	1.20	(30.5)	Cone / Disp.
4DCR5709	3/14/96	4225	4700	16.0	(71.2)	0.051	(1.30)	0.07	20.1	(89.4)	1.20	(30.5)	Cone / Disp.
4DCR5710	3/14/96	4225	4700	16.7	(74.3)	0.066	(1.68)	0.15	25.3	(113)	1.20	(30.5)	Cone / Disp.
Average				14.7	(65.5)	0.066	(1.68)	0.12	24.1	(107)	1.08	(27.4)	

Test: Cast-in-Place Anchor, Diameter=0.75 in., Embedment=4.0 in., Edge Distance=4.0 in., Far Hairpin, Dynamic Shear Loading, Cracked Concrete, River Gravel Aggregate

Legend: 4DCR5711, 4DCR5712, 4DCR5713, 4DCR5714, 4DCR5715

V_{CC} = Theoretical Concrete Cracking Load
V_H = Ultimate Shear Capacity of Hairpin

Test Name	Date	f_c psi	Normalized f_c psi	At Concrete Failure				Additional Side Crack Opening mm	At Ultimate Failure				Failure Mode
				Normalized Maximum Load		Displacement at Maximum Load			Normalized Maximum Load		Displacement at Maximum Load		
				kips	(kN)	inches	(mm)		kips	(kN)	inches	(mm)	
4DCR5711	1/30/96	4800	4700	15.5	(68.9)	0.193	(4.90)	0.16	18.7	(83.2)	0.517	(13.1)	Cone / Disp.
4DCR5712	1/31/96	4800	4700	12.4	(55.2)	0.103	(2.62)	0.03	15.5	(68.9)	1.20	(30.5)	Cone / Disp.
4DCR5713	1/31/96	4800	4700	14.5	(64.5)	0.157	(3.99)		17.4	(77.4)	1.20	(30.5)	Cone / Disp.
4DCR5714	1/31/96	4800	4700	15.7	(69.8)	0.211	(5.36)	0.09	18.7	(83.2)	1.20	(30.5)	Cone / Disp.
4DCR5715	3/14/96	4225	4700	19.7	(87.6)	0.144	(3.66)	0.15	19.7	(87.6)	0.144	(3.66)	Cone / Disp.
Average				15.6	(69.2)	0.162	(4.10)	0.11	18.0	(80.1)	0.852	(21.6)	

Results for Series 3-5

Anchor	Test Number	Loading	Diameter in. (mm)		Effective Embedment h_e in. (mm)		Front Anchor Edge Distance in. (mm)		Back Anchor Edge Distance in. (mm)		f_c psi (MPa)		Normalized f_c psi (MPa)		Concrete Cone Breakout Normalized F_u kips (kN)		Concrete Cone Breakout Displacement in. (mm)		Ultimate Failure Normalized F_u kips (kN)		Ultimate Failure Displacement in. (mm)		Failure Mode Front Anchor	Failure Mode Back Anchor
CIP No Hairpin	5SCR5701	Static	0.75	(19)	4	(100)	4	(100)	12	(300)	4460	(30.8)	4700	(32.4)	25.8	(115)	0.117	(2.97)	38.1	(169)	0.728	(18.49)	cone	fracture
	5SCR5702	Static	0.75	(19)	4	(100)	4	(100)	12	(300)	4460	(30.8)	4700	(32.4)	29.7	(132)	0.125	(3.18)	39.4	(175)	0.63	(16.00)	cone	fracture
	5SCR5703	Static	0.75	(19)	4	(100)	4	(100)	12	(300)	4460	(30.8)	4700	(32.4)	28.7	(128)	0.112	(2.84)	37.8	(168)	0.77	(19.56)	cone	fracture
	5SCR5704	Static	0.75	(19)	4	(100)	4	(100)	12	(300)	4460	(30.8)	4700	(32.4)	23.3	(104)	0.177	(4.50)	35	(156)	0.787	(19.99)	cone	fracture
	5SCR5705	Static	0.75	(19)	4	(100)	4	(100)	12	(300)	4460	(30.8)	4700	(32.4)	27.9	(124)	0.228	(5.79)	37.5	(167)	0.702	(17.83)	cone	pryout
														Average	27.1	(120)	0.152	(3.86)	37.6	(167)	0.723	(18.37)		
														COV	9.43		32.86		4.27		8.58			
CIP Close Hairpin	5SCR5706	Static	0.75	(19)	4	(100)	4	(100)	12	(300)	4460	(30.8)	4700	(32.4)	38.2	(170)	0.158	(4.01)	57.6	(256)	0.813	(20.7)	fracture	pryout
	5SCR5707	Static	0.75	(19)	4	(100)	4	(100)	12	(300)	4460	(30.8)	4700	(32.4)	35.0	(156)	0.230	(5.84)	43.6	(194)	0.570	(14.5)	cone/disp.	fracture
	5SCR5708	Static	0.75	(19)	4	(100)	4	(100)	12	(300)	4460	(30.8)	4700	(32.4)	34.9	(155)	0.160	(4.06)	54.4	(242)	0.908	(23.1)	cone/disp.	fracture
	5SCR5709	Static	0.75	(19)	4	(100)	4	(100)	12	(300)	4460	(30.8)	4700	(32.4)	32.7	(145)	0.174	(4.42)	45.4	(202)	0.746	(18.9)	cone/disp.	pryout
	5SCR5710	Static	0.75	(19)	4	(100)	4	(100)	12	(300)	4406	(30.4)	4700	(32.4)	32.3	(144)	0.169	(4.29)	43.2	(192)	0.654	(16.6)	cone/disp.	fracture
														Average	34.6	(154)	0.178	(4.53)	48.84	(217)	0.738	(18.8)		
														COV	6.79		16.66		13.69		17.90			

Test: Cast-in-Place Anchors, Diameter=0.75 in., Embedment=4.0 in., Edge Distance=4.0 in., and 12 in.,
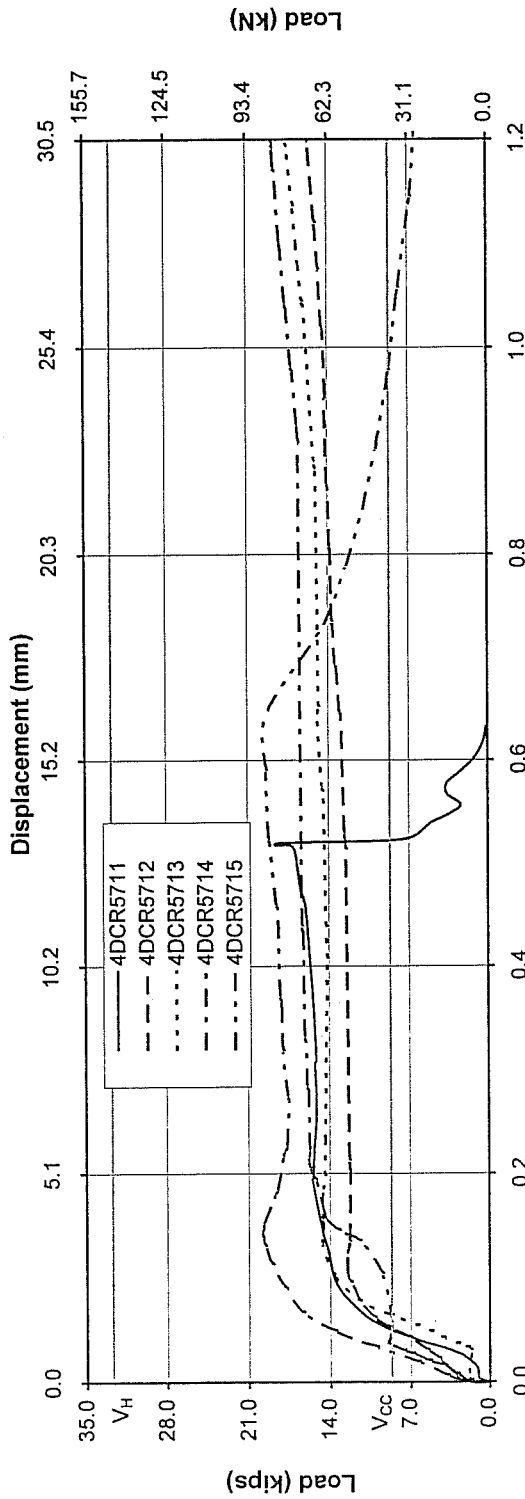No Hairpin, Static Shear Loading, Uncracked Concrete, River Gravel Aggregate
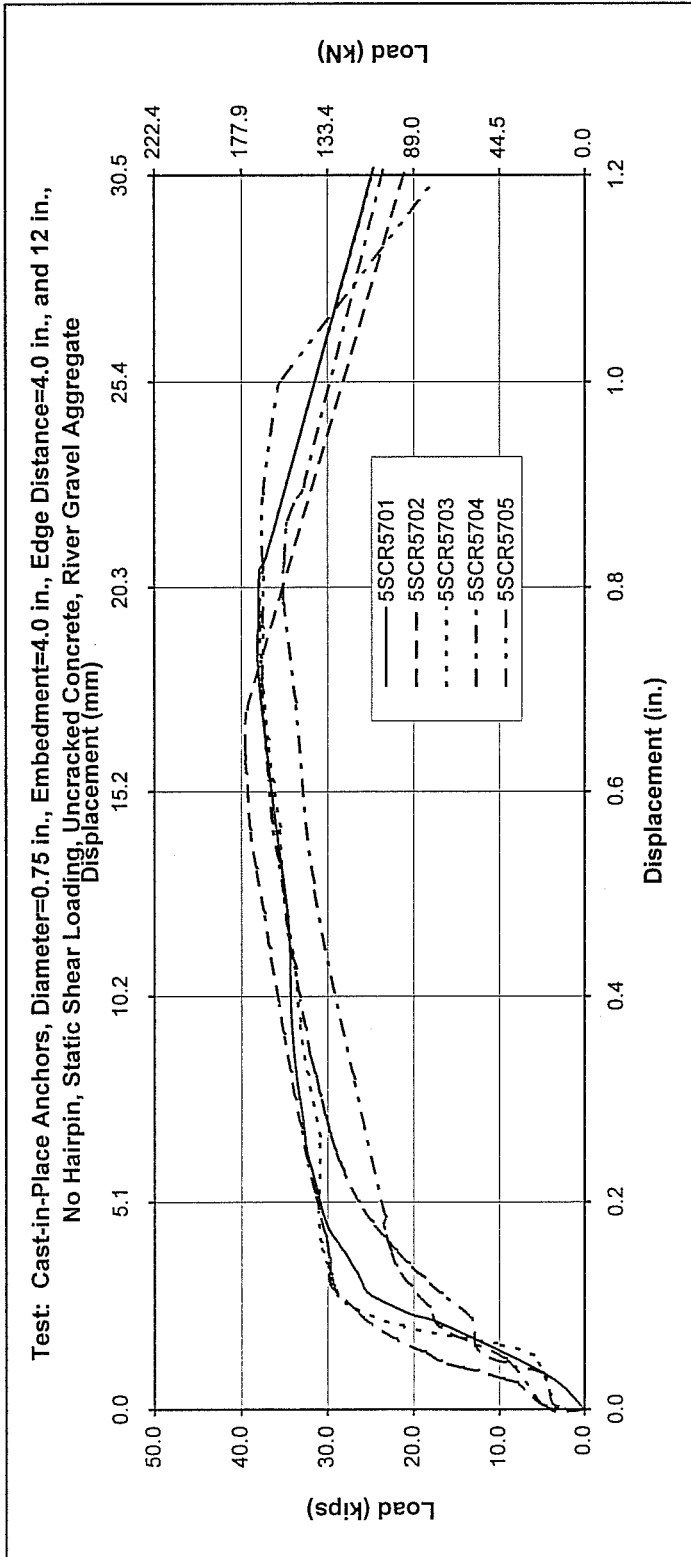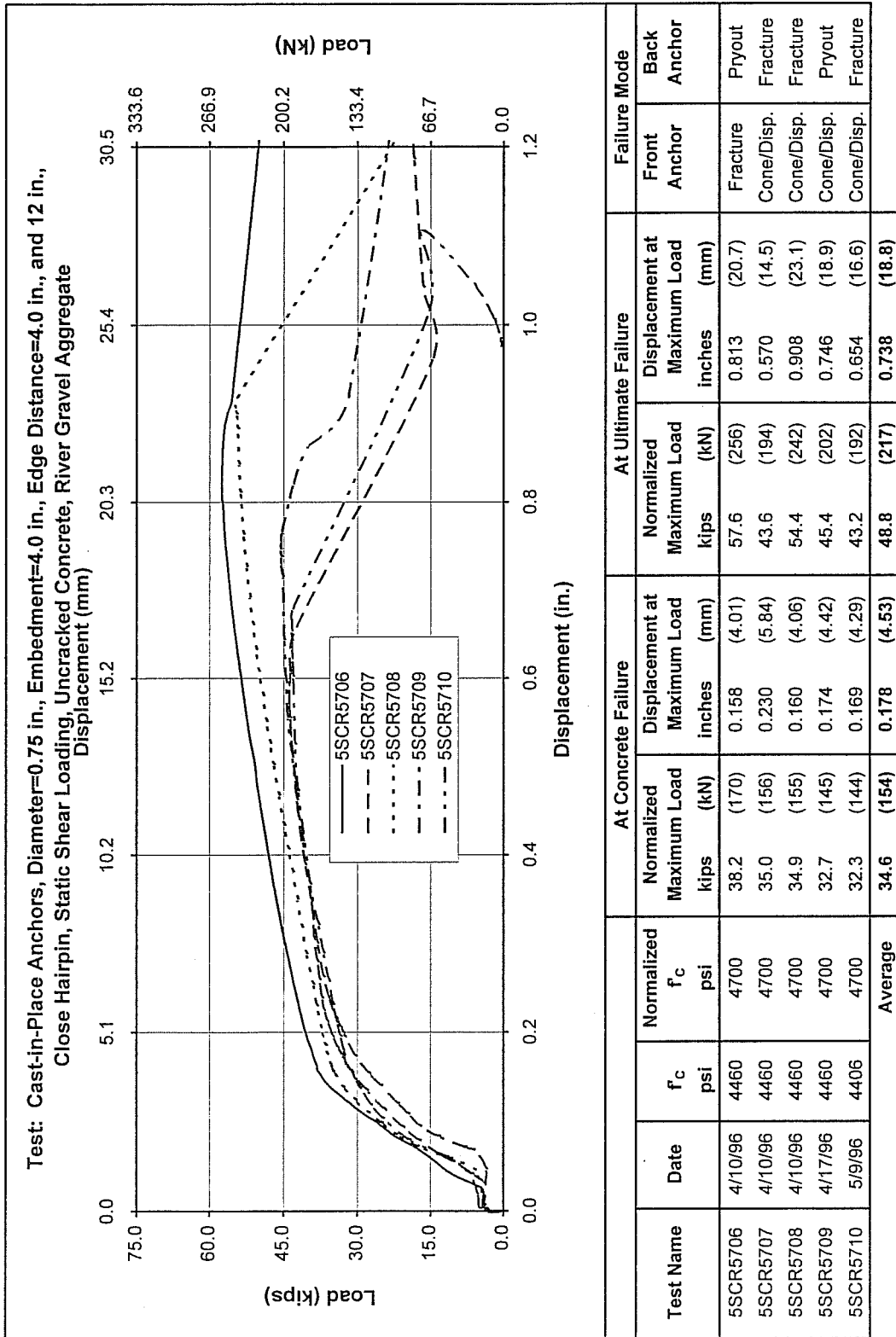

Test Name	Date	f'c psi	Normalized f'c psi	At Concrete Failure				At Ultimate Failure				Failure Mode	
				Normalized Maximum Load		Displacement at Maximum Load		Normalized Maximum Load		Displacement at Maximum Load		Front Anchor	Back Anchor
				kips	(kN)	inches	(mm)	kips	(kN)	inches	(mm)		
5SCR5701	4/2/96	4460	4700	25.8	(115)	0.117	(2.97)	38.1	(169)	0.728	(18.5)	Cone	Fracture
5SCR5702	4/2/96	4460	4700	29.7	(132)	0.125	(3.18)	39.4	(175)	0.630	(16.0)	Cone	Fracture
5SCR5703	4/2/96	4460	4700	28.7	(128)	0.112	(2.84)	37.8	(168)	0.770	(19.6)	Cone	Fracture
5SCR5704	4/4/96	4460	4700	23.3	(104)	0.177	(4.50)	35.0	(156)	0.787	(20.0)	Cone	Fracture
5SCR5705	4/4/96	4460	4700	27.9	(124)	0.228	(5.79)	37.5	(167)	0.702	(17.8)	Cone	Pryout
Average				27.1	(120)	0.152	(3.86)	37.6	(167)	0.723	(18.4)		

Test: Cast-in-Place Anchors, Diameter=0.75 in., Embedment=4.0 in., Edge Distance=4.0 in., and 12 in., Close Hairpin, Static Shear Loading, Uncracked Concrete, River Gravel Aggregate

Test Name	Date	f_c psi	Normalized f_c psi	At Concrete Failure				At Ultimate Failure				Failure Mode	
				Normalized Maximum Load		Displacement at Maximum Load		Normalized Maximum Load		Displacement at Maximum Load		Front Anchor	Back Anchor
				kips	(kN)	inches	(mm)	kips	(kN)	inches	(mm)		
5SCR5706	4/10/96	4460	4700	38.2	(170)	0.158	(4.01)	57.6	(256)	0.813	(20.7)	Fracture	Pryout
5SCR5707	4/10/96	4460	4700	35.0	(156)	0.230	(5.84)	43.6	(194)	0.570	(14.5)	Cone/Disp.	Fracture
5SCR5708	4/10/96	4460	4700	34.9	(155)	0.160	(4.06)	54.4	(242)	0.908	(23.1)	Cone/Disp.	Fracture
5SCR5709	4/17/96	4460	4700	32.7	(145)	0.174	(4.42)	45.4	(202)	0.746	(18.9)	Cone/Disp.	Pryout
5SCR5710	5/9/96	4406	4700	32.3	(144)	0.169	(4.29)	43.2	(192)	0.654	(16.6)	Cone/Disp.	Fracture
Average				34.6	(154)	0.178	(4.53)	48.8	(217)	0.738	(18.8)		

Results for Series 3-6

Anchor	Test Number	Loading	Diameter (in.)	(mm)	Effective Embedment h_e (in.)	(mm)	Front Anchor Edge Distance (in.)	(mm)	Back Anchor Edge Distance (in.)	(mm)	f'_c (psi)	(MPa)	Normalized f'_c (psi)	(MPa)	Concrete Cone Breakout Normalized F_u (kips)	(kN)	Displacement (in.)	(mm)	Ultimate Failure Normalized F_u (kips)	(kN)	Displacement (in.)	(mm)	Failure Mode Front Anchor	Back Anchor
CIP No Hairpin	6DCR5701	Dynamic	0.75	(19)	4	(100)	4	(100)	12	(300)	4406	(30.4)	4700	(32.4)	26.0	(116)	0.116	(2.95)	38.6	(172)	0.692	(17.6)	cone	fracture
	6DCR5702	Dynamic	0.75	(19)	4	(100)	4	(100)	12	(300)	4460	(30.8)	4700	(32.4)	25.3	(113)	0.112	(2.84)	32.3	(144)	0.448	(11.4)	cone	fracture
	6DCR5703	Dynamic	0.75	(19)	4	(100)	4	(100)	12	(300)	4460	(30.8)	4700	(32.4)	26.9	(120)	0.091	(2.31)	37.7	(168)	0.814	(20.7)	cone	fracture
	6DCR5704	Dynamic	0.75	(19)	4	(100)	4	(100)	12	(300)	4406	(30.4)	4700	(32.4)	25.3	(113)	0.140	(3.56)	40.5	(180)	0.709	(18.0)	cone	fracture
	6DCR5705	Dynamic	0.75	(19)	4	(100)	4	(100)	12	(300)	4406	(30.4)	4700	(32.4)	26.5	(118)	0.090	(2.29)	37.5	(167)	0.523	(13.3)	cone	fracture
											Average		26.0	(116)			0.110	(2.79)	37.3	(166)	0.637	(16.2)		
											COV		2.75				18.78		8.16		23.31			
CIP Close Hairpin	6DCR5706	Dynamic	0.75	(19)	4	(100)	4	(100)	12	(300)	4406	(30.4)	4700	(32.4)	36.5	(162)	0.161	(4.09)	53.6	(238)	0.730	(18.5)	fracture	fracture
	6DCR5707	Dynamic	0.75	(19)	4	(100)	4	(100)	12	(300)	4406	(30.4)	4700	(32.4)	39.1	(174)	0.153	(3.89)	57.3	(255)	0.665	(16.9)	yield	yield
	6DCR5708	Dynamic	0.75	(19)	4	(100)	4	(100)	12	(300)	4406	(30.4)	4700	(32.4)	40.0	(178)	0.204	(5.18)	56.6	(252)	0.828	(21.0)	fracture	fracture
	6DCR5709	Dynamic	0.75	(19)	4	(100)	4	(100)	12	(300)	4406	(30.4)	4700	(32.4)	38.3	(170)	0.154	(3.91)	57.7	(257)	0.727	(18.5)	yield	yield
	6DCR5710	Dynamic	0.75	(19)	4	(100)	4	(100)	12	(300)	4406	(30.4)	4700	(32.4)	38.0	(169)	0.185	(4.70)	44.9	(200)	0.513	(13.0)	fracture	fracture
											Average		38.4	(171)			0.171	(4.35)	54.0	(240)	0.693	(17.6)		
											COV		3.40				13.04		9.90		16.77			

Test: Cast-in-Place Anchors, Diameter=0.75 in., Embedment=4.0 in., Edge Distance=4.0 in., and 12 in., No Hairpin, Dynamic Shear Loading, Uncracked Concrete, River Gravel Aggregate
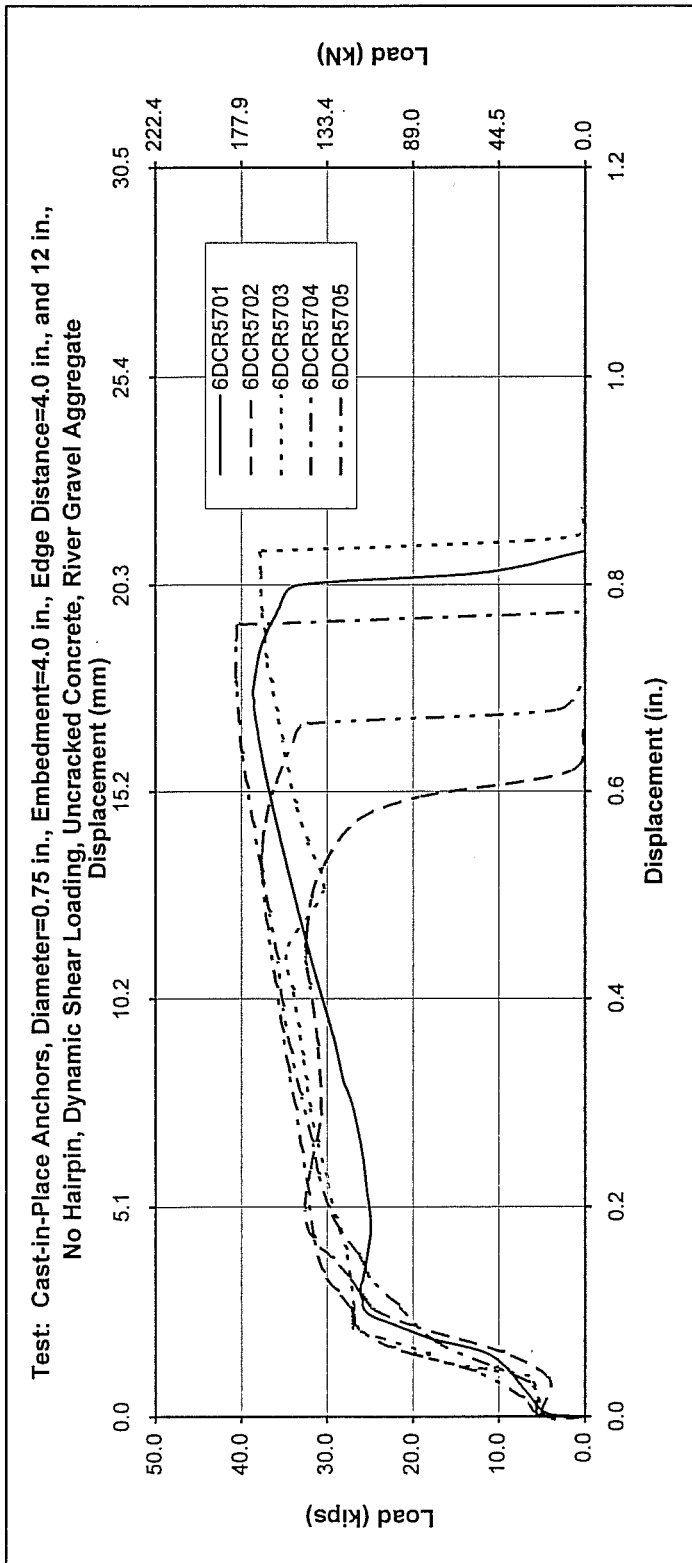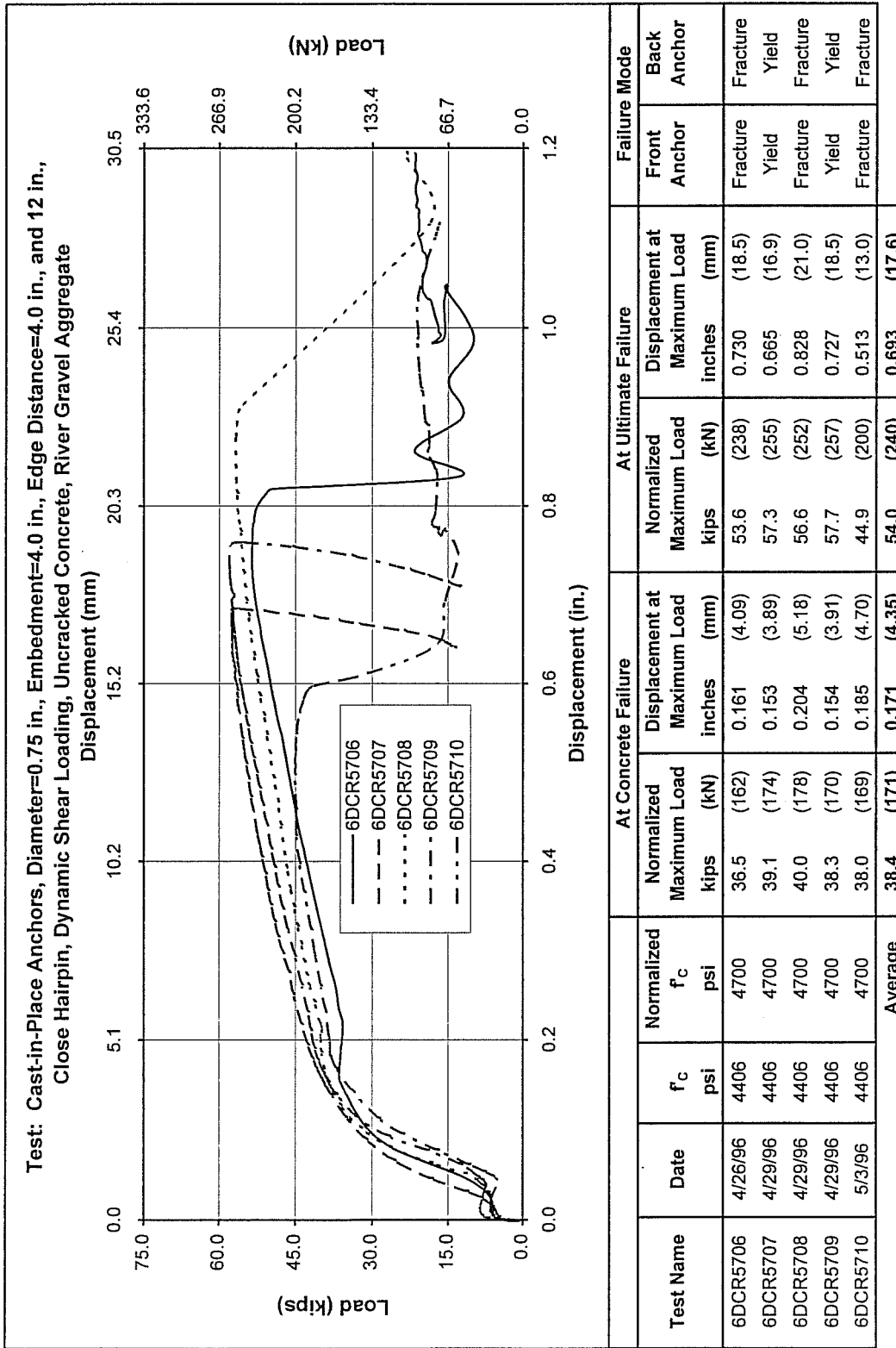

| Test Name | Date | f'c psi | Normalized f'c psi | At Concrete Failure | | At Ultimate Failure | | Failure Mode | |
				Normalized Maximum Load kips (kN)	Displacement at Maximum Load inches (mm)	Normalized Maximum Load kips (kN)	Displacement at Maximum Load inches (mm)	Front Anchor	Back Anchor
6DCR5701	5/1/96	4406	4700	26.0 (116)	0.116 (2.95)	38.6 (172)	0.692 (17.6)	Cone	Fracture
6DCR5702	4/24/96	4460	4700	25.3 (113)	0.112 (2.84)	32.3 (144)	0.448 (11.4)	Cone	Fracture
6DCR5703	4/24/96	4460	4700	26.9 (120)	0.091 (2.31)	37.7 (168)	0.814 (20.7)	Cone	Fracture
6DCR5704	4/26/96	4406	4700	25.3 (113)	0.140 (3.56)	40.5 (180)	0.709 (18.0)	Cone	Fracture
6DCR5705	4/26/96	4406	4700	26.5 (118)	0.090 (2.29)	37.5 (167)	0.523 (13.3)	Cone	Fracture
Average				26.0 (116)	0.110 (2.79)	37.3 (166)	0.637 (16.2)		

214

Test: Cast-in-Place Anchors, Diameter=0.75 in., Embedment=4.0 in., Edge Distance=4.0 in., and 12 in., Close Hairpin, Dynamic Shear Loading, Uncracked Concrete, River Gravel Aggregate

Test Name	Date	f'c psi	Normalized f'c psi	At Concrete Failure Normalized Maximum Load kips (kN)	Displacement at Maximum Load inches (mm)	At Ultimate Failure Normalized Maximum Load kips (kN)	Displacement at Maximum Load inches (mm)	Failure Mode Front Anchor	Back Anchor
6DCR5706	4/26/96	4406	4700	36.5 (162)	0.161 (4.09)	53.6 (238)	0.730 (18.5)	Fracture	Fracture
6DCR5707	4/29/96	4406	4700	39.1 (174)	0.153 (3.89)	57.3 (255)	0.665 (16.9)	Yield	Yield
6DCR5708	4/29/96	4406	4700	40.0 (178)	0.204 (5.18)	56.6 (252)	0.828 (21.0)	Fracture	Fracture
6DCR5709	4/29/96	4406	4700	38.3 (170)	0.154 (3.91)	57.7 (257)	0.727 (18.5)	Yield	Yield
6DCR5710	5/3/96	4406	4700	38.0 (169)	0.185 (4.70)	44.9 (200)	0.513 (13.0)	Fracture	Fracture
Average				38.4 (171)	0.171 (4.35)	54.0 (240)	0.693 (17.6)		

Results for Series 3-7

Anchor	Test Number	Loading	Diameter in. (mm)	Effective Embedment h_e in. (mm)	Front Anchor Edge Distance in. (mm)	Back Anchor Edge Distance in. (mm)	f'_c psi (MPa)	Normalized f'_c psi (MPa)	Concrete Cone Breakout Normalized F_u kips (kN)	Displacement in. (mm)	Additional Crack Opening side mm	top mm	Ultimate Failure Normalized F_u kips (kN)	Displacement in. (mm)	Failure Mode Front Anchor	Back Anchor
CIP No Hairpin	7SCR5701	Static	0.75 (19)	4 (100)	4 (100)	12 (300)	4460 (30.8)	4700 (32.4)	31.0 (138)	0.138 (3.51)	0.11	0.06	35.4 (157)	0.587 (14.9)	cone	pryout
	7SCR5702	Static	0.75 (19)	4 (100)	4 (100)	12 (300)	4460 (30.8)	4700 (32.4)	30.5 (136)	0.202 (5.13)	0.21	0.06	36.0 (160)	0.814 (20.7)	cone	pryout
	7SCR5703	Static	0.75 (19)	4 (100)	4 (100)	12 (300)	4460 (30.8)	4700 (32.4)	28.7 (128)	0.171 (4.34)	0.23	0.09	34.6 (154)	0.369 (9.37)	cone	pryout
	7SCR5704	Static	0.75 (19)	4 (100)	4 (100)	12 (300)	4460 (30.8)	4700 (32.4)	20.9 (93.0)	0.164 (4.17)	0.17	0.05	30.8 (137)	0.456 (11.6)	cone	pryout
	7SCR5705	Static	0.75 (19)	4 (100)	4 (100)	12 (300)	4460 (30.8)	4700 (32.4)	28.7 (128)	0.206 (5.23)	0.15	0.05	38.8 (173)	0.963 (24.5)	cone	fracture
								Average	28.0 (124)	0.176 (4.48)	0.17	0.06	35.1 (156)	0.638 (16.2)		
								COV	14.60	16.02	27.44	26.50	8.22	38.78		
CIP Close Hairpin	7SCR5706	Static	0.75 (19)	4 (100)	4 (100)	12 (300)	4460 (30.8)	4700 (32.4)	42.1 (187)	0.211 (5.36)	0.20		60.8 (270)	0.849 (21.6)	cone/disp.	pryout
	7SCR5707	Static	0.75 (19)	4 (100)	4 (100)	12 (300)	4460 (30.8)	4700 (32.4)	30.3 (135)	0.089 (2.26)	0.20	0.04	51.7 (230)	0.568 (14.4)	cone/disp.	fracture
	7SCR5708	Static	0.75 (19)	4 (100)	4 (100)	12 (300)	4460 (30.8)	4700 (32.4)	36.8 (164)	0.219 (5.56)	0.14	0.04	45.9 (204)	0.547 (13.9)	fracture	fracture
	7SCR5709	Static	0.75 (19)	4 (100)	4 (100)	12 (300)	4460 (30.8)	4700 (32.4)	33.1 (147)	0.197 (5.00)	0.17	0.04	53.1 (236)	1.01 (25.6)	cone/disp.	fracture
	7SCR5710	Static	0.75 (19)	4 (100)	4 (100)	12 (300)	4460 (30.8)	4700 (32.4)	33.3 (148)	0.145 (3.68)	0.12	0.04	46.1 (205)	0.589 (15.0)	cone/disp.	fracture
								Average	35.1 (156)	0.172 (4.37)	0.17	0.04	51.5 (229)	0.712 (18.1)		
								COV	12.91	31.77	21.55	0.00	11.87	28.90		

Test: Cast-in-Place Anchors, Diameter=0.75 in., Embedment=4.0 in., Edge Distance=4.0 in., and 12 in., No Hairpin, Static Shear Loading, Cracked Concrete, River Gravel Aggregate
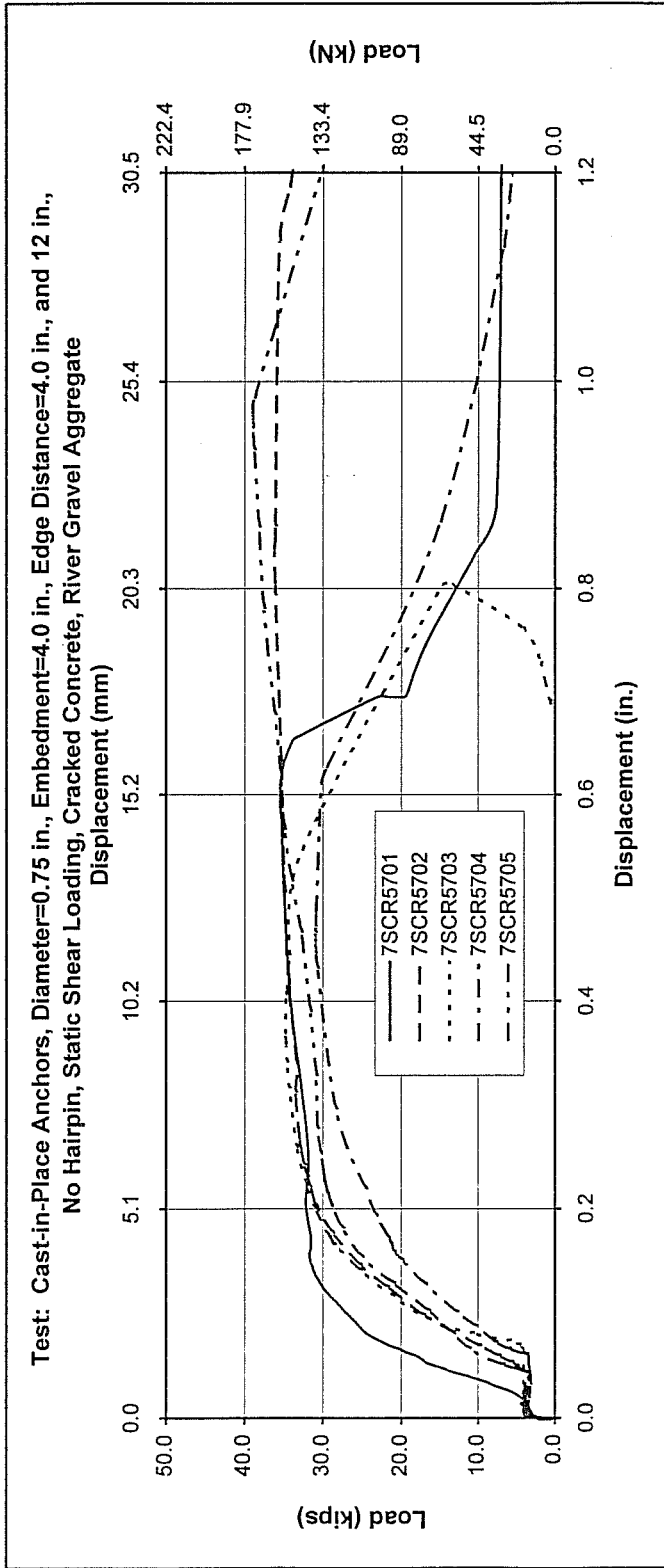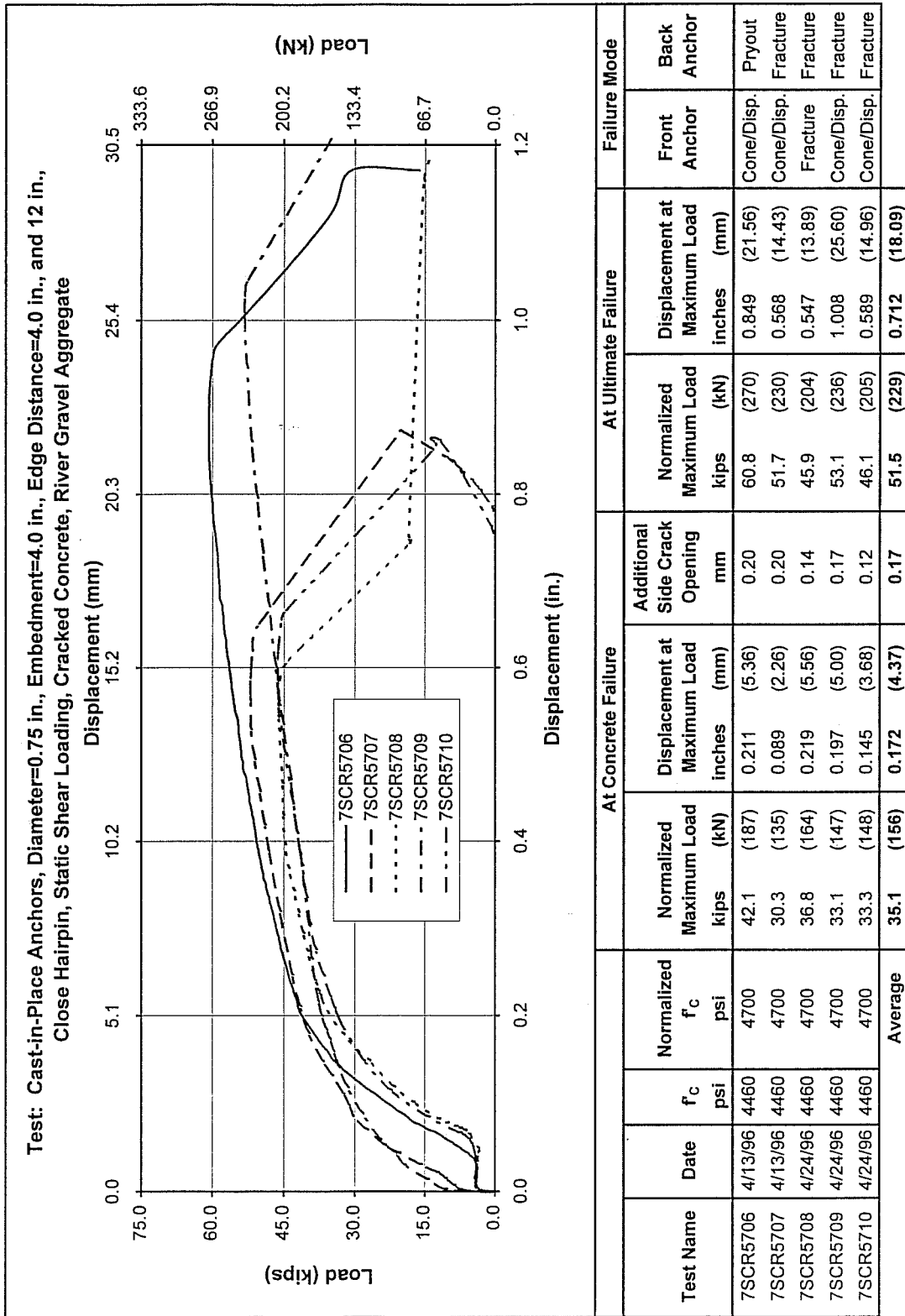
Test Name	Date	f'c psi	Normalized f'c psi	At Concrete Failure			At Ultimate Failure		Failure Mode	
				Normalized Maximum Load kips (kN)	Displacement at Maximum Load inches (mm)	Additional Side Crack Opening mm	Normalized Maximum Load kips (kN)	Displacement at Maximum Load inches (mm)	Front Anchor	Back Anchor
7SCR5701	4/10/96	4460	4700	31.0 (138)	0.138 (3.51)	0.11	35.4 (157)	0.587 (14.9)	Cone	Pryout
7SCR5702	4/12/96	4460	4700	30.5 (136)	0.202 (5.13)	0.21	36.0 (160)	0.814 (20.7)	Cone	Pryout
7SCR5703	4/12/96	4460	4700	28.7 (128)	0.171 (4.34)	0.23	34.6 (154)	0.369 (9.4)	Cone	Pryout
7SCR5704	4/12/96	4460	4700	20.9 (93.0)	0.164 (4.17)	0.17	30.8 (137)	0.456 (11.6)	Cone	Pryout
7SCR5705	4/13/96	4460	4700	28.7 (128)	0.206 (5.23)	0.15	38.8 (173)	0.963 (24.5)	Cone	Fracture
Average				28.0 (124)	0.176 (4.48)	0.17	35.1 (156)	0.638 (16.2)		

Test: Cast-in-Place Anchors, Diameter=0.75 in., Embedment=4.0 in., Edge Distance=4.0 in., and 12 in., Close Hairpin, Static Shear Loading, Cracked Concrete, River Gravel Aggregate
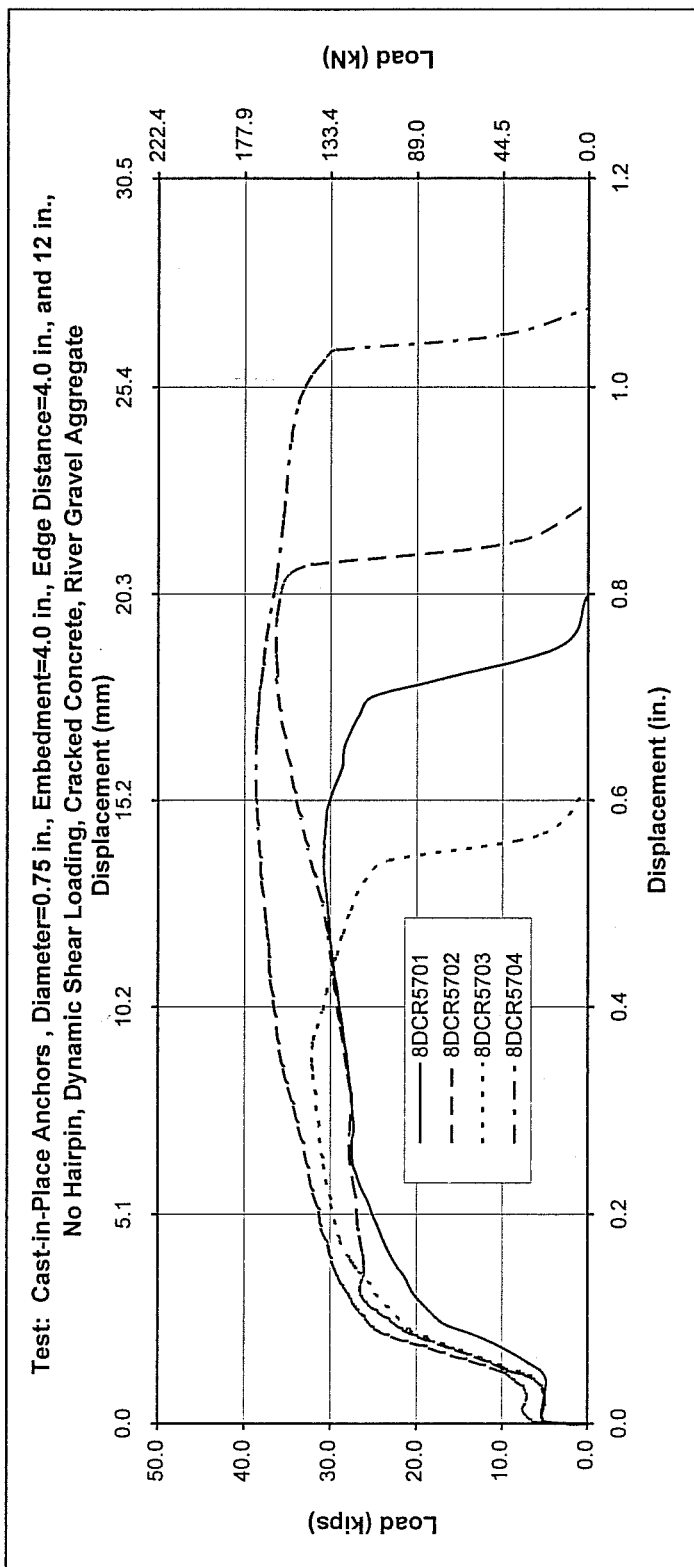

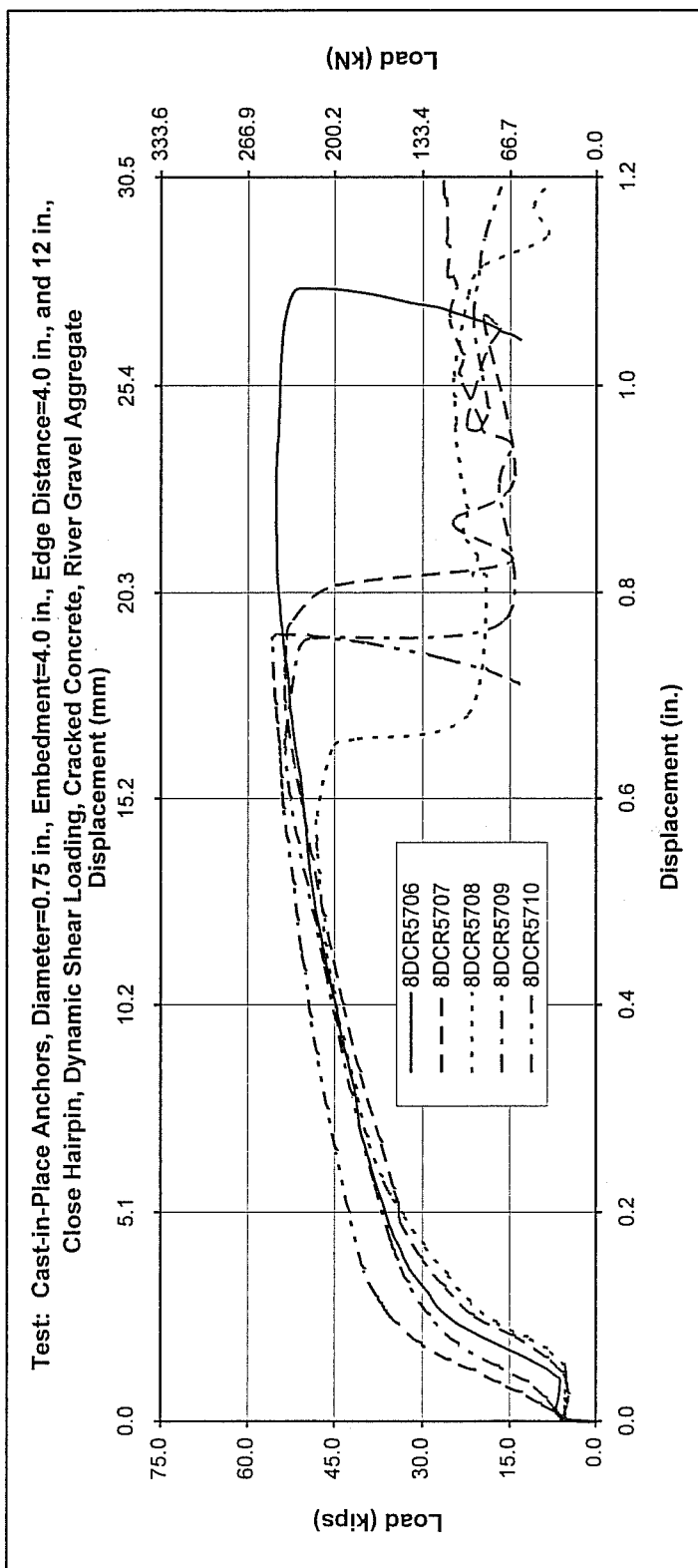| Test Name	Date	f_c psi	Normalized f_c psi	At Concrete Failure			At Ultimate Failure			Failure Mode	
				Normalized Maximum Load kips (kN)	Displacement at Maximum Load inches (mm)	Additional Side Crack Opening mm	Normalized Maximum Load kips (kN)	Displacement at Maximum Load inches (mm)		Front Anchor	Back Anchor
7SCR5706	4/13/96	4460	4700	42.1 (187)	0.211 (5.36)	0.20	60.8 (270)	0.849 (21.56)		Cone/Disp.	Pryout
7SCR5707	4/13/96	4460	4700	30.3 (135)	0.089 (2.26)	0.20	51.7 (230)	0.568 (14.43)		Cone/Disp.	Fracture
7SCR5708	4/24/96	4460	4700	36.8 (164)	0.219 (5.56)	0.14	45.9 (204)	0.547 (13.89)		Fracture	Fracture
7SCR5709	4/24/96	4460	4700	33.1 (147)	0.197 (5.00)	0.17	53.1 (236)	1.008 (25.60)		Cone/Disp.	Fracture
7SCR5710	4/24/96	4460	4700	33.3 (148)	0.145 (3.68)	0.12	46.1 (205)	0.589 (14.96)		Cone/Disp.	Fracture
Average				35.1 (156)	0.172 (4.37)	0.17	51.5 (229)	0.712 (18.09)			

Results for Series 3-8

Anchor	Test Number	Loading	Diameter in. (mm)	Effective Embedment h_e in. (mm)	Front Anchor Edge Distance in. (mm)	Back Anchor Edge Distance in. (mm)	f_c psi (MPa)	Normalized f_c psi (MPa)	Concrete Cone Breakout Normalized F_u kips (kN)	Displacement in. (mm)	Additional Crack Opening side mm	top mm	Ultimate Failure Normalized F_u kips (kN)	Displacement in. (mm)	Failure Mode Front Anchor	Back Anchor
CIP	8DCR5701	Dynamic	0.75 (19)	4 (100)	4 (100)	12 (300)	4406 (30.4)	4700 (32.4)	27.5 (122)	0.255 (6.48)	0.21	0.04	30.8 (137)	0.529 (13.4)	cone	fracture
No	8DCR5702	Dynamic	0.75 (19)	4 (100)	4 (100)	12 (300)	4406 (30.4)	4700 (32.4)	26.3 (117)	0.125 (3.18)	0.26	0.04	36.3 (161)	0.742 (18.8)	cone	fracture
Hairpin	8DCR5703	Dynamic	0.75 (19)	4 (100)	4 (100)	12 (300)	4406 (30.4)	4700 (32.4)	27.2 (121)	0.153 (3.89)	0.21	0.05	32.0 (142)	0.347 (8.81)	cone	fracture
	8DCR5704	Dynamic	0.75 (19)	4 (100)	4 (100)	12 (300)	4406 (30.4)	4700 (32.4)	27.2 (121)	0.117 (2.97)	0.20	0.04	38.5 (171)	0.603 (15.3)	cone	fracture
								Average	27.1 (120)	0.163 (4.13)	0.22	0.04	34.4 (153)	0.555 (14.1)		
								COV	1.92	39.12	12.31	11.76	10.50	29.63		
CIP	8DCR5706	Dynamic	0.75 (19)	4 (100)	4 (100)	12 (300)	4406 (30.4)	4700 (32.4)	35.0 (156)	0.179 (4.55)	0.16	0.02	55.0 (245)	0.857 (21.8)	yield	yield
Close	8DCR5707	Dynamic	0.75 (19)	4 (100)	4 (100)	12 (300)	4406 (30.4)	4700 (32.4)	33.8 (150)	0.197 (5.00)	0.19	0.05	53.4 (238)	0.723 (18.4)	fracture	fracture
Hairpin	8DCR5708	Dynamic	0.75 (19)	4 (100)	4 (100)	12 (300)	4406 (30.4)	4700 (32.4)	35.7 (159)	0.223 (5.66)	0.21	0.04	47.9 (213)	0.554 (14.1)	fracture	fracture
	8DCR5709	Dynamic	0.75 (19)	4 (100)	4 (100)	12 (300)	4406 (30.4)	4700 (32.4)	34.3 (153)	0.159 (4.04)	0.20	0.02	53.4 (238)	0.652 (16.6)	fracture	fracture
	8DCR5710	Dynamic	0.75 (19)	4 (100)	4 (100)	12 (300)	4406 (30.4)	4700 (32.4)	36.4 (162)	0.112 (2.84)	0.16	0.05	55.6 (247)	0.756 (19.2)	yield	yield
								Average	35.0 (156)	0.174 (4.42)	0.18	0.04	53.1 (236)	0.708 (18.0)		
								COV	2.98	24.08	12.51	42.13	5.74	16.03		

Test: Cast-in-Place Anchors, Diameter=0.75 in., Embedment=4.0 in., Edge Distance=4.0 in., and 12 in., No Hairpin, Dynamic Shear Loading, Cracked Concrete, River Gravel Aggregate
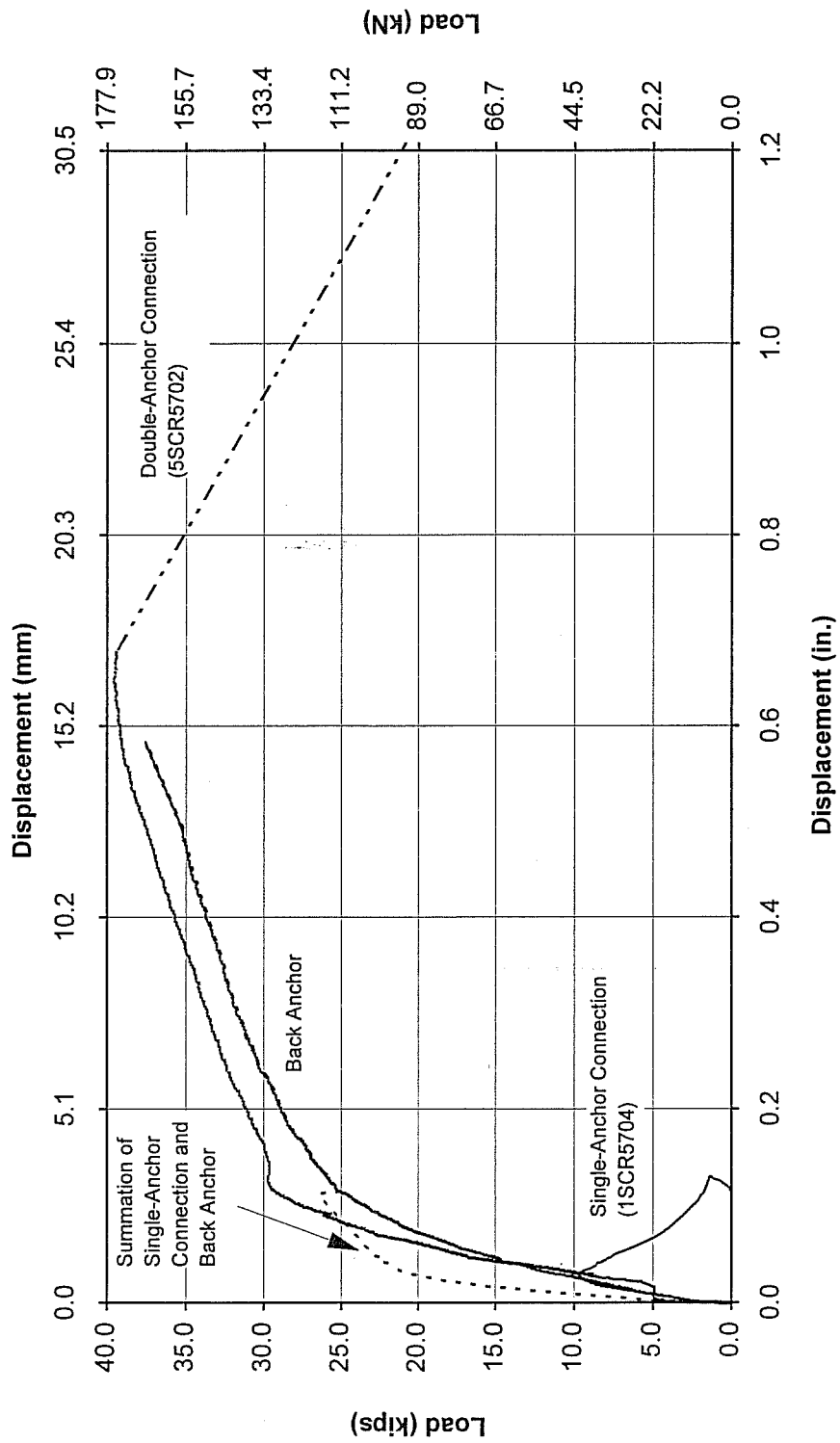

Test Name	Date	f_c psi	Normalized f_c psi	At Concrete Failure			At Ultimate Failure		Failure Mode	
				Normalized Maximum Load kips (kN)	Displacement at Maximum Load inches (mm)	Additional Side Crack Opening mm	Normalized Maximum Load kips (kN)	Displacement at Maximum Load inches (mm)	Front Anchor	Back Anchor
8DCR5701	4/26/96	4406	4700	27.5 (122)	0.255 (6.48)	0.21	30.8 (137)	0.529 (13.4)	Cone	Fracture
8DCR5702	4/29/96	4406	4700	26.3 (117)	0.125 (3.18)	0.26	36.3 (161)	0.742 (18.8)	Cone	Fracture
8DCR5703	4/29/96	4406	4700	27.2 (121)	0.153 (3.89)	0.21	32.0 (142)	0.347 (8.81)	Cone	Fracture
8DCR5704	5/1/96	4406	4700	27.2 (121)	0.117 (2.97)	0.20	38.5 (171)	0.603 (15.3)	Cone	Fracture
Average				27.1 (120)	0.163 (4.13)	0.22	34.4 (153)	0.555 (14.1)		

Test: Cast-in-Place Anchors, Diameter=0.75 in., Embedment=4.0 in., Edge Distance=4.0 in., and 12 in., Close Hairpin, Dynamic Shear Loading, Cracked Concrete, River Gravel Aggregate

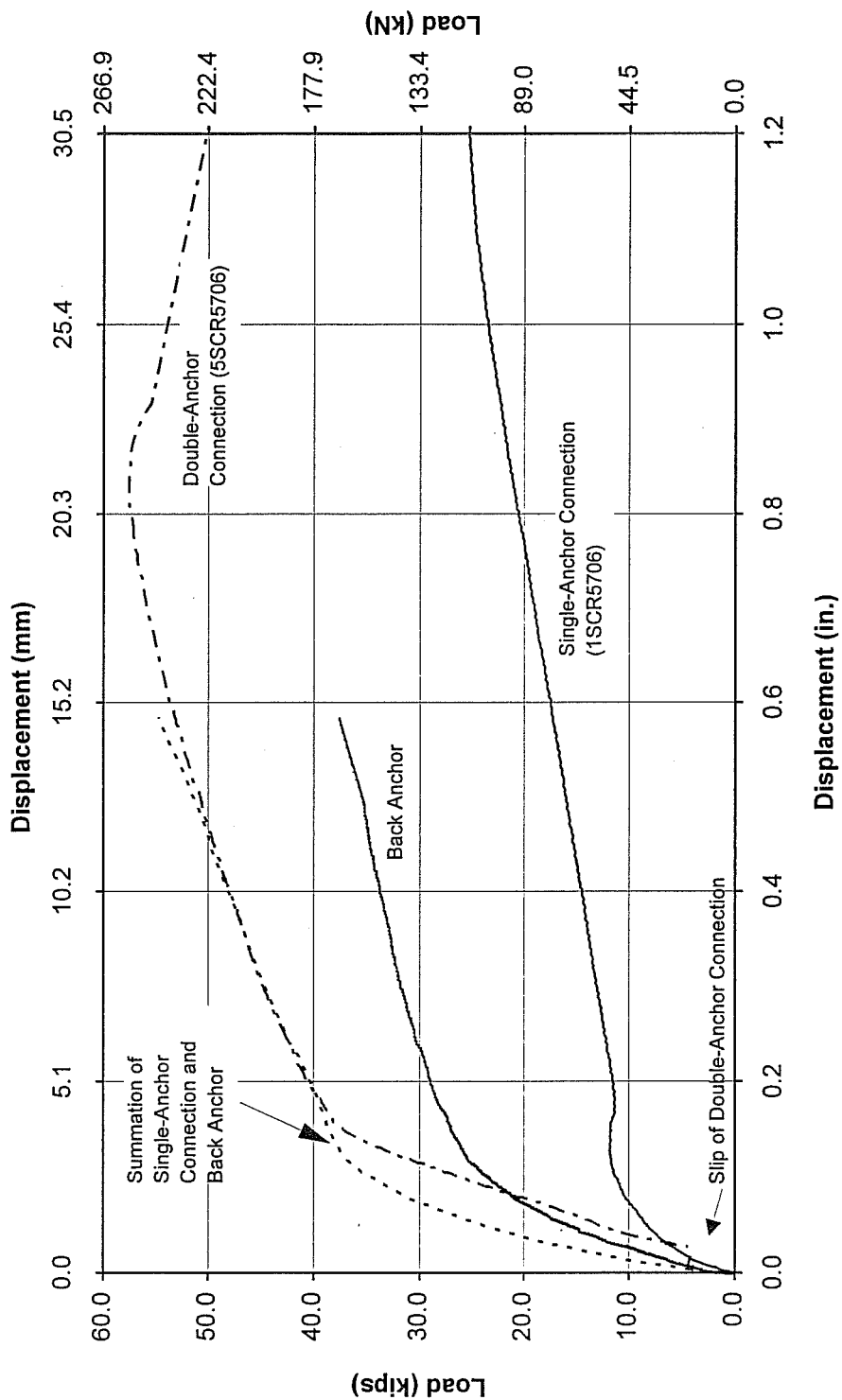| Test Name	Date	Normalized f'_c psi	f'_c psi	At Concrete Failure					At Ultimate Failure				Failure Mode	
				Normalized Maximum Load kips	(kN)	Displacement at Maximum Load inches	(mm)	Additional Side Crack Opening mm	Normalized Maximum Load kips	(kN)	Displacement at Maximum Load inches	(mm)	Front Anchor	Back Anchor
8DCR5706	5/1/96	4406	4700	35.0	(156)	0.179	(4.55)	0.16	55.0	(245)	0.857	(21.8)	Yield	Yield
8DCR5707	5/3/96	4406	4700	33.8	(150)	0.197	(5.00)	0.19	53.4	(238)	0.723	(18.4)	Fracture	Fracture
8DCR5708	5/3/96	4406	4700	35.7	(159)	0.223	(5.66)	0.21	47.9	(213)	0.554	(14.1)	Fracture	Fracture
8DCR5709	5/3/96	4406	4700	34.3	(153)	0.159	(4.04)	0.20	53.4	(238)	0.652	(16.6)	Fracture	Fracture
8DCR5710	5/9/96	4406	4700	36.4	(162)	0.112	(2.84)	0.16	55.6	(247)	0.756	(19.2)	Yield	Yield
Average				35.0	(156)	0.174	(4.42)	0.18	53.1	(236)	0.708	(18.0)		

APPENDIX C

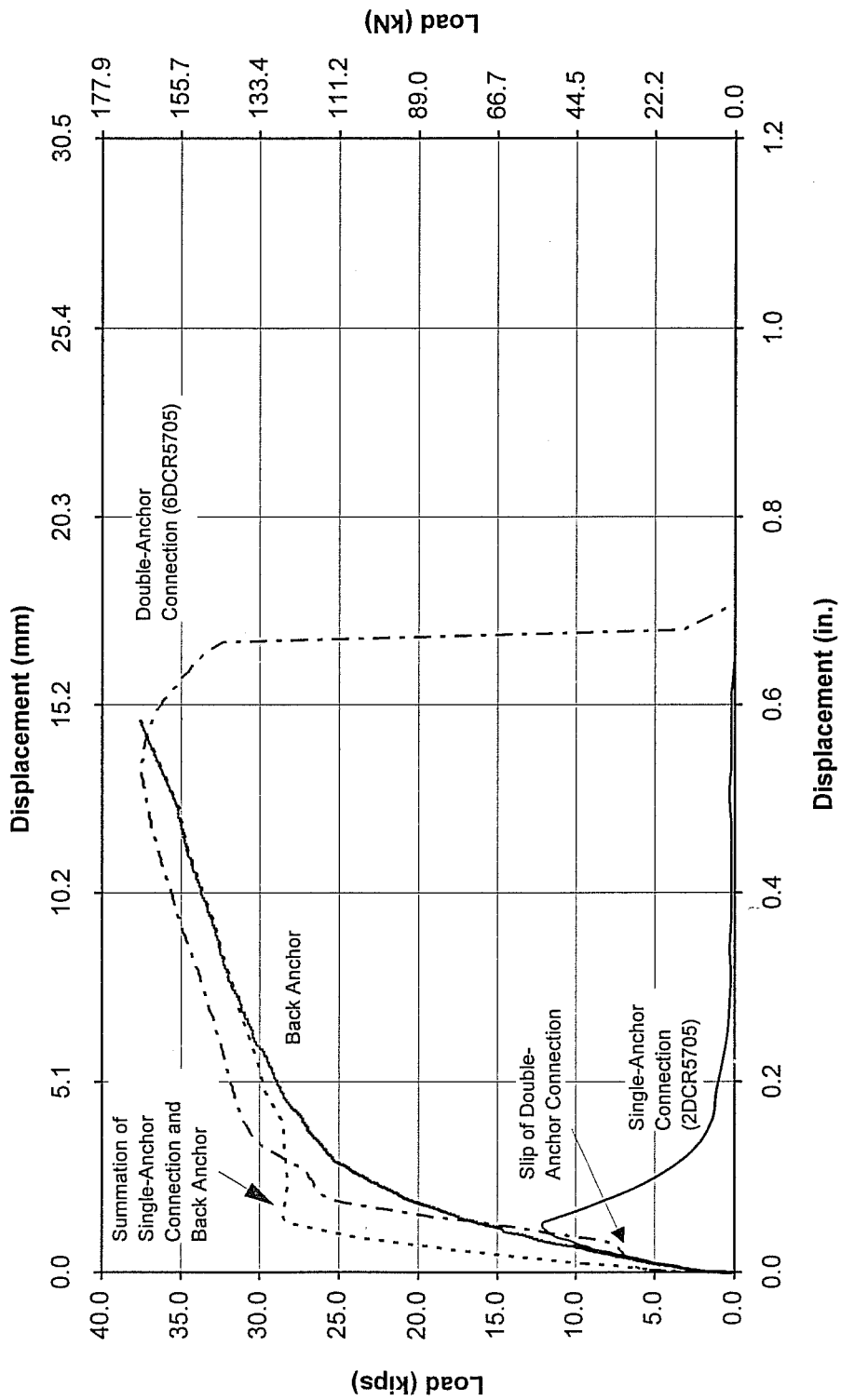# EVALUATION OF DOUBLE ANCHOR MODEL

Evaluation of Double-Anchor Model for Anchors Loaded in Shear Static Loading, No Hairpin, Uncracked Concrete
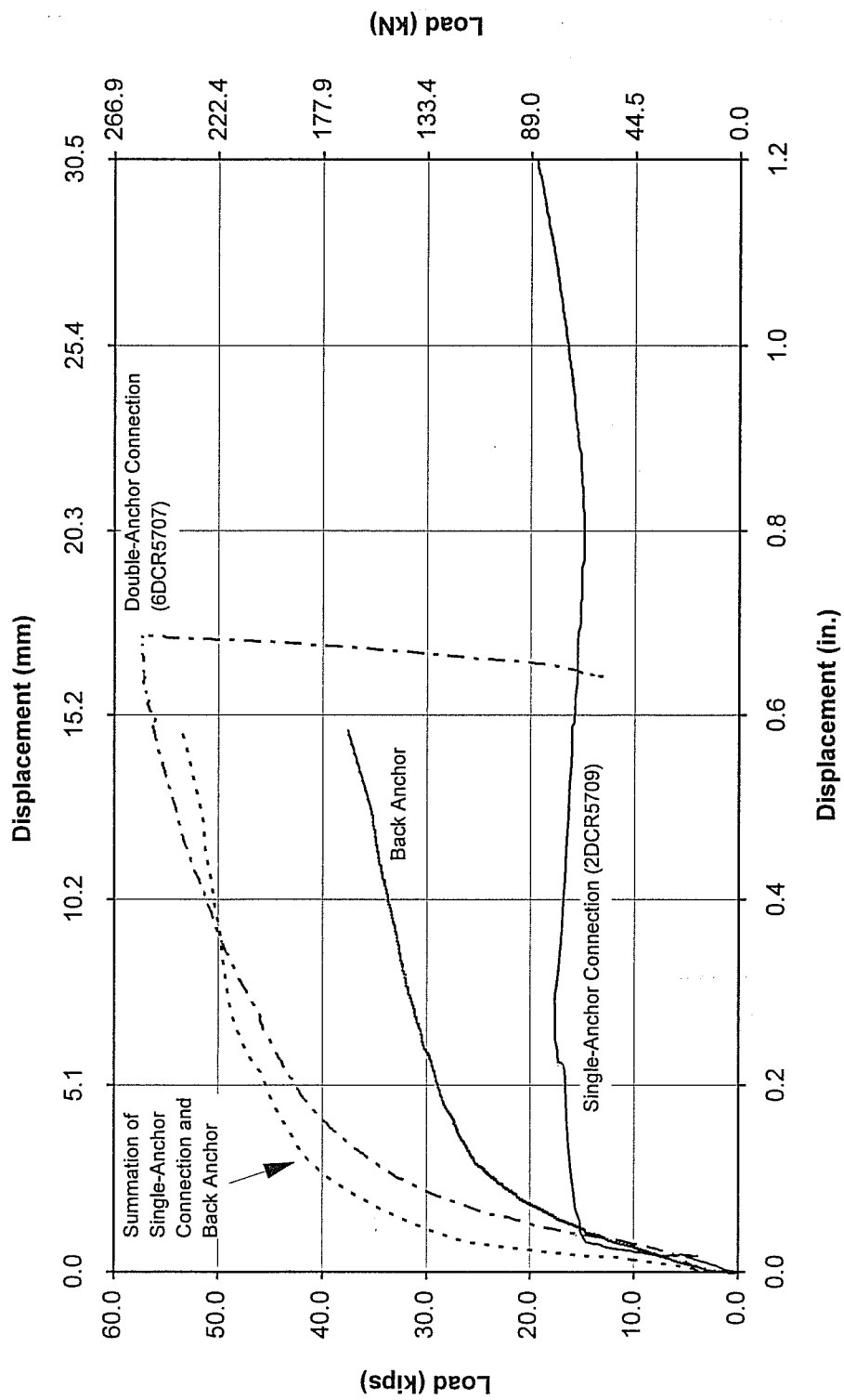
Evaluatin of Double Anchor Model for Anchors Loaded in Shear
Static Loading, Close Hairpin, Uncracked Concrete

Evaluation of Double-Anchor Connection for Anchors Loaded in Shear Dynamic Loading, No Hairpin, Uncracked Concrete

Evaluation of Double-Anchor Model for Anchors Loaded in Shear
Dynamic Loading, Close Hairpin, Uncracked Concrete

Evaluation of Double-Anchor Model for Anchors Loaded in Shear
Static Loading, No Hairpin, Cracked Concrete

Evaluation of Double-Anchor Model for Anchors Loaded in Shear Static Loading, Close Hairpin, Cracked Concrete
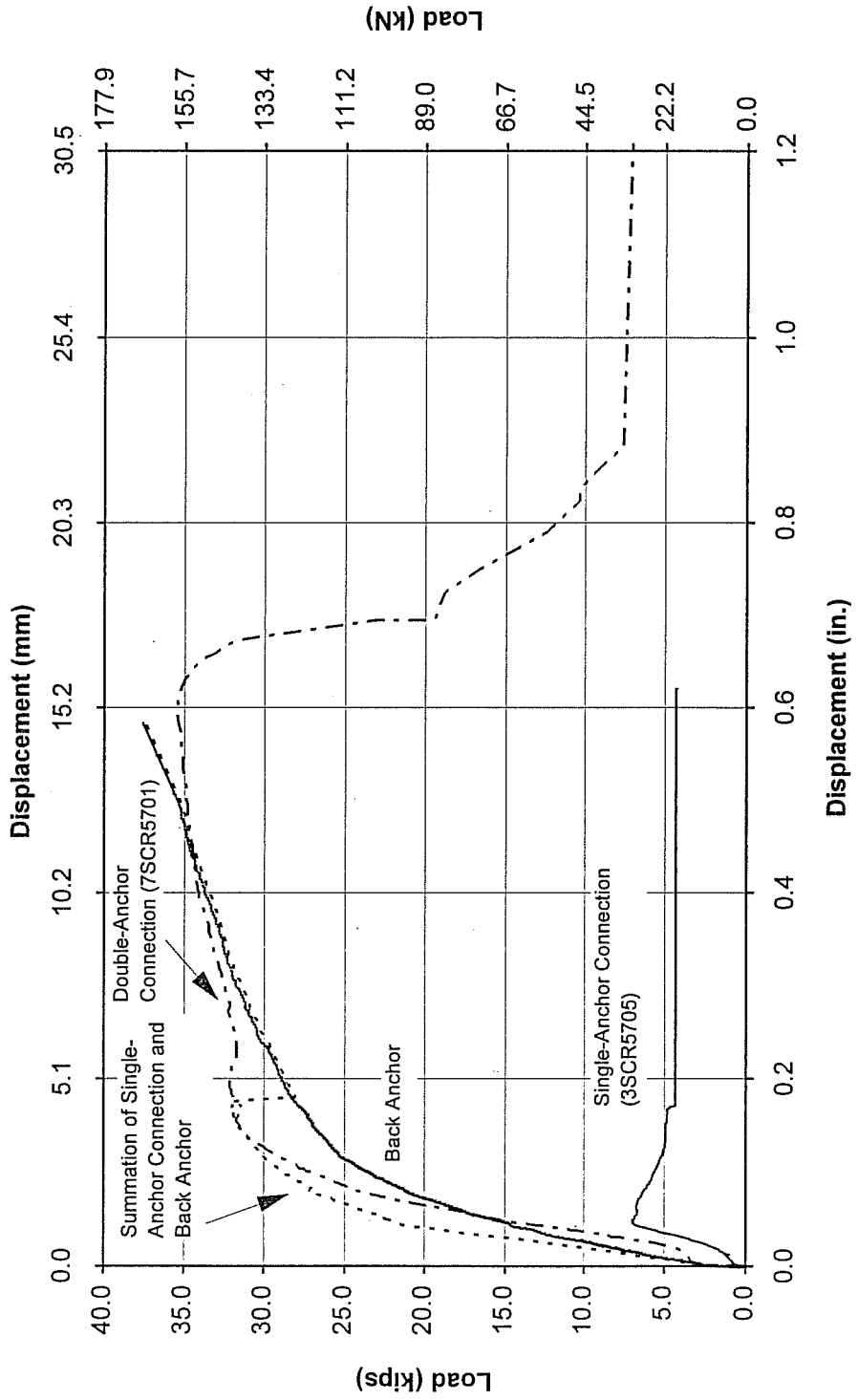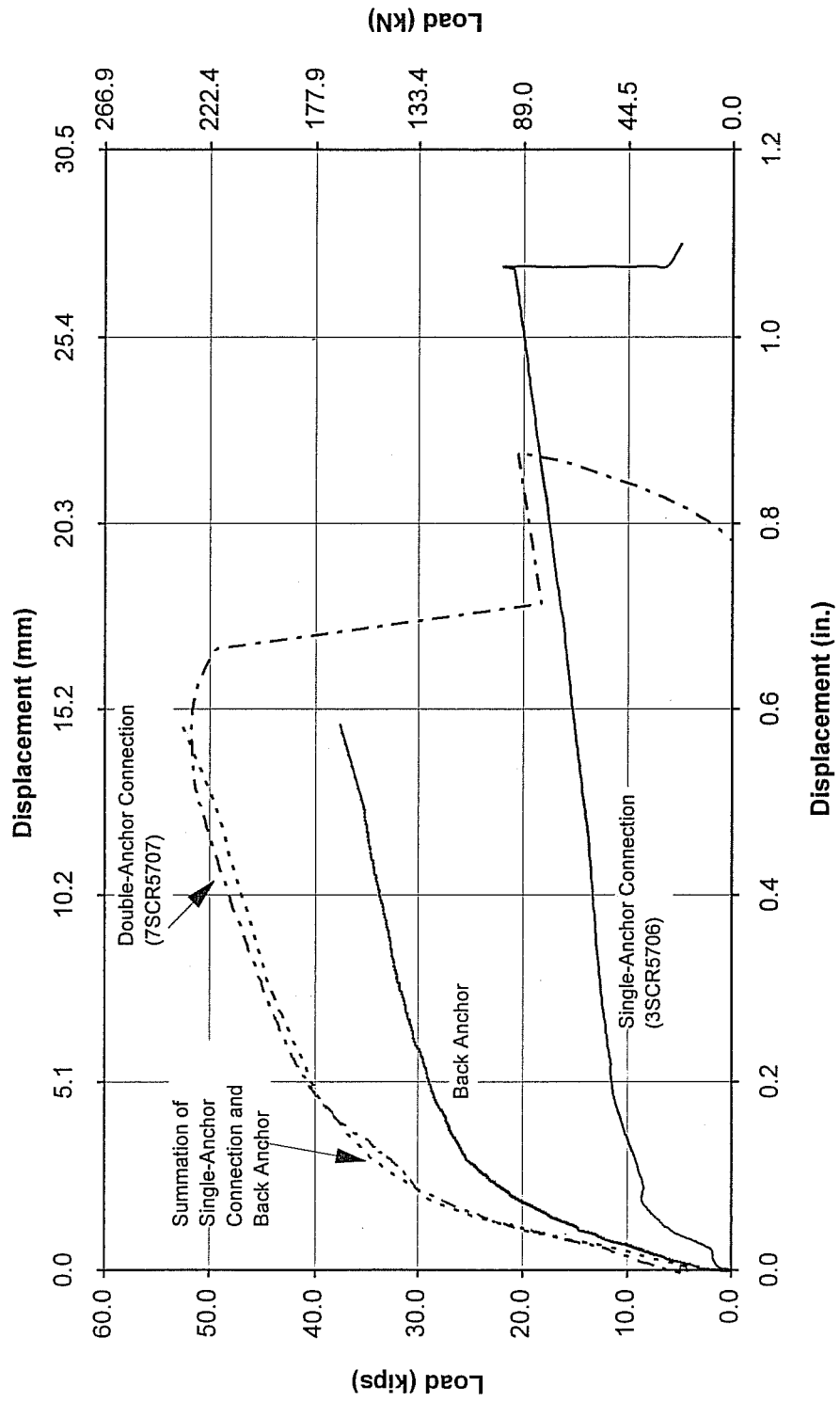
Evaluation of Double-Anchor Connection for Anchors Loaded in Shear
Dynamic Loading, No Hairpin, Cracked Concrete

Evaluation of Double-Anchor Model for Anchors Loaded in Shear
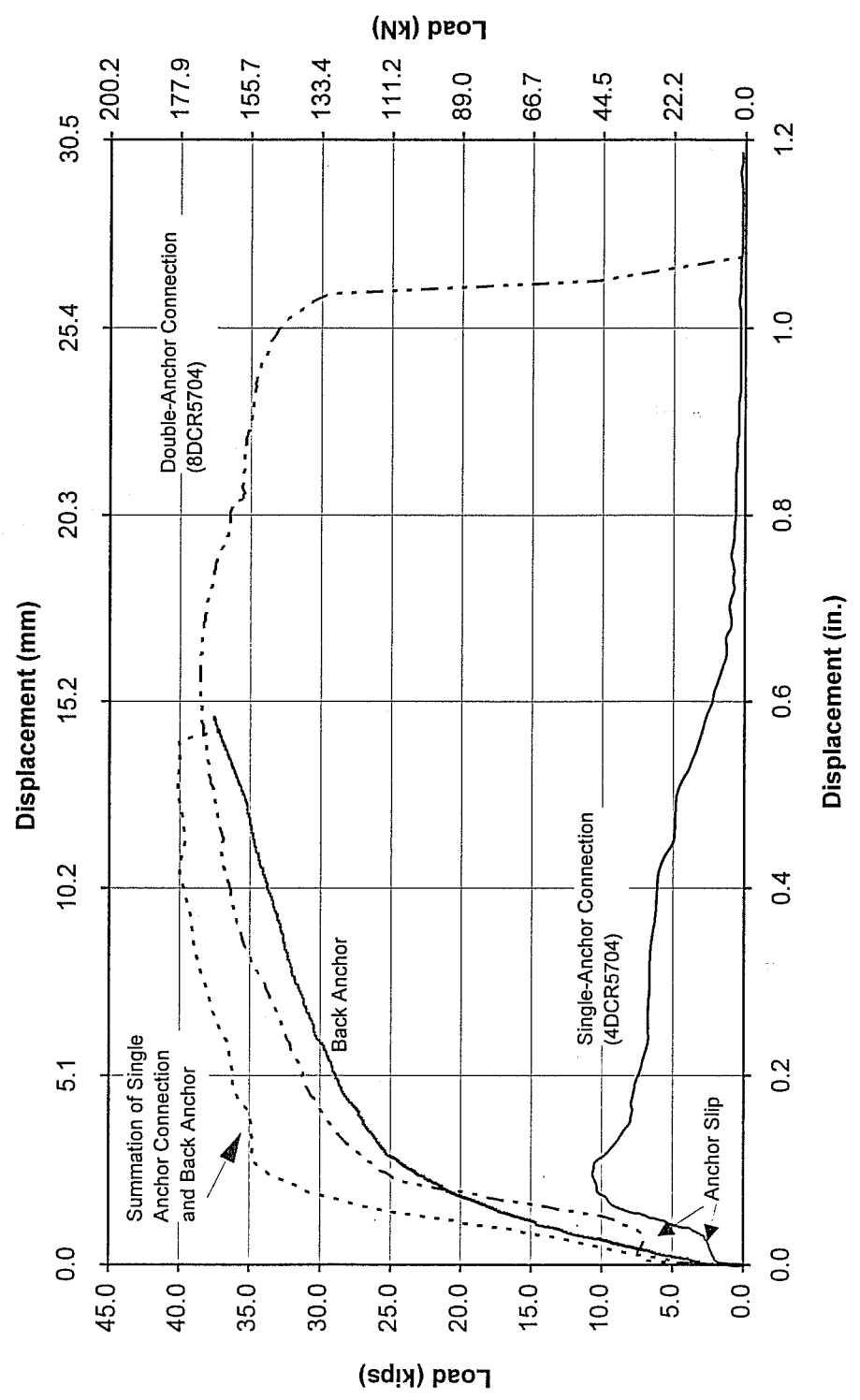Dynamic Loading, Close Hairpin, Cracked Concrete

APPENDIX D

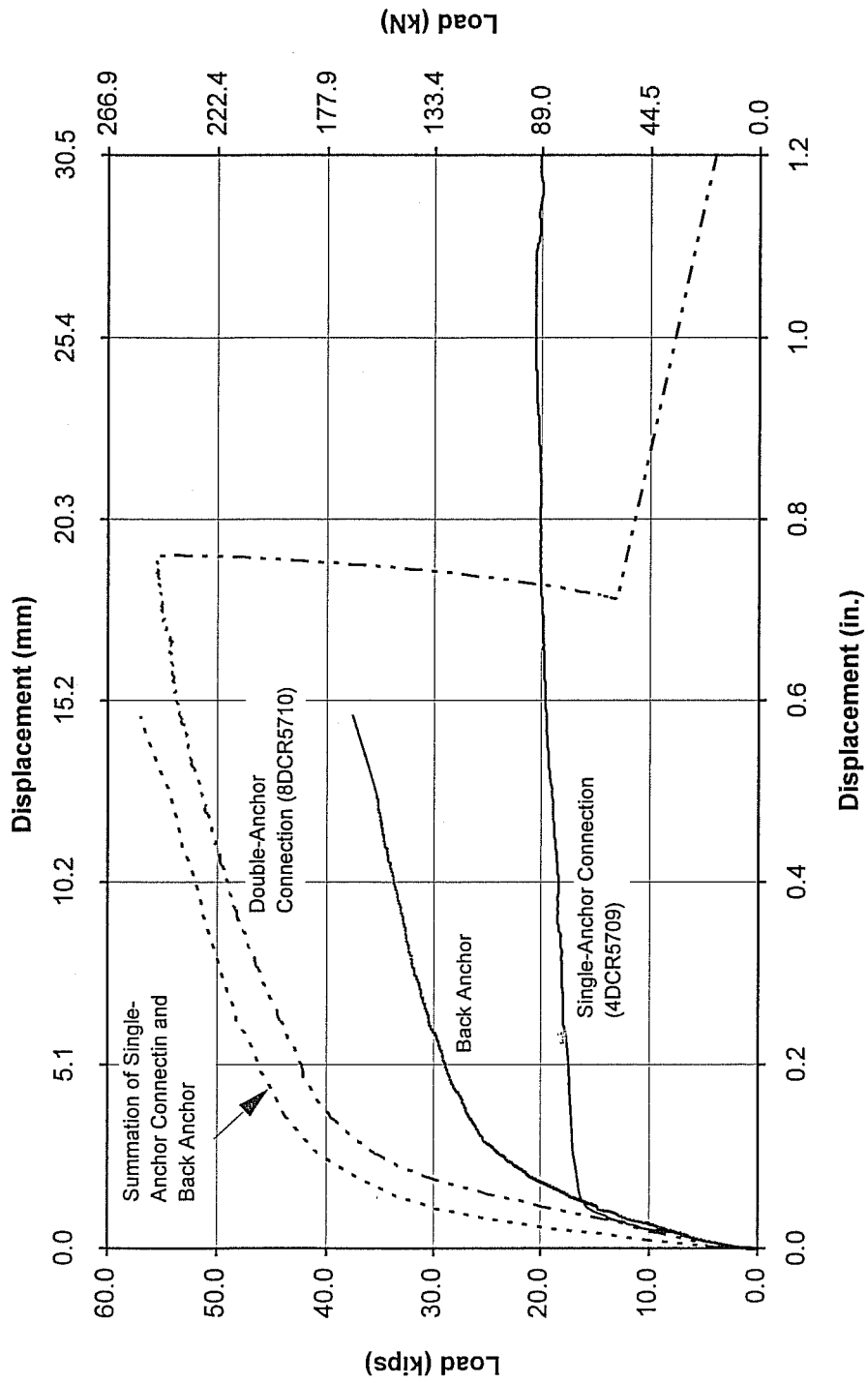# NOTATION

NOTATION

A_N	actual projected area of failure cone for tensile loading, in.^{2} or mm^2
A_{No}	projected area of the failure cone for a single anchor unlimited by overlapping cones, edge effects, or member thickness for tensile loading, in.^{2} or mm^2
A_s	effective area of steel, in.^{2} or mm^2
A_V	actual projected area of failure cone for shear loading, in.^{2} or mm^2
A_{Vo}	projected area of a single anchor unlimited by overlapping cones, edge effects, or member thickness for shear loading, in.^{2} or mm^2
c	distance from center of anchor to edge of concrete, in. or mm
c_1	distance from center of anchor to edge of concrete in loading direction for shear tests, in. or mm
d_o	outside diameter of anchor, in. or mm
d_u	diameter of anchor head, in. or mm
f_c	tested concrete compressive strength measured on 6 x 12 in. cylinders, psi
f_{cc}	tested concrete compressive strength measured on 200-mm cubes, N/mm^2
f'_c	specified concrete compressive strength measured on 6 x 12 in. cylinders, psi
f'_{cc}	specified concrete compressive strength measured on 200-mm cubes, N/mm^2
F_u	measured maximum load, lb or N
h_{ef}	effective embedment, in. or mm
k_{nc}	multiplicative constant for evaluating tensile capacity using the CC Method
ℓ	activated load bearing length of anchor, in or mm
N	tensile load, lb or N
N_{no}	nominal tensile cone breakout capacity, lb or N
N_u	ultimate tensile capacity, lb or N
V	shear load, lb or N
V_{no}	nominal shear breakout capacity, lb or N
V_u	ultimate shear capacity, lb or N

REFERENCES

[ACI 349 1990] ACI 349 1990, "Code Requirements for Nuclear Safety Related Concrete Structures," American Concrete Institute, Detroit, Michigan, 1990.

[ASTM C 1131-81 1987] ASTM C 1131-81, "Resistance to Degradation of Small-Size Coarse Aggregate by Abrasion and Impact in the Los Angeles Machine," American Society for Testing and Materials, Philadelphia, Pennsylvania, 1987.

[CEB 206 & 207 1991] Comite' Euro-International du Beton, *Fastenings to Reinforced Concrete and Masonry Structures: State-of-the-Art Report*, bulletin D'Information Nos. 206 and 207, August 1991.

[Cook 1989] Cook, Ronald A., "Behavior and Design of Ductile Multiple-Anchor Steel-to-Concrete Connections," Ph.D. Dissertation, The University of Texas at Austin, May 1989.

[Eligehausen and Balogh 1995] Eligehausen, R. and Balogh, T., "Behavior of Fasteners Loaded in Tension in Cracked Reinforced Concrete," *ACI Structural Journal*, Vol. 92, No. 3, May-June 1995, pp. 365-379.

[Farrow, Frigui, and Klingner 1996] Farrow, C.B., Frigui, I., and Klingner, R.E., "Tensile Capacity of Single Anchors in Concrete: Evaluation of Existing Formulas on an LRFD Basis", *ACI Structural Journal*, Vol. 93, No. 1, January-February 1996, pp. 128-137.

[Fuchs, Eligehausen, and Breen 1995] Fuchs, W., Eligehausen, R., and Breen J.E., "Concrete Capacity Design (CCD) Approach for Fastening to Concrete," *ACI Structural Journal*, Vol. 92, No. 1, January-February 1995, pp. 73-94.

[Klingner 1991] Klingner, R.E. "Anchor Bolt Behavior and Strength During Earthquakes: Technical and Management Proposal," Solicitation No. RS-NRR-91-031, United States Nuclear Regulatory Commission, The University of Texas at Austin, August 1991.

[Klingner and Mendonca 1982b] Klingner, R.E., and Mendonca, J.A., "Tensile Capacity of Short Anchor Bolts and Welded Studs: A Literature Review," *ACI Journal*, Vol. 79, no. 4, July-August, 1982, pp. 270-279.

[Klingner and Mendonca 1982a] Klingner, R.E., and Mendonca, J.A., "Shear Capacity of Short Anchor Bolts and Welded Studs: A Literature Review," *ACI Journal*, Vol. 79, no. 5, September-October 1982, pp. 339-349.

[Klingner, Mendonca, and Malik 1982] Klingner, R.E., Mendonca, J.A., and Malik, J.B., "Effect of Reinforcing Details on the Shear Resistance of Anchor Bolts Under Reversed Cyclic Loading," *ACI Journal*, Vol. 79, No. 1, January-February 1982, pp. 3-12.

[Lotze 1996] Lotze, Dieter, "Design of Group Fastenings According to Plastic Theory," Research Report to the U.S. Nuclear Regulatory Commission, December, 1995.

[Rodriguez 1995] Rodriguez, Milton, "Behavior of Anchors in Uncracked Concrete Under Static and Dynamic Tensile Loading," M.S. Thesis, The University of Texas at Austin, August 1995.

[Rodriguez et, al. 1994] Rodriguez, M., Zhang, Y., Lotze, D., Graves III, H.L., and Klingner, R.E. "Dynamic Behavior of Anchors in Cracked and Uncracked Concrete: A Progress Report," submitted to the Nuclear Regulatory Commission, 1994.

VITA

Jennifer Marie Hallowell was born in Silver Spring, Maryland on November 25, 1972, the daughter of Paul Lincoln Hallowell and Patricia Marie Hallowell. After graduating with high honors from Stone Ridge School of the Sacred Heart, Bethesda, Maryland in June, 1990, she entered Lehigh University in Bethlehem, Pennsylvania. At Lehigh, she was recipient of the Lehigh University Faculty and Professional Staff Scholarship, the William C. and Elizabeth H. Hittinger Scholarship, the Roger G. Slutter Memorial Scholarship, and the Alumni Association Junior Prize. She was awarded the degree of Bachelor of Science with highest honors from Lehigh University in May, 1994. In August, 1994, she entered The Graduate School at the University of Texas. She was awarded the John A. Focht Presidential Graduate Scholarship in Civil Engineering for the 1995-1996 academic year. She is currently employed as a design structural engineer with Walter P. Moore and Associates, Dallas, Texas.

Permanent Address: 18403 New Hampshire Avenue
Ashton, Maryland 20861

This thesis was typed by the author.